Heterogeneous gold, palladium and copper based catalysts for liquid phase oxidation of methane

Mohd Hasbi Ab. Rahim

ProQuest LLC
789 East Eisenhower Parkway
P.O. Box 1346
Ann Arbor, MI 48106-1346

Acknowledgements

First and foremost, I would like to express my praise and gratitude to God Almighty for giving me the chance to successfully completing this piece of research work. Surely this knowledge that I have is only a tiny piece of His many other undiscovered knowledge.

I wish to thank Prof. Graham Hutchings for giving me the possibility to involve in this research project in Cardiff Catalysis Institute and for the chance to explore field of chemistry during my time spent working on this PhD study.

Moreover, I would like to thank Dr. Nikolaos Dimitratos for his assistance in supervising and to have patiently contributed to the corrections of this thesis as well as Dr. Jose-Antonio Lopez Sanchez, Dr. Stuart Taylor, Dr. David Willock, Dr. Albert Carley and Dr. Rob Jenkins for parallel supervision.

My PhD study also would not have been possible without the help of other people. Therefore, I would like to thank all the members of GJH group especially DOW Methane Challenge Team; Izham, Mike, Ceri, Lokesh and Rob. It was a pleasure to work with them.

In addition, having carried out this research in a chemistry department, the role of all department staff has been important especially I like to mention: Mal, Alun, Steve, Richard, Gary, Robin and Jamie for their support.

I also would like to thank Malaysian Government for the financial support.

Finally, I express my deep thanks to my wife, Farhana Yunus and my little princess, Aimy Akma for being here with me during my study period, I do not think I could have made it without both of you.

Abstract

The oxidation of lower alkanes especially methane to methanol under mild reaction conditions is one of the most challenging task for industry and academia. At present, indirect utilisation via synthesis gas is the only commercially viable process for methanol production. Therefore, this study intends to investigate the direct oxidation of methane to methanol using a novel low temperature approach. Recently, gold based supported catalysts have been found to be highly effective oxidation catalysts where a number of important discoveries have been made such as in hydrogen peroxide synthesis and selective oxidation of alcohols to aldehydes. Due to these recent advances, further work into the oxidation of carbon-hydrogen bonds especially methane by gold and gold-palladium alloyed nanoparticles was the central topic of this study.

As a proof of concept for the following studies, oxidation of primary C-H bonds in toluene and toluene derivatives were carried out in a high pressure stirred autoclave with molecular oxygen as oxidant. It was evident that Au-Pd supported catalyst is capable in oxidising primary C-H bonds on toluene and toluene derivatives at lower temperature with high catalytic activity based on turnover number (TON) compared to available heterogeneous catalysts reported in literature. However, these catalysts are ineffective in the oxidation of methane with oxygen under mild conditions with water as solvent and temperature below 90 ^{o}C. In view of this, hydrogen peroxide has been used as oxidant and it was shown that Au-Pd supported nanoparticles are active for the oxidation of methane giving high selectivity to methanol especially in the reactions carried out with hydrogen peroxide generated using an *in-situ* approach. Methane oxidation reactions were carried out in aqueous medium. The main products were methanol, methyl hydroperoxide and only carbon dioxide as overoxidation product.

Investigations of reaction conditions such as concentration of oxidant, reaction time, reaction temperature and pressure of methane were investigated. It was found that the activity and selectivity of the catalyst was highly dependant on these variables. Oxygenate productivity was found to increase by increasing the H_2O_2 or H_2/O_2 concentration and methane pressure. Longer reaction times were detrimental to the methanol selectivity where overoxidation reaction occurred. Interestingly, the Au-Pd catalytic system was able to oxidise methane to methanol at temperatures as low as 2 ^{o}C. The applicability of the developed catalytic system was tested on ethane oxidation reaction and it successfully

produced ethanol as the major product. The oxygenate productivity was higher as compared to methane due to the solubility factor and the difference in the strength of carbon-hydrogen bonds.

The catalyst preparation method and pretreatment were shown to be very important in the formation of active catalysts. The Au-Pd alloy having Au core-palladium shell structure with PdO dominance on the surface and bigger particle size was preferred than analogue catalyst consists of Au and Pd in metallic state with smaller particle size. In addition to that, the choice of support is crucial and this study discovered TiO_2 as a preferred support where it could assist in stabilising the active hydroperoxy species. The Au:Pd ratio was also found to be an important variable, and equal weight ratio between Au and Pd was shown to be the optimised ratio for methane oxidation either using addition of H_2O_2 or *in-situ* H_2O_2 approach. The synergistic effect of Au and Pd was confirmed by superior catalytic activity compared to monometallic catalysts. Reaction mechanism was proposed and it was based on catalytic evaluation data, stability of the products and oxidation with radical scavengers. The proposed mechanism was in line with the theoretical modelling studies on similar catalytic systems.

Optimisation of Au based supported catalyst with copper as co-metal supported on TiO_2 was shown to improve the oxygenate productivity and methanol selectivity as well as enhanced the H_2O_2 utilisation. In particular, trimetallic 5wt%AuPd1.0wt%Cu/TiO_2 synthesised via impregnation method and calcined in static air gave more than double turn over frequency (TOF = 1.404) with methanol selectivity around 83% as compared to bimetallic 5wt%Au-Pd/TiO_2 catalyst (TOF = 0.692, methanol selectivity = 49%). It was suggested in this study that copper is responsible in enhancing the formation of intermediate methyl hydroperoxide species and in some extent to block the non-selective sites for hydrogen peroxide decomposition and hydrogenation by disrupting the surface structure of Au-Pd alloy whilst at the same time maintaining the active sites (Au-Pd alloy) responsible for selective formation of methanol. The oxidation state of copper was shown to be the main factor in controlling the catalytic activity and selectivity. Copper in a combination of multiple oxidation states was preferred than single oxidation state. A redox reaction mechanism was proposed to occur throughout the reaction.

In conclusion, a combination of catalyst evaluation and characterisation data gives structure activity relationships for the series of catalysts tested especially on methane oxidation reactions.

Table of contents

Pages

CHAPTER 1

Introduction and Literature Review

1.1. Importance and concept of catalysis

Catalysis research is central to the science of modern chemical processing, fuel technologies and environmental control. It controls more than 90% of the world's chemical manufacturing processes and is one of the most technologies in national economies.[1-3] Catalysis is a multidisciplinary science and it is a combination of fundamental and applied science as well as contributions from field of engineering. Catalytic processes may involve different stages such as catalyst synthesis, activation, operation micro/nanostructure and compositional data, structure-property correlation, deactivation, regeneration. The ultimate goal is the successful transfer to commercialisation stage of the catalytic process.

The word catalyst comes from the combination of two Greek words. The prefix *cata-* means down and the verb *–lysein* means to split or break. Berzelius firstly introduced it in 1836. It was not until 1895 that William Ostwald has written down a definition of catalyst. He defined a catalyst as "*a substance that increases the rate at which a chemical system approaches equilibrium, without being consumed in the process*".[4-6] Generally, a catalyst is a substance that enter into the process of a reaction and it might change during the reaction, but it normally restored to its original structure after completing the catalytic cycle.

The presence of catalyst in the reaction is crucial and it choice typically dependant on the catalytic performance especially the ability to select one particular route to the exclusion of the others. It might through intermediate species that are formed on it surfaces and/or directly to the target product. Interestingly, the course of the reaction of the same molecules or substrate could be fine-tuning by changing or tuning the catalyst. For instance, ethanol could be dehydrogenated to ethanal or to ethene by dehydration process.[6]

Catalyst surface acts by preparing the reactants for reaction, by converting them into forms that will react with minimum energy input, that is with lower activation energy than would otherwise needed.[6] As illustrated in figure 1.1, typically a catalytic process involves three main stages proceeding by physical adsorption which eliminates the potential energy

barrier by allowing close approach of the substrate molecule to the surface of catalyst. At later stage the chemical bond within substrate molecule breakdown to create the new bond with the catalyst surface. This path is possible if the reactant has a capability to chemisorb onto surface of catalyst. On the other hand, if the catalyst itself is the same phase as reactant, the coordination of the reactants to the active centre will replace the chemisorption process. Then, the active site of the catalyst plays a role in accelerating and tuning the reaction pathways followed by separation of the product. In ideal system, it should be a close catalytic cycle.

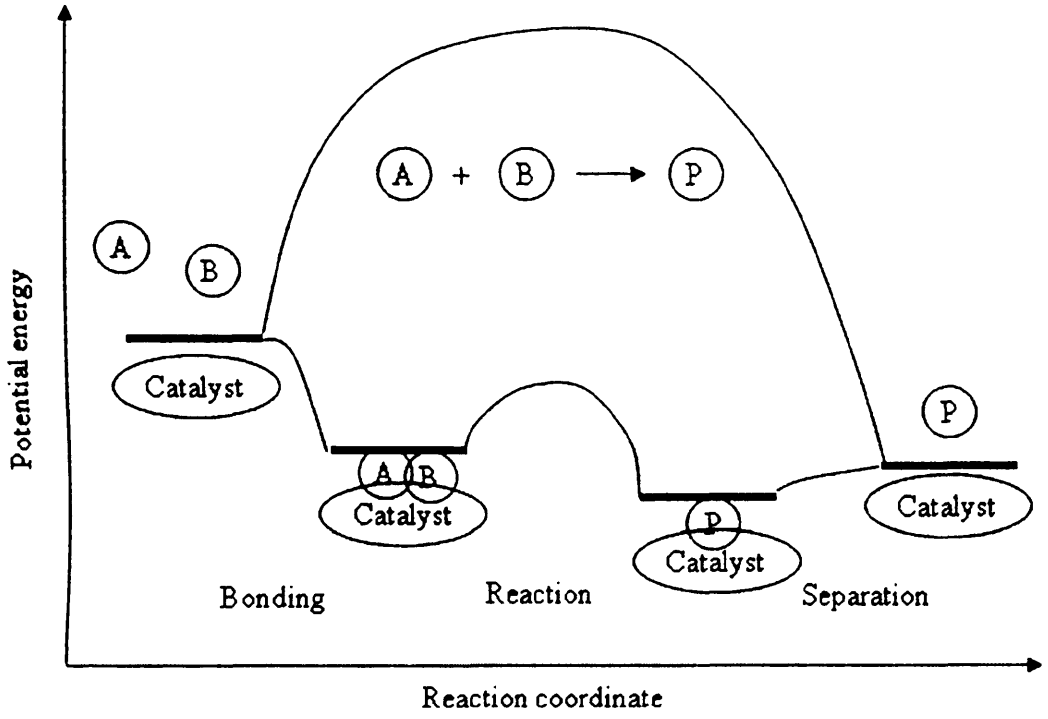

Figure 1.1 Catalytic reaction based on potential energy and reaction coordinate

1.2. Heterogeneous Catalysis

Heterogeneous catalysts have been used in different reactions such as in oil industry, production of commodity chemicals and fine chemicals also to neutralize the hazardous gases. Heterogeneous catalysts are in a different phase as compared to the reactants.[1,5] Hence, there is a phase boundary separates the catalyst from the reactant thus makes it easier for separation of catalysts from reactant and products. However, there are several

requirements need to be fulfilled by the heterogeneous system in order to obtain successful reaction. For instance, in the reaction involving solid metal catalysts in liquid solvent or reactant together with the presence of oxidant, the robustness of the catalysts are important where it should resistant to the possible metal leaches out into solution subsequently affect the catalytic activity as well as the recyclability of the catalyst.

Since the reactant and catalyst are in different phases, mass transfer limitations could exist, with later affects the overall performance. Mass transport limitations occur when diffusion of both reactants and products are slower than chemical reaction. Due to that, screenings of reaction conditions need to be carried out before proceed to the optimisation stage. In ideal heterogeneous catalytic system, the overall reaction must be in kinetic control which is based on chemical reaction on the solid catalyst. The ability of catalyst to work in kinetic control regime is important since it will provide information parameters such as activation energy, heat of adsorption and rate of chemical transformation which later can be used to reasonably compare the activities between catalysts. Given that the reaction is generally carried out with different parameters such as different mass of catalyst and volume the reactant or even with different amounts of involved product, it is important to correlate the catalytic activity based on number and nature of the active sites. However, this only can be carried out if the active site has been established, or if not on that cases, the productivity is compared based on mass of catalyst used for specific reaction time *i.e.* mol of product per kg catalyst per hour reaction time.

The advantages and some difficulties involving catalytic reaction through heterogeneous system are discussed in thought-out of the thesis.

1.3. Catalytic reactions of gold based catalysts

Gold based nanoparticles dispersed across the surfaces of certain supports have been shown to be active and selective as catalysts for a variety of important reactions. Gold as metal catalyst was emerged to be an important catalyst since two key papers published in 1980's by Hutchings and Haruta, respectively.[7,8] Hutchings made the breakthrough that gold is the preferred catalyst for acetylene hydrochlorination while Haruta discovered outstanding catalytic activity of gold at low temperature of carbon monoxide oxidation. In the following section, a brief discussion -on the importance of gold based catalysts in catalytic reactions of various substrates is described.

1.3.1. Carbon monoxide oxidation

As mentioned earlier, Haruta and co-workers was the first to discover that small Au nanoparticles supported on suitable oxide catalysts are active for carbon monoxide (CO) oxidation at low temperature.[8] Since that report, CO oxidation is one of the most studied test substrates when using gold as a catalyst. Moreover, selective oxidation of CO to CO_2 is an important reaction in industrial application such as in automotive emission control and fuel cells applications with both contributed to greener and reduced costs technology.[9] In order to find out the reason behind excellent activity of Au toward oxidation reaction of CO to CO_2, several mechanisms have been proposed mainly dependant on the catalyst itself or reaction conditions such as temperature.[10,11] None of these mechanisms alone are able to explain the origin of activity, but each of them can explain some experimental evidence. The proper choice of support and catalyst preparation as well as pre-treatment method are crucial in order to obtain the active catalyst, generally a small Au (< 5 nm) nanoparticles is required and this was proven by lower activity towards CO_2 formation obtained with larger Au catalyst prepared using an impregnation technique.[12] It was discovered that smaller Au particle alone is not capable to convert CO with high conversion, this statement based on the fact that Au supported on TiO_2 prepared through photodeposition technique which smaller particle size giving lower catalytic activity comparable to analogue impregnation catalyst.[12] Therefore, it was suggested that maximum metal-support interface is required. This can be seen from the same Au/TiO_2 catalyst prepared using impregnation and deposition-precipitation respectively, where the former shows spherical rather than hemispherical observed with latter technique.[13] In term of Au oxidation state, the main active species is believed to be Au^0, either alone or with presence some of cationic Au. A study by Zanella and Louis that Au on TiO_2 prepared in the dark followed by vacuum-dried which later produced cationic gold is inactive for CO oxidation.[14] Even though no detail discussion on CO oxidation mentions in this section, it is clear that Au as metal catalyst plays a crucial role in activating CO to CO_2 and it activity depends on a variety of parameters, such as particle size of gold, oxidation state and support which need to be carefully handled and monitored.

1.3.2. Reaction of OH containing group

The oxidation of alcohols and polyols to fine chemicals is one of the most important processes since important intermediates can be formed for industrial applications. For instance, the oxidation of diols compound such as ethylene glycol and propane-1,2-diol to corresponding glycolic acid and lactic acid respectively have great interest in industrial stage. Conventional method for the production of both acid products are not environmental friendly and expensive in economic point of view since it employed a toxic or corrosive reagents.[15,16] Currently, industrial productions of glycolic acid by DuPont involve chloroacetic acid, formaldehyde and carbon monoxide.[15] Lactic acid production involved the reaction of acetaldehyde with hydrogen cyanide followed by hydrolysis with sulphuric acid whereas the alternative biochemical process using fermentation suffered from purifications problem as well as low productivity.[16] Therefore, many catalytic systems have tried to counter the setback. Rossi and co-workers found that gold catalysts could oxidise ethylene glycol and propane-1,2-diol to corresponding glycolic acid and lactic acid respectively with high selectivity level.[17-20] A successful oxidations of both vicinal diols using gold catalysts is not surprising since supported gold catalysts have shown in earlier studies to catalysed OH containing compounds. Back to 1985, Nyarady and Sievers have utilised gold as metal catalyst for selective oxidation of alcohol using N_2O as oxidant in gas phase system. At temperature range from ambient up to 400 ^{o}C, aldehyde was detected as main product.[21] Gas-phase oxidation of alcohols at lower temperature was successfully carried out using Au/SiO_2 where it selectively activated primary and secondary aliphatic alcohols by air to the corresponding carbonyl derivatives.[22] In liquid phase system, Rossi and co-workers were the first to demonstrate that OH containing group substrate, in particular diols and sugars, can be oxidised selectively to various monoacids using molecular oxygen as oxidant, although the system still required a basic environment.[19,17,23] Further work by Carretin and co-workers have shown that Au supported catalyst gave outstanding catalytic properties on oxidation of glycerol to glycerate with 100% selectivity. Molecular oxygen was used as oxidant and the reaction was performed in relatively mild conditions.[24-26] Moreover, Au catalysts were more stable and could be reused compared to other supported nanometals such as platinum and palladium. Extended studies were carried out by Dimitratos *et al.* which used sol immobilisation and impregnation methods for the preparation of Au, Pd and bimetallic Au-Pd supported metal catalysts onto TiO_2 and carbon, respectively.[27] Strong synergistic effects was observed on Au-Pd bimetallic

supported catalysts especially with TiO_2 as support prepared via impregnation method which believed due to formation of core shell structure compared to homogeneous alloy on carbon. The smaller and narrower particle size distribution on analogue sol-immobilised catalyst produced better activity than the impregnated catalyst counterpart. The data showed that the choice of supports and the surface composition of Au nanoparticles in obtaining high activity and selectivity of glycerol oxidation are crucial. Recently, Au supported on magnesium oxide synthesised via simple impregnation method gave higher glycerol conversion with high selectivity to glycerol carbonate. Interestingly, the catalyst was stable up to 10 catalytic cycles even in the presence of urea and temperature at 150 °C. The presence of Au is crucial especially in controlling the glycerol carbonate selectivity which believed to involve in second part of the reaction involving transformation of glycerol urethane. This is the first demonstration of using Au metal catalyst on this type of reaction.[28]

In case of oxidation of compound containing monofunctional OH group, benzyl alcohol is one of the most studies substrates involving Au based catalysts. One of the significant studies on oxidation of alcohols in solvent-less system and molecular oxygen as oxidant have been carried out by Corma and co-workers. In their studies, Au supported on CeO_2 catalysts was showed to oxidise alcohols to aldehydes and ketones. This catalyst is active at relatively mild condition without the requirement of the addition of NaOH to achieve high activity.[29] Besides, the results were shown to be comparable with similar TOFs values to those obtained by Kaneda *et al.* using supported palladium catalysts.[30] The catalytic activity of monometallic Au/CeO_2 was claimed to the ability of catalyst to stabilise a reactive peroxy intermediate from molecular oxygen. An alloying of Pd with Au on TiO_2 by impregnation method was demonstrated to significantly enhance the catalytic activity of benzyl alcohol oxidation.[31] Further study on bimetallic Au-Pd supported nanoparticles catalysts on similar substrate were carried by Dimitratos and co-workers.[32,33] In this case, the Au-Pd catalyst either supported on TiO_2 or carbon were synthesised via sol-immobilisation method and the results clearly displayed higher activity when compared with analogue catalysts synthesised via impregnated method. The better catalytic activities of sol-immobilised sampled were due to the similar reasons discussed above for glycerol oxidation reactions.

In fact, there were numerous studies reported on the oxidation of OH containing compound using Au based catalysts owing to their unique catalytic properties as briefly mentioned above.

1.3.3. Hydrogen peroxide synthesis

Hydrogen peroxide is widely used as environmental friendly oxidant in various processes such as bleaching agent or as disinfectant. At present, hydrogen peroxide is commercially produced in large scale through sequential hydrogenation and oxidation of an alkyl hydroquinone.[34] Large scale productions of concentrated hydrogen peroxide create a problem due the transportation and storage given that relatively small quantities required for fine chemical industry. Moreover, hydrogen peroxide synthesis through antraquinone route involves expensive solvent system and it requires a periodic replacement of the antraquinone due to hydrogenation. Moreover, it needs a waste treatment which contributes to high capital cost.

Therefore, an alternative direct process with highly efficiency in producing dilute hydrogen peroxide has been developed. Initially, most of the catalytic system focused on Pd based catalysts.[35-39] Further works by Solsona and co-workers shown that by alloying Pd with Au metal led to an increase in rate of H_2O_2 formation with higher H_2 selectivity.[40] Similar synergistic effect of Au-Pd was reported by Ishihara *et al.* which has shown increase of the rate of hydrogen peroxide production and selectivity up to 30%, but strongly dependable on the choice of supports.[41] Earlier report from London and co-workers were the first to show that gold containing catalysts were active for hydrogen peroxide synthesis via direct route using alumina oxide as support.[42] A separate study by Haruta and co-workers showed that SiO_2 was affective as a support for Au metal catalyst at 10 °C reaction temperature and they concluded that the activity of the catalyst strongly related to the metal particle size.[43] Edwards *et al.* have reported that large Au nano-crystals on TiO_2 synthesised via an impregnation method showed higher H_2O_2 productivity (in mol/kg/hr) than smaller particle size obtained from analogue catalyst synthesised via deposition-precipitation method. The variation of overall catalytic performance dependant on particle size effect might unique on certain support and/or another factor such as presence of second metal. This was proven by catalytic data obtained from bimetallic Au-Pd supported on carbon (G-60) synthesized via sol-immobilisation technique which gave 25% higher H_2O_2 productivity compared to larger Au-Pd catalysts prepared using impregnation method. In addition to that, sol-immobilised samples used 80% less metal loading which clearly contributed to higher intrinsic activity.[44] Palladium to gold surface composition with narrow particle sizes play an important role in synthesis of hydrogen peroxide, but it still suffers from selectivity problem due to the (i) decomposition to

oxygen and water, (ii) hydrogenation to water and (iii) the direct non-selective formation of water. The mentioned pathways is summarised in figure 1.2.

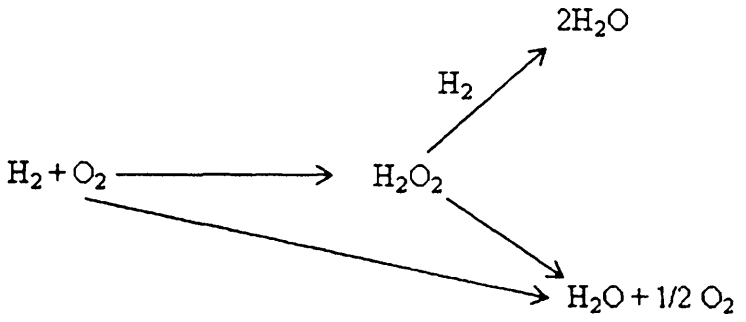

Figure 1.2: Hydrogen peroxide synthesis and its decomposition/hydrogenation pathways[45]

Therefore, various parameters have been considered and tested in order to improve the catalytic performance either by tuning the catalyst itself as mentioned before or by changing the reaction parameters such temperature, H_2 to O_2 ratio and solvent system. Clearly, the total reaction pressure has a major effect as does the composition of the solvent mixture as both these parameters affect the amount of H_2 available for reaction in solution. Additionally, the reaction temperature, the H_2/O_2 molar ratio and the solvent composition also have significant effects.[46] In order to verify the factor affected the subsequent hydrogenation step, works have been carried out by Edwin and co-workers demonstrated that carbon-based catalysts showed the lowest H_2O_2 hydrogenation and decomposition activity, indicating that carbon can be the ideal support for Pd-only and Au–Pd-supported catalysts for H_2O_2 synthesis.[47] The major parameter is the isoelectric point of the support, and supports with low isoelectronic points (*e.g.* carbon and silica) give catalysts with the highest rates for the synthesis of hydrogen peroxide. Recently, by using Au-Pd supported on acid-treat carbon, high yields of hydrogen peroxide with hydrogen selectivity greater than 95% was successfully demonstrated by Edward *et al.*[48] In this system, it is crucial to pre-treat the support prior to metal impregnation other than with catalyst itself and the increase of activity is not affected by the concentration of used acid. Higher catalytic performance on acid-pretreated catalysts due to their ability to increase the stability of generated H_2O_2 also to decrease in Au-Pd particle distribution and higher Au metal dispersion.

Interestingly, current catalytic system managed to have higher H_2O_2 productivity even using water as solvent and without presence any additive such as halide group. This discovery is vital since it will produce very clean hydrogen peroxide which suitable for medical application and it also opens the possible use as very clean oxidant in fine chemical production.

1.3.4. Activation of hydrocarbons

C-H bond activation of alkane groups emerge as interesting area given that it will open up a route to activate an abundant feedstock such natural gas. Since Au based catalysts have successfully used in couple of reaction as discussed in previous sub-section, C-H activations studies have been done mainly on cyclohexane as trial substrate. Oxidation of cyclohexane to the corresponding alcohol and ketone given an important intermediate for manufacturing of adipic acid and eta-caprolactam which further process to produce Nylon-6 and Nylon-6,6. The present commercial process for cyclohexane oxidation using molecular oxygen or air is carried out at 150–160 °C and 1–2 MPa, affording 4% conversion and 70–85% selectivity to cyclohexanone and cyclohexanol.[49] Several systems have been tried such as μ3-oxo-bridged Co/Mn cluster complex,[50] cobalt complexes[51] and metal substituted aluminophosphate[52] in order to improve the catalytic activity at mild conditions. However, some of them like cobalt complexes grafted on mesoporous silica suffered from loss of activity caused by leaching problem. Since the reaction typically involves Co, Mn and Fe as a metal, some researchers have taken a step to test the cyclohexane oxidation with the presence of Au based catalytic system. Initially, by using Au/ZSM-5 catalyst with oxygen as oxidant, Zhao *et al.* has successfully oxidised cyclohexane with 16% conversion at 92% selectivity in a solvent free system, and the catalyst can be recycled twice without any obviously loss of activity.[53] The same group also reported that Au supported MCM-41 catalyst gave comparable activity toward cyclohexane and by using mesoporous supports, easier product diffusion from active sites make it feasible for large–scale processes.[54]

Both systems mentioned above operated at temperature higher than 100 °C. Xu and co-workers have developed a system which effectively activated cyclohexane at 70 °C with high selectivity to cyclohexanol and cyclohexanone. By using graphite as a support, comparable catalytic performances were obtained with Au metal compared to Pt and Pd

metal counterpart, respectively.[55] An oxide was also tried as a support for Au metal, Xu *et al.* demonstrated that Au/Al_2O_3 with O_2 as oxidant in solvent-free system could activate cyclohexane up to 12% with high selectivity including cyclohexyl hydroperoxide which act as intermediate product.[56] The same group also used SiO_2 and SiO_2/TiO_2 as a support but both systems operated at higher temperature (> 100 °C).[57] Recently, Au supported on SiO_2 catalysts prepared by self-assembly technique were found to be very efficient catalysts for the selective oxidation of cyclohexane with air instead of molecular oxygen in the absence of any solvent or promoter where under suitable reaction conditions, 10% conversion of cyclohexane and 92% selectivity of cyclohexanone and cyclohexanol could be obtained.[58]

Other than cyclohexane as a test substrate for C-H bond activation using Au based catalysts, the catalysts were tested on the activation of lower alkanes mostly in gas phase reactions. Back to 1998, Blick and co-workers reported the methane coupling using Au/MgO catalyst.[59] In fact, the presence of gold specifically at higher loading suppressed the activity of magnesium oxide. Although, they found that as proportion of Au present as discrete particles increased, it activated methane oxidation to form carbon oxide products. Therefore, further work on Au support catalyst has been carried out on methane total oxidation to CO_2 and H_2O. Total oxidation is an important element in the worldwide fight against air pollution. Applications include the use of catalytic units for natural gas combustion (catalytic combustion). This type of oxidation also suitable for the elimination of low concentrations of volatile organic compounds (VOCs) in process outlet streams, from indoor air in the work place and in the home. One of the principles features of catalytic combustion is its capability to oxidise very low concentrations of combustibles in air at a concentration below the minimum requirement to sustain thermal combustion. By using Au supported on cobalt oxide, 99% conversion could be obtained at 350 °C.[60] Incorporating Pd or Pt on Au increases the conversion to 100%. Others support such as TiO_2, FeO_x, Al_2O_3, MnO_x have been tried at similar reaction conditions or slightly higher temperature, but with inferior activity.[60,61]

In another study, researchers have tried to selectively oxidise methane, ethane and propane to respective oxygenates products at lower temperature *i.e.* 150 to 300 °C. Au catalysts were prepared using co-precipitation and deposition-precipitation method supported on ZnO and Fe_2O_3 respectively. The conversion obtained followed the expected trend with the most active substrate to be propane followed by ethane and methane. The conversion trends were explained by the reactivity of carbon-hydrogen bond for respective alkanes

where C-H bond activation energies for propane was lower (397 kJ/mol) compared to ethane (410 kJ/mol) and methane (431 kJ/mol).[62] However, poor selectivity was obtained in methane oxidation with only 5% methanol selectivity obtained using Au/Fe_2O_3 synthesised at pH equal to 6.[63] Similar catalytic pattern also was observed in separate studies using Au/TiO_2, Au/FeO_3 and Au/CeO_2 catalysts on propane oxidation.[64]

Since most of the methane oxidation mentioned above is only in gas phase system, additional literature available involving Au catalyst in liquid phase will be discussed in another section of this chapter (see section 1.5.3).

1.4. Oxidation of toluene and derivatives of toluene

In the modern chemical industry, the liquid-phase oxidation of aromatic and derivatives aromatic hydrocarbons by molecular oxygen is a highly attractive process from an economic and environmental point of view. A range of valuable oxygenate compounds can be produced by this process. For example, benzyl alcohol, benzaldehyde, benzoic acid and benzyl benzoate could be produced from toluene oxidation[65,66] and having a commercial values for various industrial applications. For instance, benzaldehyde, C_6H_5CHO, is one of the most industrially useful members of the family of aromatic aldehyde, where it was acted as the raw material in dyestuff and pharmaceutical industries. In the latter industry, it was used for the manufacture of intermediates for chloramphenicol, analgin, ephedrin, and ampicillin[67] whereas benzyl benzoate can be used as a solvent for various chemical reactions, as food additive, antiparasite or as a raw material to synthesise benzyl alcohol and benzoic acid through hydrolysis process.

Two industrially important processes for the synthesis of benzaldehyde involve the hydrolysis of benzal chloride and the air-oxidation of toluene.[67] Other processes, such as the oxidation of benzyl alcohol, the reduction of benzyl chloride, and the reaction of carbon monoxide and benzene, have been utilised in the past, but are no longer industrially useful. Today, the air-oxidation of toluene, both in the vapour and liquid phases, is the source of most of world's synthetic benzaldehyde. The processes, however, requires rather high temperatures and pressures and give low yields.[68] Alternative processes that can overcome these disadvantages would be attractive, especially in design catalysts which are active at low-temperature of oxidation.

The liquid phase oxidation of toluene with heterogeneous catalysts is one of the promising ways to overcome the problem relating to environmental concern and separation process which later could reduce the overall production cost of benzaldehyde. Wang and co-workers have reported that 31% toluene conversion with 18.7% benzaldehyde selectivity can be achieved by using copper-based heterogeneous catalysts in molecular oxygen and *N*-Bromosuccinimide (NBS) as additive.[69] The higher benzaldehyde selectivity (86%) was obtained via pyridine as additive, however the conversion was low, *cal.* 7%.

Many reports have been published on using initiators and co-oxidant to enhance the catalytic performance of toluene and its substituted oxidation. An oxidant such as H_2O_2[70-72] and TBHP[73] emerged as a common and superior preferences. Solvent also plays an important role in this reaction, several solvents such as CH_3CN, CH_3OH, CH_2Cl_2,[70] Dichlorobenzene,[74] Benzene,[75] Dimethylformamide (DMF)[76] and water-dioxane medium[77] have been used for oxidation of toluene. Solvent-free systems gave interesting results on oxidation reaction of toluene and substituted toluene to produce benzaldehyde, benzoic acid.[75,78] High conversion with high yield (85%) of benzoic acid was obtained by Bastock and co-workers at 22 hours reaction time.[75]

Even though many studies have been reported for toluene oxidation, obviously there are still lacking of attractive systems with a capability to oxidise toluene and derivative of toluene with high activity and selectivity especially at relatively mild reaction conditions without using initiators and/or co-catalysts.

1.5. Oxidation of methane

1.5.1. Introduction

Large portions of the world's reserves of natural gas remain virtually untouched, therefore need to be effectively utilised since there is a world-wide interest in the conversion into value-added products of methane, as the main constituent of natural gas.[79] Methane is also contained in coal-bed gas, landfill gas and methane hydrate resources. Moreover, the growth for synthetic fuels and valuable chemicals annually increases, as the recovery of petroleum becomes more difficult and expensive.[79-81] Consequently, natural gas represents one promising alternative energy source to fully replace petroleum-based products in the

future. These phenomena stimulated a wide range of research activities aimed both at fundamental and applied aspects of methane chemistry.

In 2006, proven gas reserves were estimated to be at 180 trillion cubic meters.[82] At an annual production of about 3 trillion cubic meters, the current reserves will last more than 60 years. The abundance of such gas reserves continues to draw the attention and interest of the international community in how best to use them. Generally, natural gas conversion technologies can be divided into two sections *i.e.* indirect and direct process. Direct conversion normally involves oxidative coupling, oxyhalogenation, aromatization and selective oxidation whereas indirect process involves a conversion of methane via synthesis gas. Conversion of methane into useful chemicals remains as a big challenge in catalysis in the 21st century. There are large numbers of studies demonstrated the conversion of methane via selective oxidation process to produce oxygenates (methanol; CH_3OH, formaldehyde; HCHO).[83-85,66,86] Methanol is used to produce formaldehyde, methyl t-butyl ether (MTBE), acetic acid, solvents, chloromethanes, methyl methacrylate, methylamines, glycol methyl ethers, dimethyl terephthalate, antifreeze, and fuels. For the five-year period beginning from 2008, nearly 26 million tons of new capacity of methanol has been announced in industry with an average demand of about 47 million tons per year across the same timeline.[87] However, there is still no direct processes with commercial viability at this moment. Currently, the technology for chemical utilisation of methane is indirect, involving steam reforming of methane to synthesis gas (H_2 + CO) and the subsequent transformation of synthesis gas to methanol via methanol synthesis or Fischer-Tropsch synthesis (scheme 1.1).[88]

$$CH_4(g) + H_2O(g) \xrightarrow{\text{Catalyst}} CO(g) + 3H_2(g)$$

$$CO(g) + 2H_2(g) \xrightarrow{\text{Catalyst}} CH_3OH(g)$$

(Scheme 1.1)

However, the steam reforming of methane is not only an energy-intensive but also a high-cost process. Most (65–75%) of the capital cost of the indirect approach is associated with the methane reforming process.[89]

Example of steam reforming process is shown in figure 1.3 below:

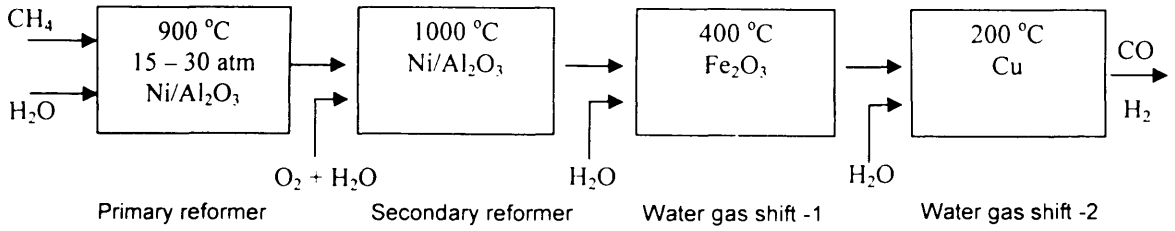

Figure 1.3: Block diagram for conventional steam reforming: CH_4 and excess H_2O are reacted in a primary reformer and the unconverted CH_4 is reacted with O_2 and more H_2O in a secondary reformer to give equilibrium CO and H_2.[89]

From the point of view of methane chemistry, it is not at all hard to see why it has proven so difficult to develop practical methods for direct conversion of methane to more valuable products. The difficulties arise from both kinetics and thermodynamics. Methane is quite inert, so that traditional approaches to activate methane require high temperatures, where the chemistry is dominated by radical pathways. Under such conditions, reactivity is primarily determined by C-H bond strength. For methane, bond dissociation energy value is higher than for most of the common organic products. Hence the organic oxygenates products such as methanol, formaldehyde and formic acid will generally be significantly more reactive than methane. It was concluded that the ratio of reactivity of CH_4:CH_3OH was about 1:6.[90] The desire products are relatively unstable intermediates compared to substrate (*i.e.* methane), which in the presence of oxygen suffer fast consecutive reactions to carbon oxides.[91] There is a consequent strict limitation on achievable yield.

All approaches to circumvent this limitation can be basically divided into two types: engineering and chemistry. The first approach uses novel reactor and process designs to optimise performance in spite of the mechanistic disadvantage. These might include separations technology, low conversion with recycle process. The second approach seeks to improve the intrinsic selectivity of the transformation, either by controlling access to the reaction site to favour conversion of methane and disfavour that of products or by finding a different mechanism whereby products are protected from undergo undesired reactions. The second approach intuitively appears more likely to succeed with low-temperature, homogeneous systems than for high-temperature heterogeneous catalysts. In general, it appears that the low temperature activation proceeds by non-radical mechanisms, and that

here the goal of oxidising methane at mild conditions can be realised. The higher temperature reaction is more likely to be radical in nature. Even though non-radical methane activation can be achieved, often under mild conditions, there are still major challenges. Most non-oxidative transformations of methane to more elaborate compounds are thermodynamically uphill at low temperatures. It is difficult to design an overall reaction system that is thermodynamically allowed, without economically excessive requirements for energy input. Oxidative routes do not have any problem with thermodynamics, but another difficulty arises, most of the metal-centre based systems that activate methane are unstable and rapidly destroyed by oxidising conditions. In addition to these issues, homogeneous approaches to methane conversion are complicated by many considerations that tend to affect such processes such as difficult in separations, inefficient energy integration.[92]

Therefore, it is necessary to perform the oxidation at mild conditions and one such route to achieve this is by activation of methane in liquid phase at lower reaction temperature using heterogeneous catalysts. Perhaps it will open opportunity for industrial practice.

1.5.2. Gas phase direct oxidation of methane

Oxidation of lower alkanes has been studied extensively in the field of catalysis and some of them were successfully transformed and utilised at industrial stage. One of the examples is the oxidation of *n*-butane to maleic anhydride using vanadium phosphate catalyst. The oxidation of other lower alkanes in gas phase is reported in many reports and it is still one of the most interesting areas to explore. In case of methane oxidation, several groups have reported good catalytic activity to oxygenate products.[92,93,84,94] Typically, the reactions were carried out at higher temperature with the presence of gases oxidant such air, molecular oxygen and nitrous oxide. The used of solid catalyst in this system produced high activity, although since it normally involved radical chemistry, the selectivity to target products was relatively low.[95-97]

By varying reaction parameters and reactor design, moderate selectivity (to methanol) could be obtained and could reach 30–40% with conversion around 5-10% under optimum conditions at higher temperatures (450–500 ^{o}C) and pressures (30–60 bar).[98,84,99] In addition, the preferred oxygenates product produced in gas phase is formaldehyde rather than methanol due to the some limitation mainly due to the mechanistic pathways. In the

presence of O_2 as oxidant, the intermediate methoxy ($CH_3O\bullet$) species is quickly oxidized which later suppressed the possibility of protonation step responsible on generating methanol. Over oxidation of methanol also contributed to the lower selectivity.

In order to mimic the methane monooxygenase system which is considered as prior-art in oxygenation of methane, researchers have tried to develop a heterogeneous catalyst mainly based on zeolite system for gas phase methane oxidation. Panov *et al.* showed that methane could be oxidised over Fe-ZSM5 to methanol using N_2O as oxidant. Decomposition of N_2O creates an anion-radical species called α-oxygen, which is responsible to selectively oxidise methane to methanol.[100-102] However, the system has negative side as it is not a continuous process, where it needs an additional step to extract the formed methanol from the solid catalyst with solvent. Sachtler *et al.* showed that activation of Fe-ZSM-5 with molecular oxygen followed by exposure to methane did only result in full combustion products.[103] Therefore, an attempt to activate methane using molecular oxygen was further studied by replacing iron metal with copper. Schoonheydt and co-workers showed that Cu-ZSM-5 materials could also selectively convert methane to methanol using O_2 (or air) as an oxidant at relatively low temperature (150 °C).[104,105] Literature involving oxidation of methane using Au related catalyst in gas phase has been discussed in section 1.3.4 of this chapter.

1.5.3. Liquid phase direct oxidation of methane

1.5.3.1. Introduction

A number of articles have been recently published on catalytic oxidation of methane in liquid phase.[106,107,84,108] Selectivity of oxygenated products (*i.e.* methanol, formic acid) is often higher than in the corresponding gas phase whereby the participation of radicals lead to the formation of deep oxidation products (e.g. CO, CO_2). In addition to that, reaction in liquid phase can be carried out at relatively mild conditions with lower pressure and temperature which can contribute to the lower capital plus higher energy efficiency in industrial stage.

The majority of liquid phase reactions have been carried out in protic media such as sulphuric acid (H_2SO_4) and oleum (H_2SO_4-SO_3). There are two reasons behind the reaction carried out in strong acids medium. First reason is based upon the nature of reaction

mechanism where it involved electrophilic carbon-hydrogen activation followed by oxidative functionalisation. The conjugate bases of strong acids are poorly co-ordinating, thereby enhancing the electrophilicity of the catalyst metal ion. The second reason seeks to chemically protect the methanol from further oxidation by forming methanol derivative through esterification process.[109,86] For instance, with the formation of methyl bisulfate instead of methanol, it was claimed that the rate constant of the oxidation step of CH_4 to methyl bisulfate was *cal.* 100 times larger than that of the further oxidation of methyl bisulfate.[84] Therefore could enhance the CH_4 conversion level. However, there are several setbacks were observed in the reaction with the presence of acid solution. Utilized a strong acid medium (H_2SO_4) in the system creating a large amount of waste which is toxic to the environment and also detrimental to the reactor system due to its corrosive behaviour. In addition to that, formation of methanol derivative as the main product requires another process to hydrolyse the ester product back to methanol.

So far, one particular high-yield system for the catalytic conversion of methane to methanol was published by Periana *et al.*[110] In this system, CH_4 could be converted to methyl bisulfate (CH_3OSO_3H) by Hg^{II} in concentrated sulphuric acid. The selectivity to CH_3OSO_3H reached 85% (methylbisulfate which further hydrolysed to methanol with 100% efficiency) at CH_4 conversion of 50% with a 0.1M solution of $Hg(OSO_3H)_2$ in concentrated sulphuric acid at 180 °C and CH_4 pressure of 34.5 bar. By replacing $HgSO_4$ to bi-pyrimidyl platinum complex, further increased CH_4 conversion up to 90% with comparable selectivity to methyl bisulphate.[106] As mentioned previously, by generating the product in the form of methanol derivative (methyl ester), over oxidation of oxygenates to combustion product can be avoided and consequently increase the selectivity toward target product *i.e.* methanol (as methanol derivative). Unfortunately, this catalyst was deactivated by the water and methanol that are produced *in-situ* during the reaction. The recovery and re-oxidation of the produced SO_2 must also be considered to complete the catalytic cycle. Even though Periana and co-workers successfully oxidised methane with high yield, it still less desirable compare to enzymatic methane monooxygenase (MMO) system. This biological system works by activates the dioxygen to a peroxy intermediate which later responsible to oxidise hydrocarbon including methane selectively to methanol at mild conditions (45 °C). However, the possible formation of combustible product *i.e.* carbon oxide did not report in the literature.[111] Despite the fact that higher methanol productivity (5 mole (CH_3OH) kg(catalyst)$^{-1}$ h^{-1})) obtained from MMO system,[111] it still required an expensive NADH as co-factor to activate the oxygen, while in the presence of H_2O_2

instead of NADH, productivity significantly decreased down to 0.076 mole (CH_3OH) h^{-1} kg(MMOH) $^{-1}$.[112] After all, it should be noted that MMO actually activates the oxidant and not methane when achieving selective primary C-H bond activation, besides that the activity does not increase with alkane chain length. Every system has advantages and disadvantages, similar to MMO even with some weakness; it still stands as a bench mark on lower alkane activation in relatively mild conditions.

Further discussions on liquid phase oxidation especially on methane are shown in the following section.

1.5.3.2. Oxidation with homogeneous catalytic system in different solvents and oxidants

In general, the main target and challenge to the researchers who are involved in catalytic oxidation of lower alkane is to operate at very mild conditions. This aim cannot be achieved if the reaction is carried out in gas phase system. Therefore, it is important to use a different approach as performing the reaction in liquid phase. The origins of transition-metal catalyzed CH_4 oxidation chemistry can be traced back to the early work of Snyder and Grosse.[113] Grosse oxidized methane with fuming sulphuric acid at 263 °C employing an $HgSO_4$ catalyst, and obtained oxygenated and sulfonated methane derivatives in a total yield of 44%. Back to 1987, Shilov and co-workers was successfully oxidised methane to methanol and methyl chloride using Pt^{II}/Pt^{IV} system at in chlorine containing aqueous solution at 120 °C.[114] At the same time, another approach to activate methane was carried out by Kao *et al.* using Pd^{II}. Instead of directly producing methanol as oxygenated products, the system works by protecting the oxygenates through formation of methyl trifluoroacetate which later could be hydrolyse to methanol.[115] The product-protected concept was later utilised in Periana's works[106,110] as detailed in section 1.5.3.1 and in addition was further studied by others groups. Catalyst were developed based on transition metal such as Pt and Pd in form of metal salt and metal complex [116-118] and/or non-metal system such as halogens.[119-121] Apart from Hg, Pd and Pt homogeneous systems, the cationic Au or gold complex also were used in methane oxidation in acidic media.[122-124] Jones and co-workers have shown that the combination of cationic gold and selenic acid (H_2SeO_4) as oxidant successfully produced 94% selectivity to CH_3OSO_3H with 28% methane conversion at relatively higher reaction temperature (180 °C).[124] It was proposed that Au cations followed similar mechanism as observed with Hg^{II} and Pt^{II} where it

involved electrophilic substitution step to form $Au^{\delta+}$-CH_3 ($Au^{\delta+}$: Au^{I}/Au^{III}) intermediate species. The intermediate species was later proceeded with oxidative functionalization reaction involving redox reactions of $Au^{\delta+}$-CH_3 to generate the oxidised product *i.e.* methanol. The ability of gold cations to activate methane via C-H electrophilic activation and oxidative functionalization mechanisms is not surprising since Au^{I} and Au^{III} have similar electronic configuration with as Hg^{II} and Pt^{II}, respectively. As previously mentioned, both Hg^{II} and Pt^{II} homogeneous catalytic system employed similar type of reaction mechanism. [110,106,66] However, difference to Hg^{II} and Pt^{II} catalytic system which used sulphuric acid (H_2SO_4), Au homogeneous catalyst required stronger acid (selenic acid) in order to keep the cationic oxidation state from being reduced to Au^0. In similar reaction condition, Au in metallic state was showed to be less active toward methane oxidation.[124]

It seems most of the initial studies on liquid phase oxidation of lower alkanes utilised strong acids as solvents. Some researchers had used other solvents such as acetonitrile as reaction medium.[125-127] However, Shulpin *et al.* reported that acetonitrile itself was oxidised at higher temperature and it may take part in the reaction. The reaction was performed at temperature range of 25 to 50 °C with pressure of up to 85 bar. The products obtained were methanol, formaldehyde, formic acid, carbon monoxide, and carbon dioxide.[125] Alternatively, it is important to use an environmental friendly solvent such as H_2O to perform the reaction and it was shown by several groups that it is possible to oxidise methane in aqueous medium.[125,128,129] It has been reported that a di-iron-substituted silicotungstate catalysed the oxidation of methane by H_2O_2 in water, and methyl formate and CO_2 were obtained as the main products.[129] At 80 °C, the turnover number (TON) for CH_4 conversion was 21.6 in 48 hours and the selectivity to methyl formate and CO_2 were respectively 54% and 44%, with a homogeneous γ-$SiW_{10}[Fe(OH_2)]_2O_{38}$ catalyst. Further studies on environmental benign solvent and oxidant using homogeneous catalyst was demonstrated by Yuan *et al.*[128] They explored the catalytic activities of a series of transition metal chlorides (Fe, Co, Ru, Rh, Cu, Au, Pt, Pd and Os chloride, respectively) for the oxidation of methane and ethane with H_2O_2 in a water medium at 90 °C. In methane and ethane, corresponding alcohol, aldehyde, acid and combustible products (CO_x) were obtained in all cases. Osmium chloride exhibited the highest activity among these transition metal chloride catalysts for selective oxidations of both methane and ethane where the selectivity to C_1 and C_2 oxygenates were respectively 61% and 85%. $HAuCl_4$ and $FeCl_3$ also showed satisfactory catalytic effects for the selective oxidations of methane and ethane with H_2O_2 in a water medium. $HAuCl_4$ provided a TOF of ~10 h^{-1} compared to

12 h^{-1} for $OsCl_3$ and a selectivity of 57% for the oxidation of methane to C_1 oxygenates at 90 °C. However, precipitation was observed after the reaction, possibly due to the formation of metallic gold, indicating that Au^{III} was unstable under the reaction conditions. At the same time, different oxidants such as $NaIO_4$, $NaClO_4$, NaClO and TBHP were tried in the presence of $OsCl_3$ catalyst, although only TBHP produced catalytic activity near to H_2O_2 as oxidant. Moreover, solubility of alkane in H_2O is known to be limiting and it will increase by increasing the pressure, consequently could enhance the catalytic activity.[128] Most of the homogeneous systems mentioned above targeted alcohol or it's substituted as a main product. On the other hand, there are several reports which tried to directly produced acetic acid from alkane oxidation in liquid phase. Nizova *et al.* for example reported the oxidation of CH_4 to CH_3OOH with O_2 in the presence of H_2O_2 catalyzed by $[NBu_4]VO_3$-pyrazine-2-carboxylic in acetonitrile (CH_3CN). H_2O_2 was suggested to be a promoter for the reaction by generation of hydroxyl radical (•OH), while oxygen works as the oxidant.[130] In latest work, another researcher has successfully used oxygen as oxidant without presence of hydrogen peroxide; the reaction was carried out in sulphuric acid media with the presence of Pd^{II} cations catalyst. Catalytic activity was strongly affected by the O_2/CH_4 ratio of the feed gas, the total pressure of the feed, the concentration of sulphur trioxide (SO_3) in the sulphuric acid, and the concentration of Pd^{II} present in solution at the onset of reaction.[131] Carbon monoxide was also established to be an essential intermediate in the formation of CH_3COOH and is the source of the carboxylate group in this product. The role of carbon monoxide in carbonylation of methane to acetic acid is well known and the similar group also demonstrated that Pt^{II} cations have an ability to catalyse this type of reaction.[132] Both systems operated at higher temperature, 180 °C. Before that, Sen *et al.* was the first utilised this concept which they catalyzed methane by aqueous Rh(III) plus I^- to give acetic acid with fairly good selectivity.[133] However, the activity was quite low and the best yield achieved is about 0.5% based on methane. Apart from CO as carbon source, Periana *et al.* reported where both carbons of acetic acid are derived directly from two methane molecules in a single reaction system where Pd^{II} cations was used as catalyst. The only other product detected is methyl bisulphate and carbon dioxide.[134] The drawback of the system is the Pd^{II} cations reduce to metal state causing the reaction to stop. In order to solve this problem, Zerella and co-workers had replicated the reaction with addition of Cu^{II} and O_2 to the reaction mixture and they observed the yield of acetic acid was enhanced without dramatically increasing the yield of methyl bisulfate or decreasing the selectivity.[135]

From the brief literatures mentioned above, it seems homogeneous catalytic systems were vastly used in activating methane and other lower alkane to corresponding oxygenates through numerous condition *i.e.* different solvent, oxidant, additive, temperature and pressure. Some have advantages and disadvantages compared to others. Therefore, further improvement needs to be carried out especially by implementing the heterogeneous catalytic system.

1.5.3.3. Oxidation with heterogeneous catalytic system in different solvent and oxidant

The utilisation of heterogeneous catalysts is the main concern for researchers involved in catalysis field which it will be more advantageous than the use of homogeneous systems especially due to the possibility of easier separation and reusability. Although it is important to note here that generally it might suffer from leaching problem, mass transport limitation and other factors associated with tri-phase systems. Back to 1997, Ratnasamy and co-workers carried out methane reaction using phthalocynine complexes of Fe, Cu, Co encapsulated in zeolite, respectively.[136] By using molecular oxygen as oxidant in the presence of TBHP as initiator and acetonitrile as solvent, they reported higher catalytic activity than homogeneous Periana's Hg systems. Interestingly, no CO_2 detected in gas phase. Low activity observed in the absence of unsubstituted metal phthalocyanines or zeolites alone and the system required both O_2 and TBHP to obtained higher catalytic performance. In the case of H_2O as solvent instead of acetonitrile, formic acid was detected as main product and other products were methanol, formic acid and CO_2. Bar-Nahum *et al.* showed that bipyrimidinylplatiumpolyoxometalate ($H_5PV_2Mo_{10}O_{40}$) hybrid complex supported on SiO_2 and carbon were also active for liquid phase methane oxidation at lower temperature (50 °C).[137] In the presence of O_2 as oxidant with dilute acid solution (*i.e.* H_2SO_4) as solvent, equivalent amount acetaldehyde and methanol were produced. Their data show an important of acid presence in the system since with only H_2O as solvent, catalytic activity decreased by factor 6 and acetaldehyde as a major product.

Recent work by Sorokin and co-workers has presented a grafted μ-nitrido iron phthalocyanine complex on silica for the selective oxidation of methane under mild reaction conditions using H_2O_2 as oxidant,[138,139] whereas Schüth and co-workers[140] have coordinated platinum onto covalent triazine-based frameworks and use this material as a solid catalyst for the synthesis of methanol using concentrated sulphuric acid as Periana *et*

al. has previously described.[106] They claimed that the solid catalyst was stable over several recycling steps with the activity comparable to Periana's system. Generally, it is apparent from the recent literature that efforts have been set to produce a bio-mimetic methane oxidation catalyst especially on using phthalocyanine based complexes either in a homo- or heterogeneous form. Apart from bio-mimetic catalyst, TS-1 as a catalyst for activating methane in liquid phase was reported by Shulpin *et al.* However, the catalytic activity was not compromising, therefore no further optimisation was done on this catalytic system.[141]

1.5.3.4. Hydrogen peroxide (H_2O_2) as oxidant

There are several works discussed on using hydrogen peroxide in oxidising methane, it could employed either as sole oxidant[138,139,128] or as initiator with molecular oxygen (or air).[130] Some of these works have been discussed in details in the previous section. One particular interest here is to look into the work by Sorokin and co-workers. In this study, methane oxidation was performed in water with H_2O_2 as oxidant in the presence of heterogeneous μ-nitrido iron phthalocyanine complex on silica catalyst. The catalyst was claimed to be stabled without any degradation and it was confirmed by performing the reaction with labelled methane ($^{13}CH_4$). Formic acid was detected as the sole product at 25 ^{o}C while at higher temperature up to 60 ^{o}C, formation of hydrated formaldehyde and methanol could be obtained but in rather minor quantity relative to formic acid. There was no carbon oxide been detected even at 20 hours reaction time. Analysis of CO_2 was carried out only in liquid phase using ^{13}C-NMR and there is no report on CO_2 quantification in gas phase sample, therefore the analysis was not completed. Recently, Rahman *et al.* had demonstrated that H-ZSM5 solid catalyst was capable in oxidising methane to formic acid in the presence of H_2O_2 and water as solvent.[142] Other observed products were methanol, acetaldehyde, acetic acid and carbon dioxide. Compared to Sorokin works, they performed the reaction at rather higher temperature (100 ^{o}C) with the presence of triphenylphosphine (PPh_3) as a promoter. Within 5 hours reaction time at 26 bar of methane, the maximum yield of formic acid obtained was around 13.0% and the selectivity calculated to be 66.8%. Carbon dioxide as consecutive oxidation product was contributed to 30% from total products. The activity of H-ZSM5 was claimed to strongly reliant on acidity of catalyst which considered as active site of the catalyst. Therefore, H-ZSM5 with SiO_2/Al_2O_3 ratio equal to 23.8 which having strong acid gave higher yield of formic acid compared to

analogue catalyst with higher SiO_2/Al_2O_3 ratio. Details mechanistic studies did not included in this article, although it was claimed that formic acid was originated from methanol as intermediate species.

1.5.3.5. Oxidation with *in-situ* capture H_2O_2

The concept of *in-situ* H_2O_2 as an oxidant could be traced back to 1966 where Hooper patented a work consisting oxidation of aromatic, cycloaliphatic or olefinic hydrocarbon to produce phenol, alcohol or glycol respectively.[143] Hydrogen peroxide was generated by contacting hydrogen and oxygen in the presence of water and acid with solid Pd based catalyst. As shown in section 1.5.3.4, hydrogen peroxide was proved to work as oxidant for oxidising methane and other lower alkane to oxygenate, although in some aspects it suffered several setbacks, both in economical and oxidant-reactivity if used as co-reactant. In fact, the cost of hydrogen peroxide is higher than target product (*i.e.* methanol) itself which make less attractive for scale-up to commercialisation stage.[144] On the other hand, it might undergo unselective hydrogenation-decomposition process which later affects the catalytic productivity. Therefore, it requires an alternative ways by introducing the concept of slow production and *in-situ* capture of H_2O_2 in a pot system together with oxidation reaction. Up to date, there are several reports on activation of alkane following this approach. Back to 1992, Sen and co-workers utilised a mixture of gas containing $CO/H_2O/O_2$ to generate the hydrogen peroxide and subsequently activate methane and ethane to oxygenates using 5% Pd on Carbon catalyst.[145] The same work patented in three years later shows that the presence of CO is crucial where it work together with H_2O in water gas shift reaction which at later stage produced dihydrogen. In second stage, catalytic reaction between H_2 and O_2 to produced H_2O_2 then catalyzed by Pd based catalytic system to oxidise alkane (see scheme 1.2).[146,147] Apart from CO, the presence of acidic solution was clearly necessary since no oxidation could be obtained in it absence. In this particular study, hydrochloric acid (HCl) was used as acid source. The overall reaction was stated to be different from Fenton-type radical reaction.

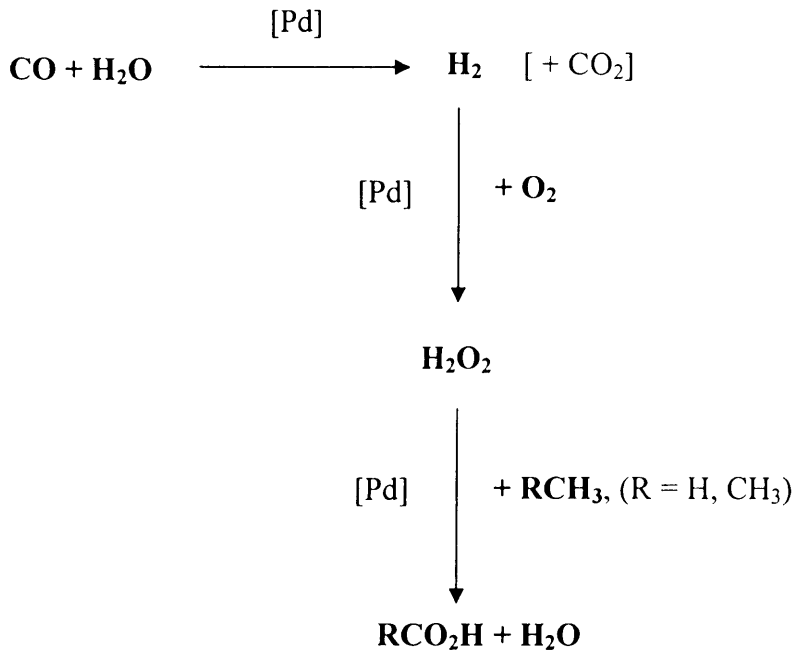

In their following works with the aims to selectively produce methanol as sole product, Sen and co-workers utilised a combination between heterogeneous Pd on carbon with soluble copper (II) salts in a mixture of trifluoroacetic acid (TFA) and water and observed the selective oxidation of methane and other lower alkanes by dioxygen. Interestingly the presence of $CuCl_2$ affected the selectivity trend where methanol and its derivatives ($CF_3CO_2CH_3$) were produced as main products instead of formic acid regardless the amount of copper added into the reaction system. Previously, similar group have successfully utilised Rhodium based homogeneous catalyst and managed to tune the selectivity by varying the solvent system. A mixture of perfluorobutyric acid and water with certain ratio generated methanol as main product with formic acid was the only significant by product observed.[148] However, again the presence of CO was essential to the system in order to maintain a high selectivity to partially oxidised products.[147] The requirement of a co-reductant (carbon monoxide) makes the overall reaction formally analogous to the monooxygenase in which only one of the two oxygen atoms in the dioxygen molecule is used for substrate oxidation.

Given that the correlation of catalytic activity and characteristics of catalyst has not been established in previous works by Sen *et al.*, further detail studies on similar system has been done by Park and co-workers.[149] The nature of co-catalyst, the presence of halide (Cl^-), and the solvent composition changed the structure of palladium species and affected the

yield of product (CF_3COOCH_3). In the presence of a copper compound and Cl^-, the metallic palladium could be partly oxidised into Pd(II) species. For the active catalyst system, copper compound appeared to be present as Cu(I). Pd(II) species coordinated with Cl^- appeared to be essential for the selective activation of methane and the metallic palladium responsible for the *in-situ* generation of H_2O_2 from CO, H_2O, and O_2.

Hydrogen peroxide produced through water gas shift reaction was claimed to generate at low rate thus was used efficiently for alkane oxidation. On the other hand, Lin and co-workers claimed that by starting with dihydrogen, hydrogen peroxide was formed rapidly, but most of it underwent subsequent metal-catalyzed decomposition at the reaction temperature around 85 to 100 °C (as evidenced by a relatively rapid drop in gas pressure) .[147] Although, this could be avoided by lowering the reaction temperature or employing the catalyst which naturally did not decompose hydrogen peroxide. Presence of CO_2 from water gas shift reaction makes it impossible to quantify the total selectivity of the product.

As mentioned previously, H_2O_2 also can be generated in *in-situ* by the presence of H_2 and O_2 gas. Park and co-workers [150.151] published their finding in liquid phase methane oxidation using *in-situ* generated H_2O_2 as oxidant. However, their works required dual catalyst, where Pd/C act as an *in-situ* H_2O_2 generator and $Cu(CH_3COO)_2$ or NH_4VO_3 as oxidation catalyst. The reaction was carried out in the presence of trifluoroacetic acid (TFA) and trifluoroacetic anhydride (TFAA) as solvent; whereas the temperature was set to 80 °C with total pressure up to 47 atm (71.4% CH_4, 14.3% H_2 and 14.3% O_2). They claim that the system advantages compared to $CO/H_2O/O_2$ since it can be carried out at lower temperature without required any Cl^- presence.

Generally, most the reports involving *in-situ* generation H_2O_2 for activating alkane either not environmental friendly or could not be classified as true heterogeneous catalysts. The activity is strongly dependant on the nature of co-catalyst, halide ion and composition of solvent. Thus, the discovery of an efficient catalyst and the choice of reaction conditions are the keys to realizing an ideal oxidation process.

1.6. Aims of the thesis

Liquid phase oxidations of lower alkanes especially methane in a stirred autoclave were studied using heterogeneous catalysts mainly based on Au based catalyst systems. Reaction parameters were investigated in detail whilst the optimisation was carried out in order to attain an advanced green catalytic system.

1.7. Scope of the thesis

1. Development of heterogeneous catalysts for liquid phase direct oxidation of methane to oxygenate products via environmental friendly approach.
2. Utilisation of catalyst as bifunctional systems which generate the hydrogen peroxide as oxidant and activate the alkanes in one pot systems.
3. Systematic study into the effect of reaction conditions on catalytic performance.
4. Description of the key parameters that control and affect catalytic activity and selectivity
5. Elucidation of the active sites of the catalyst to determine the optimum preparation route and catalyst composition.
6. Modification of the catalysts and reaction parameters in order to successfully activate methane to oxygenate at mild reaction conditions.

References:

1. Chorkendorff, I., Nietmantsverdriet, J.W. *Concepts of Modern Catalysis and Kinetics*; Wiley-VCH GmbH & Co. KGaA, 2003.
2. Bond, G. C. *Heterogeneous Catalysis: Principles and Applications*, 2nd Edition ed.; Oxford: Oxford University Press, 1987.
3. Centi, G., Cavani, F. and Trifirò, F *Selective Oxidation by Heterogeneous Catalysis*; New York: Kluwer Academic/Plenum Publishers, 2001.
4. Bowker, M. *The Basis and Applications of Heterogeneous Catalysis*; Oxford: Oxford University Press, 1998.
5. Thomas, J. M., Thomas, W.J. *Principles and Practice of Heterogeneous Catalysis*; VCH Weinheim, 1997.
6. G.C. Bond, C. L., D. T. Thompson, *Catalysis by Gold*; Imperial College Press, 2006; Vol. 6.
7. Hutchings, G. J. *Journal of Catalysis* **1985,** *96*, 292-295.
8. M. Haruta, T. K., H. Sano, N. Yamada. *Chem. Lett.* **1987,** *16*, 405.
9. Ueda, A.; Oshima, T.; Haruta, M. *Applied Catalysis B: Environmental* **1997,** *12*, 81-93.
10. G.C. Bond, D. T. T. *Gold Bulletin* **2000,** *33*.
11. Kung, H. H.; Kung, M. C.; Costello, C. K. *Journal of Catalysis*, *216*, 425-432.
12. Bamwenda, G. R.; Tsubota, S.; Nakamura, T.; Haruta, M. *Catalysis Letters* **1997,** *44*, 83-87.
13. Soares, J. M. C.; Morrall, P.; Crossley, A.; Harris, P.; Bowker, M. *Journal of Catalysis* **2003,** *219*, 17-24.
14. Zanella, R.; Louis, C. *Catalysis Today* **2005,** *107-108*, 768-777.
15. DuPont. 2011.
16. Biella, S.; Castiglioni, G. L.; Fumagalli, C.; Prati, L.; Rossi, M. *Catalysis Today* **2002,** *72*, 43-49.
17. Porta, F.; Prati, L.; Rossi, M.; Coluccia, S.; Martra, G. *Catalysis Today* **2000,** *61*, 165-172.
18. Biella, S.; Prati, L.; Rossi, M. *Inorganica Chimica Acta* **2003,** *349*, 253-257.
19. Prati, L.; Rossi, M. *Journal of Catalysis* **1998,** *176*, 552-560.
20. Prati, L.; Porta, F. *Applied Catalysis A: General* **2005,** *291*, 199-203.
21. Nyarady, S. A.; Sievers, R. E. *Journal of the American Chemical Society* **1985,** *107*, 3726-3727.
22. Biella, S.; Rossi, M. *Chemical Communications* **2003**, 378-379.
23. Bianchi, C.; Porta, F.; Prati, L.; Rossi, M. *Topics in Catalysis* **2000,** *13*, 231-236.
24. Carrettin, S.; McMorn, P.; Johnston, P.; Griffin, K.; Hutchings, G. J. *Chemical Communications* **2002**, 696-697.
25. Carrettin, S.; McMorn, P.; Johnston, P.; Griffin, K.; Kiely, C. J.; Attard, G. A.; Hutchings, G. J. *Topics in Catalysis* **2004,** *27*, 131-136.
26. Carrettin, S.; McMorn, P.; Johnston, P.; Griffin, K.; Kiely, C. J.; Hutchings, G. J. *Physical Chemistry Chemical Physics* **2003,** *5*, 1329-1336.

27. Dimitratos, N.; Lopez-Sanchez, J. A.; Anthonykutty, J. M.; Brett, G.; Carley, A. F.; Tiruvalam, R. C.; Herzing, A. A.; Kiely, C. J.; Knight, D. W.; Hutchings, G. J. *Physical Chemistry Chemical Physics* **2009,** *11*, 4952-4961.
28. Hammond, C.; Lopez-Sanchez, J. A.; Hasbi Ab Rahim, M.; Dimitratos, N.; Jenkins, R. L.; Carley, A. F.; He, Q.; Kiely, C. J.; Knight, D. W.; Hutchings, G. J. *Dalton Transactions* **2011,** *40*, 3927-3937.
29. Abad, A.; Concepción, P.; Corma, A.; García, H. *Angewandte Chemie International Edition* **2005,** *44*, 4066-4069.
30. Mori, K.; Hara, T.; Mizugaki, T.; Ebitani, K.; Kaneda, K. *Journal of the American Chemical Society* **2004,** *126*, 10657-10666.
31. Enache, D. I. E., J. K.; Landon, P.; Solsona-Espriu, B.; Carley, A. F.; Herzing, A. A.; Watanabe, M.; Kiely, C. J.; Knight, D. W.; Hutchings, G. J. . *Science* **2006,** *311*, 362-365.
32. Dimitratos, N.; Lopez-Sanchez, J. A.; Morgan, D.; Carley, A. F.; Tiruvalam, R.; Kiely, C. J.; Bethell, D.; Hutchings, G. J. *Physical Chemistry Chemical Physics* **2009,** *11*, 5142-5153.
33. Lopez-Sanchez, J. A.; Dimitratos, N.; Miedziak, P.; Ntainjua, E.; Edwards, J. K.; Morgan, D.; Carley, A. F.; Tiruvalam, R.; Kiely, C. J.; Hutchings, G. J. *Physical Chemistry Chemical Physics* **2008,** *10*, 1921-1930.
34. Hess, H. T. *Kirk-Othmer Encyclopaedia of Chemical Engineering*; Wiley: New York, 1995; Vol. 13.
35. Liu, Q.; Lunsford, J. H. *Applied Catalysis A: General* **2006,** *314*, 94-100.
36. Lunsford, J. H. *Journal of Catalysis*, *216*, 455-460.
37. Liu, Q.; Lunsford, J. H. *Journal of Catalysis* **2006,** *239*, 237-243.
38. Choudhary, V. R.; Samanta, C.; Choudhary, T. V. *Applied Catalysis A: General* **2006,** *308*, 128-133.
39. Choudhary, V. R.; Gaikwad, A. G.; Sansare, S. D. *Catalysis Letters* **2002,** *83*, 235-239.
40. Solsona, B. E.; Edwards, J. K.; Landon, P.; Carley, A. F.; Herzing, A.; Kiely, C. J.; Hutchings, G. J. *Chemistry of Materials* **2006,** *18*, 2689-2695.
41. Ishihara, T.; Ohura, Y.; Yoshida, S.; Hata, Y.; Nishiguchi, H.; Takita, Y. *Applied Catalysis A: General* **2005,** *291*, 215-221.
42. Landon, P.; Collier, P. J.; Papworth, A. J.; Kiely, C. J.; Hutchings, G. J. *Chemical Communications* **2002**, 2058-2059.
43. Okumura, M.; Kitagawa, Y.; Yamagcuhi, K.; Akita, T.; Tsubota, S.; Haruta, M. *Chemistry Letters* **2003,** *32*, 822-823.
44. Pritchard, J.; Kesavan, L.; Piccinini, M.; He, Q.; Tiruvalam, R.; Dimitratos, N.; Lopez-Sanchez, J. A.; Carley, A. F.; Edwards, J. K.; Kiely, C. J.; Hutchings, G. J. *Langmuir* **2010,** *26*, 16568-16577.
45. Samanta, C. *Applied Catalysis A: General* **2008,** *350*, 133-149.
46. Piccinini, M.; Ntainjua N, E.; Edwards, J. K.; Carley, A. F.; Moulijn, J. A.; Hutchings, G. J. *Physical Chemistry Chemical Physics* **2010,** *12*, 2488-2492.

47. Ntainjua N, E.; Edwards, J. K.; Carley, A. F.; Lopez-Sanchez, J. A.; Moulijn, J. A.; Herzing, A. A.; Kiely, C. J.; Hutchings, G. J. *Green Chemistry* **2008,** *10*, 1162-1169.
48. Edwards, J. K.; Solsona, B.; N, E. N.; Carley, A. F.; Herzing, A. A.; Kiely, C. J.; Hutchings, G. J. *Science* **2009,** *323*, 1037-1041.
49. K. Weissermel, H.-J. A. *Industrial Organic Chemistry*, 4th ed.; Wiley-VCH, Weinheim, 2003.
50. Chavan, S. A.; Srinivas, D.; Ratnasamy, P. *Journal of Catalysis* **2002,** *212*, 39-45.
51. Nowotny, M.; Pedersen, L. N.; Hanefeld, U.; Maschmeyer, T. *Chemistry – A European Journal* **2002,** *8*, 3724-3731.
52. Raja, R.; Sankar, G.; Thomas, J. M. *Journal of the American Chemical Society* **1999,** *121*, 11926-11927.
53. Zhao, R.; Ji, D.; Lv, G.; Qian, G.; Yan, L.; Wang, X.; Suo, J. *Chemical Communications* **2004**, 904-905.
54. Lü, G.; Zhao, R.; Qian, G.; Qi, Y.; Wang, X.; Suo, J. *Catalysis Letters* **2004,** *97*, 115-118.
55. Xu, Y.-J.; Landon, P.; Enache, D.; Carley, A. F.; Roberts, M. W.; Hutchings, G. J. *Catalysis Letters* **2005,** *101*, 175-179.
56. Xu, L.-X.; He, C.-H.; Zhu, M.-Q.; Fang, S. *Catalysis Letters* **2007,** *114*, 202-205.
57. Xu, L.-X.; He, C.-H.; Zhu, M.-Q.; Wu, K.-J.; Lai, Y.-L. *Catalysis Letters* **2007,** *118*, 248-253.
58. Xie, J.; Wang, Y.; Li, Y.; Wei, Y. *Reaction Kinetics, Mechanisms and Catalysis* **2011,** *102*, 143-154.
59. Blick, K.; Mitrelias, T.; Hargreaves, J.; Hutchings, G.; Joyner, R.; Kiely, C.; Wagner, F. *Catalysis Letters* **1998,** *50*, 211-218.
60. Solsona, B. E.; Garcia, T.; Jones, C.; Taylor, S. H.; Carley, A. F.; Hutchings, G. J. *Applied Catalysis A: General* **2006,** *312*, 67-76.
61. Gluhoi, A. C.; Nieuwenhuys, B. E. *Catalysis Today* **2007,** *119*, 305-310.
62. www.wikipedia.org. 2011.
63. Al-Sayari, S. A., Cardiff University, 2006.
64. Gasior, M.; Grzybowska, B.; Samson, K.; Ruszel, M.; Haber, J. *Catalysis Today* **2004,** *91-92*, 131-135.
65. Jones, W. D. *Science* **2000,** *287*, 1942-1943.
66. Shilov, A. E.; Shul'pin, G. B. *Chemical Reviews* **1997,** *97*, 2879-2932.
67. Kirk, R. E.; Othmer, D. F. *Kirk-Othmer Encyclopedia of Chemical Technology*; Wiley, New York, 1992.
68. Borgaonkar, H. V.; Raverkar, S. R.; Chandalia, S. B. *Industrial & Engineering Chemistry Product Research and Development* **1984,** *23*, 455-458.
69. Wang, F.; Xu, J.; Li, X.; Gao, J.; Zhou, L.; Ohnishi, R. *Advanced Synthesis & Catalysis* **2005,** *347*, 1987-1992.
70. Monfared, H. H.; Amouei, Z. *Journal of Molecular Catalysis A: Chemical* **2004,** *217*, 161-164.
71. Bahronowski, K.; Dula, R.; Gasior, M.; Łabanowska, M.; Michalik, A.; Vartikian, L. A.; Serwicka, E. M. *Appl. Clay. Sci* **2001,** *18*, 93.

72. Das, S.; Bhowmick, T.; Punniyamurthy, T.; Dey, D.; Nath, J.; Chaudhuri, M. K. *Tetrahedron Letters* **2003,** *44*, 4915-4917.
73. Singh, A. P.; Selvam, T. *Journal of Molecular Catalysis A: Chemical* **1996,** *113*, 489-497.
74. Yang, F.; Sun, J.; Zheng, R.; Qiu, W.; Tang, J.; He, M. *Tetrahedron* **2004,** *60*, 1225-1228.
75. Bastock, T. W.; Clark, J. H.; Martin, K.; Trenbirth, B. W. *Green Chemistry* **2002,** *4*, 615-617.
76. Gupta, M.; Paul, S.; Gupta, R.; Loupy, A. *Tetrahedron Letters* **2005,** *46*, 4957-4960.
77. Nair, K.; Sawant, D. P.; Shanbhag, G. V.; Halligudi, S. B. *Catalysis Communications* **2004,** *5*, 9-13.
78. Li, X.; Xu, J.; Zhou, L.; Wang, F.; Gao, J.; Chen, C.; Ning, J.; Ma, H. *Catalysis Letters* **2006,** *110*, 149-154.
79. Gradassi, M. J.; Wayne Green, N. *Fuel Processing Technology* **1995,** *42*, 65-83.
80. Lunsford, J. H. *Catalysis Today* **2000,** *63*, 165-174.
81. Schuurman, Y.; Mirodatos, C. *Applied Catalysis A: General* **1997,** *151*, 305-331.
82. Gist, R. "Global oil and gas market: what does the future hold?"; MAI World Methanol Conference, 2005, Miami, USA.
83. Taylor, S. H.; Hargreaves, J. S. J.; Hutchings, G. J.; Joyner, R. W.; Lembacher, C. W. *Catalysis Today* **1998,** *42*, 217-224.
84. Otsuka, K.; Wang, Y. *Applied Catalysis A: General* **2001,** *222*, 145-161.
85. Nguyen, L. D.; Loridant, S.; Launay, H.; Pigamo, A.; Dubois, J. L.; Millet, J. M. M. *Journal of Catalysis* **2006,** *237*, 38-48.
86. Sen, A. *Accounts of Chemical Research* **1998,** *31*, 550-557.
87. Thomasson, A. In *CMA News*: USA, 2007.
88. Khokhar, M. D.; Shukla, R. S.; Jasra, R. V. *Journal of Molecular Catalysis A: Chemical* **2009,** *299*, 108-116.
89. Bharadwaj, S. S.; Schmidt, L. D. *Fuel Processing Technology* **1995,** *42*, 109-127.
90. Sen, A.; Benvenuto, M. A.; Lin, M.; Hutson, A. C.; Basickes, N. *Journal of the American Chemical Society* **1994,** *116*, 998-1003.
91. Michalkiewicz, B. *Applied Catalysis A: General* **2006,** *307*, 270-274.
92. Labinger, J. A. *Fuel Processing Technology* **1995,** *42*, 325-338.
93. WANG Ye, A. D., ZHANG QingHong *Science China* **2010,** *53*, 337.
94. Wolf, D. *Angewandte Chemie International Edition* **1998,** *37*, 3351-3353.
95. Hunter, N. R.; Gesser, H. D.; Morton, L. A.; Yarlagadda, P. S.; Fung, D. P. C. *Applied Catalysis* **1990,** *57*, 45-54.
96. Foster, N. R. *Applied Catalysis* **1985,** *19*, 1-11.
97. Gesser, H. D.; Hunter, N. R.; Prakash, C. B. *Chemical Reviews* **1985,** *85*, 235-244.
98. Walker, G. S.; Lapszewicz, J. A.; Foulds, G. A. *Catalysis Today* **1994,** *21*, 519-526.
99. Thomas, D. J.; Willi, R.; Baiker, A. *Industrial & Engineering Chemistry Research* **1992,** *31*, 2272-2278.
100. Pannov, G. I.; Sobolev, V. I.; Kharitonov, A. S. *Journal of Molecular Catalysis* **1990,** *61*, 85-97.

101. Sobolev, V. I.; Kharitonov, A. S.; Paukshtis, Y. A.; Panov, G. I. *Journal of Molecular Catalysis* **1993,** *84*, 117-124.
102. Sobolev, V. I.; Dubkov, K. A.; Panna, O. V.; Panov, G. I. *Catalysis Today* **1995,** *24*, 251-252.
103. Gao, Z.-X.; Kim, H.-S.; Sun, Q.; Stair, P. C.; Sachtler, W. M. H. *The Journal of Physical Chemistry B* **2001,** *105*, 6186-6190.
104. Groothaert, M. H.; Smeets, P. J.; Sels, B. F.; Jacobs, P. A.; Schoonheydt, R. A. *Journal of the American Chemical Society* **2005,** *127*, 1394-1395.
105. Smeets, P. J.; Groothaert, M. H.; Schoonheydt, R. A. *Catalysis Today* **2005,** *110*, 303-309.
106. Periana, R. A.; Taube, D. J.; Gamble, S.; Taube, H.; Satoh, T.; Fujii, H. *Science* **1998,** *280*, 560-564.
107. Shul'pin, G. B.; Nizova, G. V.; Kozlov, Y. N.; GonzalezCuervo, L.; Süss-Fink, G. *Advanced Synthesis & Catalysis* **2004,** *346*, 317-332.
108. Seki, Y.; Min, J. S.; Misono, M.; Mizuno, N. *The Journal of Physical Chemistry B* **2000,** *104*, 5940-5944.
109. Stahl, S. S.; Labinger, J. A.; Bercaw, J. E. *Angewandte Chemie International Edition* **1998,** *37*, 2180-2192.
110. Periana, R. A.; Taube, D. J.; Evitt, E. R.; Löffler, D. G.; Wentrcek, P. R.; Voss, G.; Masuda, T. *Science* **1993,** *259*, 340-343.
111. J. Colby, D. I. S., H. Dalton, . *Biochemical Journal* **1977,** *165*, 395.
112. Y. Jiang, P. C. W., H. Dalton. *Biochimica et Biophysica Acta* **1993,** *1163*, 105.
113. J. C. Snyder, A. V. G.; USPTO Ed.; HOUDRY PROCESS CORP 1950.
114. A.E. Shilov, G. B. S. p. *Russ. Chem. Rev* **1987,** *56*, 442.
115. Kao, L. C.; Hutson, A. C.; Sen, A. *Journal of the American Chemical Society* **1991,** *113*, 700-701.
116. Michalkiewicz, B.; Kalucki, K.; Sosnicki, J. G. *Journal of Catalysis* **2003,** *215*, 14-19.
117. M. Lin, A. S. *Nature* **1994,** *836*, 613.
118. Cheng, J.; Li, Z.; Haught, M.; Tang, Y. *Chemical Communications* **2006**, 4617-4619.
119. Osako, T.; Watson, E. J.; Dehestani, A.; Bales, B. C.; Mayer, J. M. *Angewandte Chemie International Edition* **2006,** *45*, 7433-7436.
120. Periana, R. A.; Mirinov, O.; Taube, D. J.; Gamble, S. *Chemical Communications* **2002**, 2376-2377.
121. Jarosińska, M.; Lubkowski, K.; Sośnicki, J.; Michalkiewicz, B. *Catalysis Letters* **2008,** *126*, 407-412.
122. D.A Pichugina, N. E. K. m., AF Shestakov. *Gold Bulletin* **2007,** *40*, 115-120.
123. De Vos, D. E.; Sels, B. F. *Angewandte Chemie International Edition* **2005,** *44*, 30-32.
124. C. J. Jones, D. T., R. A. *Angew. Chem* **2004,** *116*, 4726.
125. Süss-Fink, G.; Nizova, G. V.; Stanislas, S.; Shul'pin, G. B. *Journal of Molecular Catalysis A: Chemical* **1998,** *130*, 163-170.

126. Süss-Fink, G.; Gonzalez, L.; Shul'pin, G. B. *Applied Catalysis A: General* **2001,** *217*, 111-117.
127. Wei, X.; Ye, L.; Yuan, Y. *Journal of Natural Gas Chemistry* **2009,** *18*, 295-299.
128. Yuan, Q.; Deng, W.; Zhang, Q.; Wang, Y. *Advanced Synthesis & Catalysis* **2007,** *349*, 1199-1209.
129. Mizuno, N.; Seki, Y.; Nishiyama, Y.; Kiyoto, I.; Misono, M. *Journal of Catalysis* **1999,** *184*, 550-552.
130. V. Nizova, G.; Suss-Fink, G.; B. Shul'pin, G. *Chemical Communications* **1997**, 397-398.
131. Zerella, M.; Kahros, A.; Bell, A. T. *Journal of Catalysis* **2006,** *237*, 111-117.
132. Zerella, M.; Bell, A. T. *Journal of Molecular Catalysis A: Chemical* **2006,** *259*, 296-301.
133. Minren Lin, A. S. *Nature* **1994,** *368*, 613.
134. Periana, R. A.; Mironov, O.; Taube, D.; Bhalla, G.; Jones, C. J. *Science* **2003,** *301*, 814-818.
135. Zerella, M.; Mukhopadhyay, S.; Bell, A. T. *Chemical Communications* **2004**, 1948-1949.
136. Ratnasamy, P.; Raja, R.; Srinivas, D. *Philosophical Transactions of the Royal Society A: Mathematical, Physical and Engineering Sciences* **2005,** *363*, 1001-1012.
137. Bar-Nahum, I.; Khenkin, A. M.; Neumann, R. *Journal of the American Chemical Society* **2004,** *126*, 10236-10237.
138. Sorokin, A. B.; Kudrik, E. V.; Bouchu, D. *Chemical Communications* **2008**, 2562-2564.
139. Sorokin, A. B.; Kudrik, E. V.; Alvarez, L. X.; Afanasiev, P.; Millet, J. M. M.; Bouchu, D. *Catalysis Today* **2010,** *157*, 149-154.
140. Palkovits, R.; Antonietti, M.; Kuhn, P.; Thomas, A.; Schüth, F. *Angewandte Chemie International Edition* **2009,** *48*, 6909-6912.
141. Shul'pin, G. B.; Sooknoi, T.; Romakh, V. B.; Süss-Fink, G.; Shul'pina, L. S. *Tetrahedron Letters* **2006,** *47*, 3071-3075.
142. Rahman, A. K. M. L.; Kumashiro, M.; Ishihara, T. *Catalysis Communications* **2011,** *12*, 1198-1200.
143. Hooper, G. W.; Office, L. P. Ed.; Imperial Chemical Industries Limited: Great Britain, 1966.
144. www.icis.com. 2011.
145. Lin, M.; Sen, A. *Journal of the American Chemical Society* **1992,** *114*, 7307-7308.
146. Sen, A. L., M. USPTO Ed., 1995.
147. Lin, M.; Hogan, T.; Sen, A. *Journal of the American Chemical Society* **1997,** *119*, 6048-6053.
148. Lin, M.; Hogan, T. E.; Sen, A. *Journal of the American Chemical Society* **1996,** *118*, 4574-4580.
149. Park, E. D.; Choi, S. H.; Lee, J. S. *Journal of Catalysis* **2000,** *194*, 33-44.
150. Park, E. D.; Hwang, Y. S.; Lee, J. S. *Catalysis Communications* **2001,** *2*, 187-190.
151. Park, E. D.; Hwang, Y.-S.; Lee, C. W.; Lee, J. S. *Applied Catalysis A: General* **2003,** *247*, 269-281.

CHAPTER 2

Experimental Procedures

2.1. Introduction

In this chapter the description of the experimental set up used thought-out this study is presented. Detail catalysts preparation, experimental rig and procedures are illustrated at the beginning of the chapter. Then the analytical method used to identify and quantify samples taken during reaction is described. Finally, the catalyst characterisation methods used including theory and experimental aspect of each instruments are presented.

2.2. Catalysts preparation

2.2.1. Synthesis of gold based catalysts

Catalytic activity of Au based catalyst is well known to have a significant effect based on catalyst preparation method. Typically, different techniques were used purposely to obtain different metal particle size and distribution, oxidation state and other important aspect in nanocrystal metal catalyst. Therefore, two different methods were chosen (impregnation and sol immobilisation) to prepare a series of Au catalysts whether in form of mono/bi or trimetallic with other metal. There were certain notations used for the catalysts prepared by these methods. IW denoted for impregnation whilst SI denoted for catalysts synthesised via sol-immobilisation techniques. Detail preparations for each method are shown below:

2.2.1.1. Synthesis of gold based supported catalyst via an impregnation technique

Pd-only, Au-only and Au-Pd bimetallic catalysts supported on TiO_2 (Degussa, P25), CeO_2 (Aldrich), γ-Al_2O_3 (Alfa Aesar), SiO_2 (Degussa) and Carbon (Aldrich) respectively were prepared by the impregnation method. The preparation was carried out as follows:

Materials containing a total of 5wt% total metal were prepared and the Au and Pd were presented in equal weights. For the 2.5%Au-2.5%Pd/TiO_2 catalyst, the detailed preparation procedure employed is described below.

Pd precursor ($PdCl_2$, Johnson Matthey, 0.083 g) was dissolved in gold solution (5.0 mL, $HAuCl_4 \cdot 3H_2O$, Johnson Matthey (5.0 g) dissolved in water 250 mL) by vigorous stirring. After the complete dissolution of the palladium salt, the support (1.90 g) was added very slowly into the solution and continued stirring until a homogeneous slurry solution was obtained. The slurry was kept in the oven for 16 hours at 110 °C. The dried form was typically calcined in static air using a horizontal tube Carbolite CWF 1200 furnace for 3 hours at 400 °C. The heating rate was set to 20 °C/min and calcination time was calculated or started whilst temperature achieved 400 °C. The same experimental procedure was carried out during the synthesis of Au/Pd supported nanoparticles with different Au/Pd ratio and as well as using a different support.

For the series of catalysts where copper was introduced as monometallic/or co-metal with gold and palladium, the procedure is similar as described above. Copper Chloride ($CuCl_2 \cdot 2H_2O$, Sigma-Aldrich, 5.0 g in 250 mL distilled water) was used as precursor and it was calculated to have required metal loading. For instance, in case of trimetallic 2.5wt%Au2.5wt%Pd2.5wt%Cu supported on TiO_2, the synthesis of catalyst was done by dissolving the Pd precursor ($PdCl_2$, 0.083 g) in gold solution (5 mL, $HAuCl_4 \cdot 3H_2O$ (5g) dissolved in water 250 mL) and copper solution (6.7 mL, $CuCl_2 \cdot 2H_2O$ (5g) dissolved in water 250 mL) by vigorous stirring. After the complete dissolution of the palladium salt, the TiO_2 (1.85 g) was added slowly into the solution and continued stirring until homogeneous slurry solution was obtained. The slurry was kept in the oven for 16 hours at 110 °C and then, the dried form was calcined at 400 °C for 3 hours in static air at heating rate set of 20 °C/min.

2.2.1.2. Synthesis of Au-Pd support catalyst via sol-immobilisation technique

Au-Pd bimetallic sols (1:1 molar ratio or wt ratio) were prepared using the following procedure: An aqueous $PdCl_2$ and $HAuCl_4$ solution of the desired concentration was prepared. The desired amount of a PVA (1 wt %) solution was added (PVA/Au (wt/wt) = 1.2) (in some cases used PVA/Au (wt/wt) = 0.65; a 0.1 M freshly prepared solution of $NaBH_4$ ($NaBH_4$/Au (mol/mol) = 5) was then added to form a dark-brown sol. After 30 minutes of sol generation, the colloid was immobilised by adding a support (acidified at

pH 1, by sulphuric acid) under vigorous stirring. The amount of support was calculated as having a required total final metal loading. After 2 hours the slurry was filtered, the catalyst washed thoroughly with distilled water and dried at 110 °C overnight. The catalyst was used as dried or by subjecting to reflux treatment with hot water for 0.5 to 2 hours to remove the coating polymer.[1]

2.2.2. Synthesis of copper oxide catalyst

In this study, copper oxide was synthesised via three different procedures *i.e.* co-precipitation, quick-precipitation and sol-gel technique. Detail preparations for each method are shown below:

2.2.2.1.Synthesis of copper oxide via co-precipitation (CuO_{Cp}) technique

Copper oxide catalyst was prepared by precipitation of copper chloride ($CuCl_2 \cdot 2H_2O$) precursor with urea. It was carried out by refluxing with 100 mL H_2O at 100 °C for 16 hours.[2] A slurry solution obtained was filtered and washed with 2 L of water and dried at 110 °C for 16 hours. Dried catalyst was calcined in air at temperature range from 200 – 500 °C. Copper oxide synthesised via this technique was denoted as CuO_{Cp}.

2.2.2.2. Synthesis of copper oxide via quick-precipitation (CuO_{Qp}) technique

In a typical procedure, 300 mL of 0.02 M copper acetate aqueous solution was mixed with 1 mL glacial acetic acid in a round-bottomed flask equipped with a reflux condenser.[3] The solution was heated to 100 °C with vigorous stirring, and then 0.8 g of sodium hydroxide (NaOH, analytical grade) was rapidly added into the above boiling solution until the pH value of the mixture reached 6–7, which a large amount of black precipitate was simultaneously produced. After being cooled to room temperature, the precipitate was centrifuged, washed once time with distilled water (1 L) and followed by absolute ethanol, respectively and dried in air at room temperature or calcined at 400 °C in static air for 3.0 hours. Copper oxide synthesised via this technique was denoted as CuO_{Qp}.

2.2.2.3. Synthesis of copper oxide via sol gel (CuO_{Sg}) technique

Copper nitrate solution with copper/citric acid mole ratio equal to 1.0 was added drop wise into citric acid solution. HNO_3 or NH_4OH was added to the slurry solution to adjust the pH value to 1.0.[4] Then, the formation of a homogeneous and transparent solution was stirred and slow evaporation at 70 °C was followed until a viscous residual was generated which later dried at 110 °C for 16 hours before subjected to heat treatment at 250 and 400 °C in static air for 3 hours, respectively. Copper oxide synthesised via this technique was denoted as CuO_{Sg}.

2.3. Catalyst evaluation

Catalysts synthesised in this study were evaluated for different reactions, namely oxidation of toluene, 4-methoxytoluene and lower alkanes (*i.e.* methane and ethane), respectively. Specific procedures for each system were shown in the following sub-section:

2.3.1. Solvent-free oxidation of toluene and 4-methoxytoluene

The oxidation of toluene was carried out in a stirred batch reactor (100 mL, Parr Instruments, USA). In typical reaction, the vessel was charged with substrate (40 mL) and catalyst. The autoclave was then purged five times with oxygen, leaving the vessel at 10 bar gauge. The reaction mixture was raised to the required temperature and the stirrer was set to 1500 rpm. Samples from the reactor were taken periodically, via sampling system, ensuring that the volume purged before sampling was higher than the tube volume. Similar procedure was applied for oxidation of 4-methoxytoluene.

2.3.2. Liquid phase alkane oxidation

In this study, liquid phase alkane oxidations were carried out in a batch stirred autoclave system. Detail procedures were shown in following sub-section:

2.3.2.1. Experimental procedure involving addition of H_2O_2 as oxidant

The liquid phase catalytic oxidations of methane (and other alkane *i.e.* ethane) were carried out using a stainless-steel autoclave (Parr Instruments, Model 4842) containing a Teflon vessel with total volume of 50 ml (see figure 2.1 for reactor set-up). In a typical run, a measured amount of catalyst was added into the Teflon vessel, which was pre-charged with a 10 mL solution of distilled water and the desired amount of H_2O_2 (50 wt% H_2O_2). The total volume of the reaction solution was 10 mL. The system was purged three times with methane to remove the available air in the autoclave. The methane inlet valve was closed after autoclave pressurized with methane (Research grade, 99.999%, BOC) to desire reaction pressure (typically at 30.5 bar). Then, the autoclave was heated to the desire reaction temperature (typically at 50 ^{o}C). After reaching the reaction temperature, the reaction solution was vigorously stirred at 1500 rpm (or otherwise stated) and maintained at the reaction temperature for a fixed period. After the reaction, the autoclave reactor was cooled with ice-water mixture to temperature below 12 °C in minimizing the possible loss of volatile products. The gas mixture of the reactor was slowly removed using a special gas sampling bag (PVF Gas Sampling Bag 9x9 On/Off 1.6 L, LabPure). For the reaction involving solid heterogeneous catalyst, the liquid solution was filtered using filter paper. In the case of the homogeneous catalyst, the solution was placed directly into a sample vial. Finally, the solutions were analysed or kept into fridge to prevent the loss of volatile products.

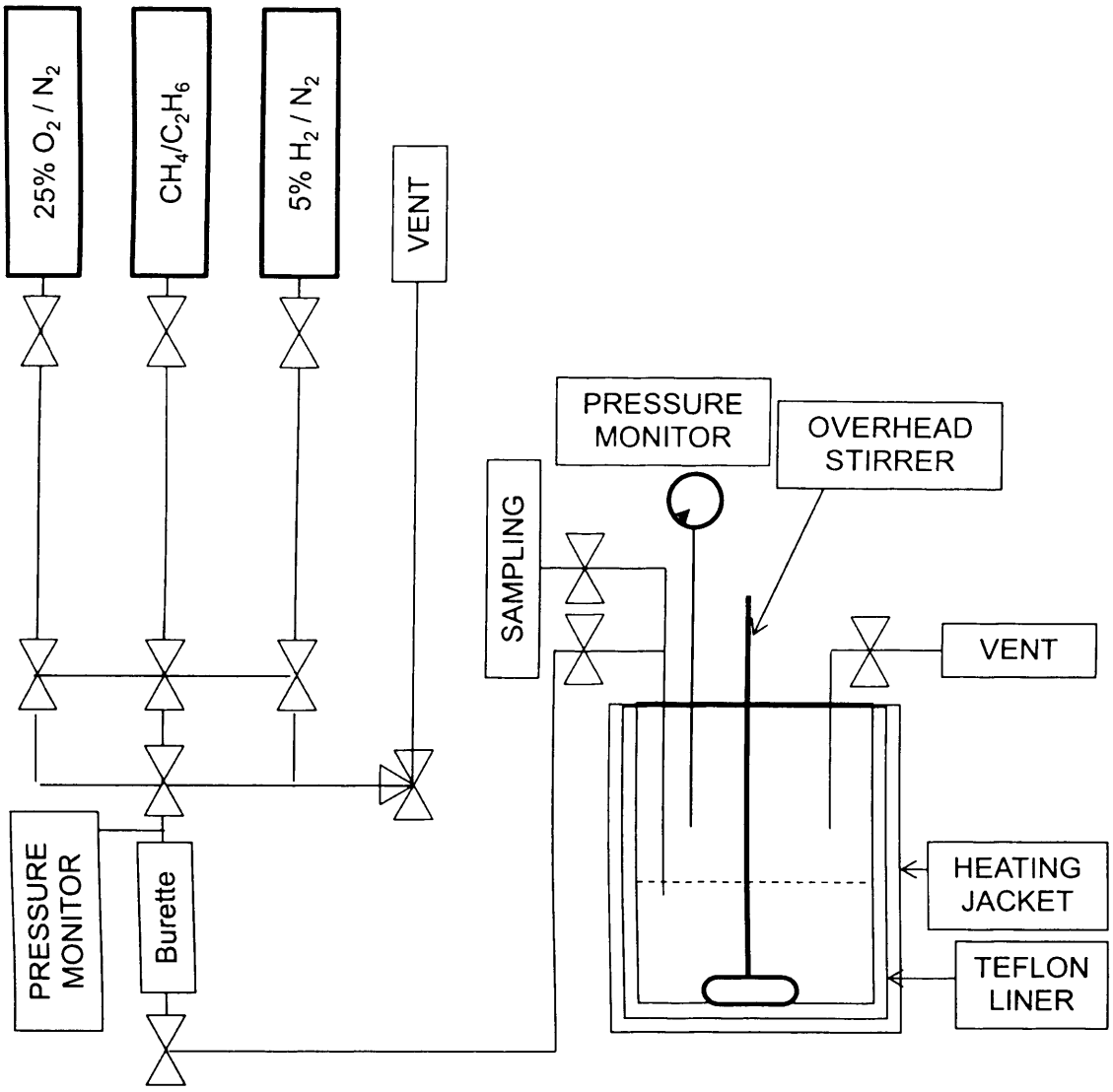

Figure 2.1: Schematic representation of the autoclave batch reactor

2.3.2.2. Experimental procedure involving *in-situ* generated H_2O_2 as oxidant

The liquid phase catalytic oxidations of methane (and other alkane *i.e.* ethane) through *in – situ* generated H_2O_2 as oxidant were carried out using a similar stainless-steel autoclave (Parr Instruments, Model 4842) as shown in figure 2.1 which contain a Teflon vessel with total volume of 50 mL. In a typical run, a measured amount of catalyst was added into the Teflon vessel, which was pre-charged with a 10 mL solution of distilled water. The autoclave was purged three times with $5\%/H_2/N_2$ and then filled successively with $5\%H_2/N_2$ (BOC), $25\%O_2/N_2$ (BOC) and CH_4 (Research grade, 99.999%, BOC). The desired composition of the gases mixture was outside the range of explosive limits. Then,

the autoclave was heated to the desired reaction temperature (typically at 50 °C). In case of reaction in sub-ambient temperature, the ice-batch was used to lower the temperature. Then, similar protocols as described in section 2.3.2.1.1 above were followed.

2.3.2.3. Batch autoclave washing procedures

Washing procedures has been set up to avoid cross contamination of products. After each reaction, all the internal and external parts of autoclave systems were subjected to several washing steps and cleaned using distilled water. In typical washing procedure, the vessel was filled with water and the temperature was set at 100 °C with vigorous stirring. In some cases, the liquid solution after washing was kept to verify the contamination by subjecting to NMR analysis of the solution before performing the next reaction. In addition to washing procedure, the contamination of the reactor was also regularly checked by performing the blank reaction or the standard reaction with a reference catalyst.

2.4. Analysis of products

Product analysis and validation have been carried out exclusively for each reaction. It comprises a calibration, products identification and quantification.

2.4.1. Toluene and 4-methoxytoluene oxidation

For the identification and analysis of the products, a Gas Chromatography equipped with Flame Ionisation Detector (a Varian star 3400 cx equipped with a 30 m CP-Wax 52 CB column), were used and checked by comparison with known commercially pure samples. Catalytic data for reactions were calculated using external calibration curve and external standard (2-propanol). External standard also was used to determine the carbon balance of the reaction. Detail calibration factor (CF) and calculation for both standards were shown in appendix A.1 (a, b, c, d).

2. 4.2. Methane oxidation

In order to have qualitative and quantitative analysis of products obtained from methane oxidation, two different procedures were used *i.e.* ^{1}H-NMR and GC-FID, respectively.

2.4.2.1. Analysis of liquid phase product from methane oxidation using proton NMR (^{1}H-NMR)

Nuclear magnetic resonance (NMR) is widely used technique to obtain structural information of compounds, especially organic species and it is mainly used in this work to analyse the liquid-phase products. The principle of the technique is the resonant absorption of radio frequency radiation by nuclei exposed to magnetic field. In order to be NMR active, the nuclei need to have zero spin angular momentum *I*, as for ^{1}H which has *I*=1/2 as well as ^{13}C. Nuclei like ^{16}O and ^{12}C are not NMR active since having I=0.[5] In fact, the most widely used nuclei in NMR are ^{1}H and ^{13}C since these two nuclei are the most abundant in organic compound and its possess a significant magnetogyric ratio which leads to a high NMR signal which important to the instrument sensitivity. Considering the amount of product to be analysed could be in the range of micromole, the analysis was carried out in highly sensitive 500 MHz machine (^{1}H- NMR, Bruker 500 MHz).

Typically, the 0.7 ml volume of liquid solution was placed into NMR tube and 0.1 ml of Deuterium oxide, D_2O (99.9%, Fluorochem) was added as a lock reference. A solution of Deuterium chloroform ($CDCl_3$) containing tetramethylsilane (TMS) ($CDCl_3$ 99.8 atom% D contain 1% (v/v) TMS, from Aldrich) was used as external standard. This external standard was sealed in glass ampoule, provides a signal resonance at 0 ppm where all other product resonances can be standardised.

A series of different concentrations of methanol were prepared using the following concentration in NMR tube 0.7, 3.5, 5.3, 7.0 and 10.5 μmol, respectively. These different methanol standards were subjected to ^{1}H-NMR analysis together with D_2O and glass sealed external standard. The ^{1}H-NMR spectra (figure 2.2) of methanol were recorded and standardised against TMS signal generating the calibration curve illustrated in figure 2.3. A linear correlation between actual and calculated methanol concentrations was observed across the whole concentration range tested. The concentration of TMS obtained in sealed tube was used to calibrate and quantify the products in liquid phase.

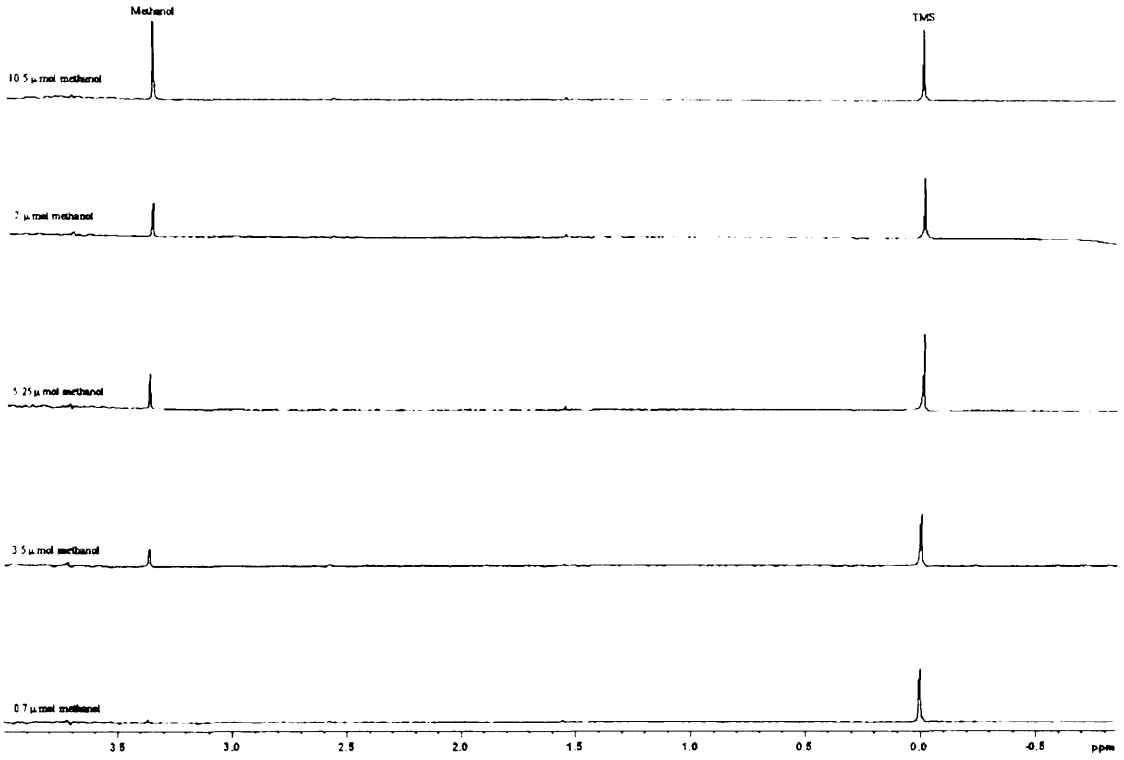

Figure 2.2: ^{1}H-NMR spectra of the various solution concentrations of methanol

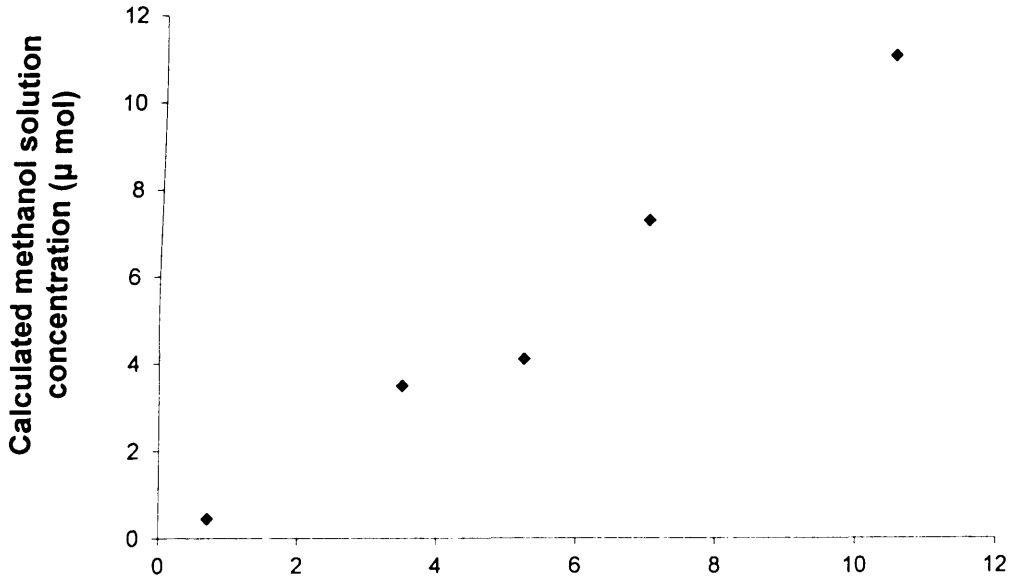

Figure 2.3: ^{1}H-NMR methanol calibration curve

During ^{1}H-NMR analysis, proton in the range of -15 to 15 ppm scan was used followed by solvent suppression pulse sequence to minimise the interference from the dominant water signal and permits the detection of products as low as 0.1 μmol. In some cases, the reaction was carried out in D_2O instead of H_2O in order to have better signal for the products.
In order to estimate the error during analysis, the analysis of known concentration of methanol was analysed three times. This will generate an average value which could estimate the error of analysis. The procedure was carried periodically to ensure the reliability of the analysis. At the same time, similar procedure was carried out to analyse a liquid sample from reaction. Based on several analyses, it was estimated that the error of analysis was around 5%. Besides, the concentration of TMS as external standard in sealed tube was monitored periodically by analysing at least four different known concentrations of methanol. In another approach to verify and validate the data obtained from ^{1}H-NMR analysis, similar liquid samples were subjected to gas-chromatography analysis (see section 2.4.2.2). The results indicated that the mole of each product was in agreement with the value observed with ^{1}H-NMR.

The ^{1}H-NMR chemical shift of products and standard was shown in table 2.1 below:

Table 2.1: The ^{1}H-NMR chemical shifts of possible products from methane oxidation and chemical shift for external standard

Entry	Products and/or std	Chemical Shift (ppm)
1	Methanol, CH_3OH	3.4
2	Methyl hydroperoxide, CH_3OOH	3.9
3	Formaldehyde, HCHO	9.1
4	Hydrated formaldehyde	5.1
5	Formic acid, HCOOH	8.3
6	Tetramethyl silane, TMS (as standard)	0
7	Deuterated chloroform, $CDCl_3$ (as standard)	7.2

Example of ^{1}H-NMR spectrum from the oxidation of methane in liquid phase using Au based supported heterogeneous catalyst was displayed in figure 2.4

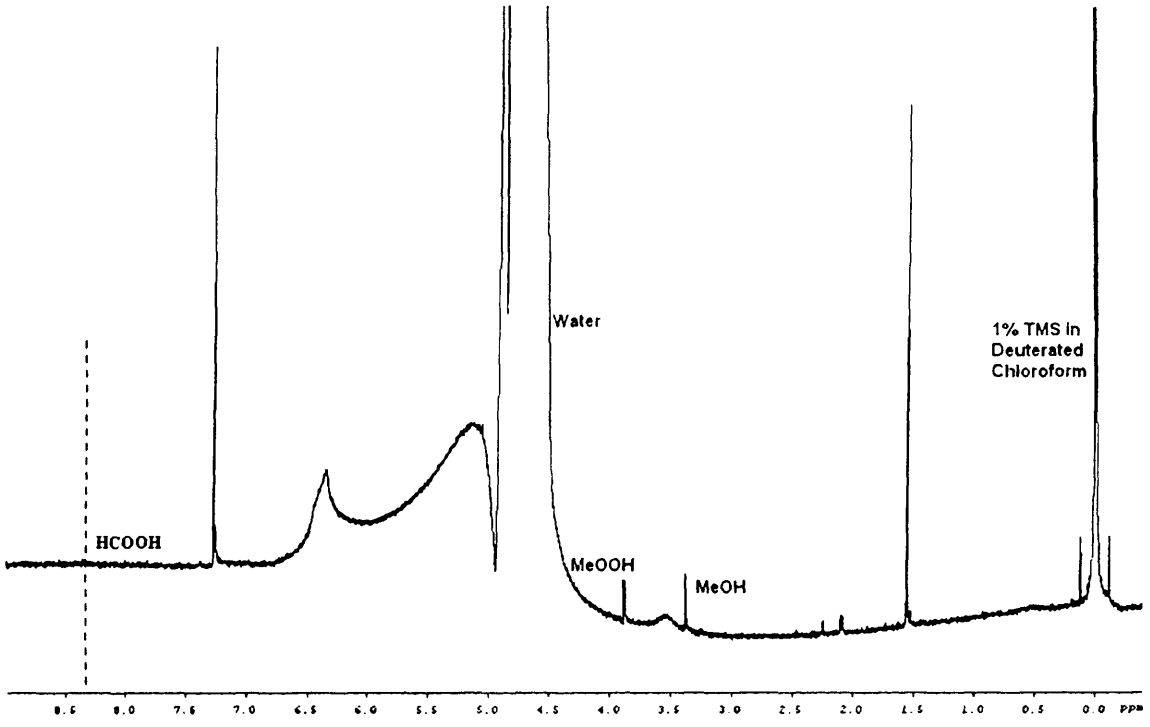

Figure 2.4: Typical ^{1}H-NMR spectrum with Au based supported catalyst.

2.4.2.2. Analysis of liquid phase products from methane oxidation using Gas Chromatography with Flame Ionisation Detector (GC-FID) and Mass Spectroscopy (MS) detector

In addition to ^{1}H-NMR, GC-FID (Varian 450-GC fitted with a CP-Sil 5CB capillary column (50m length, 0.32mm ID)) was used to corroborate the assignment of the peaks. A sample is first injected into the entrance of the column (injection port) by a sample syringe, and vaporized. It is subsequently flushed onto the column by an inert gas, such as helium or nitrogen, which is known as the mobile phase. The interaction between the molecules in the mobile phase and stationary phase sets up an exchange equilibrium that causes individual products to be retained on the column for different lengths of time. Each separate compound therefore elutes inside the column at different speeds, depending on their specific interaction. For instance, different in polarity of the samples will caused different interaction with column stationary phase, generally the more polar solute will

more tenaciously adsorbed onto the surface of an adsorbent consequently elute at higher retention time.[6] In case of samples with almost similar polarity, the solute with bigger formula molecule will eluted slower than the smaller formula molecule counterpart. An example of this can be seen in this study where retention time for methane was shorter compared to ethane in similar analysis condition. In general, the choice of column normally relies on the nature of the samples to analyse. A FID (flame ionisation detector) detector was used to analyse the effluent stream. Products in a sample are therefore individually detected by a computer, with the comparison of the retention times with authentic standards allowing the identification of the products. To obtain reliable quantitative data for liquid oxygenates, isopropyl alcohol (IPA) was used as external standard. Three different concentration of methanol were used in obtaining methanol calibration curve and the calibration factor was calculated as follows;

$$CF = \frac{mol(MeOH)}{mol(isopropanol)} x \frac{PA(isopropanol)}{PA(MeOH)} \qquad \text{(Equation 1)}$$

Equation 1: Formula for calculating the calibration factor with respect to the concentration and peak area of constituent.

In addition to FID as detector, gas-chromatography equip with mass spectrometry (GC-MS, column: 30 m CP-Wax 52 CB column) also was used to identify and verify the product obtained in liquid phase reaction solution (see appendix A.2).

2.4.2.3. Method to establish the presence of alkyl hydroperoxide in reaction solution

Even though two independent procedures have been developed and established, most of the liquid product analyses were carried out through ^{1}H-NMR technique. This is due to the stability issue of the product since alkyl hydroperoxide was detected as primary product. This intermediate species is not stable at higher temperature and it decomposes thermally in the GC's injector port during injection. However, periodically both ^{1}H-NMR and GC-FID were used in qualitative and quantitative verifying of obtained products. This was carried out by following the procedure developed by Shulpin and co-workers.[7,8] The liquid sample was analyzed twice, *i.e.* before and after the addition of excess of sodium borohydrate ($NaBH_4$). The reason is that the alkyl hydroperoxide formed are quantitatively

transformed under the action of reducing agent into the corresponding alcohol, therefore, this method allowed to calculate the real concentrations of the product in the solution. In standard test, an excess (*i.e.* 2:1 mol/mol ratio) of this reducing agent was added into the solution before subjected to ^{1}H-NMR analysis and it then was compared to the analysis data of the solution before addition of $NaBH_4$.

2. 4.2.4. Analysis of gas products from methane oxidation

2.4.2.4.1. Gas phase analysis using gas chromatography

Gas Chromatography system (Varian 450-GC equipped with FID & TCD detectors, CP-SiL5CB column (50m, 0.33mm diameter, Helium carrier gas) was used to identify and quantify the gas phase product from the reaction. To establish the identification of each possible gas involved in the reaction, authentic samples of each gas (methane, CO, CO_2) were analysed separately. Since the retention time of each samples was established, three known CO_2 standards (10, 103 and 1011ppm in air) were injected in to the GC via the manual injection port to construct a calibration curve (see appendix A.3). In order to increase the detectability limit of the products, the GC was also equipped with a methanizer. A plot of the average counts for each sample versus the CO_2 concentration was used to construct a calibration curve, which would later allowed determining the CO_2 concentration of a sample.

To obtain accurate area and minimising systematic error from the peaks obtained, the GC's column was purged until no peak of CO_2 was observed before performing the analysis. Quantification of CO_2 in gas sample was done by calculating theoretical mole of CH_4 based on Ideal Gas Law (see equation 2).

$$PV = nRT, \text{ rearranged to, } \quad n = \frac{PV}{RT} \qquad \text{(Equation 2)}$$

Where, P is pressure of use gas

V is volume of gas on top of the liquid in autoclave

R is gas constant

T is temperature

n is mol of gas

2.4.2.4.2. Analysis of gas in liquid using gas chromatography

In order to fully quantify the carbon oxide (CO_x), the liquid solution also was subjected to GC analysis. Similar to gas phase analysis, the retention time of each possible gases especially CO and CO_2 were established using authentic samples. The sum of moles of CO_2 obtained in liquid and gas giving the exact amount of CO_2 produced during reaction. In this procedure, nitrogen (N_2) is used to flush the GC injection port for 5 minutes before performing any analysis and a nitrogen atmosphere was maintained above the GC injection ports. Using previously degassed water, a solution of oxidant for the reaction was prepared and quickly analysed for CO_2 in liquid phase by injection of the solution into the GC injection port. The reaction was carried out as usual taking care to note the amount of gas phase CO_2 presented in the reaction gas at the start of the run. After reaction was completed and cooled, a degassed solution sample was injected into the GC under N_2 atmosphere, to ensure that the CO_2 detected was around the same value as noted in the first instance. Then the reactor was quickly degassed and the Teflon/glass liner removed. The mixture should not be greatly disturbing during removal. Within 1-2 minutes after removal, 20 μL of the reaction mixture was injected into the GC for analysis and this is always done under N_2 atmosphere. For reproducibility the second sample was injected after 5-6 minutes as well. The standard CO_2 in gas analysis was performed on the previously collected sample. The sum of the liquid and gas analyses gives the number of moles of the CO_2 produced in the reaction.

2.4.3. Ethane oxidation.

2.4.3.1. Analysis of liquid phase products from ethane oxidation using proton NMR (^{1}H-NMR)

Similar procedures as shown in section 2.4.2.1 were used in liquid-phase products analysis from ethane oxidation where ^{1}H nuclear magnetic resonance (^{1}H-NMR, Bruker 500 MHz) was used as primary instrument. ^{1}H-NMR chemical shift of possible products also external standard was shows in table 2.2. For each compound, the authentic sample was subjected to 1H-NMR analysis and the chemical shift obtained was compared with available literature.

Table 2.2: Proton NMR (^{1}H-NMR) chemical shift of possible liquid products from ethane oxidation and chemical shift for external standard

Entry	Product	Chemical Shift, ppm
1	Acetaldehyde	3H, duplet, 2.25
		1H, quartet, 9.70
2	Acetaldehyde, hydrate	3H, duplet, 1.33
		1H, quartet, 5.25
3	Methanol	3H, singlet, 3.35
4	Ethanol	3H, triplet, 1.19
		2H, quartet, 3.67
5	Ethyl hydroperoxide	3H, triplet, 1.21
		2H, quartet, 4.06
6	Acetic acid	3H, singlet, 2.08
7	Ethyl acetate	3H, triplet, 1.25
		3H, singlet, 2.08
		2H, quartet, 4.15
8	Formic acid	H, singlet, 8.35
9	Tetramethyl silane, TMS (as standard)	0, singlet
10	Deturated chloroform, $CDCl_3$ (as standard)	7.2, singlet

An example of the ^{1}H-NMR spectrum for some of the products is shown in figure 2.5 – 2.7. The confirmation of chemical shift responsible for acetaldehyde and as well as of its hydrated form (figure 2.5) was verified by an analysis of authentic acetaldehyde and by comparing the spectrum with available literature.[9]

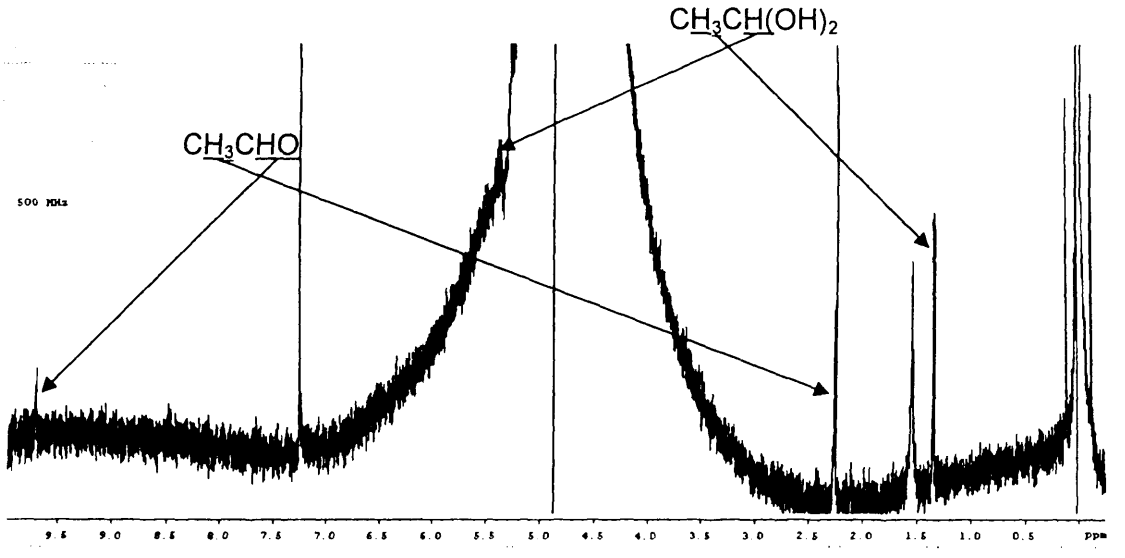

Figure 2.5: ^{1}H-NMR spectrum of acetaldehyde and hydrated form of acetaldehyde.

Due to the lack of commercial availability of ethyl hydroperoxide (CH_3CH_2OOH), as alternative step has been taken to synthesis it locally in the lab. This was carried out by performing the typical reaction of ethane in the presence of copper oxide catalyst. As discussed in detailed in chapter 6, copper based catalyst selectively produced alkyl hydroperoxides as the main product. The presence of ethyl hydroperoxide (figure 2.6) as main product in reaction solution was confirmed by following the same method used in section 2.4.2.3. It was proven in this study where the reduction of solution containing ethyl hydroperoxide solely produced ethanol.[10]

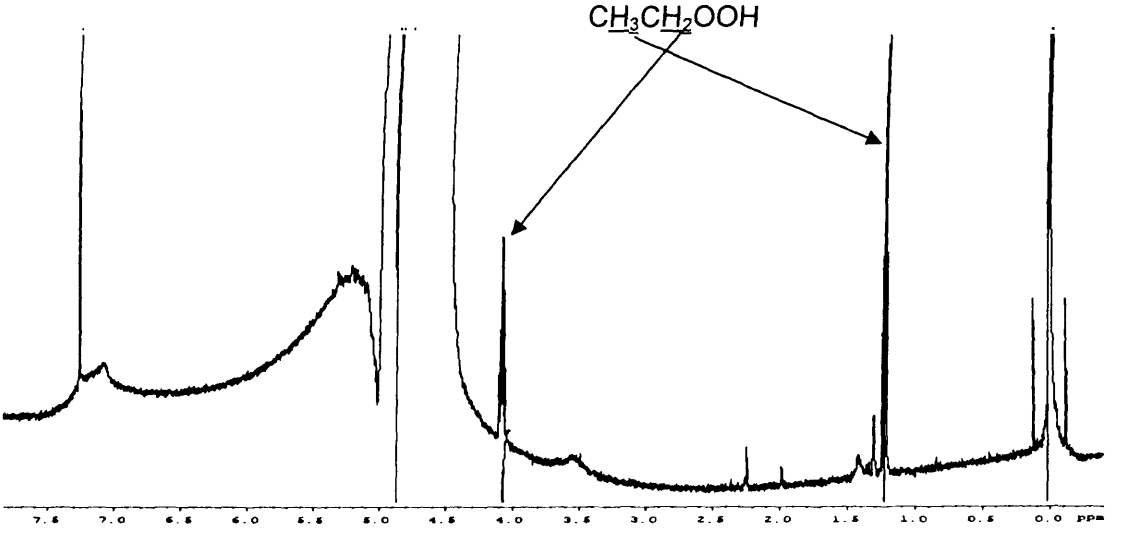

Figure 2.6: ^{1}H-NMR spectrum of ethyl hydroperoxide

In order to support this analysis and due to the fact that the only signal corresponds to ethyl acetate which possibly interfere with the chemical shift signal observed in solution-containing ethyl hydroperoxide, the solution containing ethyl hydroperoxide was spiked with ethyl acetate. The ^{1}H-NMR spectrum of spike sample clearly showed the difference between ethyl hydroperoxide and ethyl acetate (figure 2.7).

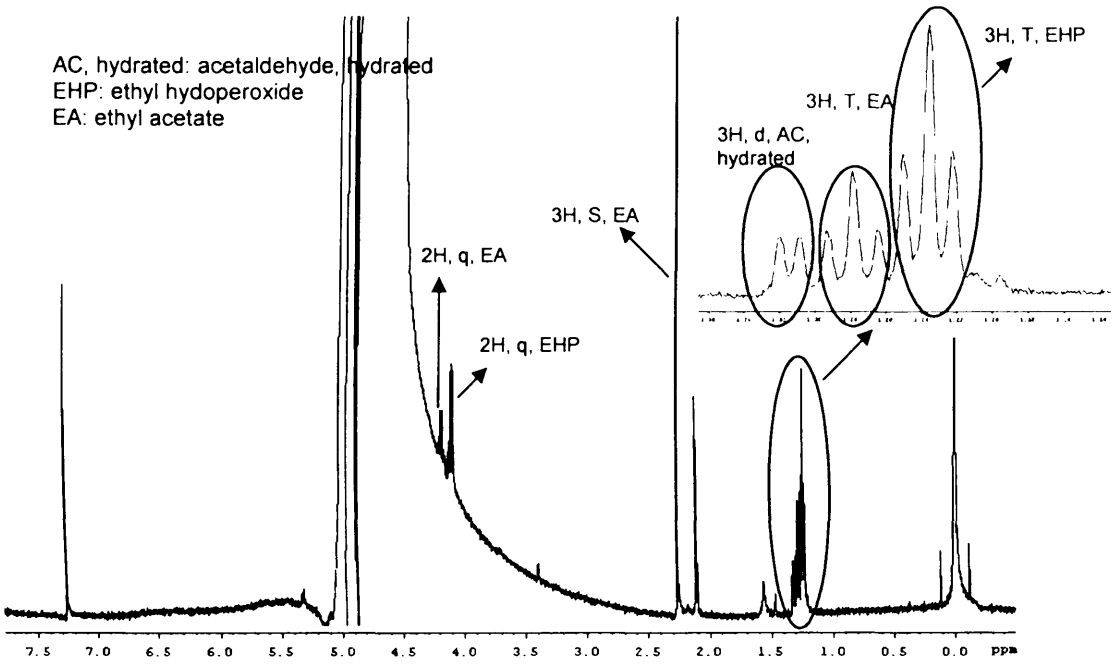

Figure 2.7: ^{1}H-NMR spectrum of solution containing ethyl hydroperoxide with ethyl acetate

Then, chemical shift attained from the analysis as discussed above was used as standard reference for ethyl hydroperoxide identification in ^{1}H-NMR. In addition, the presence of ethyl hydroperoxide (EtOOH) also has been checked using Gas Chromatography (GC-FID). The solution was treated with $NaBH_4$ as demonstrated above. The intensity of ethanol peak and area were increased due to the formation of ethanol from ethyl hydroperoxide. For confirming the authentication of the peaks of the products in GC-FID, authentic samples were injected and the retention time of each product is shown in table 2.3:

Table 2.3: Gas Chromatography retention time of possible liquid products from ethane oxidation

Entry	Product	Retention Time, min
1	Acetaldehyde	5.99
2	Methanol	6.01
3	Ethanol	8.46
4	Acetic acid	19.19
5	Ethyl acetate	24.78
6	Formic acid	Not detected

Even though proton NMR is a suitable instrument to analyse the liquid-phase sample, the difficulty may be arisen from the overlapping of chemical shift of certain product especially between ethyl hydroperoxide and ethanol (in some cases). This may have an effect on the integration of the respective products. Therefore, a combined analysis of liquid-phase product in both GC-FID and ^{1}H-NMR together with reduction treatment could solve the problem.

2.4.3.2. Analysis of gas products from ethane oxidation

Similar procedure as shown in section 2.4.2.4 was used for the analysis of gas-phase products a from ethane oxidation.

2. 5. Catalyst stability

One of the key factors that must be considered for heterogeneous catalysts operating in three phase systems is the possibility that active metal components can leach into the reaction mixture, thereby leading to catalyst deactivation or, to the formation of an active homogeneous catalyst. Therefore, the reaction solutions were filtered to remove the particles of catalyst and analysed by atomic absorption spectroscopy (AAS) or inductive couple plasma with mass spectrometer detector (ICP-MS) in order to determine the amount of leached metal.

To ensure if the catalyst retained its original activity and selectivity, two procedures have been set up *i.e.* drying and decantation procedure. In the first procedure, the reaction mixture was filtered and the recovered catalyst was dried typically at room temperature or at 110 °C overnight or recalcined at 400 °C in static air for 3 h. Then, the recovered powder was used to perform a new reaction as the same as fresh catalyst. In most cases, the procedures were repeated at least three times.

On the second procedure, the decantation method was developed to eliminate the factor that may arise from the catalyst recovering protocol. After completion of the reaction, the liquid solution above the solid catalyst was completely decanted, then a fresh solution was added and the reaction was repeated. The solution after final used also has been subjected to leaching test. Moreover, the metal loading of fresh and used catalyst was analyzed by AAS analysis and a detailed analysis is shown in section 2.9.3.

2.6. Stability of products

In order to verify the stability of the products produced during reaction, the experiments have been set up by mimicking the typical reaction conditions. Inert gas such as Helium or Nitrogen was used instead of alkane in the presence of each possible product at the start of the reaction, respectively. Typically, for each compound the experiment was carried out twice, either in the absence or presence of catalyst. In some cases, labelled compound *i.e.* $^{13}CH_3OH$ was used and the reaction solution has been subjected to ^{1}H-NMR analysis. The percentage of product transformation was calculated based on comparing the concentration of initial and final compound. In addition, consecutive oxidation of each product was monitored in ^{1}H-NMR spectrum.

2.7. Hydrogen peroxide synthesis

Hydrogen peroxide synthesis was performed using in the same reaction set up as used on alkane oxidation. For the standard test conditions, the autoclave was charged with the catalyst and solvent (typically H_2O), and purged three times with 5%H_2/N_2 and then filled with 5%H_2/N_2 and 25%O_2/N_2 at a calculated total pressure. Stirring (1500 rpm) was commenced after reaching the desired temperature, and experiments were carried out for the desired time. Hydrogen peroxide produced was determined using the procedure mentioned in section 2.8.

2.8. Determination of hydrogen peroxide content

In order to determine the hydrogen peroxide (H_2O_2) remained after reaction or from *in-situ* H_2O_2 synthesis itself, titrimetric method was used by titrating aliquots of the fresh solution and the solution after reaction with acidified $Ce(SO_4)_2$. $Ce(SO_4)_2$ solutions were standardized against $(NH_4)_2Fe(SO_4)_2\ 6H_2O$ using ferroin as indicator.[11]

2.9. Catalysts characterisation

2.9.1. Powder X-ray diffraction (XRD)

2.9.1.1. Background

The XRD is used to characterise the bulk of a crystal structure, to monitor the kinetics of bulk transformations and to estimate the crystallite size by diffraction of an X-ray beam (Cu Kα with an energy of 8.04 keV and a wavelength of 0.154 nm) as a function of the angle 2θ of the incident beam. X-rays scattered by atoms in ordered lattice interference constructively in directions given by Bragg's Law (Equation 3).[6,12]

$$n\lambda = 2d\sin\theta,\ n = 1,2,... \qquad \text{(Equation 3)}$$

Where, λ is the wavelength of the X-rays

d is the distance between two lattice planes

θ is the angle between the incoming X-rays and the normal to the reflecting lattice plane

n is an integer called the order of the reflection

The atomic planes of a crystal cause an incident beam of X-rays to be refracted at specific angles. This allows the identification of the structure when compared to a database of XRD patterns and the crystallite size from the width of the peaks. When sample is polycrystalline powder, the diffraction pattern is formed by a small fraction of the particles only and it can be improved by rotation of the sample during measurement in order to enhance the number of particles that contribute to diffraction.[12]

2.9.1.2. Experimental

The crystallographic phases composition present in the catalysts mentioned in this thesis has been characterised by using X-ray diffraction analysis (PANalytical MPD diffractometer) employing $CuK_{\alpha 1}$ radiation (λ□= 0.154098 nm) on the catalyst at ambient temperature and was scanned typically in the range of 10–70 degrees at setting of 40 kV and 40 mA. All powder samples were mounted on sample holders. The values of the d-spacing, intensity and full width at half maximum (FWHM) were calculated using X'Pert HighScore Plus software. The diffractogram obtained was matched against the Powder Diffraction File (PDF) database to confirm the catalysts phases. Crystallite size calculations were determined using the Scherrer equation (equation 4).[13]

$$\text{Crystallite size} = \frac{(K * \lambda)}{(FWHM * \cos\theta)} \qquad \text{(Equation 4)}$$

Where, K is the Scherrer constant

λ is the wavelength of X-ray

FWHM is the full peak width at half maximum

θ is the angle of diffraction

However, the applicability of the technique is normally limited to compounds with particle sizes greater than 5 nm, since extensive broadening occurs for smaller particles, and clear diffraction peaks are only observed when the sample possesses sufficient long-range order. In some cases, relative intensity of the peak was used to roughly determine the changes in metal composition.

2.9.2. Brunauer Emmet Teller (BET) surface area measurements

2.9.2.1. Background

Nitrogen adsorption at boiling temperature (77 K) represents the most widely used technique to determine catalyst surface area and to characterize its porous texture. The model, developed by Brunauer, Emmet and Teller in 1940s,[14] still remains the most diffuse tool to determine the monolayer volume (V_m) of the adsorbate, and then the surface area of solids by the equation 5:

$$Surface\ area = (Vm/22414)Na\sigma \qquad \text{(Equation 5)}$$

Where N_a is Avogadro number and σ the area covered by one nitrogen molecule. The σ value generally accepted is 0.162 nm^2.[15] Monolayer volume (V_m) can be estimated by the three parameters BET equation by assuming that:[16]

1. The heat of adsorption of first monolayer is constant (the surface is uniform as concerns the adsorption),
2. The lateral interaction of adsorbed molecules is negligible,
3. The adsorbed molecules can act as new adsorption surface and the process can repeat itself,
4. The heat of adsorption of all monolayer however the first is equal to the heat of condensation.

Nowadays, BET method is the most widely used to determine surface area of solids and it can be regarded as a reference method.

2.9.2.2. Experimental

The analysis of BET surface area measurements was obtained by performing nitrogen adsorption-desorption isotherm at liquid nitrogen temperature (77 K) using Micrometics Gemini 2360 surface analyzer. Typically, at least ~0.1 g sample was used at each time. The catalyst was previously degassed at 120 ^{o}C for 45 minutes. For the surface area experiment, there is a ±10% error in the recorded values due limitations in the technique and the varying amounts of catalyst tested in each analysis. Due to the some limitations of the instrument mentioned above, the analysis also has been carried out on an Autosorb 1, Quantachrome instrument.

2.9.3. Atomic absorption spectroscopy (AAS)

2.9.3.1. Background

Atomic absorption measure the absorption of radiation by gaseous atoms.[6] Samples are atomized using thermal energy from either a flame or a graphite furnace. Because the width of an atom's absorption band is so narrow, the continuum sources common for molecular absorption cannot be used. Instead, a hollow cathode lamp provides the necessary line source of radiation. The amount of energy, *i.e.*, wavelength, is specific to a particular electron transition and in a particular element the width of an absorption line is only of the order of a few picometers (pm), which gives the technique its elemental selectivity. Therefore, for each element need a specific lamp. Typically, AAS analysis requires standards with known analyte content to establish the relation between the measured absorbance and the analyte concentration. Since the technique is only capable in analysing the liquid sample, the solid sample to be analysed have to be dissolved in other solution such aqua regia or other appropriated solvent. In addition to that, it is crucial that the properties of the standard solutions such as the acidity or viscosity are similar with the sample's solution. This is important to reduce and avoid any systematic errors due to the difference in properties of the solution.

2.9.3.2. Experimental

The chemical composition was determined by using atomic emission spectroscopy (AAS) Perkin-Elmer 2100 Atomic Absorption spectrometer using an air-acetylene flame. Analysis of actual metal loading incorporated into the support was performed by digesting a known quantity of the dried catalyst (0.1 g) in an aqua regia solution, followed by the addition of 250 ml deionised water to dilute the sample. At least three standards were prepared for each related metal. As a control, a blank solution was used. Blank solutions were added with similar amount of aqua regia to be consistent with the solution of the samples. Absorbance obtained from the fresh and used catalyst was compared to the standard and the percentages of metal loss were calculated by comparing the obtained metal loading.

In addition to that, the concentration of metal that had leached out into solution during reaction was tested. This was carried out by analyzing the filtrate sample from the reaction. The obtained value was then calculated and compared to the actual percentages of each metal in fresh catalyst.

2.9.4. Thermogravimetric analysis (TGA)

2.9.4.1. Background

Thermogravimetric analysis measures the weight loss of material as a function of temperature.[6] Weight losses are given as percentage of the total sample weight and can be used to identify the species lost during course of the temperature ramp. A specific mass of sample is placed into crucible and heated to a required temperature under specified atmosphere and temperature ramping. Normally the data is plotted as weight loss against temperature and a large variation in mass over a small temperature suggests a phase change within the sample. The use of gas is depending on the required information to be obtained. In this study, TGA was used to determine the phase transformation for copper oxide catalyst.

2.9.4.2. Experimental

Analysis was conducted using a Setaram Setsoft TG/DTA machine. A typical example for obtaining a TGA pattern is as follows. 50 mg of a sample was placed into an aluminium oxide crucible for analysis. The analysis was performed in air. The temperature programmed was used to have an isothermal time period at 30 °C for 16 minutes, and then a temperature ramp to 800 °C at a ramp rate of 5 °C/min was used.

2.9.5. Scanning electron microscopy (SEM)

2.9.5.1. Background

Electron microscopy is a technique to determine the morphology and size of the sample together with the information on the composition and structure of the particles.[12] The principle is similar to the simple light microscope, however instead using light the electron microscope use high energy of electron beam. In case of scanning electron microscopy (SEM), it uses a beam of high energy electrons to examine the topology, morphology and composition of a sample. The electron beam is generated from a field emission gun which comprises a very fine single crystal of tungsten. A series of fine apertures and lenses focus the beam to a fine point and directly onto sample producing secondary electrons, which are detected and accumulated into the final image (figure 2.8). In addition to secondary electron, backscattered electron also has been used in this study to observe the metal catalyst dispersion on the support. The secondary electrons have mostly low energies and originate from the surface of the sample whilst the backscattered electrons come from deeper regions and carry the information on the composition of the sample due to the heavy elements are more efficient scatterers and appear brighter in the image.[12] Although it has limitation up to certain resolution and inferior compared to transmission electron microscopy. In this study, SEM mostly used to observe the morphology of series of copper oxide catalyst.

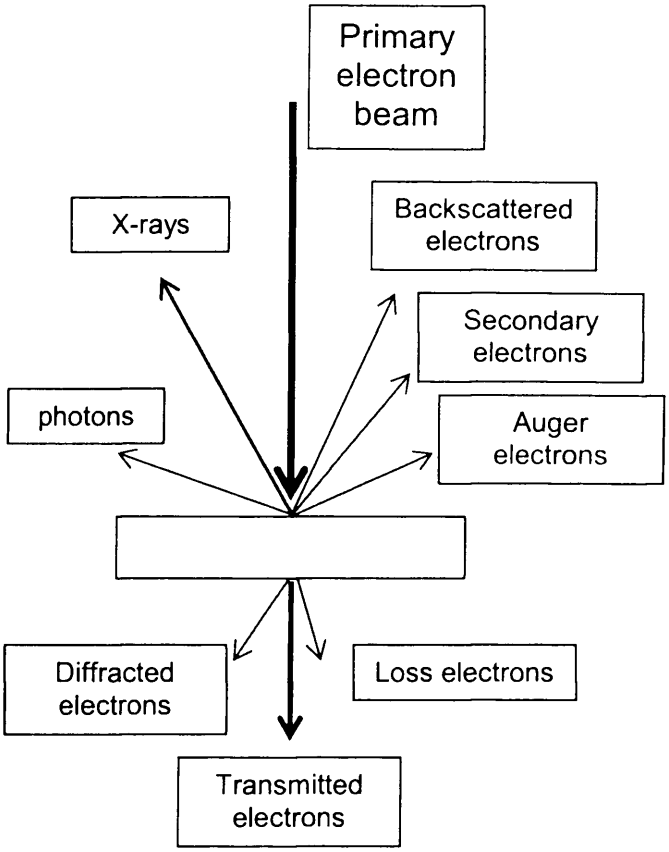

Figure 2.8: The interaction between the primary electron beam and the sample in an electron microscope

2.9.5.2. Experimental

SEM analysis was performed using Carl Zeiss SMT EVO series electron microscope at department of chemistry, Cardiff University. The samples were adhered on the aluminium stub using carbon conductive tape. The stub was then mounted on the stub holder and loaded into the chamber and evacuated for analysis. The SEM micrographs were captured and recorded using image capture and processing software at various magnifications.

2.9.6. X-ray photoelectron spectroscopy analysis (XPS)

2.9.6.1. Background

X-ray photoelectron spectroscopy is based on the photoelectric effect where a sample is irradiated with a monochromatic beam of X-rays.[12,17] The X-rays provide an energy in term of photon which later been absorbed by atom leading to ionisation and emission of valence electrons with specific kinetic energy. This information was used to calculate the binding energy of photoelectron using equation given below:

$$E_k = h\nu - E_b - \varphi \qquad \text{(Equation 6)}$$

Where, E_k is the kinetic energy of the photoelectron

h is Planck's constant

v is the frequency of the exciting radiation

E_b is the binding energy of the photoelectron with respect to the Fermi level of the sample

φ is the work function of the spectrometer

Given that for each element there is a characteristic binding energy associated with each core atomic orbital, it will give to a characteristic peak for each element. Therefore, it make XPS among the most commonly used techniques in characterisation of the catalyst where it has a capability to quantitatively measures the elemental composition, the oxidation state and in some cases determine the dispersion of one phase over another.

2.9.6.2. Experimental

X-Ray photoelectron spectroscopy (XPS) was performed using a VG EscaLab 220i spectrometer, using a standard Al-Kα X-ray source (300 W) and analyzer pass energy of 20 eV. Samples were mounted using double-sided adhesive tape, and binding energies were referenced to the C 1s binding energy of adventitious carbon contamination, which taken to be 284.7 eV.

2.9.7. Temperature programmed reduction analysis (TPR)

2.9.7.1. Background

Temperature programmed analysis is a very useful method to investigate the interaction between a test molecule and a catalyst surface and this application has been applied to study the gas adsorption on metals and metal oxides. Temperature programmed reduction (TPR) analysis allows to determine the number and quantity of the reducible species present in the sample.[18] It is also used as "finger-print" to investigate the different types of oxygen present in the catalyst which involved in the oxidation process under that catalyst. In this work, TPR has been used to collect the information on the oxidation state species of supported metals and to identify metal mixing in the case of alloy formation using bimetallic or trimetallic supported catalyst.

2.9.7.2. Experimental

Temperature programmed reduction (TPR) profile of the catalysts were obtained using ThermoElectron TPDRO 1100 instrument utilizing with thermal conductivity detector (TCD). All the experiments were carried out by *in-situ* procedure using 10% H_2 in Argon (25 mL min^{-1}). The catalysts were pretreated under Helium flow (20 mL min^{-1}) at 383 K for 30 minutes before cooling them to 308 K. Then the flow was switched to 10 % H_2/Ar (15 mL min^{-1}) stream and the temperature was raised to 973 K at 5 K min^{-1}. The reduction was measured by monitoring the hydrogen consumption through the TCD detector

References:

1. Lopez-Sanchez, J. A.; Dimitratos, N.; Hammond, C.; Brett, G. L.; Kesavan, L.; White, S.; Miedziak, P.; Tiruvalam, R.; Jenkins, R. L.; Carley, A. F.; Knight, D.; Kiely, C. J.; Hutchings, G. J. *Nat Chem* **2011,** *advance online publication.*
2. Matijević, S. K. a. E. *Journal of Material Research* **1991,** *6*, 766-777.
3. Zhu, J.; Li, D.; Chen, H.; Yang, X.; Lu, L.; Wang, X. *Materials Letters* **2004,** *58*, 3324-3327.
4. Wu, Y.; He, Y.; Wu, T.; Chen, T.; Weng, W.; Wan, H. *Materials Letters* **2007,** *61*, 3174-3178.
5. Atkins, P. W. *Physical Chemistry*; Oxford University Press, 1998.
6. D. Kealey, P. J. H. *Analytical Chemistry*; BIOS Scientific Publishers Limited: Oxford, 2002.
7. Süss-Fink, G.; Nizova, G. V.; Stanislas, S.; Shul'Pin, G. B. *Journal of Molecular Catalysis A: Chemical* **1998,** *130*, 163-170.
8. Süss-Fink, G.; Yan, H.; Nizova, G. V.; Stanislas, S.; Shul'pin, G. B. *Russian Chemical Bulletin* **1997,** *46*, 1801-1803.
9. Nagai, Y.; Morooka, S.; Matubayasi, N.; Nakahara, M. *The Journal of Physical Chemistry A* **2004,** *108*, 11635-11643.
10. Nizova, G. V.; Süss-Fink, G.; Shul'pin, G. B. *Tetrahedron* **1997,** *53*, 3603-3614.
11. Ntainjua N, E.; Edwards, J. K.; Carley, A. F.; Lopez-Sanchez, J. A.; Moulijn, J. A.; Herzing, A. A.; Kiely, C. J.; Hutchings, G. J. *Green Chemistry* **2008,** *10*, 1162-1169.
12. Niemantsverdriet, J. W. *Spectroscopy in Catalysis, An introduction*; Wiley-VCH Publisher, 2000.
13. Klug, P. H., Alexander, E. *X-ray Diffraction Procedures for Polycrystalline and Amorphous Materials*, 2nd edition ed.; John Wiley and Sons New York, 1974.
14. Brunauer, S. *The Adsorption of Gases and Vapors*; University Press Oxford, 1945.
15. Partyka, S.; Rouquerol, F.; Rouquerol, J. *Journal of Colloid and Interface Science* **1979,** *68*, 21-31.
16. Leofanti, G.; Padovan, M.; Tozzola, G.; Venturelli, B. *Catalysis Today* **1998,** *41*, 207-219.
17. Hollas, J. M. *Modern Spectroscopy*, Fourth Edition ed.; Wiley: Sussex, England, 2004.
18. Lucarelli, M. F. A. L., 1999; pp. 1-5.

CHAPTER 3

Selective Activation of Primary C-H Bonds – Toluene as a Proof of Concept Study

3.1. Introduction

In recent years, the unexpected high activity of gold as a low-temperature CO oxidation catalyst has initiated intensive research in the use of gold nanoparticles for reactions involving C-H hydrocarbon.[1-3] Gold-based catalysts have demonstrated a very promising activity with different types of homogeneous and heterogeneous catalysts based on nano-particles or metal complexes developed for the oxidation of alcohols as discussed in chapter 1. Enache and co-workers have investigated the effect of Au-Pd ratio on catalytic oxidation of benzyl alcohol.[4,5] They used Au-Pd nanoparticles supported on the surface of TiO_2 with the optimum weight ratio for this bimetallic system being 2.5% Au and 2.5% Pd. By performing the reaction in solvent-less conditions, toluene was observed as one of the by-products and the selectivity profile changed progressively with time. Moreover, Au-Pd supported nanoparticles as a catalyst is known to work by creating reactive hydroperoxy intermediates[6,7] which is similar to active oxygen species responsible for activating primary C-H bonds in the enzymatic methane monooxygenase (MMO) system.[8] Therefore, these observations have led to further possible studies on oxidation of primary C-H bonds in toluene or even in lower alkanes such as methane and ethane using this approach.

The goal of this study was to use a supported gold-palladium bimetallic nanoparticles as a catalyst in a proof-of-concept studies on oxidation of primary C-H hydrocarbons. Toluene and 4-methoxytoluene were selected as substrates and the reactions were carried out using a high pressure autoclave reactor and molecular oxygen (O_2) as oxidant. The Au-Pd supported catalysts were selected as they have been well characterised in literature also in most cases showing superior catalytic activity compared to equivalent monometallic catalysts.[4-6,9] The reaction parameters such as reaction temperature and time, mass of catalyst, catalyst preparation methodology and different support are presented in this chapter.

3.2. Oxidation of toluene

3.2.1. Oxidation at lower temperature and influence of catalyst preparation technique

The ability to activate and oxidise alkanes at relatively mild reaction conditions, specifically at lower temperature and pressure with molecular oxygen or air as the oxidant is highly challenging and target reaction for the catalysis community. Detailed discussion on the toluene oxidation process employed in industry as well as the available literature on both homogeneous and heterogeneous catalytic systems used in this reaction were previously mentioned in section 1.4 of Chapter 1. In general, the available catalytic systems for toluene oxidation reaction either involved undesirable approaches that was not environmental friendly or utilised homogeneous catalysts with stoichiometric oxidants. In addition to that, the reactions were carried out at relatively high temperature (>190 °C) which involved autogeneous processes and consequently it is difficult to control the selectivity to desire products. Industrial processes for oxidation of toluene either to produce benzaldehyde or benzoic acid as a target product utilised toxic substances. In the production of benzaldehyde, the reaction undergoes chlorination of toluene followed by saponification process.[10] The commercial production of benzoic acid, from the oxidation of toluene, is achieved by heating a solution of the substrate, cobalt acetate and bromide promoter in acetic acid to 250 °C, under an atmosphere of oxygen.[11] Although the commercial process involved homogeneous catalysts, there are many reported studies which utilise heterogeneous catalytic systems. However, at present, most of the literature on toluene oxidation with heterogeneous catalysts indicates that the reaction was carried out at high temperature range around 190 °C[12-14] and presence of solvent such as dichlorobenzene, benzene and dimethylformamide (DMF).[15-17] There are a few studies reported on toluene oxidation in solvent-less system[13,16] and there are still requirements for initiators or co-catalysts such as a sacrificial aldehyde to promote the oxidation process.[16]
In this study, the blank reaction in the absence of catalyst was performed primarily in order to verify the contribution from homogeneous reaction which possibly occurred especially when using molecular oxygen (O_2) as oxidant at elevated temperature and pressure. The experiment was conducted in a closed autoclave with O_2 at a constant reaction pressure, so that as the reaction proceeded and O_2 was consumed, oxygen was replenished. It is evident in figure 3.1 that blank reaction at 160 °C only gave less than 0.2% conversion after 7 hours reaction time. This provides an indication that autogeneous

reaction is not significant at this level of temperature and pressure. Given that the baseline reaction was established, the reaction was carried out with 5wt%Au-Pd/TiO_2 synthesised via an impregnation technique. Initially a very high substrate/metal molar ratio (S/M: 52000) with catalyst mass around 20 mg was used and the catalytic data showed an increase of toluene conversion by a factor of 3 compared to the blank reaction. In view of the general assumption that catalytic reactions are surface-based, then the catalytic activity and selectivity could be tuned by changing the catalyst properties or other catalyst related parameters. Thus by increasing catalyst mass (20 to 200 mg) in the reaction, a further increase in conversion to 1.6% after 7 hours was achieved. Theoretically, catalytic activity (based on turn over number (TON), see table 3.1) for both reaction should be the same, the difference might show the diffusion limitations evolved with higher mass of catalyst and since this study was focused to prove the concept, further detail on kinetic parameter effect is not reported here.

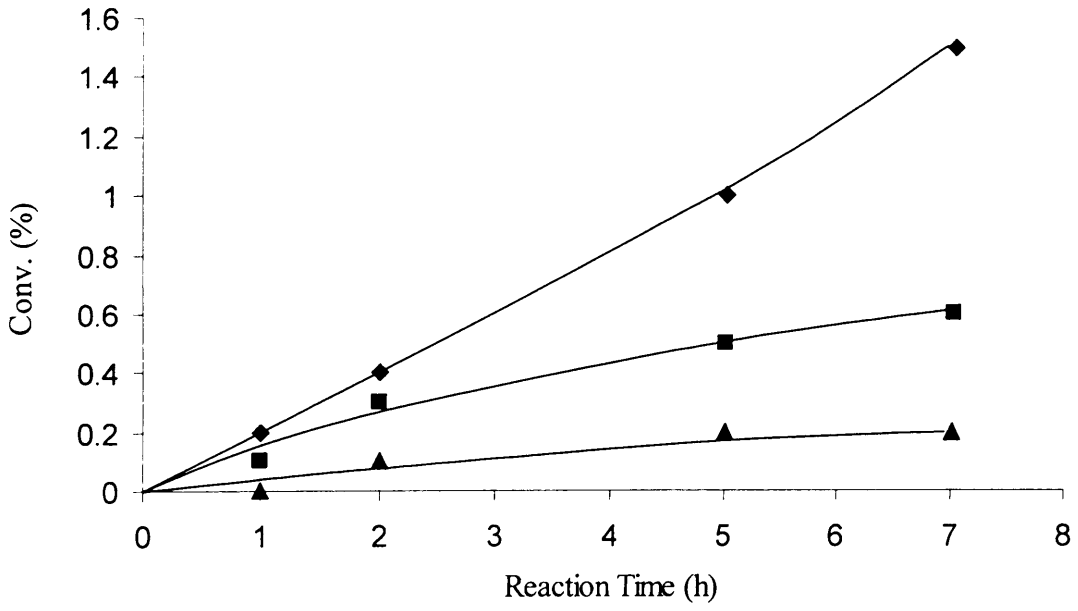

Figure 3.1: Conversion profile of blank and presence of the 5wt%Au-Pd/TiO_{2IW} catalyst in the liquid phase oxidation of toluene as a function of time. Reaction conditions: toluene = 40 mL, 20 and 200 mg of catalyst, temperature = 160 °C, pO_2 = 10 bar, time = 7 hours, stirring rate = 1500 rpm. Key: ▲blank conversion (%), ■ conversion (20 mg) (%),◆ conversion (200 mg) (%).

In terms of selectivity in blank reaction, benzaldehyde was observed as main product followed by benzyl alcohol then benzyl benzoate and trace of benzoic acid. It was reported that sequential oxidation of benzyl alcohol is rapid at similar range of reaction temperature.[4] Similar to blank reaction, benzaldehyde was the major product and by increasing the mass of catalyst not only increases the rate of reaction but also changing the product distribution (table 3.1). Consecutive oxidation of benzyl alcohol as a first product was observed and it was slower when a lower mass of catalysts was used.

Table 3.1: Comparison on product distribution in liquid phase oxidation of toluene in the presence of two different mass of 5wt%Au-Pd/TiO_{2IW} impregnated catalyst

Mass (mg)	Conv.	Selectivity (%)				TON[b]
	(%)	Benzyl alcohol[a]	Benzaldehyde[a]	Benzoic acid[a]	Benzyl Benzoate[a]	
-	0.2	18.0	76.3	2.3	3.4	-
20	0.6	37.4	49.7	9.9	3.0	325
200	1.5	5.4	60.9	23.6	10.2	78

Reaction conditions: toluene = 40 mL, time = 7 hours, temperature = 160 °C, pO_2 = 10 bar, stirring rate = 1500 rpm. [a] Analysis using GC- FID, [b] Turn over number (TON) = ((% conv. * mol of substrate) / mol of metal / 100 %)

Initially with higher catalyst loading (200 mg of catalyst), the selectivity to benzaldehyde was high (75% selectivity). However, as the reaction proceeded, the formation of benzoic acid increased indicating the over oxidation of benzaldehyde to benzoic acid (figure 3.2). In addition, benzyl benzoate was formed with low selectivity and could be originated from two different possible pathways.[7,18] Firstly as benzyl alcohol and benzoic acid are produced in the reaction solution, esterification could occur to generate benzyl benzoate product. Alternatively, the mechanism of benzyl benzoate generation could occur through oxidation of a hemiacetal. The hemiacetal itself originated via coupling of benzaldehyde and benzyl alcohol products. The latter route was previously shown in the studies on benzyl alcohol oxidation using Au supported on CeO_2 catalyst.[7] The combination of both pathways was possible and considered in this study.

In all cases, carbon mass balances were ~100%, and no carbon oxides were formed with Au-Pd/TiO_{2IW} catalysts.

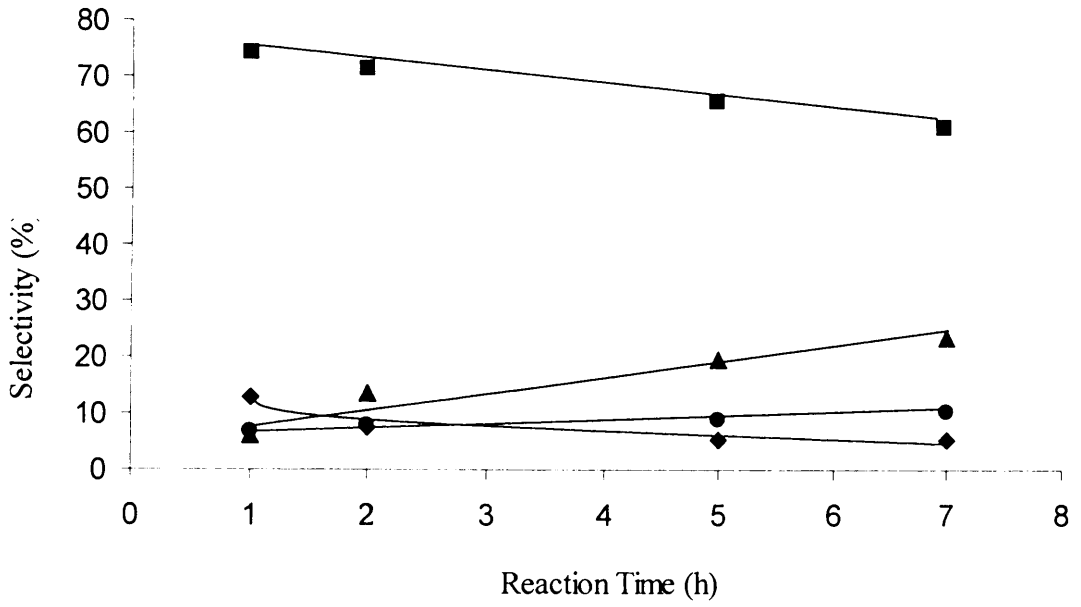

Figure 3.2: Selective oxidation of toluene in the presence of the 5wt%Au-Pd/TiO_{2IW}. Reaction conditions: toluene = 40 ml, 200 mg of catalyst, temperature = 160 °C, pO_2 = 10 bar, time = 7 hours, stirring rate = 1500 rpm. Key: ◆benzyl alcohol selectivity (%),■benzaldehyde selectivity (%),▲benzoic acid selectivity (%), ● benzyl benzoate selectivity (%).

As mentioned earlier in chapter 1, changing the catalyst preparation technique could alter the catalytic profile of the reaction. Specifically sol-immobilisation technique has been employed to obtain Au/Pd metal nanoparticles with smaller and narrower particle size distribution (3-5 nm, median at 3.8 nm)[19] compared to the bimodal distribution of particles with small size distribution (2-10 nm) and minority (*ca.* 8%) of larger particles (35-80 nm) using the impregnation technique and calcined in static air.[20,4,21] Besides, sol-immobilisation techniques generate homogeneous Au-Pd alloys with Au and Pd in metallic state whereas Au core-Pd shell type alloy structure with Pd^{2+} (PdO) dominance the Au-Pd impregnated catalysts calcined at high temperature (*i.e.* 400 °C) in static air. It was shown in the earlier literature studies on benzyl alcohol oxidation that Au-Pd supported nanoparticles synthesised via sol-immobilisation produced higher catalytic activity compared to the analogous impregnated catalyst.[22,23] For instance, sol-immobilised 1%Au-Pd/C catalyst has almost 4 times higher TOF value compare to analogue catalyst synthesised with impregnation technique.[22,4] The higher activity observed in sol-immobilised catalyst in benzyl alcohol oxidation was strongly related to Au-Pd particle size effect as well as the metal oxidation state. Recently, Miedziak *et al.* claimed that

particle size factor and especially their distribution has more prominence than the effect of oxidation state in benzyl alcohol oxidation.[24,25] Therefore, taking into account the observation from benzyl alcohol oxidation, a 1%Au-Pd/TiO_2 sol-immobilised catalyst has been used in toluene oxidation. As expected from benzyl alcohol oxidation, toluene oxidation with molecular oxygen in the presence of sol-immobilised catalyst demonstrated higher catalytic activity. Turn over number values calculated for 1%Au-Pd/TiO_{2SI} was higher (TON: 260) compared to 78 observed with 5%Au-Pd/TiO_{2IW} within similar range of reaction time. Hence, the data supports the idea that smaller Au-Pd particle with narrower particle distribution is required to obtain better catalytic activity for toluene oxidation.

Since the metal loading and mass of catalyst use for sol-immobilised catalyst during the reaction is different with impregnation catalyst, the selectivity data were compared at iso-conversion (table 3.2). Contrasting product distributions at similar conversion level is necessary for comparing the intrinsic selectivity of different catalyst.

Table 3.2: Liquid phase oxidation of toluene using bimetallic Au-Pd supported TiO_2 catalysts synthesised via impregnation and sol-immobilisation methods, respectively. Comparison of distribution of products at iso-conversion level

Catalyst	Preparation technique	Conv. (%)	Selectivity (%)			
			Benzyl alcohol[a]	Benzaldehyde[a]	Benzoic acid[a]	Benzyl Benzoate[a]
5%Au-Pd/TiO_2	Impregnation	0.4	7.4	71.3	13.4	7.9
1%Au-Pd/TiO_2	Sol-immobilisation	0.4	1.1	48.1	21.2	29.6

Reaction conditions: toluene = 40 mL, temperature = 160 °C, pO_2 = 10 bar, stirring rate = 1500 rpm. Impregnation: 200 mg of catalyst, Sol-immobilization: 100 mg of catalyst, [a] Analysis using GC- FID

The highest selectivity to benzaldehyde was obtained with impregnated catalyst (71%) whereas with the sol-immobilised Au-Pd supported catalyst, the major products were benzoic acid and benzyl benzoate. This selectivity pattern is contradictory to the selectivity trend observed in benzyl alcohol oxidation for both sol-immobilised and impregnated Au-Pd catalysts. In that case, benzaldehyde seemed to be stable against consecutive oxidation

as higher benzaldehyde selectivity with minor consecutive products (benzoic acid and benzyl benzoate) was observed with impregnated catalyst. However, the difference could be explained by the generation of toluene as one of the product which is in competition with benzaldehyde production. Higher toluene formation in impregnated samples decreased the benzaldehyde selectivity and the higher toluene formation was explained by the presence of Pd rich surface together with surface acidity (presence of chlorine).[25,26] On the other hand, in terms of benzyl benzoate selectivity, sol-immobilised catalyst shows 29.6% compared to 7.9% with impregnated catalyst counterpart. It was found in this study that benzyl benzoate formation from toluene oxidation with sol-immobilised Au-Pd supported nanoparticles catalyst was originated from oxidation of hemiacetal species.[27] These results indicated that product distribution was affected by tuning the catalyst properties. From the aforementioned results it can be suggested that the stability of benzaldehyde is higher with the impregnated catalyst, whereas when the reaction is catalysed by the sol-immobilised catalyst, there is an enhancement in the consecutive oxidation of benzaldehyde to benzoic acid and the formation of benzyl benzoate. In addition to that, the synergistic effect of Au-Pd was confirmed by inferior catalytic activity obtained for both Au and Pd monometallic supported catalysts, respectively.[27]

This initial study clearly indicated that Au-Pd supported nanoparticles, even at relatively lower temperature (160 ^{o}C) was capable in activating primary C-H bond in toluene with higher activity compared to previous published reports. This comparison was based on turn over number (TON) value (see table 3.1) which shows at least 4 times higher than those of previous heterogeneous catalysts for this reaction.[12-14]

3.3. Oxidation of 4-methoxytoluene

3.3.1. Blank reaction at different temperature

In second part of this chapter, 4-methoxytoluene was chosen as a substrate to be oxidised under the same reaction conditions as toluene oxidation in order to investigate the effect of substituting one proton of the toluene compound with one methoxy group. In this case, it is expected to give higher activity compared to toluene. This argument is based on the substituent effects on toluene aromatic ring. The substituent group will affect the strength of C-H bond dissociation energies of system. In the benzylic system, bond dissociation

energies of C-H are dependant on two effects; ground state effect and radical effect.[28] Ground state effect is associated with a polar effect, whereas radical effect is based on spin delocalization effect. Since the methyl group of toluene is a weak donor; a *para*-donor causes a destabilization of ground state but stabilizes the benzyl radical. Thus, both the ground effect and radical effect reduces the benzylic C-H bond dissociation energies. Hence, the presence of methoxy (OCH_3) substituent, which is a strong electron-donating group at carbon *para* in toluene aromatic ring, will reduce the C-H bond dissociation energies of system. This facilitates the activation of C-H bond and therefore it is easier to activate 4-methoxytoluene compared to toluene.

Initially, in order to obtain the appropriate temperature for oxidation of 4-methoxytoluene, a series of blank reactions was carried out between four difference temperatures in the range of 160 - 190 °C. The conversion determined by gas chromatography analysis is plotted as a function of time. The conversion profile was shown in figure 3.3 below:

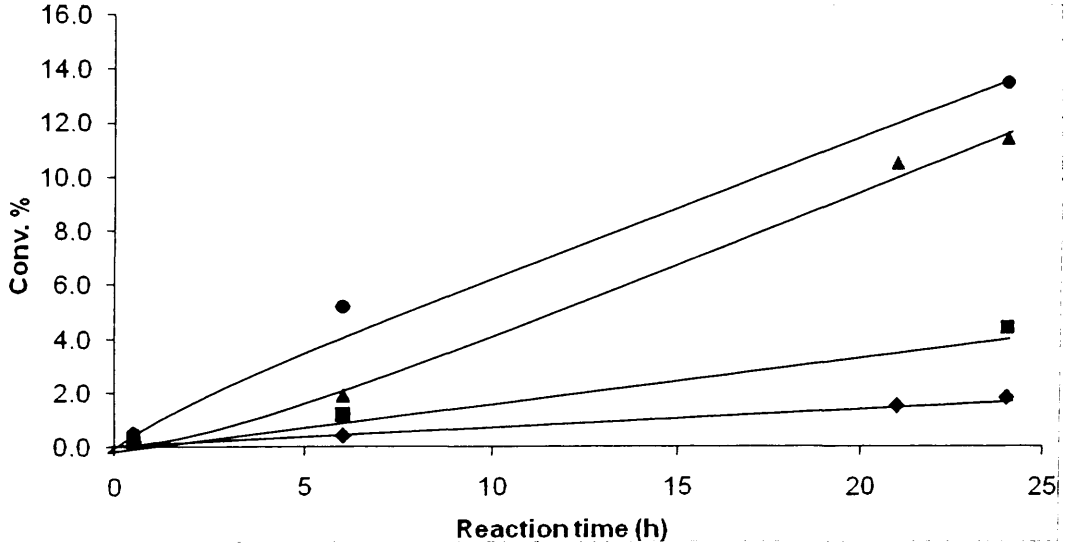

Figure 3.3: Blank oxidation of 4-methoxytoluene at different temperature. Reaction conditions: 4-methoxytoluene = 40 mL, pO_2 = 10 bar, time = 6 hours, stirring rate = 1500 rpm. Key: (◆) 160 °C; (■) 170 °C; (▲) 180 °C; (●) 190 °C

It can be seen that the conversion of 4-methoxytoluene was apparently higher at temperature 180 and 190 °C with almost 14% conversion at 24 hours reaction time. This value is about 7 times higher compared to conversion at 160 °C with same reaction duration. The main product for blank reaction at 160 °C is 4-methoxybenzaldehyde compared to 4-methoxybenzoic acid for higher temperature counterpart (see table 3.3). At

temperature higher than 160 °C, 4-methoxybenzaldehyde was easily oxidised to 4-methoxybenzoic acid with ~71-75% selectivity within 24 hours reaction time. These results show that the radical type reaction involving O_2 is more significant at temperatures higher than 160 °C, therefore the oxidation of 4-methoxytoluene was carried out at 160 °C.

Table 3.3: Blank oxidation of 4-methoxytoluene

Temp. (°C)	Conv. (%)	Product Distributions (%)			
		4-Methoxy benzyl alcohol[a]	4-Methoxy benzaldehyde[a]	4-Methoxy benzoic acid[a]	*Others [a]
160	1.8	17.1	48.0	28.9	6.0
170	4.4	5.4	13.9	71.3	9.3
180	11.4	2.4	13.4	72.4	12.0
190	13.5	1.5	12.3	74.6	11.6

Reaction conditions: 4-methoxytoluene = 40 mL, Time = 24 hours, temperature = 160 °C, pO_2 = 10 bar, stirring rate = 1500 rpm. [a] Analysis using GC- FID
*Others: consist family of esters and C-C coupling products

3.3.2. Influence of support and catalyst preparation technique

Types of supports were shown to be important in determining the catalytic activity of Au-Pd supported nanoparticles catalysts.[29,26] Different types of support could produce catalysts with different characteristics such as metal dispersion, acidity/basicity, morphology and particle size of the metal.[30] In this section, four different supports (TiO_2, SiO_2, CeO_2, and C) were impregnated with Au and Pd and tested in 4-methoxytoluene oxidation in the presence of molecular oxygen as oxidant. All catalysts were calcined at 400 °C in static air before subjected to reaction. The significant point of this process is to avoid the possibility of leached of the active metals into reaction media and also to enhance the metal support interaction. In all cases, the main products detected were 4-methoxybenzyl alcohol, 4-methoxybenzaldehyde and 4-methoxybenzoic acid. The additional products formed were identified as a family of esters and C-C coupling products.[27] After 48 hours of reaction time (table 3.4), the order of activity based on turn over number (TON) was the following; Carbon $\geq$ TiO_2 > SiO_2 > CeO_2.

Table 3.4: Liquid phase oxidation of 4-methoxytoluene in the presence of 5w%Au-Pd bimetallic with different supported materials catalysts prepared by impregnation method

Support	Time	Conv.	Selectivity (%)				TON [b]
		(%)	4-Methoxy benzyl alcohol[a]	4- Methoxy benzaldehyde [a]	4-Methoxy benzoic acid [a]	*Others [a]	
-	24	1.8	17.1	48.0	28.9	6.0	-
TiO_2	24	6.6	3.0	21.7	57.1	18.2	287
	48	8.6	2.2	11.1	63.1	23.6	373
Carbon	24	6.5	1.3	17.5	74.5	6.7	282
	48	8.7	1.9	5.8	77.4	14.9	376
CeO_2	24	5.0	3.9	33.1	44.8	18.1	217
	48	6.2	4.4	23.2	49.0	23.4	267
SiO_2	24	4.5	5.5	38.1	43.5	12.9	195
	48	7.3	4.7	8.3	62.3	24.7	316

Reaction conditions: 4-methoxytoluene = 40 mL, mass of catalyst = 200 mg, temperature = 160 °C, pO_2 = 10 bar, stirring rate = 1500 rpm. [a] Analysis using GC- FID, [b] Turn over number (TON) = ((% conv. * mol of substrate) / mol of metal / 100 %)
*Others: consist family of esters and C-C coupling products

In term of selectivity profile, it was evident from table 3.4 that Au-Pd on oxide (TiO_2, SiO_2, CeO_2 supports) material show almost similar selectivity level for all range of product. For example, after 24 hours reaction time, 4-methoxybenzoic acid was observed as main product followed by 4-methoxylbenzaldehyde and then the products from combination of esters family and C-C coupling reaction. The 4-methoxybenzyl alcohol was only detected in minor quantity with selectivity less than 7%. In contrast to the oxide supports, Au-Pd on carbon displayed 75% selectivity to 4-methoxybenzoic acid compound indicating that over-oxidation process was higher in this particular catalyst. Although, similar to oxide supports, insignificant amount of alcohol (6.5%) was observed. As stated in toluene

oxidation, sequential oxidation of alcohol compound was higher at this level of temperature.

It was reported in the earlier studies by Enache *et al.* on benzyl alcohol oxidation using molecular oxygen as oxidant and gold catalysts that the formation of by-products (benzoic acid and benzyl benzoate) were associated with the presence of strong acid sites on the catalysts.[29] In general, the acidity of each support used in this study is weak. This statement is based on ammonia TPD analysis on Au on different supported materials reported in literature where TiO_2, CeO_2, carbon and SiO_2 only showed physisorbed ammonia indicating weaker acidity.[29] However, a close examination on ammonia TPD with Au-Pd supported on TiO_2, CeO_2, SiO_2 and carbon demonstrated that the acidity strength of Au-Pd/C_{1W} was higher compared to Au-Pd on oxide supports. The stronger acidity nature of the Au-Pd/C_{1W} could explain the higher formation of benzoic acid produced.[31]

The selectivity profile with time-online reaction of the 5wt%Au-Pd/TiO_{21W} catalyst is shown in figure 3.4 as an example. As the reaction time increased, the selectivity to 4-methoxybenzaldehyde decreased, whereas the selectivity to 4-methoxybenzoic acid increased indicating the consecutive oxidation of 4-methoxybenzaldehyde to 4-methoxybenzoic acid.

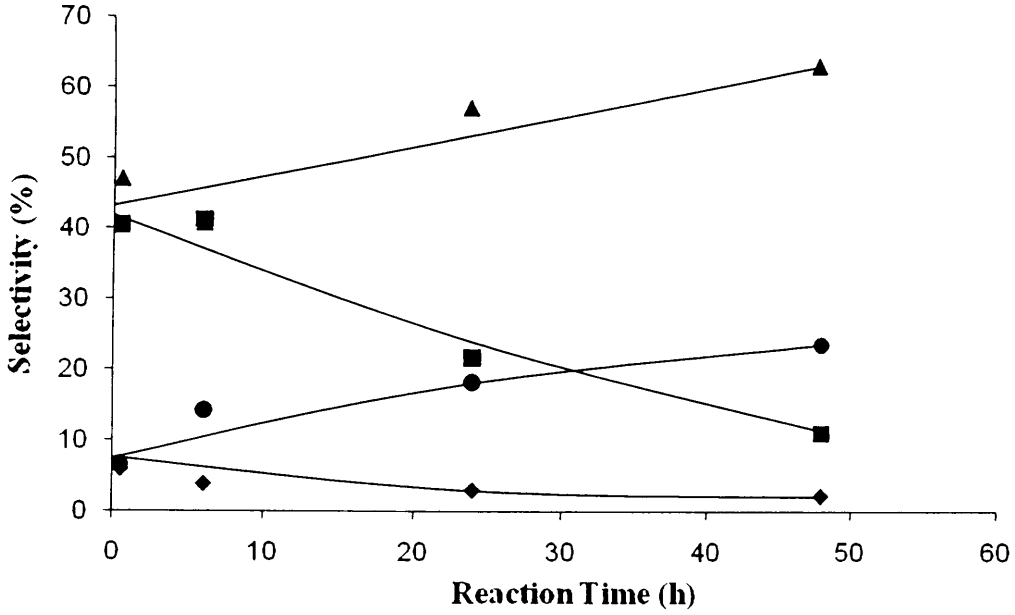

Figure 3.4: Selective oxidation of 4-methoxytoluene in the presence of the 5wt%Au-Pd/TiO_{2IW}. Reaction conditions: 4-methoxytoluene= 40 ml, 200 mg of catalyst, temperature = 160 °C, pO_2 = 10 bar, time = 48 hours, stirring rate = 1500 rpm. Key: ◆4-methoxybenzyl alcohol selectivity (%),■4-methoxybenzaldehyde selectivity (%),▲4-methoxybenzoic acid selectivity (%), • selectivity to family of esters and C-C coupling products (%).

All catalysts with different support materials were calcined in static air at high temperature *i.e.* 400 °C. It was expected from previous literature that Au-Pd with TiO_2, SiO_2 and CeO_2 to have Au core-Pd shell structure whereas with carbon as support material, formation of homogeneous alloy should occur. However, it seems the catalytic activity is not strongly related to the structure of Au-Pd alloy evolved in catalyst. This statement was based on lower TONs values observed in similar range of reaction time on Au-Pd/SiO_{2IW} and Au-Pd/CeO_{2IW} compared to TON of Au-Pd/TiO_{2IW} catalyst. Moreover, Au-Pd/C_{IW} with homogenous alloy structure having comparable activity to Au-Pd/TiO_{2IW} catalyst. Another factor should be considered here is the particle size and distribution of metals on each supports. Detailed studies on particle size and metals distribution of Au/Pd on different supports synthesised using similar procedure as used in this study have been carried out in earlier works by Edwards *et.al.*[21,32] by using STEM technique, all catalysts were shown to have bi-modal particle size. In term of mean particle size, Au-Pd catalyst support on TiO_2, Al_2O_3 and carbon were calculated (based on XRD data, see section 4.6.1 of Chapter 4) to have almost similar average crystallite size (23 nm) whereas Au-Pd metal

in SiO_2 as support shows around 14 nm in size. Since the SiO_2 support catalyst displayed inferior catalytic activity than TiO_2 and carbon supported catalyst counterpart, again the particle size effect alone could not clearly explain the activity patterns.

According to the available literature, Au-Pd supported catalyst synthesised using impregnation method and calcined in static air at higher temperature typically consist Au in metallic state and Pd in oxidised state (Pd^{2+}).[21] However, detailed XPS analyses reported in literature on each catalyst illustrated that the surface molar ratio of Pd and Au could be different. Compared to SiO_2 as support, TiO_2 was shown to give the higher Pd to Au surface molar ratio.[32,33] Therefore, it could be considered here that the surface composition of Au-Pd would affect the catalytic performance of the Au-Pd supported oxide catalyst.

Other than different structure of Au-Pd alloy, compared to TiO_2, carbon has higher surface area which provided superior metal dispersion and more important it may increase the availability of exposed corner/edges sites on metal nanoparticles with carbon as support. Higher metal exposition is due to the formation of spherical structure rather than hemisphere as observed on TiO_2 as support. In view of the fact that alloy type or particle size alone could not give a clear correlation to the demonstrated catalytic activity pattern, the origin of superior activity might be derived from the combination of several factors such as Au-Pd surface composition also the dispersion of metal on support.

In general, the catalytic data based on the effect of substrates (toluene versus 4-methoxytoluene) are an agreement with the theory as discussed previously where methoxy (OCH_3) decreased the dissociation energy of primary C-H bond and consequently increased the conversion of 4-methoxytoluene compared to toluene. For example, with TiO_2 as support, the conversion obtained with toluene as substrate was half compare to analogue reaction with 4-methoxytoluene.

In order to study the effect of catalyst preparation technique on catalytic activity as observed in section 3.2.1, 1%Au-Pd/TiO_{2SI} sol immobilised catalyst was subjected to 4-methoxytoluene oxidation at similar conditions. Table 3.6 obviously shows that sol-immobilised catalyst gave higher TON compared to its impregnated catalyst counterpart. The catalytic data observed in 4-methoxytoluene oxidation was in agreement with the data observed with toluene as substrate. Superior catalytic activity of sol-immobilised samples over impregnated samples was established on several oxidation reactions with different substrate. [9,19,25]

Table 3.5. Liquid phase oxidation of 4-methoxytoluene using bimetallic Au-Pd supported TiO_2 catalysts synthesised via impregnation and sol-immobilisation methods, respectively.

Catalyst	Conv. (%)	Selectivity (%)				TON[b]
		4-Methoxy benzyl alcohol[a]	4- Methoxy benzaldehyde [a]	4-Methoxy benzoic acid [a]	*Others [a]	
5%Au-Pd/TiO_{2IW}	2.2	3.3	35.2	60.3	1.2	92
1%Au-Pd/TiO_{2SI}	0.6	4.5	65.2	30.2	0	139

Reaction conditions: toluene = 40 mL, time = 6 hours, temperature = 160 °C, pO_2 = 10 bar, stirring rate = 1500 rpm. Impregnation: 200 mg of catalyst, Sol-immobilized: 100 mg of catalyst, [a] Analysis using GC- FID, [b] Turn over number (TON) = ((% conv. * mol of substrate) / mol of metal / 100 %) *Others: consist family of esters and C-C coupling products

As it was mentioned in section 3.2.1 and based on catalyst characterisation carried out in this study (section 4.5 of chapter 4), the characteristics of Au-Pd/TiO_2 catalyst synthesised via sol-immobilisation technique was clearly different as compared to the calcined catalyst synthesised using impregnation method. It was thought here that combination of small metal particle size and higher metal dispersion as well as presence of Au and Pd in metallic state in sol-immobilised catalyst are more efficient in activating aromatic hydrocarbons and consequently increase the rate of reaction.

3.4. Conclusions

In this chapter, the selective oxidation of toluene and derivatives toluene using Au-Pd supported nanoparticles catalysts as a proof of concept study for primary carbon-hydrogen bond (C-H) activation is briefly studied. The experimental results are contrasts on the basis of catalyst preparation method and effect of support material. In general, supported Au-Pd nanoparticles are shown to be active for the oxidation of toluene and 4-methoxytoluene at relative mild solvent-free reaction conditions with molecular oxygen as oxidant. Specifically, the reactions were carried out at lower temperature (160 °C) without utilisation of any initiators or co-catalysts. The catalytic activities observed based on turn over numbers (TONs), were found at least 4 times higher than those of previous

heterogeneous catalysts for this reaction.[12-14] Moreover, higher catalytic activity was observed with 4-methoxytoluene than toluene indicating the role of the methoxy group.

Varying the catalyst preparation technique leads to significant differences in activity and product distribution. Depending on the nature of the metal and the reaction conditions, the distribution of the products could be tuned. Smaller metal particle size with narrow sized distribution and metallic oxidation state (Au^0, Pd^0) was observed to be responsible for high activity. Therefore, Au-Pd supported catalysts synthesised via sol immobilisation method was more active compared to Au-Pd supported catalysts by the impregnation method. Furthermore, the use of different supports (TiO_2, C, SiO_2, CeO_2) for depositing Au-Pd emphasises the importance of the support on the activity and selectivity to the desired product.

Overall, the findings of the ability of Au-Pd supported nanoparticles catalyst in oxidising primary C-H bonds with molecular oxidant seems to hint at the possibility of selective oxidation of other alkanes such as methane under relatively mild reaction conditions.

References:

1. Haruta, M. *Studies in Surface Science and Catalysis*; Elsevier, **2003**.
2. Hutchings, G. J. *Catalysis Today* **2005,** *100*, 55-61.
3. Hutchings, G. J. H., M. *Applied Catalysis A: General* **2005,** *291*, 2-5.
4. Enache, D. I. E., J. K.; Landon, P.; Solsona-Espriu, B.; Carley, A. F.; Herzing, A. A.; Watanabe, M.; Kiely, C. J.; Knight, D. W.; Hutchings, G. J. *Science* **2006,** *311*, 362-365.
5. Enache, D. I. B., D.; Edwards, J. K.; Taylor, S. H.; Knight, D. W.; Carley, A. F.; Hutchings, G. J. *Catalysis Today* **2007,** *122*, 407-411.
6. Edwards, J. K.; Solsona, B.; N, E. N.; Carley, A. F.; Herzing, A. A.; Kiely, C. J.; Hutchings, G. J. *Science* **2009,** *323*, 1037-1041.
7. Abad, A.; Concepción, P.; Corma, A.; García, H. *Angewandte Chemie International Edition* **2005,** *44*, 4066-4069.
8. J. Colby, D. I. S., H. Dalton, . *Biochemical Journal* **1977,** *165*, 395.
9. Pritchard, J.; Kesavan, L.; Piccinini, M.; He, Q.; Tiruvalam, R.; Dimitratos, N.; Lopez-Sanchez, J. A.; Carley, A. F.; Edwards, J. K.; Kiely, C. J.; Hutchings, G. J. *Langmuir* **2010,** *26*, 16568-16577.
10. Partenheimer, W. *Catalysis Today* **1995,** *23*, 69-158.
11. H. D. Holtz, L. E. G.; USPTO Ed.; Phillips Petroleum Co., 1978.
12. Wang, F.; Xu, J.; Li, X.; Gao, J.; Zhou, L.; Ohnishi, R. *Advanced Synthesis & Catalysis* **2005,** *347*, 1987-1992.
13. Li, X.; Xu, J.; Zhou, L.; Wang, F.; Gao, J.; Chen, C.; Ning, J.; Ma, H. *Catalysis Letters* **2006,** *110*, 149-154.
14. J. Gao, X. T., X. Li, H. Miao, J. Xu. *J. Chem. Technol. Biotechnol* **2007,** *82*, 620.
15. Yang, F.; Sun, J.; Zheng, R.; Qiu, W.; Tang, J.; He, M. *Tetrahedron* **2004,** *60*, 1225-1228.
16. Bastock, T. W.; Clark, J. H.; Martin, K.; Trenbirth, B. W. *Green Chemistry* **2002,** *4*, 615-617.
17. Gupta, M.; Paul, S.; Gupta, R.; Loupy, A. *Tetrahedron Letters* **2005,** *46*, 4957-4960.
18. Choudhary, V. R.; Jha, R.; Jana, P. *Green Chemistry* **2007,** *9*, 267-272.
19. Dimitratos, N.; Lopez-Sanchez, J. A.; Anthonykutty, J. M.; Brett, G.; Carley, A. F.; Tiruvalam, R. C.; Herzing, A. A.; Kiely, C. J.; Knight, D. W.; Hutchings, G. J. *Physical Chemistry Chemical Physics* **2009,** *11*, 4952-4961.
20. Edwards, J. K.; Carley, A. F.; Herzing, A. A.; Kiely, C. J.; Hutchings, G. J. *Faraday Discussions* **2008,** *138*, 225-239.
21. Edwards, J. K.; Solsona, B. E.; Landon, P.; Carley, A. F.; Herzing, A.; Kiely, C. J.; Hutchings, G. J. *Journal of Catalysis* **2005,** *236*, 69-79.
22. Dimitratos, N.; Lopez-Sanchez, J. A.; Morgan, D.; Carley, A. F.; Tiruvalam, R.; Kiely, C. J.; Bethell, D.; Hutchings, G. J. *Physical Chemistry Chemical Physics* **2009,** *11*, 5142-5153.

23. Lopez-Sanchez, J. A.; Dimitratos, N.; Miedziak, P.; Ntainjua, E.; Edwards, J. K.; Morgan, D.; Carley, A. F.; Tiruvalam, R.; Kiely, C. J.; Hutchings, G. J. *Physical Chemistry Chemical Physics* **2008,** *10*, 1921-1930.
24. Miedziak, P. J.; He, Q.; Edwards, J. K.; Taylor, S. H.; Knight, D. W.; Tarbit, B.; Kiely, C. J.; Hutchings, G. J. *Catalysis Today* **2011,** *163*, 47-54.
25. Miedziak, P.; Sankar, M.; Dimitratos, N.; Lopez-Sanchez, J. A.; Carley, A. F.; Knight, D. W.; Taylor, S. H.; Kiely, C. J.; Hutchings, G. J. *Catalysis Today* **2011,** *164*, 315-319.
26. Meenakshisundaram, S.; Nowicka, E.; Miedziak, P. J.; Brett, G. L.; Jenkins, R. L.; Dimitratos, N.; Taylor, S. H.; Knight, D. W.; Bethell, D.; Hutchings, G. J. *Faraday Discussions* **2010,** *145*, 341-356.
27. Kesavan, L.; Tiruvalam, R.; Rahim, M. H. A.; bin Saiman, M. I.; Enache, D. I.; Jenkins, R. L.; Dimitratos, N.; Lopez-Sanchez, J. A.; Taylor, S. H.; Knight, D. W.; Kiely, C. J.; Hutchings, G. J. *Science* **2011,** *331*, 195-199.
28. Wu, Y.-D.; Wong, C.-L.; Chan, K. W. K.; Ji, G.-Z.; Jiang, X.-K. *The Journal of Organic Chemistry* **1996,** *61*, 746-750.
29. Enache, D. I.; Knight, D. W.; Hutchings, G. J. *Catalysis Letters* **2005,** *103*, 43-52.
30. G.C. Bond, C. L., D. T. Thompson, *Catalysis by Gold*; Imperial College Press, 2006; Vol. 6.
31. Saiman, M.I., Cardiff University, 2012.
32. Edwards, J. K., Cardiff University, 2006.
33. Pritchard, J. C.; He, Q.; Ntainjua, E. N.; Piccinini, M.; Edwards, J. K.; Herzing, A. A.; Carley, A. F.; Moulijn, J. A.; Kiely, C. J.; Hutchings, G. J. *Green Chemistry* **2010,** *12*, 915-921.

CHAPTER 4

Liquid Phase Oxidation of Lower Alkanes via Supported Au and Pd Mono/Bimetallic Catalysts with Addition of Hydrogen Peroxide as Oxidant at Mild Conditions

4.1. Introduction

In this chapter the oxidation of methane with supported Au based catalyst is described. Mainly hydrogen peroxide (H_2O_2) was used as oxidant and added as co-reactant. The heterogeneously developed catalytic system is compared with analogue homogeneous systems, and further studies were carried out by varying reaction conditions *i.e.* temperature, pressure, time, oxidant concentration and catalyst screenings. The section also highlights the applicability of this catalytic system on ethane oxidation followed by catalyst characterisation.

4.2. Methane oxidation using molecular oxygen

As shown in chapter 3, in the presence of Au based supported catalysts, toluene and toluene derivatives were successfully used as proof-of-concept studies for the selective oxidation of primary C-H bonds by using molecular oxygen as oxidant. Consequently, this opens a possibility for the activation of lower alkane primary C-H bonds with dioxygen (O_2), either in pure form or as air under mild reaction conditions. The understandings gained from previous literature suggest that the future catalyst for oxygen atom transfer to hydrocarbons must be capable of both activating oxygen as well as the relevant hydrocarbon. Therefore, as initial approach, a reaction involving methane and molecular oxygen in the form of 25% O_2 in N_2 was carried out with the presence of well-characterised 2.5wt%Au2.5wt%Pd/TiO_2 synthesised via an impregnation method. This is the same catalyst that was used in oxidation of toluene and 4-methoxytoluene reported in chapter 3. Due to several factors detailed in chapter 1, H_2O was selected as reaction medium. In addition to its inertness, water attracts particular attention since it is cheapest

and is an ecologically pure solvent. The initial partial pressures of CH_4 and O_2 were chosen to avoid compositions that would result in an explosive mixture during reaction. The temperature was set-up at 50 °C and the reaction was carried out for up to 2 hours. This specific reaction temperature was decided based on the fact that the benchmark methane monooxygenase system as detailed in chapter one operated at similar range of temperature (45 °C).[1] However, an analysis of solution after reaction using ^{1}H-NMR did not show any trace of C_1-oxygenated product, as illustrated in table 4.1. As impregnated Au catalysts usually have larger metal particle sizes, and considering that gold with sufficiently small particles is able to chemisorbs oxygen as O_2^-, which believed the key species in securing oxidation,[2] the analogue catalyst (1wt%Au-Pd/TiO_{2SI}) synthesised via sol-immobilisation method has also been subjected to methane reaction under similar condition. The results in table 1 clearly show that in this particular reaction, no oxygenated product was observed, regardless of the characteristics of the catalyst. This generally indicates that the current system does not have the capability of activating the species responsible for the activation of primary C-H bond in methane into oxygenates. However, it must to remember here that the oxidation of methane using molecular oxygen has not being optimised, and thus the actual behavior of Au based supported nanoparticles toward this particular reaction may not be negligible and could be further examined in the future, by tuning both the reaction conditions and the morphology and characteristics of the metal supported catalysts.

Table 4.1: Catalytic selective methane oxidation with molecular oxygen in the presence of Au-Pd/TiO_2 catalyst

Entry	Catalyst	Product amount (μmol)				Methanol Selectivity (%)[c]	Oxygenate productivity (Mol/kg_{cat}/ Hour)[d]	TOF [e]
		CH_3OH [a]	HCOOH [a]	MeOOH [a]	CO_2 in gas[b]			
1	5.0wt%Au-Pd/ TiO_{2IW}	0	0	0	<0.2	0	0	0
2	1wt%Au-Pd/ TiO_{2SI}	0	0	0	<0.2	0	0	0

Reaction time: 2 hours, Temp: 50 °C, Pressure: 30 bar, Stirring rate: 1500 rpm, Catalyst: 1.0 x 10^{-5} mol of metals, Solvent: H_2O, 10 mL. [a] Analysis using ^{1}H-NMR, [b] Analysis using GC- FID [c] Methanol selectivity = (mol of CH_3OH/ total mol of products) * 100, [d] Oxygenates productivity = mol of oxygenates / Kg_{cat} / reaction time (h), [e] Turn over frequency (TOF) = mol of oxygenates / mol of metal / reaction time (h), Gases:6.25%O_2/75.0%CH_4/18.75%N_2

In the well-known biological methane monooxygenase (MMO) system, dioxygen is activated to a peroxy intermediate which can then oxidise hydrocarbons selectively, such as the selective oxidation of methane to methanol at mild conditions. Haruta has also demonstrated during the epoxidation of alkenes that sacrificial H_2 is required during the reaction, as this aids the activation of oxygen into peroxy species which are then stabilised by the supported Au catalyst.[3] Alternatively, the research conducted by Hughes and co-workers has shown that hydrogen is not required if catalytic amounts of a peroxide are added to the reactant.[4] Therefore, an attempt has been made to use hydrogen peroxide (H_2O_2) as initiator in order to activate dioxygen during the selective oxidation of methane (table 4.2). As the total amount of oxygenates produced is less than the amount observed in an analogous reaction containing only H_2O_2, this suggests that at these conditions, only H_2O_2 contributed to the obtained catalytic activity in both reactions. This is further strengthened by the observation that in the absence of H_2O_2, no product was detected by ^{1}H-NMR, which confirmed that H_2O_2 is the only oxygen donor in this present system. Whilst the catalytic activity of both reactions should theoretically be the same (given that equal amounts of hydrogen peroxide were used), the lower activity of the H_2O_2/O_2 system could be due to the rapid decomposition of hydrogen peroxide. A separate study showed that the presence of an inert gas did indeed accelerated hydrogen peroxide decomposition.

Table 4.2: Catalytic selective methane oxidation with O_2/N_2 and H_2O_2 as initiator in the presence of 5wt%Au-Pd/TiO_{2IW} catalyst

Entry	Oxidant	Product amount (μmol)				Oxygenate productivity (Mol/kg_{cat}/ Hour)[c]	H_2O_2 Remain (μmol)[d]
		MeOH [a]	HCOOH [a]	MeOOH [a]	CO_2 in gas[b]		
1[e]	H_2O_2	0.50	0	0.47	0.16	0.08	54
2[f]	H_2O_2/O_2	0.24	0	0	0.20	0.04	50

Reaction Time; 30 min, Temp: 50°C, Pressure: 30 bar, Stirring rate: 1500 rpm, Catalyst: 1.0 x 10^{-5} mol of metals (27.6 mg), solvent: H_2O, 10 mL. [a] Analysis using ^{1}H-NMR, [b] Analysis using GC- FID [c] Oxygenates productivity = mol of oxygenates / Kg_{cat} / reaction time (h), [d] Assayed by Ce^{+4} (aq) titration, [e] 500 μmol H_2O_2, [f] Gases: 6.25%O_2/75.00%CH_4/18.75%N_2 and 500 μmol of H_2O_2

Therefore in the later stages of this study, the catalytic selective oxidation of methane was carried out with hydrogen peroxide as oxidant, where H_2O_2 itself was produced in *in-situ* (see chapter 5) or added as a reactant together with the solvent.

4.3. Methane oxidation by addition of hydrogen peroxide

As described in chapter 1, there are several studies on catalytic oxidation of methane using hydrogen peroxide as oxidant. However, the majority of the systems explored are homogeneous, which include polyoxometallate systems, vanadium and iron complexes and the use of solvents such as trufluoroacetic acid and acetonitrile.[5-10] However, the use of the aforementioned solvents is problematic where these solvents can participate in the oxidation reaction as reported previously in the literature.[11,12] The utilisation of heterogeneous catalysts will be more advantageous than the use of homogeneous systems due to the possibility of easier reusability. Recent work by Sorokin and co-workers demonstrated that a grafted μ-nitrido iron phthalocyanine complex on silica was active for the selective oxidation of methane under mild reaction conditions and H_2O_2 as oxidant.[13,14] In view of this, design of the initial experiments was based on the work of Yuan *et al.* where they illustrated the possibility of oxidising methane in aqueous medium using metal chlorides and H_2O_2.[15]

4.3.1. Comparison of heterogeneous with homogeneous catalyst

Initially the oxidation of methane was performed at 90 °C (table 4.3) using a gold precursor ($HAuCl_4$) following the conditions described by Yuan and co-workers.[15] Formation of methanol, formic acid and carbon dioxide with comparable TOF values was observed in this test. However, compared to the work of Yuan *et al.*,[15] the main product was formic acid instead of methyl hydroperoxide (CH_3OOH), and indeed no trace of CH_3OOH was observed in this test. In order to confirm the data, the reaction has been repeated and it gave similar results (formic acid as product). Based on further study of the stability of CH_3OOH, it has been determined that this species is relatively unstable at higher temperature and that it can easily overoxidise, mainly to CO_2. Detailed discussion on the alkyl hydroperoxide is presented in the following chapter, section 5. 4. 2.

It is essential to note here that in the reaction with homogeneous catalyst, even though the turnover frequency (TOF) and oxygenates productivity values were high, the selectivity to

methanol was poor (less than 14%) due to the high formation of formic acid and CO_2, showing that at these conditions and using a homogeneous catalyst, over oxidation products were favoured. In addition, the precipitation of the homogeneous catalyst was observed and this is in agreement with the data reported in literature.[15,16] The precipitation of gold cations has been reported previously by Jones and co-workers, and it was found that selenic acid (H_2SeO_4) was required in order to maintain the cationic oxidation state of Au, and to prevent the reduction to metallic gold.[17] Precipitation of the metal would lead to the loss of the active site, and would not provide reusable homogeneous catalysts.

Table 4.3: Liquid phase oxidation of methane using homogeneous and heterogeneous catalysts with H_2O_2

Entry	Catalyst	Product amount (μmol)				Methanol Selectivity (%)[c]	TOF [d]	H_2O_2 Remain (μmol) [e]
		CH_3OH [a]	HCOOH [a]	MeOOH [a]	CO_2 in gas[b]			
1	5wt%Au-Pd/TiO_{2IW}	2.49	0	0	1.01	71.1	0.498	15
2	$HAuCl_4$	7.74	37.93	0	10.25	13.8	9.134	27
3	$HAuCl_4/TiO_2$	3.40	29.60	25.78	14.02	4.7	14.560	109

Reaction Time; 30 min, Reaction Temp; 90 °C, CH_4 pressure: 30 bar, Catalyst: 1.0 x 10^{-5} mol of metal, [H_2O_2]: 0.5M, Solvent: H_2O, 10 mL. [a] Analysis using ^{1}H-NMR, [b] Analysis using GC-FID, [c] Methanol selectivity = (mol of CH_3OH/ total mol of products) * 100, [d] Turn over frequency (TOF) = mol of oxygenates / mol of metal / reaction time (h), [e] Assayed by Ce^{+4} (aq) titration.

Therefore, the challenges that arise are the design of a heterogeneous catalyst that can be easily recovered and recycled, and the decrease in the formation of formic acid and especially CO_2. Hence, the analogue reaction has been carried out using 2.5wt%Au2.5wt%Pd/TiO_{2IW} and the catalytic data showed a completely different selectivity profile. By using a heterogeneous catalyst based on Au-Pd supported nanoparticles, the selectivity to methanol was 71%, and no formation of formic acid was observed. On the other hand, there is a clear difference in terms of catalytic activity as shown from the TOF values of the homogeneous gold catalyst, which is *ca.* 18 times larger compared to heterogeneous 5wt%Au-Pd/TiO_{2IW} catalyst. At relatively higher temperature, the role of radical reaction could be important. At this temperature and pressure, and particularly in the presence of Au, hydrogen peroxide might decompose to produce radical

species *i.e.* hydroxyl (•OH) and hydroperoxyl (•OOH) radicals, or unselectively decompose to water and O_2 by thermal effects. It was reported in literature that Au is highly efficient catalyst for Fenton type reaction where hydroxyl radicals are generated from H_2O_2.[18,19] The involvement of radical type mechanism reaction with gold solution as catalyst was later proven by the addition of hydroquinone as radical scavenger where it's ceased the CH_4 oxidation.[15] In addition to this, the formation of formic acid and CO_2 as main products again indicates that a radical type reaction was involved and this further supported by the absence of formaldehyde, which rapidly transforms in to formic acid in the excess of hydroxyl radicals.[20] On the contrary from initial catalytic data, homogeneous type reaction was not observed with heterogeneous 5wt%Au-Pd/TiO_{2IW} catalyst. It is important to know whether TiO_2 plays any role in controlling the radical type reaction. Hence, standard methane oxidation has been carried out in the presence of Au solution and TiO_2. Contrast to the reaction without TiO_2, the result in table 4.3 (entry 3) showed the formation of methyl hydroperoxide. Formation of methyl hydroperoxide in the presence of TiO_2 was believed to relate with the nature of TiO_2 where it was known to generate hydroperoxy species during interaction with hydrogen peroxide.[21,22] However, formic acid was still observed as the main product, and methanol selectivity was still low suggesting that TiO_2 does not have the capability to assist the selective formation of methanol. In addition to that, slightly lower amount of HCOOH could be due to the limited role of TiO_2 in radical-related reaction pathways. TiO_2 presumably acts as a scavenger for the hydroxyl (•OH) species, possibly by absorbing them into its surface oxide layer.[23]

4.3.2. Variation of reaction conditions

It is essential in development a new catalytic system to evaluate the reaction parameter of the reaction. Thus the oxidation of methane was further studied by varying various experimental conditions such as temperature, pressure of methane and hydrogen peroxide concentration. As a reference catalyst, the well characterised 5wt%Au-Pd/TiO_{2IW} was used.

4.3.2.1. Effect of reaction temperature

As shown in table 4.4, the major products were methanol and methyl hydroperoxide followed by CO_2. By increasing the reaction temperature from 2 °C to 90 °C, an increase in methane conversion was observed. The selectivity to the alcohol was highest at 90 °C, since all the intermediate species (in-form of methyl hydroperoxide (CH_3OOH)) may have transformed selectively to methanol. This data is in agreement with the literature where it is reported that methyl hydroperoxide can still be observed at temperatures of up to 70 °C[15] but at higher temperatures, the transformation of methyl hydroperoxide would increase. It is highly noteworthy that even at 2 °C, the conversion of methane to methanol was observed with an exceptionally high selectivity to oxygenate products (93%). The ability of this catalyst to generate alcohol at this level of temperature is extraordinary observationas the reports by Süss-Fink *et al.* at a similar temperature using homogeneous vanadate and pyrazine-2-carboxylic acid (PCA) system only produce methyl hydroperoxide as a product, and therefore certainly requires another step in order to selectively transform it to methanol.[24] This is the first demonstration of a heterogeneous catalyst that can activate methane at very mild conditions, and at the time this thesis is written, there is no literature reporting a similar observation.

Table 4.4: Effect of reaction temperature on catalytic performance of 5wt%Au-Pd/TiO_{2IW} for the selective oxidation of methane with H_2O_2

Entry	T (°C)	Product amount (μmol)				Methanol Selectivity (%)[c]	Oxygenate productivity (Mol/kg_{cat}/ Hour)[d]	TOF [e]	H_2O_2 Remain (μmol) [f]
		CH_3OH [a]	HCOOH [a]	MeOOH [a]	CO_2 in gas[b]				
1	2	1.31	0	1.40	0.19	45.2	0.196	0.542	4471
2	30	1.55	0	1.28	0.20	51.2	0.205	0.566	935
3	50	1.89	0	1.57	0.37	49.3	0.250	0.692	383
4	70	2.02	0	1.38	0.76	48.6	0.246	0.680	43
5	90	2.49	0	0	1.01	71.1	0.180	0.498	15

Reaction Time; 30 min. Catalyst: 27.6 mg (1.0×10^{-5} mol of metal), CH_4 pressure: 30 bar, Stirring rate: 1500 rpm, [H_2O_2]: 0.5M,, Solvent: H_2O, 10 mL, [a] Analysis using ^{1}H-NMR, [b] Analysis using GC-FID, [c] Methanol selectivity = (mol of CH_3OH/ total mol of products) * 100, [d] Oxygenates productivity = mol of oxygenates / Kg_{cat} / reaction time (h), [e] Turn over frequency (TOF) = mol of oxygenates / mol of metal / reaction time (h), [f] Assayed by Ce^{+4} (aq) titration

It is essential to emphasise that the amount of oxidant remained after reaction, at 2 °C was about 90%, indicating that only 10% of H_2O_2 was decomposed and/or used in 30 minutes reaction, compared to 19-99% at higher reaction temperature.

It is also important to notice here that for each experiment, the time required to reach reaction temperature is different, and that it takes longer to reach the higher reaction temperatures. This could affect the decomposition of hydrogen peroxide and subsequently influence the total activity.

Due to the fact that at 50 °C, high productivity to oxygenate with high selectivity to methanol (49%) and oxygenates (methanol and methyl hydroperoxide) (90%) was observed, and taking into account that the methane monooxygenase system works at a similar reaction temperature (45 °C),[1] the majority of the reactions were carried out at this temperature. In addition to this, no oxygenates products could be observed in blank reaction without catalyst at this temperature, and this is in agreement with the data reported in the literature.[24]

By using the methyl monooxygenase (MMO) system, it has been reported that the activity for methanol synthesis is 5 mol (CH_3OH) kg(catalyst)$^{-1}$ h^{-1} for sMMO (C.bath) as a complete enzyme with NADH present (5μmol NADH, 45 °C, 12 min, 2 mg protein, pH 7, CH_4 6 mL at atmospheric pressure).[1] However, no data on CO_2 production *in vitro* has been given. In addition, when H_2O_2 is used as oxidant the catalytic activity decreases to 0.076 mole (CH_3OH) h^{-1} kg(MMOH) $^{-1}$(120 μmol sMMO hydroxylase, 100 mmol H_2O_2, 15min, 45°C).[25] Therefore, these studies demonstrate that Au-Pd supported nanoparticles are more efficient in the liquid phase oxidation of methane using hydrogen peroxide than MMO when hydrogen peroxide is the oxidant.

Another point to be emphasised here is that by using the Au-Pd/TiO_{2IW} catalyst, only CH_3OOH, CH_3OH and CO_2 were observed within the range of temperature employed. This has been confirmed by comparing the ^{1}H-NMR spectrum of each reaction solution to spectra of authentic standards of other potential reaction products, such as methyl formate, dimethyl ether and formaldehyde. Methyl formate as a product from oxidation of methane with H_2O_2 in water was reported by Mizuno *et al.* when using a di-iron-substituted silicotungstate catalyst.[10]

It is important to state here that in order to calculate the total reaction selectivity, which takes into account the presence of gas phase products in the liquid solution after reaction, an analysis has been carried out as described in detail in chapter 2 (section 2.4.2.4.2). Based on the average of several analyses, the amount of CO_2 detected in solution was only

20% from the value observed in gas phase. Therefore, at standard reaction (50 °C, 30 bar CH_4, 30 minutes reaction time) with 0.37 μmol of CO_2 in gas phase, the contribution from liquid phase is relatively insignificant, and the total oxygenates/methanol selectivity is considered to be at a similar level. This is the first work to show total selectivity including possible gas products in the liquid phase. Previous studies on liquid phase alkane oxidation present CO_x selectivity based on the gas products analysed only in gas phase.[13,15]

4.3.2.2. Effect of methane pressure

The variation of the CH_4 pressure from 5 to 60 bars has been studied by maintaining the same concentration of H_2O_2 (0.5 M). It has been reported in the literature that methanol productivity can be improved by increasing the pressure of CH_4,[15] and therefore the concentration of solubilised CH_4 in liquid medium (water) during reaction. For instance, the solubility of methane at 60 bar of pressure was 38% higher compared to the solubility of methane with 30 bar of pressure.[26] In figure 4.1, catalytic data of variation of methane pressure from 5 to 60 bars while maintaining similar H_2O_2 concentration are presented. It was evident that by increasing the pressure, the total amount of oxygenates as well as of each individual oxygenate increased, and therefore the productivity to oxygenate followed a progressive increase from 0.12 at 5 bar to 0.28 based on $moles_{product}\ Kg_{cat}^{-1}\ h^{-1}$ at 60 bar.

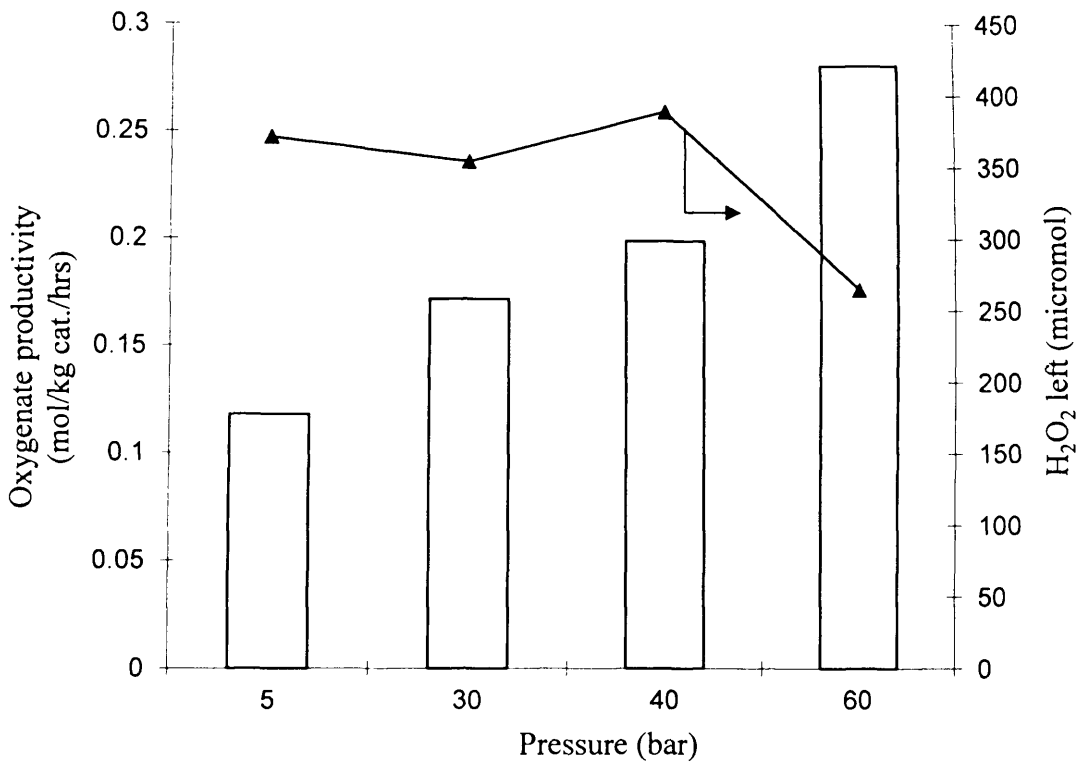

Figure 4.1: Pressure plot of methane oxidation with addition of H_2O_2 in the presence of 5wt%Au-Pd/TiO_{2IW} catalyst. Conditions: Time = 0.5 hours, [H_2O_2] = 0.5M, T = 50°C, 1500 rpm, catalyst mass = 28 mg.

However, there is contradiction from the literature in-term of H_2O_2 converted after reaction. It was reported by Yuan *et al.* that the conversion of hydrogen peroxide would be inhibited under higher methane pressure.[27] In that case, they explain that the decomposition of H_2O_2 proceeds via radical pathways and the presence of CH_4 may affect the radical reactions and thus exert influence on H_2O_2 conversion. Conversely in this study, the amount of H_2O_2 remaining after reaction was in a similar range in all cases, thus suggesting either that the mechanism involved is different, or due to the dominating role of the catalyst in accelerating the decomposition of H_2O_2 regardless of the pressure of methane. In-order to verify the later factor, analogue experiments at shorter reaction times (5 min) was performed. In these cases, it was found that the amounts of H_2O_2 available was always more than 0.1 M, therefore could probably minimise the effect of H_2O_2 concentration on influencing the exact effect of pressure. Figure 4.2 displayed the effect of methane pressure at 5 minutes reaction time. It was evident that oxygenates productivity still followed a similar pattern to that observed at longer reaction times, where the value increased with

increasing methane pressure. However, the conversion of hydrogen peroxide was clearly inhibited at increasing methane pressure up to 30 bar, and then slightly decreased within experimental error at 40 bar. It seems that at some point, the inhibiting effect of pressure in suppressing the utilization of H_2O_2 was probably less effective, and that the decomposition of H_2O_2 was dominated by the catalyst and/or reaction conditions. At first instance, it seems that the reaction would follow the same mechanism to that mentioned above, where H_2O_2 is radically decomposed to •OH/•OOH radical species which then react with solubilised methane. Though, reaction mechanistic study on this system did not support the observation and the detail discussions are presented in the following chapter (section 5.4.6).

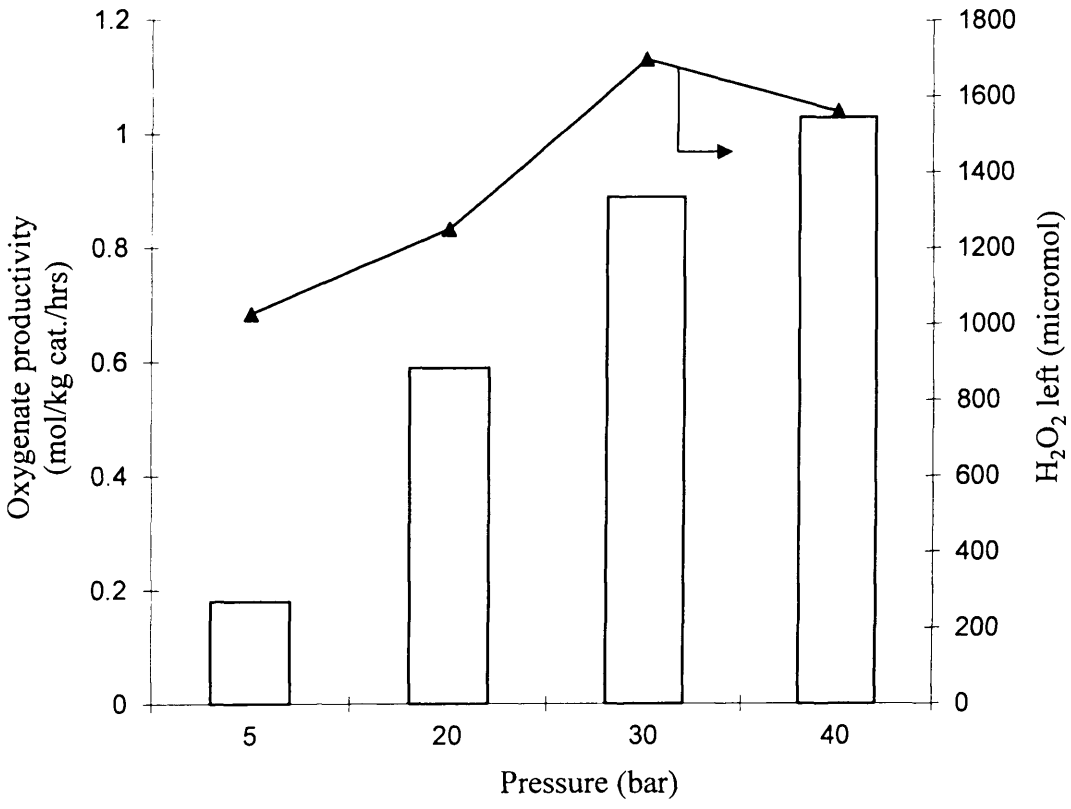

Figure 4.2: Pressure plot of methane oxidation with addition of H_2O_2 in the presence of 5wt%Au-Pd/TiO_{2IW} catalyst. Conditions: Time = 5 min, [H_2O_2] = 0.5M, T = 50 °C, 1500 rpm, catalyst mass = 28 mg.

4.3.2.3. Time on-line profile

Time on-line studies are crucial in determining the product distribution and to identify the reaction pathways involved in this particular reaction. The effect of reaction time on product formation was studied at 50 °C and it is shown in figure 4.3. Increasing the time of reaction from 5 minutes to 4 hours led to an overall increase in the total products. Time online study also indicates that methyl hydroperoxide, CH_3OOH is the primary product and that it gradually transforms to methanol in the presence of catalyst. Carbon dioxide as over oxidation product of methanol and methyl hydroperoxide (mainly from methyl hydroperoxide) is increased throughout the reaction progress.

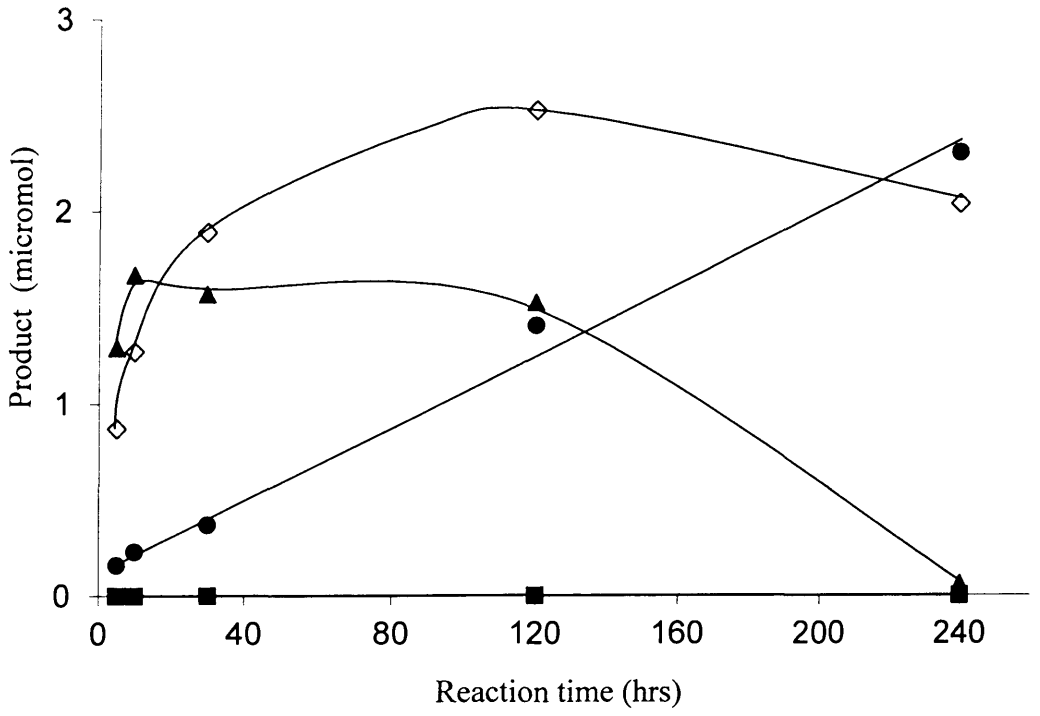

Figure 4.3: Time online plot of methane oxidation with addition of H_2O_2 in the presence of 5wt%Au-Pd/TiO_{2IW} catalyst. Key: ▲ methyl hydroperoxide, ◊ methanol, ■ formic acid, ● carbon dioxide. Conditions P(CH_4) = 30 bar, [H_2O_2] = 0.5M, T = 50 °C, 1500 rpm, catalyst mass = 28 mg.

Prolonging the reaction time from 0.5 to 2 hours was accompanied with an enhancement of methanol formation whereas further increase of reaction time led to a decrease in methanol formation with significant increase of CO_2 formation. It was observed in the range of

reaction times studied; neither formic acid nor formaldehyde was produced during the reaction. Based on the product stability studies in the presence of 5wt%Au-Pd/TiO_{2IW} catalyst, formic acid was discovered to less stable with more than 70% oxidised to carbon dioxide after 30 minutes reaction time. Similar to formic acid, formaldehyde also displayed a higher tendency to over oxidise (>80%) into formic acid and combustible CO_x products. This value was rather higher compared to only 29% of methanol converted mainly to carbon oxide (80% CO_x, 20% HCOOH) within similar range of reaction time. Hence, the unobservable formic acid and formaldehyde in methane oxidation with Au-Pd supported catalyst was rationalised to their low stability under reaction conditions. Therefore, proper choice of reaction time is necessary.

4.3.2.4. Effect of hydrogen peroxide concentration

A series of experiments varying the hydrogen peroxide concentration were carried out to determine the dependency of Au-Pd/TiO_{2IW} catalyst with oxidant. The reaction conditions such as methane pressure, reaction temperature and time were kept constant in each experiment except the concentration of H_2O_2. The results are illustrated in figure 4.4. Increasing the concentration from 0.15 M to 0.5 M of H_2O_2 significant increase in the formation of oxygenates as well as CO_2 was observed, with enhancement in oxygenate productivity. Nevertheless, the selectivity to methanol was not affected in the studied range of hydrogen peroxide concentration and it was in the range of 51-56 %. It seems, methane oxidation in this particular system is first order to H_2O_2 concentration.

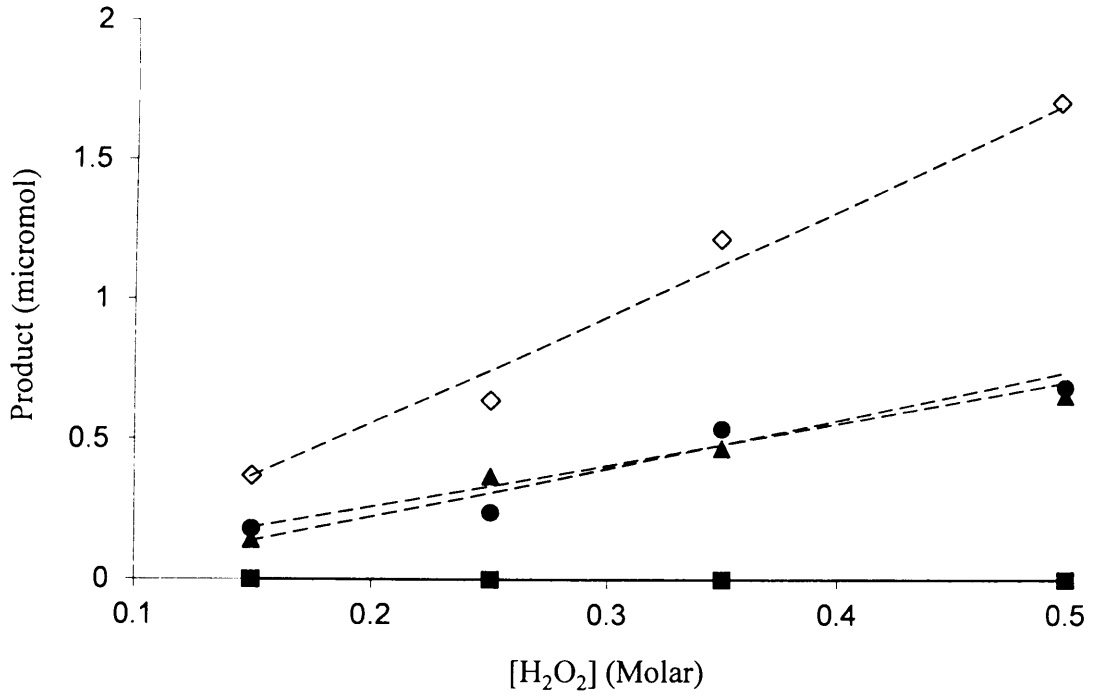

Figure 4.4: Effect of hydrogen peroxide plot on catalytic performance of 5wt%Au-Pd/TiO_{2IW} for selective methane oxidation with H_2O_2. Key: ▲ methyl hydroperoxide, ♦ methanol, ● carbon dioxide. Conditions: Time=0.5 hours, $P(CH_4)$=30 bar, T=50°C, 1500 rpm, catalyst mass = 28 mg.

Availability of the H_2O_2 throughout the reaction is crucial since it will probably form an active peroxy/hydroperoxy species which is capable of oxidizing methane to oxygenate. The molar ratio of methyl hydroperoxide and CO_2 are almost similar regardless the concentration of oxidant. Taking into account that the methyl hydroperoxide is the primary product, it could be speculated here that the origin of CO_2 arises from unselective transformation of methyl hydroperoxide instead of consecutive oxidation of methanol. It was reported in the literature that this primary product (CH_3OOH) is less stable than methanol and that it thermally decomposes at a temperature of around 46 °C to CO_2.[28] This speculation was further strengthened by product stability studies in the presence of 5wt%Au-Pd/TiO_{2IW}, which showed that more than 71% of methanol still remained after a similar length of reaction in an inert gas (detailed discussion in section 5.4.3 of chapter 5).

4.3.2.5. Effect of catalyst mass

The amount of catalyst used is an important variable in methane oxidation since there are a number of competing processes that also lead to the decomposition of hydrogen peroxide, which can significantly affect catalytic activity. The influence of increasing the amount of catalyst in the autoclave is shown in figure 4.5 for the 5wt%Au-Pd/TiO_{2IW} catalyst. The reactions were carried out at shorter reaction time (5 min) in order to minimise the effect of hydrogen peroxide concentration on the rate of reaction. Between 5 – 28 mg of catalyst, methane conversion increased linearly, but then decreased at higher catalyst loadings. It seems that by increasing the mass of catalyst above 28 mg, the decomposition of hydrogen peroxide was accelerated, and this subsequently affected the amount of oxidant available during the reaction and therefore the rate of reaction.

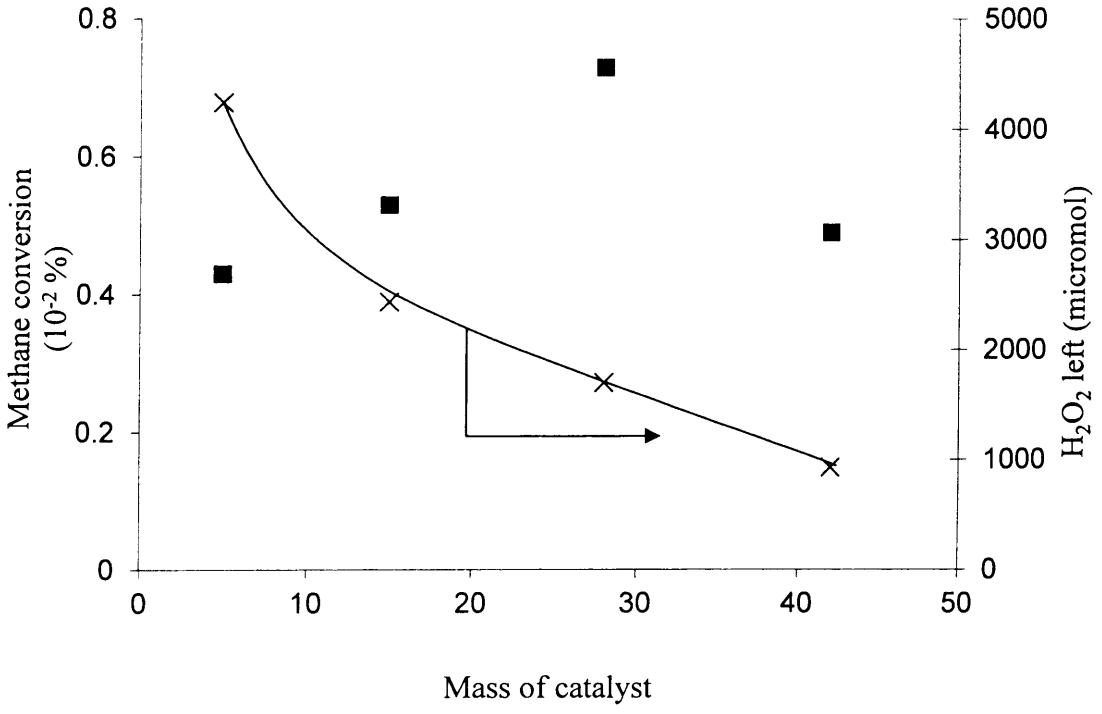

Figure 4.5: Effect of catalyst mass on catalytic performance of 5wt%Au-Pd/TiO_{2IW} for selective methane oxidation with H_2O_2. Key: ■ methane conversion, x H_2O_2 remains after reaction. Conditions: Time = 5 min, P(CH_4) = 30 bar, [H_2O_2] = 0.5M, T = 50 °C, 1500 rpm.

On the other hand, an opposite trend was observed for the selectivity profile, where similar methanol selectivity (24 – 26%) was observed over the range of 5 to 28 mg of catalyst. These values were in fact lower than the 39% methanol selectivity observed with 42 mg of catalyst. This could due to the limited accessibility of the catalyst active site in transforming the intermediate methyl hydroperoxide species into methanol at short reaction time.

However at longer reaction time (30 min), methanol selectivity increased linearly with increasing the catalyst mass whereas at the same time selectivity to methyl hydroperoxide was decreased due to the consecutive transformation of methyl hydroperoxide to methanol (figure 4.6). Interestingly, the mass of catalysts did not give a significant influence on formation of CO_2 suggesting the presence of Au-Pd catalyst is crucial in controlling the transformation of methyl hydroperoxide to methanol.

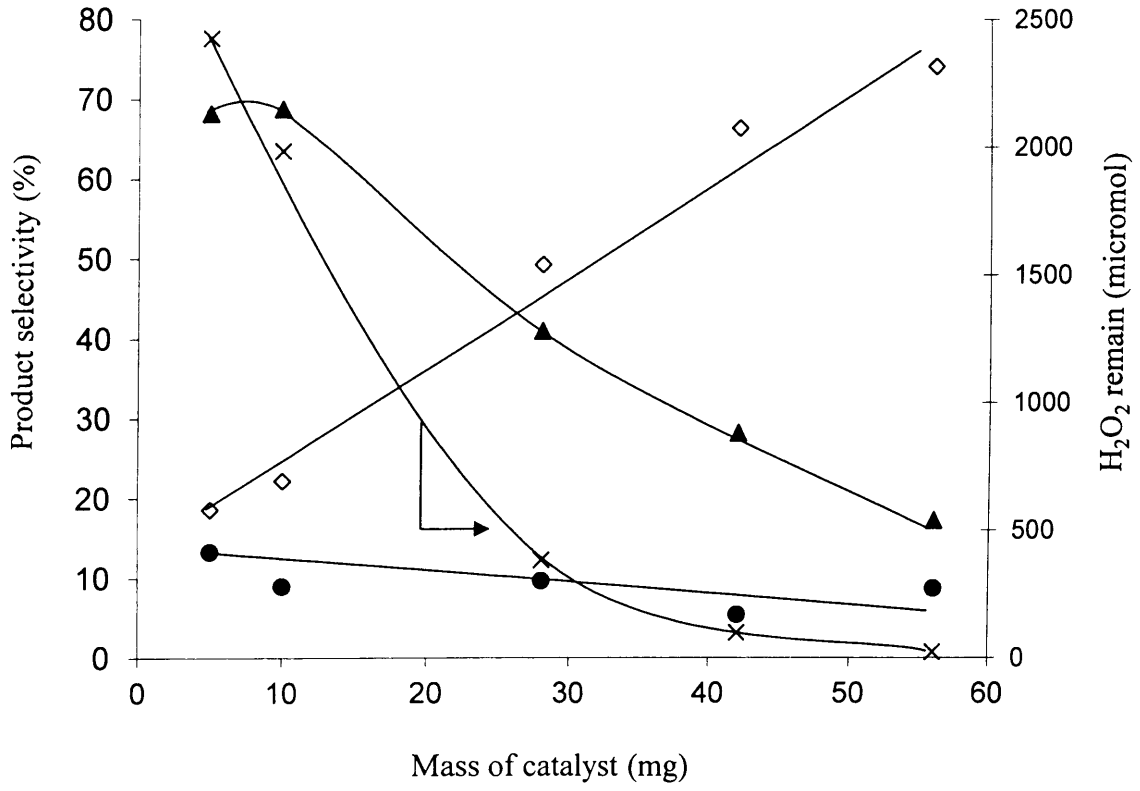

Figure 4.6: Effect of catalyst mass on catalytic performance of 5wt%Au-Pd/TiO_{2lw} for selective methane oxidation with H_2O_2. Key: ▲ methyl hydroperoxide, ◊ methanol, • carbon dioxide, x H_2O_2 remain after reaction. Conditions: Time = 0.5 hours, P(CH_4) = 30 bar, [H_2O_2] = 0.5M, T = 50 °C, 1500 rpm.

4.3.3. Effect of support on catalytic activity of Au-Pd bimetallic catalyst

The catalytic properties of supported metal catalysts are easily affected by the nature of the support material. The choice of support is vital in synthesising the metal supported catalyst with different structure and particle size, and as such a series of catalysts were prepared on other oxide supports. Considering the fact that hydrogen peroxide is more stable on acidic materials, the choice of support focus on acidic or neutral materials such as Al_2O_3, SiO_2, CeO_2 and Carbon. The Au-Pd nanoparticles catalysts with different support were synthesised using the impregnation method, and were thoroughly characterised and later tested for the *in-situ* synthesis of H_2O_2.[29-33] The results shown in table 4.5 demonstrate that TiO_2 is the preferred support, for both oxygenates productivity and methanol selectivity. In general, both activity and selectivity to methanol has the following order: $TiO_2 > Al_2O_3 > CeO_2 > Carbon > SiO_2$.

Table 4.5: Effect of different support on catalytic performance of 5wt% Au-Pd supported catalyst for the selective oxidation of methane with H_2O_2.

Entry	Support	Product amount (μmol)				Methanol Selectivity (%)[c]	Oxygenate productivity (Mol/kg_{cat}/ Hour) [d]	TOF [e]	H_2O_2 Remain (μmol) [f]
		CH_3OH [a]	HCOOH [a]	MeOOH [a]	CO_2 in gas[b]				
1	TiO_2	1.89	0	1.57	0.37	49.3	0.250	0.692	383
2	Carbon	0.63	0	0	1.55	28.9	0.046	0.126	87
3	CeO_2	0.63	0	0.74	0.16	41.2	0.099	0.274	192
4	SiO_2	0.30	0	0	1.31	18.6	0.022	0.060	58
5	γ-Al_2O_3	0.94	0	1.37	0.43	34.3	0.167	0.462	2942

Reaction Time; 30 min, Reaction Temp; 50°C, CH_4 pressure: 30 bar, Catalyst: 27.6 mg (1.0×10^{-5} mol of metal), [H_2O_2]: 0.5M, Solvent: H_2O, 10 mL, [a] Analysis using ^{1}H-NMR, [b] Analysis using GC-FID [c] Methanol selectivity = (mol of CH_3OH/ total mol of products) * 100, [d] Oxygenates productivity = mol of oxygenates / Kg_{cat} / reaction time (h), [e] Turn over frequency (TOF) = mol of oxygenates / mol of metal / reaction time (h), [f] Assayed by Ce^{+4} (aq) titration

Bimetallic Au-Pd supported on acidic alumina oxide gave lower hydrogen peroxide consumption where almost 60% oxidant left after 30 minutes reaction time. As stated in section 4.3.2, the larger availability of H_2O_2 during the reaction provides a possibility to produce a higher amount of oxygenate products, although this is clearly not the only factor given that a lower activity and selectivity to methanol was obtained with alumina as

support material compared to TiO_2. Based on EDX analysis of the STEM/HREM images, the composition and morphology of Au-Pd nanoparticles supported on Al_2O_3 should be similar as observed on TiO_2 which both consist of a core-shell structure where a gold-rich core surrounded by a palladium-rich shell is formed.[32,34] Therefore, the nature of core-shell structure might have a role in obtaining higher overall catalytic activity and selectivity. However, the core-shell structure is not the only factor since poor activity was obtained using SiO_2 as support; as mentioned in chapter 3, Au-Pd/SiO_{2IW} also consist of Au core-Pd shell structures. In order to clarify this observation and with the aim to find out the differences between Au-Pd/SiO_{2IW} catalyst compared to analogue TiO_2 and Al_2O_3, an examination with X-ray diffraction analysis has been carried out (see section 4.5.1). It was found that the crystallite size calculated based on XRD data for Au-Pd particles was lower (14.5 nm) for SiO_2 as support compared to 23.0 and 23.6 nm for catalyst supported with TiO_2 and Al_2O_3, respectively. In addition to that, based on XPS analysis of 5wt%Au-Pd/SiO_{2IW} reported by Edwards *et al.*, the signal correspond to metallic Pd (minor phase composition) was evidently observed together with Pd^{2+}.[31] In contrasts, Pd^{2+} signal dominate the XPS of Au-Pd on TiO_2 as support material (see section 4.5.4). Hence, it was believed here that lower oxygenate activity and selectivity observed for Au-Pd/SiO_{2IW} could due to the smaller metal particle size and presence of Pd^0 oxidation state. Both factors (particle size and oxidation state) could accelerate the H_2O_2 decomposition as confirmed by lower H_2O_2 detected after reaction.

In view of the fact that neither the structure of the alloy nor the crystallite size could explain the inferior catalytic performance of Au-Pd/Al_2O_{3IW} compared to Au-Pd/TiO_{2IW} catalyst, another approach has been taken by examined the nature of support itself. It was reported in literature that TiO_2 has an ability to interact with H_2O_2 and later produce and stabilise surface-peroxo (TiO_2-O_2^-) and/or hydroperoxy (Ti-OOH) species (See Scheme 4.1).[21] On the other hand, others support material used in this study did not have a capability to generated hydroperoxy species as TiO_2.

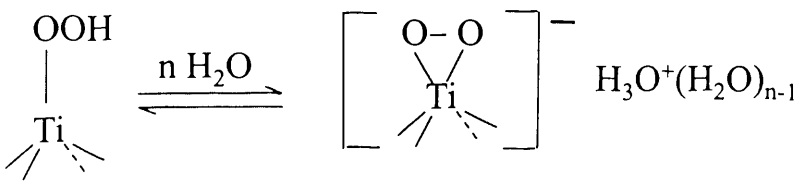

(Scheme 4.1)

The presence of surface-peroxo species is further indicated by the yellow colour change observed for the material upon interaction of TiO_2 with H_2O_2/H_2O.[21,22] However, TiO_2 itself is not principally active as it gives only a trace of methyl hydroperoxide without any formation of methanol. Additionally, it was proposed by theoretical modelling study[35] that the Au/Pd especially in oxide form (*i.e.* PdO) is capable in generating surface-peroxyl/hydroperoxyl species. It was reported in literature[36] that both Au-Pd supported catalysts either on TiO_2 or Al_2O_3 showed Pd (PdO) rich shell. However, details XPS calculation on surface molar ratio of Pd over Au demonstrated that Au-Pd/TiO_{2IW} consisted more than double Pd/Au ratio compared to Au-Pd/Al_2O_{3IW} catalyst. Thus could further enhance the catalytic activity of Au-Pd/TiO_{2IW} catalyst. Based on discussion above, it was suggested that the combination of Au-Pd and TiO_2 as support are important in oxidising methane selectively to methanol with high oxygenate productivity using H_2O_2 as oxidant at mild reaction conditions.

4.3.4. Effect of different preparation techniques on Au-Pd supported TiO_2 catalyst

It is well-known in catalysis that different preparation techniques affect catalyst morphologies, such as the oxidation state of the deposited metal, the average particle size and structure, and therefore overall catalytic activity. As discussed in chapter 1, there are several techniques that have been developed for synthesising metal supported catalysts, and in addition, even using the same technique, each additional parameter, such as heat treatments procedure is carefully manipulated and tuned to attain the target catalyst.[2] Generally, catalysts with higher surface areas and smaller metal particles are superior for catalytic oxidation reactions. Both factors can improve the accessibility of the substrate onto catalyst active site, and in some cases the electronic and geometric properties of the metal could be modified by having a small metal particle.[2] However, this is not always the rule. A unique catalyst property in many cases has to be developed for each substrate and reaction conditions.

In this section, attempts have been made to compare the catalytic activities of the catalysts based on preparation techniques such as impregnation and sol-immobilisation. The conventional impregnation technique has been chosen due to the fact that the preparation is relatively straightforward. Furthermore, the method is broadly used on synthesising commercial catalysts where the simplicity and cost are important. The Au-Pd/TiO_2 catalyst

synthesised via impregnation method and calcined in static air at higher temperature (400 °C) resulted in the formation of metal particles with bimodal particle size distribution where the smaller particle distribution was between 2-10 nm, whereas most of the large particles were 35-80 nm in size.[37] The metal particle size distribution obtained on analogue Au-Pd/TiO_2 catalyst prepared by sol-immobilisation was found to be much narrower *i.e.* between 6-7 nm.[38,39] Catalysts synthesized via the sol-immobilisation method are therefore typically more active than impregnation counterparts for several reactions such as benzyl alcohol and hydrogen peroxide synthesis.[40] This trend was also observed for toluene oxidation with molecular oxygen as oxidant as discussed in chapter 3. However, in the case of methane oxidation with addition of H_2O_2 as co-reactant as shown in table 4.6, the trend is opposite. A dried 1%Au-Pd/TiO_2 sol-immobilised catalyst with polyvinyl alcohol (PVA) as ligand gives inferior catalytic activity compared to an equivalent impregnation catalyst.

Table 4.6: Effect of preparation technique on catalytic performance of Au-Pd/TiO_2 for the selective oxidation of methane with H_2O_2

Entry	Catalysts/ preparation technique	Product amount (μmol)				Methanol Selectivity (%)[c]	TOF [d]	H_2O_2 Remain (μmol) [e]
		CH_3OH [a]	HCOOH [a]	MeOOH [a]	CO_2 in gas[b]			
1[f]	Impregnation (5wt%AuPd/TiO_2)	1.89	0	1.57	0.37	49.3	0.69	383
2[g]	Impregnation (1wt%AuPd/TiO_2)	0.30	0	1.82	0.10	14.2	6.43	2155
3[g]	Sol-Immobilisation (1wt%AuPd/TiO_2)	0.60	0	0	0.41	59.4	1.82	<15
4[g]	Sol-Immobilisation (1wt%AuPd/TiO_2) *(reflux)	0.34	0	0	0.25	57.6	1.03	<15

Reaction Time; 30 min, Reaction Temp; 50 °C, CH_4 pressure: 30 bar, [H_2O_2]:0.5M, Solvent: H_2O, 10 mL, [a] Analysis using ^{1}H-NMR, [b] Analysis using GC-FID, [c] Methanol selectivity = (mol of CH_3OH/ total mol of products) * 100, [d] Turn over frequency (TOF) = mol of oxygenates / mol of metal / reaction time (h), [e] Assayed by Ce^{+4} (aq) titration, [f] 28 mg of catalyst, [g] 10 mg of catalyst

*The 1wt%Au-Pd/TiO_{2SI} catalyst has been pre-treated with hot water reflux. Then the catalyst was filtered and washed with water.

As shown in literature, sol-immobilisation technique creates a different structure of bimetallic particles where it consist a homogeneous Au-Pd alloy with both Pd and Au in

metallic state.[40,39] Other issue may arise due to the presence of the ligand (polyvinyl alcohol (PVA)) which may cover the active metal and therefore possibly reduced the accessibility of the metal. In view of this, an additional step has been taken to remove the ligand by means of refluxing method as detailed in chapter 2. However, the catalytic data obtained following this additional step was in fact lower compared to the catalyst containing the ligand, indicating that the metal state of the catalyst strongly affects the overall activity. After all, it must to remember here that the sol-immobilisation method also includes the reduction of metal using sodium borohydride ($NaBH_4$), and therefore regardless of if the catalyst is dried or proceed with heat treatment, the oxidation state is mostly metallic.[39] Therefore, lower activity may due to the significantly higher rate of H_2O_2 decomposition with most of the oxidant converted after reaction. It is crucial to state here that bubbling of gas upon contact between water containing H_2O_2 and the sol-immobilised catalyst, indicating the presence of O_2 gas originated from decomposition of hydrogen peroxide. Separate experiments demonstrated that at the start of reaction (time = 0 without stirring) in the presence of Au-Pd/TiO_{2SI} catalyst, the amount of H_2O_2 available was around 42% (0.21M) of the initial concentration. This value is significantly lower compared to the 76% (0.38M) observed for the analogous Au-Pd/TiO_2 catalyst synthesised via impregnation technique.

In order to fairly compare the effect of preparation techniques on Au-Pd supported TiO_2 catalyst, similar loading of metal was prepared using an impregnation method and calcined in static air at 400 °C. This catalyst is expected to have bigger metal particle size with wider metal particle size distribution compared to sol-immobilised catalyst counterpart as well as difference in composition of metal oxidation state. By using similar mass of catalyst, it is apparent from table 4.6 (entry 2) that impregnated catalyst gave higher activity by a factor of 3 based on TOF values and only half of hydrogen peroxide used or decomposed during the reaction. In contrast to the sol-immobilised catalyst, the impregnated catalyst produced methyl hydroperoxide as main product, suggesting that there is another factor that must be considered in order to obtain superior activity coupled with higher selectivity to methanol as target product. In view of this, it seems that the combination of metal oxidation state with a specific composition is vital and should be overseen in order to improve the catalyst performance.

In general, the outcome from the effect of preparation technique is in line with the hydrogen peroxide-activity trend discussed in early section 4.3.2.4 in this chapter. As stated above, a unique catalyst property may be specific for the type of reaction and this

was proven since the sol-immobilised catalyst provided superior catalytic activity than impregnated catalyst in toluene and toluene derivative as shown in chapter 3.

4.3.5. Oxidation with different Au/Pd metal ratio supported on TiO_2

Following on from the work described in section 4.3.3, it is clear that TiO_2 is the best support for methane oxidation with H_2O_2 as oxidant. A series of Au-Pd bimetallic catalysts with different Au to Pd (wt% ratio) were prepared on this support using an impregnation method, and their activity for methane oxidation was evaluated after the catalysts had been calcined at 400 °C for 3 hours in static air. All catalysts have similar total metal loading equal to 5wt%. The results shown in table 4.7 illustrate that the catalysts are active toward methane oxidation but with different catalytic performance.

Table 4.7: Effect of Au:Pd ratio on catalytic performance of Au-Pd/TiO_{2IW} catalyst for the selective oxidation of methane with H_2O_2.

Entry	Au:Pd ratio (wt%:wt%)	Product amount (μmol)				Methanol Selectivity (%)[c]	TOF [d]	H_2O_2 Remain (μmol) [e]
		CH_3OH [a]	HCOOH [a]	MeOOH [a]	CO_2 in gas[b]			
1	5Au	0.74	0	0.93	0.29	37.8	0.334	2979
2	4Au: 1Pd	0.93	0	2.53	0.15	25.8	0.692	798
3	2.5Au: 2.5Pd	1.89	0	1.57	0.37	49.3	0.692	383
4	1Au: 4Pd	1.64	0	0.54	0.13	71.0	0.436	85
5	5Pd	1.74	0	0.67	0.22	72.2	0.482	110

Reaction Time; 30 min, Reaction Temp; 50 °C, CH_4 pressure: 30 bar, Catalyst: 1.0 x 10^{-5} mol of metal, [H_2O_2]:0.5M, Solvent: H_2O, 10 mL, [a] Analysis using ^{1}H-NMR, [b] Analysis using GC-FID, [c] Methanol selectivity = (mol of CH_3OH/ total mol of products) * 100, [d] Turn over frequency (TOF) = mol of oxygenates / mol of metal / reaction time (h), [e] Assayed by Ce^{+4} (aq) titration
Catalysts: synthesized via impregnation method and calcined at 400 °C in static air for 3 hours.

Since the TiO_2 as support itself showed a negligible catalytic activity, the mass of catalyst used is based on total mol of metal and the catalytic comparison should be evaluated based on turn over frequency (TOF). Monometallic Au catalyst exhibited the lower activity toward oxygenates, but used significantly less H_2O_2 during the reaction. The addition of Pd to Au significantly enhanced the catalytic performance, with the optimum Au-Pd

composition being 1 to 1 weight (2.5wt%Au2.5wt%Pd), where a compromise between catalytic activity and selectivity toward methanol was achieved. It is important to note here, at this particular reaction conditions, a higher Pd content enhanced the selectivity to methanol whereas the trend is different with higher Au contents, where higher selectivity towards to methyl hydroperoxide was obtained. In the presence of Au, decomposition of H_2O_2 seems to be suppressed. This is in agreement with the literature studies on decomposition/hydrogenation of hydrogen peroxide which shows the following trend; Au < Au-Pd < Pd.[41]

Differences in the catalytic pattern could be explained by detailed examinations of the catalyst properties. According to XRD data in section 4.5.1 of this chapter, the average crystallite size for both 4.0wt%Au1.0wt%Pd and 1.0wt%Au4.0wt%Pd were almost similar (20 nm); therefore in this case, it seems the particle size did not play a major role in controlling the selectivity of methanol. Indeed the metal surface composition factor is believed to be responsible for selectively transforming methyl hydroperoxide to methanol as well as the decomposition of hydrogen peroxide. This is supported by the catalytic data obtained with 2.5wt%Au2.5wt%Pd catalyst which showed an identical TOF value and higher methanol selectivity compared to 4.0wt%Au1.0wt%Pd even in the presence of slightly bigger metal particle size (23 nm). A detail XPS analysis in section 4.5.4 showed that all bimetallic Au-Pd/TiO_{2IW} catalysts tested in table 4.7 in some extent were believed to have core-shell structure with palladium rich shell and gold rich core. This statement was based on the unobservable Au signal in the combined Au (4d) and Pd (3d) XPS spectra. In addition to this, the relative Pd to Au atomic ratio calculated for 4.0wt%Au1.0wt%Pd/TiO_{2IW} catalyst was higher (6.95 atom/atom) than the theoretical value (0.47 atom/atom), calculated by assuming a random solid solution. This Pd to Au atomic ratio value was almost similar to 2.5wt%Au2.5wt%Pd/TiO_{2IW} (6.91 atom/atom) catalyst. However, the atomic percentage of each Au and Pd was different which almost double in 2.5wt%Au2.5wt%Pd/TiO_{2IW} compared to 4.0wt%Au1.0wt%Pd/TiO_{2IW} catalyst. Therefore, this suggests that the Au core-Pd shell structure with appropriate surface atomic percentages of both Au and Pd was important in controlling the catalytic activity and selectivity to methanol as well as the hydrogen peroxide utilization. An excess Pd species on the surface of 1.0wt%Au4.0wt%Pd/TiO_{2IW} (Pd/Au atomic ratio equal to 20.3 atom/atom) catalyst increased the methanol selectivity but at the same time accelerated the hydrogen peroxide decomposition-hydrogenation process and therefore decreased the catalytic performance (lower TOF value).

4.3.6. Catalyst pretreatment and its influence on methane oxidation

In view of the fact that the optimum composition of the Au-Pd supported on TiO_2 was determined to be an equal weight ratio (2.5wt%Au2.5wt%Pd) as described in section 4.3.5, further steps towards catalyst optimisation have been taken by pre-treating the catalyst. Either the dried catalyst was used, or the catalyst was calcined prior to use. It is reported in the literature that catalyst pretreatment will affect the catalyst properties and consequently their catalytic activity.[2] The data are compared with the standard calcinations procedure as shown in entry 1, table 4.8. It was apparent that a reductive pretreatment, either by flowing 5% hydrogen in argon over the catalyst, or chemically reducing the catalyst with sodium borohydride, ($NaBH_4$) led to a decrease in the productivity of the catalyst, as determined over 30 minutes of reaction time. A similar trend was obtained with monometallic Au or Pd catalytic systems where both of reduced samples showed lower activity compared to calcined counterparts.

Table 4.8: Effect of catalyst pretreatment on catalytic performance of 5wt%Au-Pd/TiO_{2IW} for the selective oxidation of methane with H_2O_2

Entry	Pretreatment	Product amount (μmol)				Methanol Selectivity (%)[c]	TOF [d]	H_2O_2 Remain (μmol) [e]
		CH_3OH [a]	HCOOH [a]	MeOOH [a]	CO_2 in gas[b]			
1	Static air	1.89	0	1.57	0.37	49.3	0.692	383
2	Flowing 5%H_2/Ar	0.58	0	0	<0.05	92.1	0.116	27
3	Reduced $NaBH_4$	0.30	0	0	<0.05	85.7	0.060	27
4	H_2O_2 treatment	0.40	0	0	<0.05	88.8	0.080	61
5	Flowing 50%O_2/He	1.14	0	0.29	0.53	65.9	0.286	30

Reaction Time; 30 min, Reaction Temp; 50 °C, CH_4 pressure: 30 bar, Catalyst: 27.6 mg (1.0×10^{-5} mol of metal), [H_2O_2]:0.5M, Solvent: H_2O, 10 mL, [a] Analysis using ^{1}H-NMR, [b] Analysis using GC-FID, [c] Methanol selectivity = (mol of CH_3OH/ total mol of products) * 100, [d] Turn over frequency (TOF) = mol of oxygenates / mol of metal / reaction time (h), [e] Assayed by Ce^{+4} (aq) titration
Catalyst: Synthesised via impregnation method.

The reason for the lower activity obtained in reduced catalysts could be attributed to the higher rate of non-selective H_2O_2 decomposition. As previously shown in section 4.3.4, catalysts with smaller particle size and higher metallic Pd content decomposed a higher amount of H_2O_2 without having sufficient contact time to generate the active species responsible for oxidising methane to oxygenate species. Structural analysis of catalysts by means of X-ray diffraction (XRD) illustrates that a smaller crystallite size (16 nm) was observed for the reduced catalysts, as compared to 23 nm crystallite size obtained in the case of calcined sample (see section 4.5.1 of this chapter). The XRD pattern also clearly shows the peak corresponding to Pd in metallic state based on the JCPDS reference file. Metallic palladium was also observed in the H_2O_2 treated catalyst, and the crystallite size was calculated using Scherer equation to be 15 nm.

Further analysis with XPS in section 4.5.4 confirmed the data obtained by XRD where a PdO (Pd^{2+}) signal dominated the calcined catalyst whereas the reduced catalysts had a mixture of Pd^0 and Pd^{2+}. In particular, the Au-Pd/TiO_{2IW} catalyst pre-treated in hydrogen environment have 50.3% Pd^0 and 49.7% Pd^{2+} phase whereas catalyst reduced with sodium borohydride having 30.9% Pd^0 and 60.1% Pd^{2+}. The presence of Pd^0 seems to be detrimental towards methane oxidation activity; therefore a step has been taken to generate higher concentration of Pd^{2+} phase on the surface of the catalyst by subjecting the dried catalyst into flow of O_2 for 3 hours at 400 °C. It was reported in previous studies that bulk Pd-Au alloys heated in oxygen atmosphere at temperature greater than 300 °C will enrich the surface layer of catalyst with PdO species. Thermodynamically, this is a consequence of the exothermic heat of formation of PdO compared with the endothermic heat of formation of Au_2O_3.[42] Although, the catalytic activity toward methane oxidation observed with catalyst calcined in O_2/He environment was inferior compared to standard calcinations in air, it was still higher than reduced samples, and it clearly demonstrates the positive role of PdO on the surface. The lower activity could be ascribed to the smaller crystallite size (13 nm) which, as it was discussed previously, is one of the main factors accelerating the unselective decomposition of hydrogen peroxide.

However, whilst the oxygenate productivity with reduced Au-Pd/TiO_2 catalyst was inferior, the selectivity to methanol was improved up to 92%. The reason behind the higher selectivity of reduced catalyst was due to the unobservable methyl hydroperoxide as one of the oxygenate products. Noteworthy that similar observation was obtained with sol-immobilised catalyst discussed in section 4.3.4. Therefore, the data suggested that mechanism related to the formation of methanol on reduced catalyst could be different to

the calcined catalyst. As reported in the literature, metallic Au and Pd have a higher tendency to split H_2O_2 into hydroxyl rather than to hydroperoxyl species.[43,44] Thus increases the possibility to directly produced methanol from the reaction between methyl and hydroxyl species without undergo methyl hydroperoxide route. Details mechanisms are presented in the following chapter.

In general, at these particular conditions, methane oxidation with H_2O_2 added as co-reactant, high catalytic activity requires Au-Pd catalyst with metal particle size probably more than 20 nm and the palladium should be in the oxidised state.

4.4. General applicability of the Au-Pd catalytic system on ethane oxidation

4.4.1. Introduction

The successful utilisation of hydrogen peroxide for the selective oxidation of methane to methanol either by the addition or *in-situ* synthesis of the oxidant (see chapter 5) opens a window for the possibility to explore the general applicability of the catalytic system on higher alkanes, such as ethane oxidation with hydrogen peroxide as oxidant. Theoretically ethane with slightly lower C-H bond dissociation energy (410 kJ/mole) than methane (431 kJ/mole)[45] should be more active toward oxidation. Moreover, the solubility of ethane in water was higher compare to solubility of methane. For instance, at 50 °C, the amount of ethane solubilised in water at atmospheric pressure was calculated to be around 2.3 times higher than as estimated with methane.[46] However, due to the fact that it has two carbon atoms, the reaction could progress through C-C bond cleavage and potentially generate C_1 products which could affect the product distribution. From an industrial point of view, and since natural gas consists of a mixture of gases (mainly methane), this phenomenon is highly interesting given the formation of same end product from different alkanes, thus in some extent avoiding the need to separate the alkanes in natural gas. For example, natural gas is principally methane with 5-10% ethane. A system that converts both methane and ethane to the same C_1 product, such as methanol, would not require the prior separation of the alkanes. Given that the oxidation was carried out purposely to prove the applicability of the developed catalytic system, the reactions were carried out at standard reaction conditions followed with the oxidation at optimised conditions.

4.4.2. Oxidation at standard reaction conditions

The standard reaction conditions were set to the shorter reaction time (0.5 hours) in the presence of 0.5M hydrogen peroxide and at a temperature range of 50 to 70 °C. The results are summarised in table 4.9. It is clear from this that the oxidation of ethane is possible at low temperature (50-70 °C), and that selectivity to oxygenate products in the range of 97-99% can be achieved. At 50 °C the major product is ethanol, with selectivity around 72%. Interestingly at this particular condition (50 °C), only ethanol, ethyl hydroperoxide and acetaldehyde in hydrated form were observed which indicates the C-C bond cleavage did not occur. From the bond energies of the C-C and C-H bonds in the ethane molecule, it would be predicted that the lower bond energy of the C-C bond (330 kJ/mol) versus the C-H bond (410 kJ/mol) would lead to higher activity, and that C_1 oxygenated could be produced via C-C bond scission. Moreover, similar trends to methane oxidation were observed, as there is no formation of acetic acid, showing the unique role of Au-Pd supported nanoparticles size in controlling the selectivity to alcohol. However, increasing the reaction temperature from 50 to 70 °C leads to the formation of C-C bond cleavage products, but at rather lower selectivity relative to C_2 products. In view of the fact that at these particular conditions, as shown in the analogue methane oxidation reaction, methanol is relatively stable and therefore no formic acid is detected. Conversely, higher temperature affected the reaction pathway and acetic acid accounted for about 11% of the total oxygenates product. From this, it is believed that consecutive oxidation of ethanol and acetaldehyde products took place. In general, the overall activity at 70 °C is 36% higher than at 50 °C, whereas the oxygenate selectivity dropped slightly from 99.2 to 97.6 %. It is noteworthy that the overall catalytic activity based on both oxygenates productivity (moles (oxygenates) kg^{-1} (cat) h^{-1}) and TOF (moles (oxygenates)/moles of metal (cat) h^{-1}) increased by a factor of 3 compared to the methane oxidation at similar reaction conditions. The data indicate that the catalytic activity strongly related to the solubility factor as well as C-H bond strength of alkane. The solubility factor was believed to be more prominent than the effect of different C-H bond strength, based on the only slight different (21 kJ/mole) between C-H bond strength of ethane compared to methane. The difference in catalytic activity (3 times higher in ethane) was in line with the difference in gas solubility value (>2 times). Similar reactivity patterns with showed higher catalytic activity with ethane compared to methane as a substrate were also observed in literature with homogeneous gold solution.[15,16]

Entry	Temp. (°C)	Product amount (μmol)							Oxygenates selectivity (%)[c]	Ethanol selectivity (%)[d]	Oxygenate Productivity (Mol/kg_{cat}/ Hour) [e]	TOF [f]	H_2O_2 Remain (μmol) [g]
		EtOH [a]	CH_3COOH [a]	EtOOH [a]	MeOH [a]	CH_3CHO/ CH_3CHO, hydrated [a]	CO (g) [b]	CO_2 (g) [b]					
1	50	8.80	0	1.80	0	0	0	0.23	99.2	72.4	0.873	2.410	101
2	70	11.15	2.24	0.87	1.27	3.39	0.18	0.73	97.6	59.5	1.371	3.784	68

Reaction Temp; 50 °C, Total pressure: 30 bar, rpm: 1500 rpm, Catalyst: 1.0×10^{-5} mol of metals, $[H_2O_2]$:0.5M, Volume: H_2O, 10 mL.

[a] Analysis using ^{1}H-NMR, [b]Analysis using GC-FID, [c] Oxygenates selectivity based on Carbon = (mol of oxy./ total mol of products) * 100 [d] Ethanol selectivity based on Carbon = (mol of EtOH/ total mol of products) * 100, [e] Oxygenates productivity = mol of oxygenates / Kg_{cat} / reaction time (h), [f] Turn over frequency (TOF) = mol of oxygenates / mol of metal / reaction time (h), [g] Assayed by Ce^{+4} (aq) titration

Taking into account the literature for ethane oxidation at mild conditions, Suss-Fink *et al.* have reported the oxidation of ethane in water solution using homogeneous vanadium-containing polyphosphomolybdates (ethane, 30 bar; air, 10 bar; $[H_2O_2]$ = 2.35 mol dm^{-3}, $[PMo_{11}VO_{40}]^{4-}$ = 1.0 × 10^{-4} mol dm^{-3}, 100 °C, 24 hours). However, only small concentrations of ethanol were observed, and the concentrations of acetaldehyde and acetic acid did not exceed the concentrations obtained in the blank (*i.e.* uncatalysed) experiment in the absence of the catalyst.[6] The alcohol product was only observed in the place of acetonitrile as solvent instead of water. By using vanadium complex -pyrazine-2-carboxylic acid with presence of H_2O_2 and air in acetonitrile, similar group reported that ethane could be activated at 40 °C yield ethanol, acetaldehyde and acetic acid in addition to ethyl hydroperoxide, acetic acid being obviously a secondary product.[47] However, at temperatures as low as 5 °C using manganese (IV) complex–carboxylic acid in acetonitrile and H_2O_2 as oxidant, no acid product was observed.[48] It is important to emphasise that in all cases, the total amount of alcohol is not directly produced during reaction, but from the reduction of alkyl hydroperoxide using an excess of solid triphenylphosphine (PPh_3).[6,48]
It was noticed here that most of the available literature did not report any formation of C_1 oxygenates regardless of the reaction conditions except the works by Sen *et al,*[49,50] although in contrast to the data obtained for 5wt%Au-Pd/TiO_{2IW} catalyst, Sen and co-workers observed the formation of formic acid together with ethanol and acetic acid at rather lower temperature, 30 °C. No methanol formation was observed and the formation of formic acid is claimed to be originated from further oxidation step of acetic acid involving C-C bond cleavage.

4.4.3. Ethane oxidation at optimised reaction conditions

Following on the work presented in section 4.3.1 to 4.3.6, it seems that the overall catalytic activity could be improved by varying selected parameters. In this study, 5wt%Au-Pd/TiO_2 synthesised via impregnation method and calcined at 400 °C was selected as the test catalyst given the fact it gave the best compromise between catalytic activity and selectivity to oxygenates, especially the alcohol product. In addition to this, the oxidation at optimised conditions was carried for ethane instead of methane based on the 3-fold increase in total oxygenates obtained for the C_2 substrate, which makes it easier to monitor the possible changes in catalytic pattern. The reaction parameters such as, pressure,

reaction time, catalyst mass and concentration of hydrogen peroxide were altered where in each case, some parameters were kept constant. The catalytic data are summarised in table 4.10 and it is apparent that in all cases, oxygenates selectivity is more than 98%. The highest ethane conversion obtained was around 2.21 %, however it is strongly believed that this value could still be improved. In contrast to the standard reaction at 50 °C, where C-C splitting is not observed, the higher concentration of H_2O_2 probably cause the formation of acetic acid as well as assist the formation of methanol. However, formic acid was only observed in test with higher pressure and longer reaction time (entry 4).

The presence of formic acid at this particular test could be due to the consecutive oxidation of methanol and/or from C-C cleavage of ethyl hydroperoxide or acetic acid as mentioned above. Experiments using acetic acid as substrate under the standard reaction conditions but in the presence of helium instead of ethane indicated that acetic acid is rather stable as only 2% converted to carbon oxide during the reaction period. Additionally, it was reported that formic acid is less stable than acetic acid, and that it might decompose to CO and water and/or over-oxidise to CO_2 and water.[49] Another point to make was the higher amount of hydrogen peroxide left after reaction as shown in entry 4 compared to entry 5, and this is in agreement with data reported in the literature[15] where they claimed that higher pressure stabilised and suppressed the decomposition of hydrogen peroxide.

In view of the fact that higher concentrations of hydrogen peroxide could affect the stability of the metal during reaction, an atomic absorption spectroscopy (AAS) analysis was carried out on filtrate of reaction solution after reaction. It was evidence from analysis that the amount of metal leaching was negligible.

Entry	Product amount (μmol)								Conv.(%) [c]	Oxygenates selectivity (%)[d]	Ethanol selectivity (%)[e]	Oxygenate productivity (Mol/kg_{cat}/ Hour)[f]	TOF [g]	H_2O_2 Remain (μmol) [h]
	EtOH [a]	CH_3COOH [a]	EtOOH [a]	MeOH [a]	HCOOH [a]	CH_3CHO + CH_3CHO hydrated [a]	CO in gas [b]	CO_2 in gas [b]						
1	8.8	0	1.8	0	0	1.45	0	0.20	0.04	99.2	72.4	0.873	2.410	101
2	14.4	11.6	9.0	3.0	0	3.6	0	0.28	1.39	99.6	35.8	1.486	4.160	1838
3	4.2	2.9	12.6	0.7	0	7.0	0.08	0.74	0.93	98.5	15.3	2.740	2.740	6803
4	60.3	27.7	14.5	9.6	5.2	43.0	0.15	3.82	0.53	98.7	38.9	4.008	4.008	2794
5	10.7	11.3	23.6	1.4	0	17.1	0.12	2.14	2.21	98.2	16.6	1.603	4.423	1773

[a] Analysis using ^{1}H-NMR, [b]Analysis using GC-FID, [c] Conversion (%) = (total mol of products./ theoretical mol of CH_4 in gas phase) * 100 [d] Oxygenates selectivity based on Carbon = (mol of oxy./ total mol of products) * 100 [e] Ethanol selectivity based on Carbon = (mol of EtOH/ total mol of products) * 100, [f] Oxygenates productivity = mol of oxygenates / Kg_{cat} / reaction time (h), [g] Turn over frequency (TOF) = mol of oxygenates / mol of metal / reaction time (h), [h] Assayed by Ce^{+4} (aq) titration

Entry 1: Reaction Time; 30 min, Reaction Temp; 50°C, pressure: 30 bar, Stirring rate: 1500 rpm, Catalyst: 28 mg of catalyst, H_2O_2:0.5M, solvent: H_2O, 10 mL.
Entry 2: Reaction Time; 30 min, Reaction Temp; 50°C, pressure: 5 bar, Stirring rate: 1500 rpm, Catalyst: 56 mg of catalyst, H_2O_2:2.0M, solvent: H_2O, 20 mL.
Entry 3: Reaction Time; 60 min, Reaction Temp; 50°C, pressure: 5 bar, Stirring rate: 1500 rpm, Catalyst: 10 mg of catalyst, H_2O_2:2.0M, solvent: H_2O, 20 mL.
Entry 4: Reaction Time; 240 min, Reaction Temp; 50°C, pressure: 30 bar, Stirring rate: 1500 rpm, Catalyst: 10 mg of catalyst, H_2O_2:2.0M, solvent: H_2O, 20 mL.
Entry 5: Reaction Time; 240 min, Reaction Temp; 50°C, pressure: 5 bar, Stirring rate: 1500 rpm, Catalyst: 10 mg of catalyst, H_2O_2:2.0M, solvent: H_2O, 20 mL

4.5. Catalyst Characterisation

A number of different spectroscopic techniques were employed in an attempt to elucidate the nature of the supported Au-Pd catalysts. Mainly, the catalysts were studied using two different techniques, namely X-ray diffraction analysis (XRD) and X-ray photoelectron spectroscopy (XPS). In addition to this, selected catalysts were subjected to BET surface area measurements in to obtain the catalysts surface area and an analysis with Atomic Absorption Spectroscopy (AAS) in order to verify the actual percentages of metal loading in prepared catalysts. The characterisation data obtained in this study were then corroborated and combined with the related published data available on this type of catalysts.

4.5.1. X-ray diffraction (XRD) analysis

X-ray diffraction analysis was conducted on the samples as detailed in chapter 2. The characterisations were carried out purposely to determine the crystal structure and the mean crystallite size of the involved metal as well as their oxidation state.[51,2] The powder XRD diffractogram of the fresh mono or bimetallic Au/Pd supported on TiO_2 with different percentages of weight ratio were displayed in figure 4.7. All catalysts have been calcined in static air at 400 °C for 3 hours. The XRD pattern of 5wt%Au/TiO_{2IW} indicated the presence of characteristic peaks of Au at $2\theta = 38.2^{\circ}$, 44.3° and 64.5° which are assigned to the (111), (200), (311) planes respectively. These particular reflections were obtained by referring to the JCPDS file no. 03-065-2870. On the other hand, the diffraction pattern of 5wt%Pd/TiO_{2IW} did not show any clear peaks assigned to either metallic Pd or PdO. The diffraction peaks for Pd in metallic state could be examined at $2\theta = 40.4^{\circ}$, 46.9° and 68.6° (JCPDS file 01-087-0645) whereas the formation of PdO (Pd^{2+}) was identified by main peaks at $2\theta = 33.6^{\circ}$, 33.9° and 54.8° (JCPDS file 00-006-0515) corresponds to (002), (101) and (112) reflections, respectively. An observed Pd peak could be attributed to the smaller crystallite size which is lower than detectability limit of XRD (<5 nm) or due to the high metal dispersion on the TiO_2 support.[2] XRD diffraction patterns of all Au-Pd bimetallic catalysts evidently indicated the presence of Au or Au-Pd alloy peaks, whereas the Pd species were not detected probably due to the reason mentioned above.

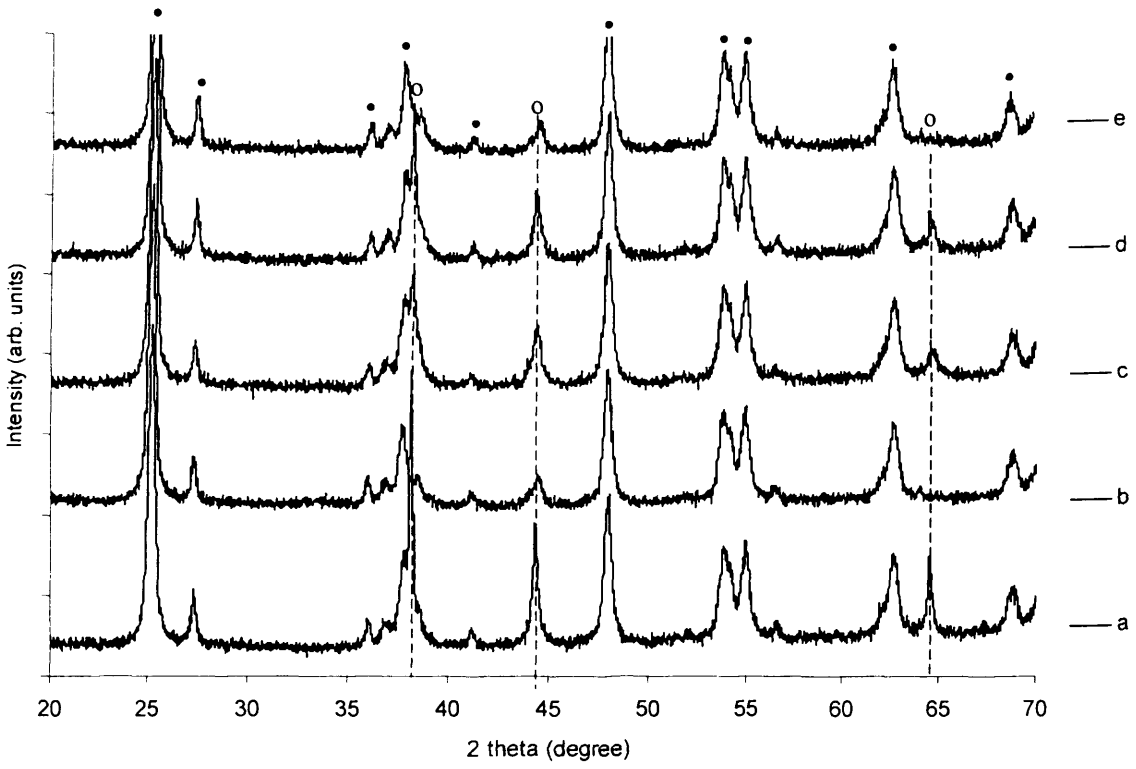

Figure 4.7: X-ray diffraction patterns of Au/Pd-TiO_{2IW} catalyst with different Au:Pd ratio calcined in air 400°C. Key: (a) 5.0wt%Au, (b) 5.0wt%Pd, (c) 2.5wt%Au2.5wt%Pd, (d) 4.0wt%Au1.0wt%Pd, (e) 1.0wt%Au4.0wt%Pd, Symbol: (•) TiO_2, (o) Au/Au-Pd alloy

For 2.5wt%Au2.5wt%Pd/TiO_{2IW}, the slight shift of the Au peaks to the right (slightly higher of 2θ value) in figure 4.7 was observed indicating the formation of Au-Pd alloy as reported in literature. [52,32,53] The gradual shift was further emphasised (figure 4.8), where the X-ray diffraction patterns of a series of Au–Pd/TiO_{2IW} with different Au/Pd weight ratio was contrasted. The possible formation of Au-Pd alloy on 1.0wt%Au4.0wt%Pd/TiO_{2IW} catalysts could be observed by the shifting of Au peak to more closely into Pd phase which is observed at higher angles in comparison with the equal weight catalyst (2.5wt%Au2.5wt%Pd).

In all cases, the diffraction lines corresponding to the TiO_2 (P25) support were clearly observed at 2θ = 25.3°, 37.8°, 48.0°, 53.9°, 55.1° and 62.7° for anatase phase (JCPDS file no: 01-078-2486) whereas diffraction peaks corresponds to rutile phase TiO_2 could be examined by characteristic peaks at 27.4°, 36.1°, 56.5° and 68.7° (JCPDS file no: 01-072-4812). The ratio between anatase and rutile phase calculated in this study (77% anatase and

23% rutile) was comparable with the expected value (75% anatase and 25% rutile) for P25 type TiO_2 (Degussa) support material.

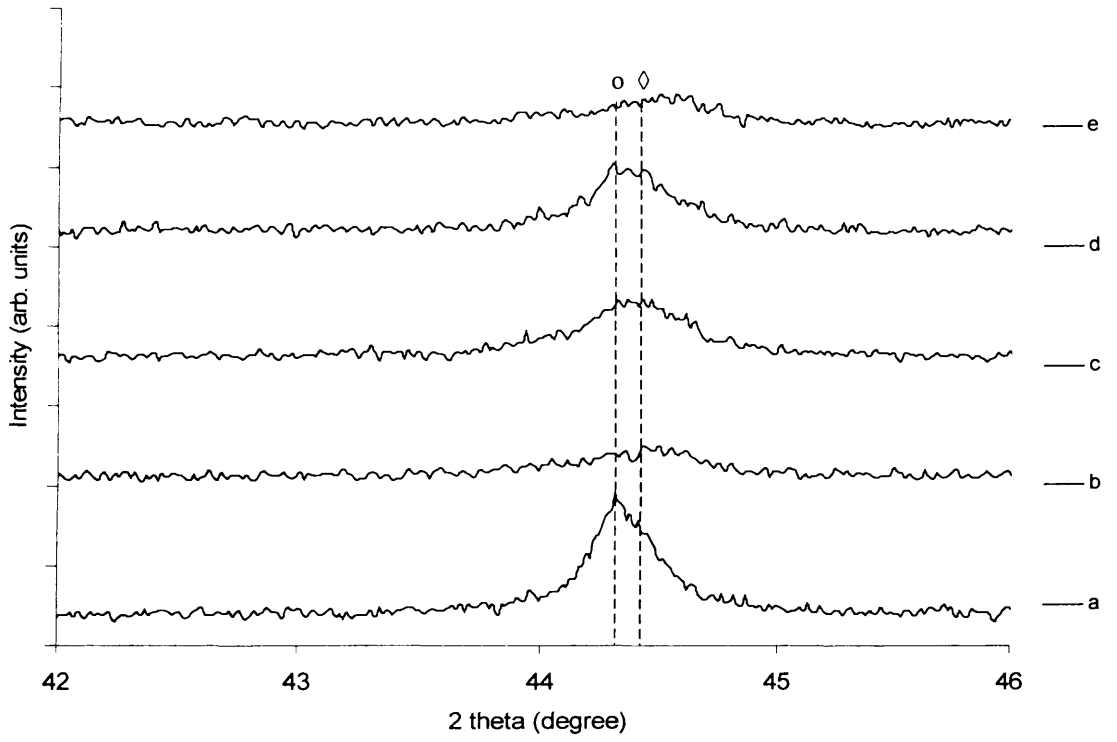

Figure 4.8: X-ray diffractogram of Au/Pd-TiO_{2IW} catalyst with different Au:Pd ratio calcined in air 400°C. Key: (a) 5.0wt%Au, (b) 5.0wt%Pd, (c) 2.5wt%Au2.5wt%Pd, (d) 4.0wt%Au1.0wt%Pd, (e) 1.0wt%Au4.0wt%Pd, Symbol: (o) Au, (◊) Au-Pd alloy

In order to calculate the mean crystallite size of the Au or Au-Pd metal in all catalysts, the Scherer's equation[54] was used. The diffraction peak at 44.3° correspond to (200) reflection was chosen instead of (111) reflection based on the fact that the peak at 38.2° was not fully resolved due to the overlapping with TiO_2 peak. Table 4.11 showed that the average crystallite size of Au on 5wt%Au/TiO_{2IW} monometallic catalyst was bigger (29 nm) compared to the one calculated in bimetallic catalyst. The bigger crystallite size could be explained by the higher metal loading and a theoretically lower metal dispersion as well as presence of chloride species on the surface of catalyst.[2] Both factors could induce the agglomeration of Au particles during heat treatment and consequently generate larger metal crystallite sizes. In addition, it was claimed in the literature that the pure metal particles are generally bigger than alloyed particles.[55] In the case of Au-Pd bimetallic catalysts, a similar crystallite size of Au-Pd (20 nm) was calculated especially for 4 to 1

weight ratio of either Au or Pd, whereas a slight increase of crystallite size was observed in the equal weight 2.5wt%Au2.5wt%Pd/TiO_{2IW} catalyst (23.0 nm).

Table 4.11: Crystallite size of Au/Pd-TiO_2 catalysts with different Au:Pd ratio. All catalysts were synthesised using impregnation method and calcined in static air at 400 °C for 3 hours.

Catalysts	Au, Au-Pd, FWHM (200) (2θ; 44.3°)	Au, Au-Pd, FWHM (200) Crystallite size[a] (nm)
4.0wt%Au1.0wt%Pd	0.422	20.3
2.5wt%Au2.5wt%Pd	0.373	23.0
1.0wt%Au4.0wt%Pd	0.417	20.5
5wt%Au	0.300	28.6

[a]Crystallite size by means of Scherer's formula: $\frac{0.9 * \lambda}{\beta_{hkl} * \cos\theta}$

In figure 4.9, the effect of different pretreatments on the structural properties of 2.5wt%Au2.5wt%Pd/TiO_{2IW} catalyst were studied and compared with as synthesised dried catalyst at 110 °C. The diffraction peaks match to Au-Pd peaks were clearly observed in all catalysts whilst the formation of Pd^0 peaks were observed in catalysts pretreated in flow of hydrogen in argon and hydrogen peroxide. In all cases, the identification of each peak was referred to similar JCPDS reference files stated above. The presence of metallic Pd in both samples was expected since either hydrogen gas or hydrogen peroxide have a capability to reduce the metal catalyst. An unobservarble Pd^0 peak for the catalyst pretreated with sodium borohydride could be explained by the amount of $NaBH_4$ used. In this case, the amount of $NaBH_4$ with an equal mole ratio to the metal was probably not sufficient to visibily reduced the catalyst.

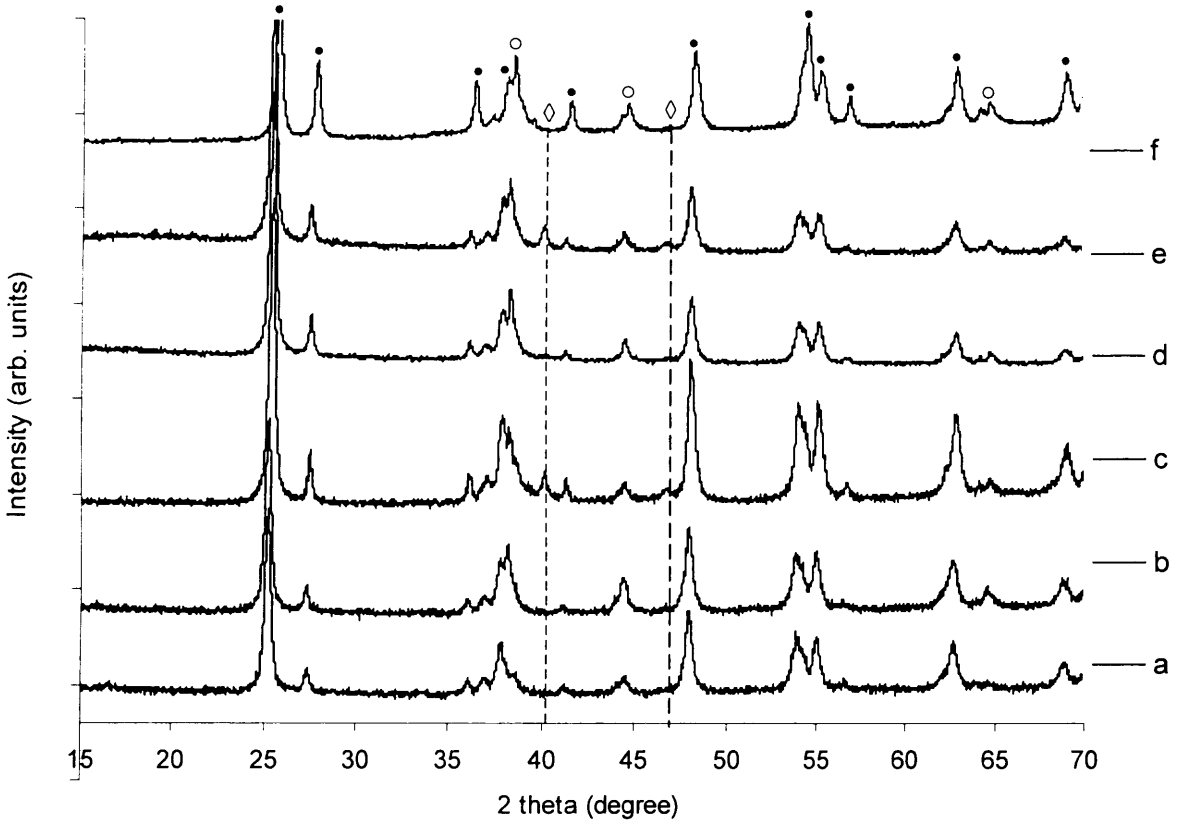

Figure 4.9: X-ray diffractogram of 5wt%Au-Pd/TiO_{2IW} catalyst with different pretreatment. Key: (a) Dried in static air at 110 °C for 16 h, (b) Calcined in static air at 400 °C for 3 hours, (c) Reduced in 5% hydrogen in argon at 400 °C for 3 hours, (d) Calcined in static air at 400 °C for 3 hours, followed by sodium borohydride treatment, (e) Calcined in static air at 400 °C for 3 hours, followed by hydrogen peroxide treatment, (f) Calcined in flow of 50%O_2/He at 400 °C for 3 hours. Symbol: (•) TiO_2, (o) Au/Au-Pd alloy, (◊) metallic Pd

The crystallite size of Au-Pd phase was shown in table 4.12. The 2.5wt%Au2.5wt%Pd/TiO_{2IW} catalyst calcined at 400 °C displayed the biggest Au-Pd crystallite size compared to the uncalcined dried catalyst (16 nm) as well as to catalysts with other types of pretreatment. The bigger crystallite size compared to the dried catalyst was explained by the sintering effect of metal particles during the calcinations process at higher temperature. Further treatment of the calcined catalyst either by H_2O_2 or $NaBH_4$ decreased the crystallite size of the metal. In addition to a reducing effect, which lead to a decrease in the crystallite size,[56,57] pretreatment in flowing gas could enhance the removal of chloride species and consequently suppress the metal agglomeration.[2] Catalyst calcined in 50% O_2 in helium produced the smallest Au-Pd crystallite size (13.1 nm).

Table 4.12: Crystallite size 5wt%Au-Pd/TiO_2 catalyst synthesised using impregnation method followed by different pretreatment

Pretreatment	Au-Pd, FWHM (200) (2θ; 44.3°)	Au-Pd, FWHM (200) Crystallite size[a] (nm)
Dried in air, 110 °C	0.535	16.0
Static air, 400 °C	0.373	23.0
5%H_2/Ar, 400 °C,	0.521	16.5
Static air, 400 °C & $NaBH_4$ treat	0.482	17.8
Static air, 400 °C, & H_2O_2 treat	0.584	14.7
50%O_2/He, 400 °C,	0.655	13.1

[a]Crystallite size by means of Scherer's formula: $\frac{0.9 * \lambda}{\beta_{hkl} * \cos\theta}$

The following figure (figure 4.10) displayed the XRD diffractogram of 2.5wt%Au2.5wt%Pd supported on different materials (TiO_2, SiO_2, γ-Al_2O_3, carbon and CeO_2) respectively. The peaks correspond to each support materials were compared to each JCPDS reference file. In term of metal, only peaks correspond to Au-Pd alloy were clearly observed at 38.2° and 44.3°. The peaks indicating the presence of metallic Pd were not observed as all the catalysts were subjected to calcinations in static air at 400 °C for 3 hours.

Switching the type of support from TiO_2 into γ-Al_2O_3, carbon and CeO_2 respectively gave comparable Au-Pd crystallite size (table 4.13). The clear difference was only observed with SiO_2 as support material, where an average crystallite size of 14.5 nm was observed. The smaller crystallite size on SiO_2 supported Au-Pd catalyst contradicts with the available literature on similar catalyst.

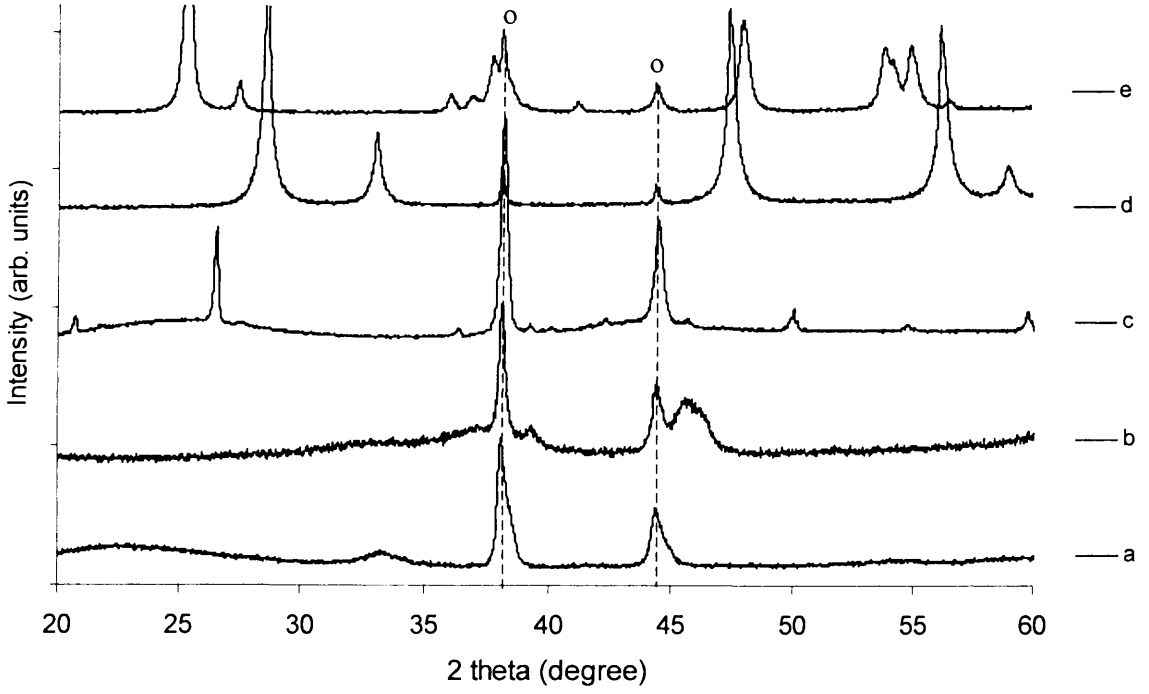

Figure 4.10: X-ray diffractogram of 5wt%Au-Pd with different support catalyst and calcined in static air at 400°C for 3 hours. Key: (a) SiO_2, (b) γ-Al_2O_3, (c) Carbon (G-60), (d) CeO_2, (e) TiO_2, Symbol: (o) Au or Au-Pd alloy. Other peaks were corresponded to reflection for each respective supports.

Table 4.13: Crystallite size of 5wt%Au-Pd nanoparticles catalyst supported on different materials. All catalysts were synthesised using impregnation method and calcined in static air at 400 °C for 3 hours.

Supports	Au-Pd, FWHM (200) (2θ; 44.3°)	Au-Pd, FWHM (200) Crystallite size[a] (nm)
TiO_2	0.373	23.0
CeO_2	0.342	25.1
SiO_2	0.591	14.5
γ-Al_2O_3	0.363	23.6
Carbon (G-60)	0.367	23.4

[a]Crystallite size by means of Scherer's formula: $\frac{0.9*\lambda}{\beta_{hkl}*\cos\theta}$

A small average crystallite size for Au-Pd/TiO_2 synthesised using the sol-immobilisation technique was determined by the lack of diffraction peaks corresponding to the deposited metals (Au, Pd) in the XRD spectra of 1.0wt%Au-Pd/TiO_{2SI} sample (figure 4.11 (c)). This is likely due to the detectability limit of XRD instrument as detailed above. It was reported in literature that transmission electron microscopy analysis (TEM) of a 1%Au-Pd/TiO_2 catalyst prepared through sol-immobilisation technique produced metal catalyst with mean particle size around 4 nm.[39] In addition, the lower total metal loading could also contribute to this observation. This is supported by the fact that a 1%Au-Pd/TiO_2 catalyst synthesised via an impregnation technique (figure 4.11 (b)) also did not contain any peaks corresponding to Au or Pd. The XRD diffractogram for both impregnated and sol-immobilized samples look identical with diffractogram of bulk TiO_2 (figure 4.11 (a)) sample.

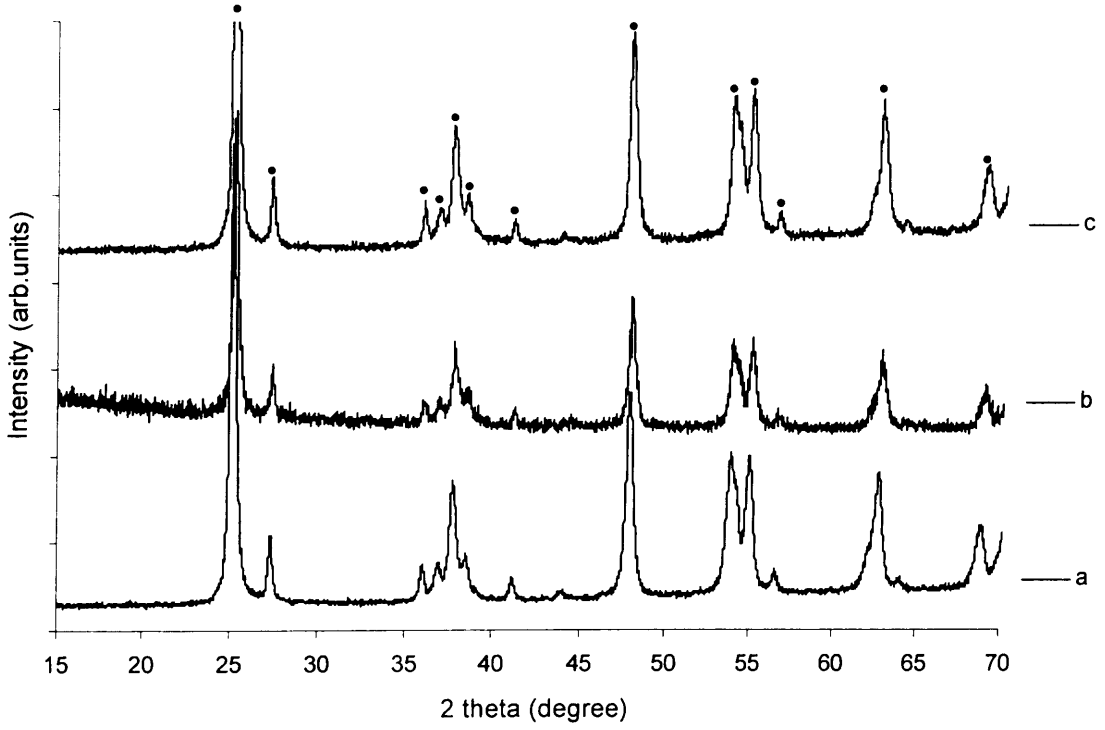

Figure 4.11: X-ray diffractogram of 1wt%Au-Pd/TiO_2 synthesized via sol-immobilisation technique and comparison with analogue impregnated samples. Key: (a) TiO_2, (b) 1wt%Au-Pd/TiO_{2IW}, (c) 1wt%Au-Pd/TiO_{2SI}, Symbol: (•) TiO_2

4.5.2. BET surface area measurement

The surface area of the catalyst is well known to play an important role in determine the catalytic performance of the catalyst.[58] In case of metal supported catalyst, the area of metal (accessibility and dispersion) is one of the crucial factors in determining the efficiency of catalysis process and in the absence of support material; the metal would undergo sintering rapidly and would therefore lose activity. In this study, the surface areas of synthesised catalysts were measured in order to know the effect of total surface area on catalytic reaction. Depositing Au and Pd metal into TiO_2 catalyst slightly decreased the surface area from 55 to 49 m^2/g (table 4.14). Lower surface area in metal supported catalyst could possibly due to the blockage of the surface or pore of the TiO_2 by the metals, or another possible compound such as chloride (Cl^-). Subjecting the 2.5wt%Au2.5wt%Pd/TiO_{2IW} catalyst to different pretreatments did not alter the BET surface area, indicating the stability of TiO_2 support. Almost similar BET surface areas were also was obtained for the 1wt%Au-Pd/TiO_2 catalyst synthesised via sol-immobilisation method (table 4.15).

Table 4.14: BET analyses of 5wt%Au-Pd/TiO_2 catalyst synthesized using impregnation method followed by different pretreatment

Catalyst	Pretreatment	BET surface area (m^2/g)
TiO_2	Static air, 400 °C	55.3
2.5wt%Au2.5wt%Pd/TiO_2	Static air, 400 °C	49.7
2.5wt%Au2.5wt%Pd/TiO_2	5%H_2/Argon, 400 °C	49.3
2.5wt%Au2.5wt%Pd/TiO_2	Static air, 400 °C and H_2O_2 treatment	49.5

Table 4.15: BET analyses of 1%Au-Pd/TiO_2 synthesized via sol-immobilisation techniques

Catalyst	Preparation technique	BET surface area (m^2/g)
0.5wt%Au0.5wt%Pd/TiO_2	Sol-immobilisation, dried in air, 110 °C	49.5

However, different catalyst surface areas were obtained by using different supports material (table 4.16). As expected, Au-Pd metals catalyst supported on highly porous carbon displayed highest surface area (748 m^2/g) followed by SiO_2, while Au-Pd supported on CeO_2 and Al_2O_3 show BET surface area comparable to TiO_2 as support. Therefore, it was believed that Au-Pd metals were highly dispersed on carbon and SiO_2 compared to TiO_2, CeO_2 and γ-Al_2O_3 supported catalysts, which later might contribute to the difference in catalytic performance. However, in this study, the total BET surface area was not considered as an important factor with respect to catalytic activity and selectivity obtained with methane oxidation reaction using hydrogen peroxide as oxidant (in both cases either with addition H_2O_2 (chapter 4) or with *in-situ* generated approaches (chapter 5)). The statement was based on lower oxygenates productivity and selectivity observed with high surface area catalyst (Au-Pd/SiO_{2IW} and Au-Pd/C_{IW}) compared to the lower surface area catalysts especially Au-Pd/TiO_{2IW}.

Table 4.16: BET analyses of 5wt%Au-Pd with different supports prepared using impregnation technique and calcined in static air at 400 °C for 3 hours.

Catalysts	BET surface area (m^2/g)
2.5wt%Au2.5wt%Pd/TiO_2	49.7
2.5wt%Au2.5wt%Pd/CeO_2	58.3
2.5wt%Au2.5wt%Pd/SiO_2	239.9
2.5wt%Au2.5wt%Pd/γ-Al_2O_3	53.0
2.5wt%Au2.5wt%Pd/Carbon	748.9

4.5.3. Atomic absorption spectroscopy (AAS) analysis

Atomic absorption analysis spectroscopy analysis was used in this study to determine the actual loading of Au and Pd available in the prepared catalysts. Since the Au-Pd supported on TiO_2 were prepared via impregnation technique where both metal precursors were impregnated into TiO_2 supported material without proceeded into any washing step, the actual metal loading for both Au and Pd metals were expected to be close to the theoretical values. In this study, the AAS analyses were carried only for 2.5wt%Au2.5wt%Pd/TiO_{2IW} dried and calcined catalysts since most of the catalytic reactions carried out in these studies

were performed with these particular catalysts. Details AAS analysis procedures have been shown in chapter 2.

As displayed in table 4.18, the actual loadings of Au and Pd for both dried and calcined samples were calculated around 2.2wt% for Au and 2.4wt% for Pd. The deviation from actual values could attributed from the possible error occurred during catalyst preparation and AAS analysis. The data demonstrated that the calcinations procedure did not affect the percentages of metal in catalysts. Moreover, the AAS analysis data was used to corroborate and confirm the discussion on Au-Pd alloy structure as well as surface composition in the following section.

Table 4.17: Determination of actual metal loading on 5wt%Au-Pd/TiO_{2IW} catalyst

Catalyst	Treatment	Metal	Metal, (wt %), Theoretical	Metal, (wt %), Actual
2.5wt%Au2.5wt%Pd/TiO_{2IW}	Uncalcined (Dried in air, 110 °C, 16 hours)	Au	2.5	2.2
		Pd	2.5	2.4
2.5wt%Au2.5wt%Pd/TiO_{2IW}	Calcined (Static air, 400 °C, 3 hours)	Au	2.5	2.2
		Pd	2.5	2.4

4.5.4. X-ray photoelectron spectroscopy (XPS) analysis

It is well reported in literature that not only the particle size of the supported Au-Pd metal be important, but also its oxidation state and surface composition could also affect catalytic performance.[2,59] For this reason, measurements using X-ray photoelectron spectroscopy have been carried out. XPS is an analytical technique with the ability to give information regarding to which elements present on the surface of the catalyst, and more detailed information on their oxidation state. In addition to qualitative analysis, quantitative information such as atomic percentages of each metal can also be determined using XPS analysis.[51] This information is important in order to examine the surface composition of each metal, especially in the sample with more than one metal involved. In this study, the

5wt%Au-Pd/TiO_{2IW} catalysts after different pretreatments were analyzed by XPS and the obtained Au (4d) and Pd (3d) combined spectra were plotted in figure 4.12.

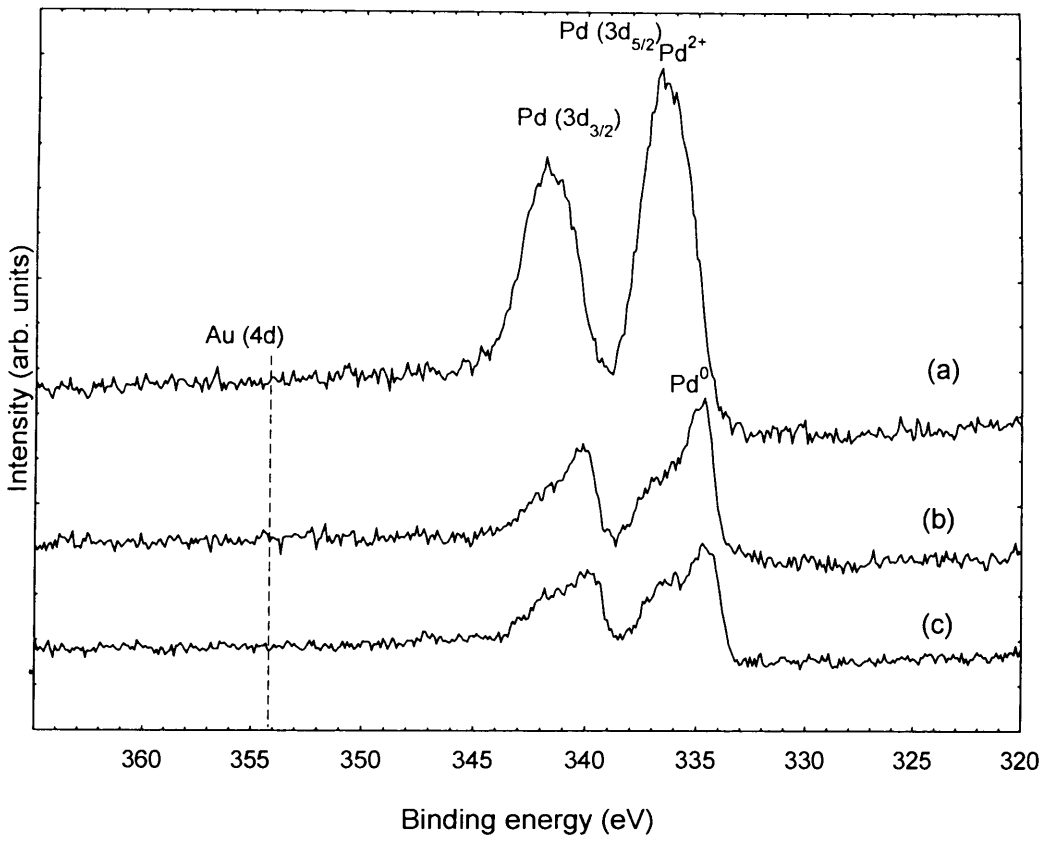

Figure 4.12: Pd (3d) and Au (4d) spectra of 5wt%Au-Pd/TiO_{2IW} catalysts with different pretreatment (a) 400 °C in static air, (b) 400 °C in 5%H_2/Ar flow, (c) 400 °C in static air and hydrogen peroxide treatment

In all cases, the intensity of the Au ($4d_{3/2}$) feature at higher binding energy around 355-358 eV was below detection limits and the signals correspond to Pd species were clearly observed. The Pd ($3d_{5/2}$) feature has a binding energy around 334-337 eV, and the Pd ($3d_{3/2}$) feature has a characteristic binding energy around 5.4 eV higher than Pd ($3d_{3/2}$) signals (see the following paragraph for detailed discussion on the metal oxidation state and respective binding energy). Detailed XPS binding energies of each metal and its specific oxidation state are presented in table 4.18.

Table 4.18: XPS binding energies of Au and Pd with respective oxidation state on 5wt%Au-Pd/TiO_{2IW} with different pretreatments[a]

Pretreatments	Pd ($3d_{5/2}$):Pd^{2+}, Pd^0 BE, eV^b (%)[c]	Au ($4d_{3/2}$):$Au^{\delta+}$, Au^0 BE, eV^b(%)[c]	Au ($4f_{7/2}$): $Au^{\delta+}$, Au^0 BE, eV^b(%)[c]
Static air, 400 °C.	336.8(85.5), 335.1(14.5)	Nd[d]	-, 83.5(100)
Flow 5%H_2/Ar,400 °C.	336.5(49.7), 334.8(50.3)	Nd[d]	-, 82.2(100)
Static air, 400 °C and H_2O_2 treatment.	336.3(60.1), 334.7(39.9)	Nd[d]	-, 83.6(100)

[a]All binding energies referenced to C 1s=284.7 eV

[b]The specific binding energies of each metal were referred to the literature[60-62]

[c]Relative % amount of different species

[d]Nd: Not detectable

The XPS spectra of the catalysts shown in figure 4.12 were clearly different compared to uncalcined fresh 5wt%Au-Pd/TiO_{2IW} catalyst reported in literature,[63] synthesized using a similar method. Typical Au(4d)-Pd(3d) XPS spectra of the uncalcined 5wt%Au-Pd/TiO_{2IW} sample showed clear Au and Pd signals leading to several overlapping peaks. Given that atomic absorption spectroscopy (AAS) measurements on 5wt%Au-Pd/TiO_{2IW} (section 4.5.3) showed no loss of gold after heat treatment (compared to AAS of uncalcined sample), which could contribute to the unobserved Au (4d) signal on XPS spectra, it is reasonable to conclude that the metal particles have a core-shell alloy structure where photoelectron emitted from the gold atoms in the core is strongly attenuated due to the inelastic scattering of the electrons during transport through the Pd shell, leading to a much reduced Au signal intensity compared with Pd.

The calcined 5wt%Au-Pd/TiO_{2IW} catalyst with the shell structure enriched with PdO phase showed an XPS feature mainly corresponding to Pd^{2+} species (see figure 4.12 (a)), whereas the catalyst reduced in a hydrogen environment (see figure 4.12 (b)) as well as the catalyst pretreated with hydrogen peroxide (see figure 4.12 (c)) displayed a mixture of Pd^{2+} (336.3-336.8 eV) and Pd^0 (334.7-334.8 eV). These XPS spectra are in agreement with the XRD analysis demonstrated in section 4.5.1. The presence of Pd^{2+} was confirmed by the observable shoulder peaks signal around 336.3-337.0 eV. The deconvulation of each Pd ($3d_{3/2}$) spectrum (figure 4.13) proved the presence of 50.3% of Pd^0 with 49.7% of Pd^{2+} for

catalyst pretreated in H_2/Ar environment whilst for catalyst pretreated with H_2O_2 gave 39.9% of Pd^0 with 60.1% of Pd^{2+}.

(i)

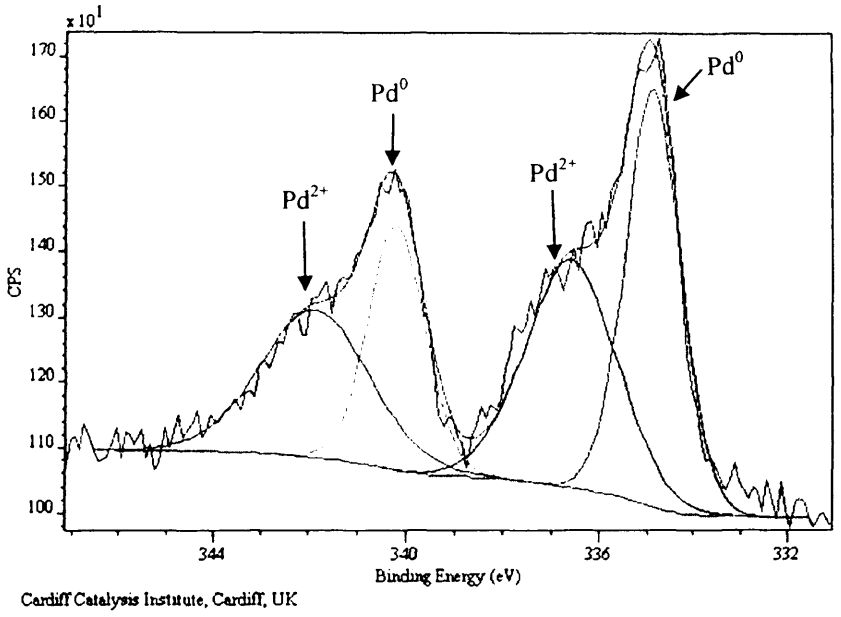

(ii)

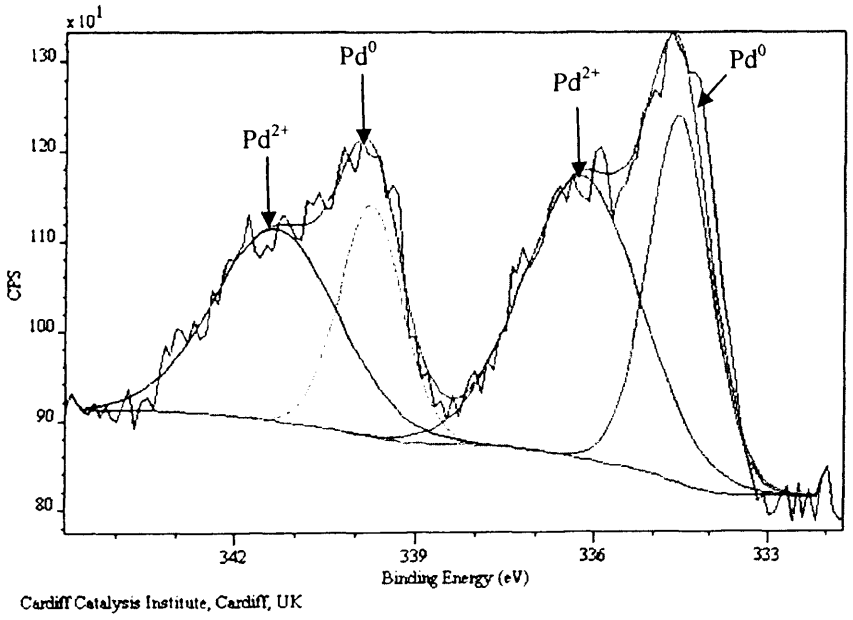

Figure 4.13: Deconvulation of Pd (3d) spectra of 5wt%Au-Pd/TiO_{2IW} catalyst, (i) Catalyst was reduced in 5%H_2/Ar for 3 hours at 400 °C, (ii) Catalyst was calcined in static air at 400 °C for 3 hours followed by H_2O_2 treatment

In view of the fact that oxidation state of Au cannot be observed and determined form the Au ($4d_{3/2}$) feature, the Au ($4f_{7/2}$) transition has instead been used and in all cases. From this, it was found that Au was in the metallic state i.e. the oxidation state of Au is 0. It was

claimed that metallic gold (Au^0) could be obtained under heating treatment in any gases because of the instability of Au_2O_3.[2]

In order to calculate and verify the overall surface composition of both Au and Pd metals, area integration of each XPS signal were carried out and the results were displayed in table 4.19. It was clear that the Pd:Au atomic ratios obtained for bimetallic 2.5wt%Au2.5wt%Pd/TiO_{2IW} catalyst calcined in static air was found to be higher (6.89) than the expected value of 1.86 (by assuming a random solid solution) for the catalyst with Au and Pd present in 1:1 atomic ratio. This trend was expected and is in agreement with the available literature reporting the formation of Au core and Pd rich structure on 2.5wt%Au2.5wt%Pd/TiO_2 catalysts synthesized using an impregnation method and calcined in static air at higher temperature (> 200 °C).[63] The Pd/Au ratio calculated for both hydrogen and H_2O_2 treatment catalysts were lower compared to calcined catalyst, although high enough in order to assume a core-shell structure.

Table 4.19: Surface elemental compositions derived from XPS for the 5wt%Au–Pd/TiO_{2IW} catalysts prepared by impregnation method followed by different pretreatment

Entry	Catalyst/treatment	Composition (atom %)		Atom ratio (Pd/Au)	
		Au/Ti	Pd/Ti	Measured	Theoritically expected[a]
1	Static air, 400 °C	0.0075	0.0518	6.91	1.86
2	Flow 5%H_2/Ar,400 °C	0.0049	0.0217	4.43	1.86
3	Static air, 400 °C and H_2O_2 treatment	0.0049	0.0267	5.49	1.86

[a] Assuming a random solid solution

The Au-Pd nanoparticles supported on TiO_2 with different Au to Pd weight (wt %) ratios were also subjected to XPS analyses, and the combined Au (4d) and Pd (3d) spectra are displayed in figure 4.14. It can be seen that both 4.0wt%Au1.0wt%Pd/TiO_{2IW} and 1.0wt%Au4.0wt%Pd/TiO_{2IW} generated similar pattern of spectra compared to equal weight catalyst (2.5wt%Au2.5wt%Pd/TiO_{2IW}) counterpart. The intensity of Pd (3d) signal was clearly intense for 1.0wt%Au4.0wt%Pd/TiO_{2IW} sample in figure 4.14 (a) due to the highest Pd loading on the support material. In addition to this, the Pd (3d) signal of this sample

also shifted to higher binding energy which indicates the presence of highly dispersed and polarised Pd^{2+} ions in the close vicinity of chloride anions as it was reported by Pawelec and co-workers.[64] In all samples, the Au (4d) feature was below the instrument detectability limit whereas Pd (3d) signals in the range of 336.4-336.9 eV were matched with the Pd^{2+} phase. These data suggest that Au core-Pd rich structure might evolved in both 4.0wt%Au1.0wt%Pd/TiO_{2IW} and 1.0wt%Au4.0wt%Pd/TiO_{2IW} catalysts. Whilst some of the Au in the 4.0wt%Au1.0wt%Pd/TiO_{2IW} catalyst may have evolved in pure form given the fact that the amount of impregnated Pd was not sufficient to fully cover the Au species. In all cases, the oxidation state based on Au ($4f_{7/2}$) signal indicates the formation of metallic gold (Au^0).

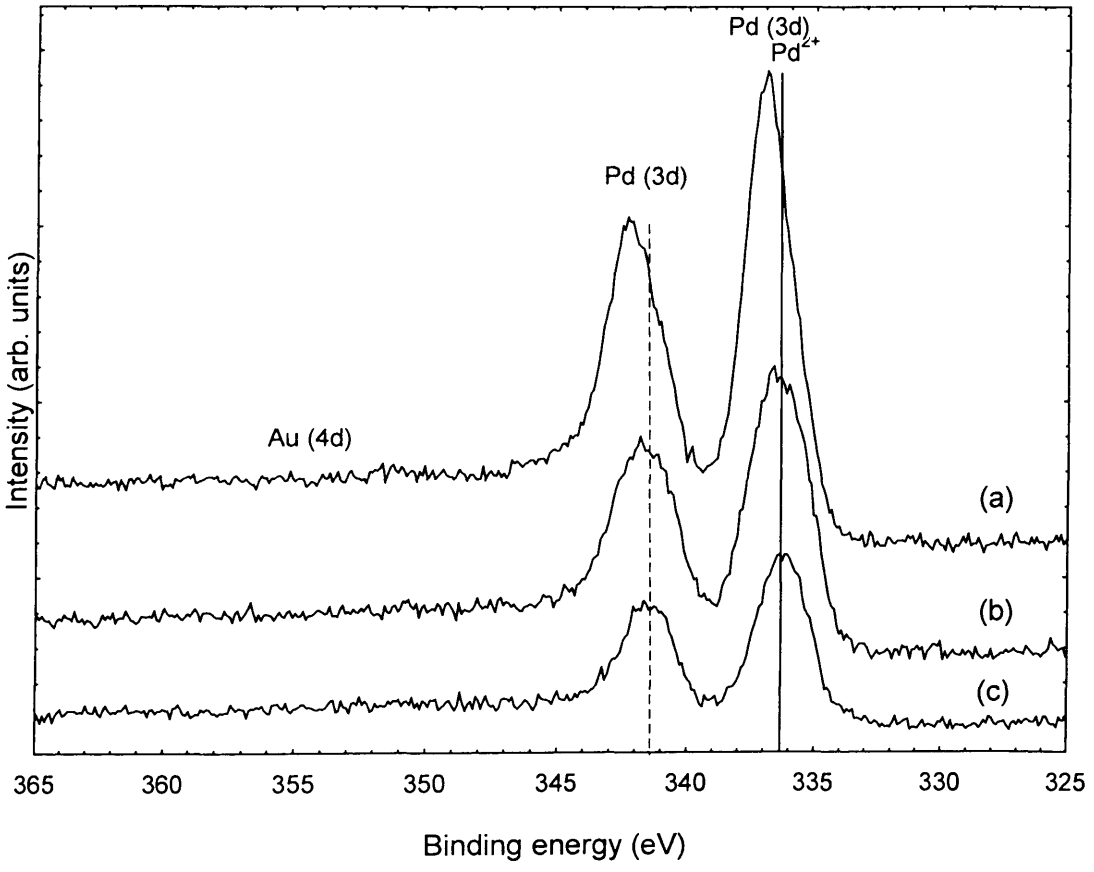

Figure 4.14: Pd 3d and Au 4d spectra of Au-Pd/TiO_{2IW} catalysts (a) 1.0wt%Au4.0wt%Pd, (b) 2.5wt%Au2.5wt%Pd, (c) 4.0wt%Au1.0wt%Pd

Further examination of the XPS data by calculating the atomic percentages of each metal with higher Pd/Au atom ratio evidently showed that some of the particle in 4.0wt%Au1.0wt%Pd/TiO_{2IW} resembled a core-shell structure (table 4.20). The theoretical

Pd/Au ratio (assuming a random solid solution) for 4.0wt%Au1.0wt%Pd/TiO_{2IW} catalyst is 0.47, which is much lower compared to 6.95 calculated from XPS data. The statement regarding to the type of alloy evolved on 4.0wt%Au1.0wt%Pd/TiO_{2IW} catalyst was based on similar reasons to those mentioned previously.

Table 4.20: Surface elemental compositions derived from XPS for the different Au/Pd ratio on TiO_2 catalysts prepared by impregnation method

Entry	Catalyst	Composition (atom %)		Atom ratio
		Au/Ti	Pd/Ti	(Pd/Au)
1	1.0wt%Au4.0wt%Pd	0.0038	0.0773	20.34
2	2.5wt%Au2.5wt%Pd	0.0075	0.0518	6.91
3	4.0wt%Au1.0wt%Pd	0.0040	0.0278	6.95

In another set of XPS analysis, the 1wt%Au-Pd/TiO_2 catalyst synthesised via sol-immobilisation technique was subjected to XPS characterisation. The major difference observed in samples prepared by sol-immobilisation compared to an impregnation catalyst is in the electronic states of Pd, which is mostly in the metallic state for the sol-immobilised catalyst (figure 4.15). In addition to this, the signal for the Au (4d) feature is now observed, and the lower signal intensity was likely due to the low catalyst metal loading, though it could also be due to the presence of ligand (PVA), which covers the surface of the metals. In order to quantify the surface composition of the sample, the spectral envelope was deconstructed into its respective Pd (3d) and Au (4d) components. Following this, the contribution from Au (4d) was subtracted out. The surface Pd/Au atomic ratio (table 4.21) shows limited evidence of Pd enrichment and therefore indicates the presence of a homogeneous random Au-Pd alloy. Similar types of alloy have also been claimed for similar catalyst characterised in earlier studies.[39]

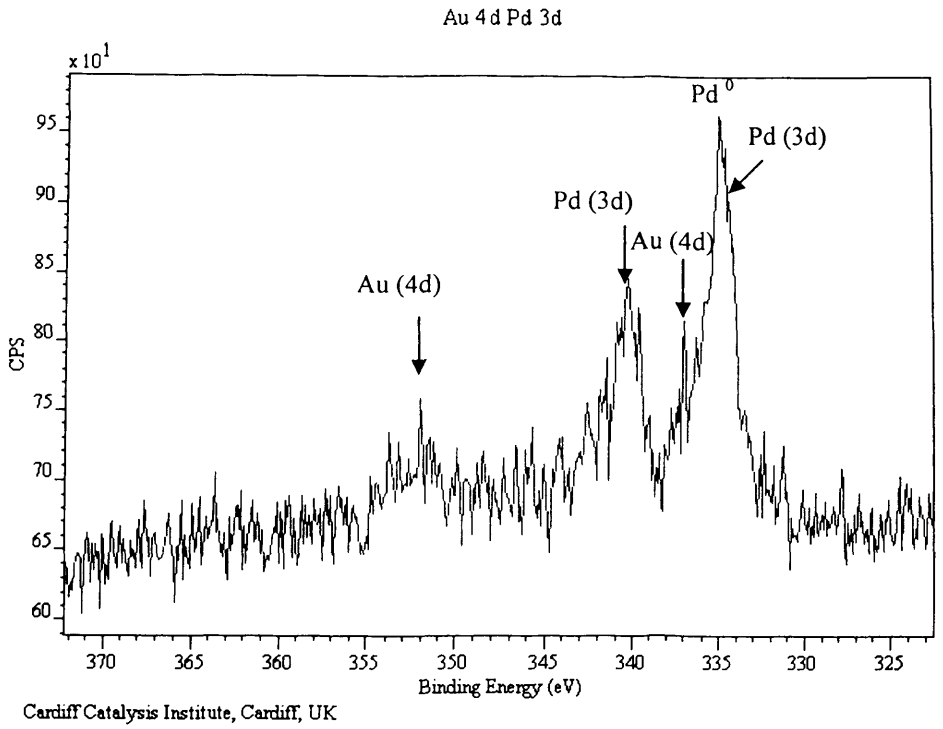

Figure 4.15: Pd (3d) and Au (4d) spectra of 1%Au–Pd/TiO_2 catalysts prepared by sol-immobilisation method.

Table 4.21: Surface elemental compositions derived from XPS for the Au–Pd/TiO_2 catalysts prepared by sol-immobilisation method.

Entry	Catalyst	Composition (atom %)		Atom ratio
		Au	Pd	(Pd/Au)
1	0.5wt%Au0.5wt%Pd/TiO_{2SI}	0.0083	0.0107	1.29

4.6. Conclusions

In this chapter, lower alkanes (mainly methane) have been examined by oxidation reactions with the addition of hydrogen peroxide using supported Au-Pd nanoparticles catalysts. The obtained experimental and catalytic data are well correlated with catalyst structure as well as the reaction parameters. It was previously shown in chapter 3 that Au-Pd alloy nanoparticles are highly effective catalysts for the oxidation of primary C-H bonds in toluene and toluene derivatives. However, these catalysts were found to be ineffective for the oxidation of methane with oxygen under mild conditions. In view of this,

another environmental friendly oxidant *i.e.* hydrogen peroxide was used and it was found that Au-Pd supported nanoparticles were active for the oxidation of methane, giving high selectivity to methanol. In a typical reaction, the oxidation of methane is performed in the liquid phase using an autoclave reactor with water as the preferred solvent. By utilising water as solvent, it permits the facile analysis of all the carbon containing products. In all cases of methane oxidation involving heterogeneous Au-Pd catalyst used in this study, only methyl hydroperoxide, methanol and carbon dioxide were detected as oxidation products. For homogeneous Au/Pd catalysts, formic acid was also observed at low temperature (50 ^{o}C), and lower amount of oxygenates and the precipitation of homogeneous catalyst were also observed.

Comparison of the catalyst supports at 50 ^{o}C clearly shows that TiO_2 is the best support as higher oxygenate productivity and methanol selectivity were observed compared to carbon, CeO_2, SiO_2 and Al_2O_3. Therefore, Au-Pd supported on TiO_2 catalyst synthesised via impregnation method and calcined in static air at higher temperature was used for reaction parameters studies. By increasing the reaction temperature from 2 °C to 90 °C, an increase in methane conversion is observed; nevertheless a drop in the selectivity to oxygenate products is also observed working at 90 °C, due to the increasing formation of CO_2. It is noteworthy that even at 2 °C, the Au-Pd catalyst successfully produced methanol with exceptionally high selectivity to oxygenate (93%). The total amount of oxygenates as well as of each individual oxygenate increased by increasing the methane pressure. The concentration of hydrogen peroxide was found to be first order toward methane oxidation, and the selectivity toward methanol was not affected in the studied range of hydrogen peroxide concentration and was found to be between 51-56% in all cases. Furthermore, the effect of the reaction time on product formation was studied at 50 °C, and from this it has been shown that methanol formation is enhanced at longer reaction times. Time online study also demonstrates that methyl hydroperoxide (CH_3OOH) is the primary product, and that it gradually transforms to methanol in the presence of Au-Pd catalyst.

Further studies also illustrated the synergistic effect of Au and Pd and the equal weight ratio (2.5wt%2.5wt%Pd) of both metals was found to be the optimised loading for obtaining higher oxygenates productivity and selectivity.

In order to study the effect of catalyst pretreatment, the reduced 5wt% Au-Pd/TiO_{2IW} (following heat treatment with H_2/Ar) was subjected to standard reaction conditions, and it was found that the selectivity to methanol improved up to 92 %. Similar observations were obtained following chemical reduction by sodium borohydrate or following hydrogen

peroxide treatment, though the overall catalytic activity for these samples is lower than the calcined catalyst. Au-Pd/TiO_2 synthesized via sol-immobilisation technique was also found to oxidise methane with a similar catalytic activity and selectivity to reduced Au-Pd impregnated catalyst. The slightly lower oxygenates productivity were reasoned to the higher hydrogen peroxide decomposition, also associated with mechanistic pathways.

The successive utilisation of hydrogen peroxide for the selective oxidation of methane to methanol opens the opportunity to explore the general applicability of alkane oxidation and for that reason, ethane was selected as another model substrate. It was found that the oxidation of ethane to ethanol and acetic acid is possible at low temperature (50-70 °C) with selectivity to oxygenated products in the range 97-99%. At 50 °C the major product is ethanol with selectivity around 72%. Optimisation of reaction conditions increased the ethane conversion up to 2.2%.

In summary, the work discussed could be considered as the first example of a detailed study on the selective oxidation of methane and ethane with hydrogen peroxide using gold-palladium supported nanoparticles onto TiO_2, with high selectivity to oxygenated products and low formation of CO_x products.

References:

1. J. Colby, D. I. S., H. Dalton, . *Biochemical Journal* **1977,** *165*, 395.
2. G.C. Bond, C. L., D. T. Thompson, *Catalysis by Gold*; Imperial College Press, 2006; Vol. 6.
3. Haruta, M. *Gold Bulletin* **2004,** *37*, 27.
4. Hughes, M. D.; Xu, Y.-J.; Jenkins, P.; McMorn, P.; Landon, P.; Enache, D. I.; Carley, A. F.; Attard, G. A.; Hutchings, G. J.; King, F.; Stitt, E. H.; Johnston, P.; Griffin, K.; Kiely, C. J. *Nature* **2005,** *437*, 1132-1135.
5. V. Nizova, G.; Suss-Fink, G.; B. Shul'pin, G. *Chemical Communications* **1997,** 397-398.
6. Süss-Fink, G.; Gonzalez, L.; Shul'pin, G. B. *Applied Catalysis A: General* **2001,** *217*, 111-117.
7. Shul'pin, G. B.; Nizova, G. V.; Kozlov, Y. N.; Gonzalez Cuervo, L.; Süss-Fink, G. *Advanced Synthesis & Catalysis* **2004,** *346*, 317-332.
8. Seki, Y.; Mizuno, N.; Misono, M. *Applied Catalysis A: General* **1997,** *158*, L47-L51.
9. Seki, Y.; Min, J. S.; Misono, M.; Mizuno, N. *The Journal of Physical Chemistry B* **2000,** *104*, 5940-5944.
10. Mizuno, N.; Seki, Y.; Nishiyama, Y.; Kiyoto, I.; Misono, M. *Journal of Catalysis* **1999,** *184*, 550-552.
11. Reis, P. M.; Silva, J. A. L.; Palavra, A. F.; Fraústo da Silva, J. J. R.; Kitamura, T.; Fujiwara, Y.; Pombeiro, A. J. L. *Angewandte Chemie International Edition* **2003,** *42*, 821-823.
12. Wilcox, E. M.; Roberts, G. W.; Spivey, J. J. *Applied Catalysis A: General* **2002,** *226*, 317-318.
13. Sorokin, A. B.; Kudrik, E. V.; Bouchu, D. *Chemical Communications* **2008**, 2562-2564.
14. Sorokin, A. B.; Kudrik, E. V.; Alvarez, L. X.; Afanasiev, P.; Millet, J. M. M.; Bouchu, D. *Catalysis Today* **2010,** *157*, 149-154.
15. Yuan, Q.; Deng, W.; Zhang, Q.; Wang, Y. *Advanced Synthesis & Catalysis* **2007,** *349*, 1199-1209.
16. Wang Y, A. D.; Zhang, A.D.; Hong, Q. *Science China* **2010,** *53*, 337.
17. C. J. Jones, D. T., R. A. *Angew. Chem* **2004,** *116*, 4726.
18. Navalon, S.; Martin, R.; Alvaro, M.; Garcia, H. *Angewandte Chemie International Edition* **2010,** *49*, 8403-8407.
19. Han, Y.-F.; Phonthammachai, N.; Ramesh, K.; Zhong, Z.; White, T. *Environmental Science & Technology* **2007,** *42*, 908-912.
20. Olivera, P. P.; Patrito, E. M.; Sellers, H. *Surface Science* **1995,** *327*, 330-357.
21. Bonino, F.; Damin, A.; Ricchiardi, G.; Ricci, M.; Spanò, G.; D'Aloisio, R.; Zecchina, A.; Lamberti, C.; Prestipino, C.; Bordiga, S. *The Journal of Physical Chemistry B* **2004,** *108*, 3573-3583.
22. Antcliff, K. L.; Murphy, D. M.; Griffiths, E.; Giamello, E. *Physical Chemistry Chemical Physics* **2003,** *5*, 4306-4316.

23. G.C. Taylor, R. J. W., R. Moseley, K.R. Williams, G. Embery. *Biomaterials* **1996,** *17*, 13.
24. Süss-Fink, G.; Nizova, G. V.; Stanislas, S.; Shul'pin, G. B. *Journal of Molecular Catalysis A: Chemical* **1998,** *130*, 163-170.
25. Y. Jiang, P. C. W., H. Dalton. *Biochimica et Biophysica Acta* **1993,** *1163*, 105.
26. Kiepe, J.; Horstmann, S.; Fischer, K.; Gmehling, J. *Industrial & Engineering Chemistry Research* **2003,** *42*, 5392-5398.
27. Wei, X.; Ye, L.; Yuan, Y. *Journal of Natural Gas Chemistry* **2009,** *18*, 295-299.
28. Kirk, A. D. *Canadian Journal of Chemistry* **1965,** *43*, 2236.
29. Landon, P.; Collier, P. J.; Papworth, A. J.; Kiely, C. J.; Hutchings, G. J. *Chemical Communications* **2002**, 2058-2059.
30. Solsona, B. E.; Edwards, J. K.; Landon, P.; Carley, A. F.; Herzing, A.; Kiely, C. J.; Hutchings, G. J. *Chemistry of Materials* **2006,** *18*, 2689-2695.
31. Edwards, J. K.; Thomas, A.; Carley, A. F.; Herzing, A. A.; Kiely, C. J.; Hutchings, G. J. *Green Chemistry* **2008,** *10*, 388-394.
32. Edwards, J. K.; Thomas, A.; Solsona, B. E.; Landon, P.; Carley, A. F.; Hutchings, G. J. *Catalysis Today* **2007,** *122*, 397-402.
33. Edwards, J. K.; Carley, A. F.; Herzing, A. A.; Kiely, C. J.; Hutchings, G. J. *Faraday Discussions* **2008,** *138*, 225-239.
34. Sheldon, R. A.; Arends, I. W. C. E.; ten Brink, G.-J.; Dijksman, A. *Accounts of Chemical Research* **2002,** *35*, 774-781.
35. Thetford, A., Cardiff University, 2011.
36. Landon, P.; Collier, P. J.; Carley, A. F.; Chadwick, D.; Papworth, A. J.; Burrows, A.; Kiely, C. J.; Hutchings, G. J. *Physical Chemistry Chemical Physics* **2003,** *5*, 1917-1923.
37. Edwards, J. K., Cardiff University, 2006.
38. Kesavan, L.; Tiruvalam, R.; Rahim, M. H. A.; bin Saiman, M. I.; Enache, D. I.; Jenkins, R. L.; Dimitratos, N.; Lopez-Sanchez, J. A.; Taylor, S. H.; Knight, D. W.; Kiely, C. J.; Hutchings, G. J. *Science* **2011,** *331*, 195-199.
39. Dimitratos, N.; Lopez-Sanchez, J. A.; Anthonykutty, J. M.; Brett, G.; Carley, A. F.; Tiruvalam, R. C.; Herzing, A. A.; Kiely, C. J.; Knight, D. W.; Hutchings, G. J. *Physical Chemistry Chemical Physics* **2009,** *11*, 4952-4961.
40. Pritchard, J.; Kesavan, L.; Piccinini, M.; He, Q.; Tiruvalam, R.; Dimitratos, N.; Lopez-Sanchez, J. A.; Carley, A. F.; Edwards, J. K.; Kiely, C. J.; Hutchings, G. J. *Langmuir* **2010,** *26*, 16568-16577.
41. Ntainjua N, E.; Edwards, J. K.; Carley, A. F.; Lopez-Sanchez, J. A.; Moulijn, J. A.; Herzing, A. A.; Kiely, C. J.; Hutchings, G. J. *Green Chemistry* **2008,** *10*, 1162-1169.
42. Hilaire, L.; Légaré, P.; Holl, Y.; Maire, G. *Surface Science* **1981,** *103*, 125-140.
43. Thetford, A.; Hutchings, G. J.; Taylor, S. H.; Willock, D. J. *Proceedings of the Royal Society A: Mathematical, Physical and Engineering Science* **2011**.
44. Li, J.; Staykov, A.; Ishihara, T.; Yoshizawa, K. *The Journal of Physical Chemistry C* **2011,** *115*, 7392-7398.
45. www.wikipedia.org. 2011.

46. www.engineeringtoolbox.com. 2011.
47. Nizova, G. V.; Süss-Fink, G.; Shul'pin, G. B. *Tetrahedron* **1997,** *53*, 3603-3614.
48. Shul'pin, G. B.; Süss-Fink, G.; Shul'pina, L. S. *Journal of Molecular Catalysis A: Chemical* **2001,** *170*, 17-34.
49. Lin, M.; Sen, A. *Journal of the American Chemical Society* **1992,** *114*, 7307-7308.
50. Sen, A. *Accounts of Chemical Research* **1998,** *31*, 550-557.
51. Niemantsverdriet, J. W. *Spectroscopy in Catalysis, An introduction*; Wiley-VCH Publisher, 2000.
52. Han, Y.-F.; Zhong, Z.; Ramesh, K.; Chen, F.; Chen, L.; White, T.; Tay, Q.; Yaakub, S. N.; Wang, Z. *The Journal of Physical Chemistry C* **2007,** *111*, 8410-8413.
53. Venezia, A. M.; La Parola, V.; Nicoll; V.; Deganello, G. *Journal of Catalysis* **2002,** *212*, 56-62.
54. H. P. Klug, L. E. A. *X-ray Diffraction Procedures for Polycrystalline and Amorphous Materials* 2nd Edition ed.; Wiley-Blackwell: New York, 1974.
55. Venezia, A. M.; La Parola, V.; Deganello, G.; Pawelec, B.; Fierro, J. L. G. *Journal of Catalysis* **2003,** *215*, 317-325.
56. Zanella, R.; Louis, C. *Catalysis Today* **2005,** *107-108*, 768-777.
57. Tsubota, S.; Cunningham, D. A. H.; Bando, Y.; Haruta, M. In *Studies in Surface Science and Catalysis;* G. Poncelet, J. M. B. D. P. A. J.; Grange, P. Eds.; Elsevier, 1995; pp. 227-235.
58. Bowker, M. *The Basis and Applications of Heterogeneous Catalysis*; Oxford: Oxford University Press, 1998.
59. Samanta, C. *Applied Catalysis A: General* **2008,** *350*, 133-149.
60. Batista, J.; Pintar, A.; Mandrino, D.; Jenko, M.; Martin, V. *Applied Catalysis A: General* **2001,** *206*, 113-124.
61. K.S. Kim, A. F. G., N. Winograd. *Analytical Chemistry* **1974,** *46*, 197.
62. M. Visco, A.; Neri, F.; Neri, G.; Donato, A.; Milone, C.; Galvagno, S. *Physical Chemistry Chemical Physics* **1999,** *1*, 2869-2873.
63. Edwards, J. K.; Solsona, B. E.; Landon, P.; Carley, A. F.; Herzing, A.; Kiely, C. J.; Hutchings, G. J. *Journal of Catalysis* **2005,** *236*, 69-79.
64. B. Pawelec, A. M. V., V. La Parola, E. Cano-Serrano,; J.M. Campos-Martin, J. L. G. F. *Applied Surface Science* **2005,** *242*, 380-391.

CHAPTER 5

Oxidation of Methane using *In-Situ* Synthesised H_2O_2, Stability and Mechanistic Studies

5.1. Introduction

This chapter is divided into two main sections; the first section concerns the selective oxidation of methane with Au based catalysts using *in-situ* generated hydrogen peroxide (H_2O_2) as the oxidant. The second part of the chapter describes the possible mechanism involved in the reaction. The heterogeneously developed catalytic system is compared with analogue homogeneous systems, and further studies were carried out by varying the reaction conditions *i.e.* temperature, time, oxidant concentration and the choice of catalyst. Finally, characterisation of the catalysts under investigation is discussed, and this is related to the observed catalytic activity.

5.2. Methane oxidation using *in-situ* generation hydrogen peroxide

5.2.1. Introduction

As presented in chapter 4, supported Au-Pd nanoparticles catalyst was capable in oxidising methane with a high selectivity to methanol under very mild conditions. The hydrogen peroxide was added to the system as an oxidant, and its effect on the rate of methane oxidation was determined to be first order. Whilst this single step process represents a potential improvement over the current two-step process practiced industrially for the conversion of methane to methanol (methane is initially steam reformed to synthesis gas (H_2 + CO) and subsequently transformed to methanol or hydrocarbon fuels via methanol synthesis or Fischer-Tropsch synthesis).[1,2] The oxidation of methane with addition of H_2O_2 as oxidant still needs to be developed given that the price of hydrogen peroxide itself is relatively higher than the target product (methanol). Currently, the average price of

hydrogen peroxide was reported to be around 3 times higher than that of methanol.[3] Therefore, from an industrial point of view, it is essential to develop a system where the oxidant can be generated in the same pot during alkane oxidation, thereby avoiding the current (expensive) industrial route for hydrogen peroxide synthesis. Haruta has shown that the addition of hydrogen with molecular oxygen decreases the energy requirement for the activation of the oxygen, as this leads to the formation of hydroperoxy species *in-situ* which are then able to selectively epoxidise propene.[4] It was assumed that similar species are required for methane oxidation under the reaction conditions employed in this study. Further studies by the group of Hutchings have demonstrated that similar Au-Pd catalytic systems could synthesise hydrogen peroxide from a mixture of hydrogen and molecular oxygen at high rates even at sub-ambient temperatures and with high H_2 selectivity.[5,6] The combination of alkane oxidation with *in-situ* generated H_2O_2 has been shown in several reports (see section 1.5.2.5). The use of *in- situ* produced H_2O_2 over externally added H_2O_2 does have one major advantage; there is no large-scale H_2O_2 decomposition due to the lower availability of oxidant, and therefore less oxidant is lost through unwanted side reactions (such as hydrogen peroxide decomposition to water and oxygen). This should provide a higher selectivity based on H_2O_2 and limits the waste and cost of replenishing H_2O_2 externally.

In this instance, the selective oxidation of methane with *in-situ* generated hydrogen peroxide was carried out with a gas-phase composition of methane, hydrogen, oxygen and suitable diluents (typically N_2 or CO_2). The role of hydrogen and oxygen introduced into the reactor was to concurrently synthesise hydrogen peroxide *in-situ,* and use this oxidant to selectively form partial oxygenates from methane.

5.2.2. Comparison between heterogeneous with analogue homogeneous catalysts

In order to establish the reaction conditions, an initial series of reactions were carried out in the absence of a catalyst and at different reaction temperatures (2, 30, 50, 70 and 90 °C, respectively). From these experiments, it was evident that neither H_2O_2 nor methanol can be generated without the presence of a catalyst (see appendix B (1)). Given that no activity was observed in the absence of a catalyst, studies then focused on using homogeneous metal catalysts in order to compare the reaction to analogue heterogeneous counterparts. The initial experiments were performed at 50 °C, as previous studies with the addition of hydrogen peroxide demonstrated that at this temperature, high oxygenate productivity as

well as high selectivity to methanol was observed. As shown in table 5.1, it is important to notice that the homogeneous Au catalyst was not capable of oxidising methane to methanol using the *in-situ* approach, whereas homogeneous Pd or combination of homogeneous Au and Pd showed activity for the oxidation of methane, albeit with low selectivity to methanol. The activity observed with homogeneous palladium was expected given that Pd was used in earlier studies to synthesise H_2O_2 under *in-situ* conditions,[7-9] as well as being used for oxidation of alkane.[10]

Table 5.1: Liquid phase oxidation of methane using homogeneous and heterogeneous Au and Pd based catalysts with *in-situ* formation of H_2O_2

Entry	Catalyst	Product amount (μmol)				Methanol Selectivity (%) [c]	TOF [d]	H_2O_2 Remain (μmol) [e]
		CH_3OH [a]	HCOOH [a]	MeOOH [a]	CO_2 in gas [b]			
1	5%Au-PdTiO_{2IW}	1.31	0	0.29	0.32	68.2	0.320	56
2	TiO_2	0	0	0	<0.1	-	-	0
3	$HAuCl_4$	0	0	0	0.23	0	0	27
4	$PdCl_2$	0.41	1.80	0.21	1.93	9.4	0.484	12
5[f]	$HAuCl_4$/ $PdCl_2$	0.26	0.70	0.61	1.07	9.8	0.314	19

Reaction Time; 30 min, Reaction Temp; 50 °C, Total pressure: 32 bar, Stirring rate: 1500 rpm, Catalyst: 1.0 x 10^{-5} mol of metals, Solvent: H_2O, 10 mL, [a] Analysis using ^{1}H-NMR, [b] Analysis using GC-FID, [c] Methanol selectivity = (mol of CH_3OH/ total mol of products) * 100, [d] Turn over frequency (TOF) = mol of oxygenates / mol of metal / reaction time (h), [e] Assayed by Ce^{+4} (aq) titration, [f] 1:1 mol ratio of metal. Gases: 0.86% H_2/1.72%O_2/75.86%CH_4/21.55%N_2.

It was previously mentioned in section 4.3.1 that the homogeneous system suffers from poor recyclability given that precipitation of the homogeneous metal catalyst is observed after reaction. This precipitation was later confirmed by UV-Vis analysis of the filtrate solution (see appendix B (2)). Therefore, it is evident that the heterogeneous system presents a significant advantage over the homogeneous system, in that it can be easily recovered and reused for additional reaction cycles. In addition to this, the data in table 5.1 demonstrates that the 5wt%Au-Pd/TiO_{2IW} heterogeneous catalyst gave much higher methanol selectivity compared to the homogeneous mono or bimetallic Au/Pd counterpart. This data is also in agreement with the catalytic results obtained in the analogue reaction with the addition of hydrogen peroxide (reported in section 4.3.1) where there was no

formic acid observed after 30 minutes reaction time using the heterogeneous system, whereas for homogeneous Pd, selectivity to formic acid was 41%. Additionally, it is important to note that the support itself was not active as catalyst for methane activation using *in-situ* generated H_2O_2 in the absence of Au and Pd. This is presumably due to the fact that TiO_2 itself cannot produce H_2O_2 from H_2 and O_2.

This is the first truly bi-functional heterogeneous catalytic system since earlier studies of methane oxidation using H_2/O_2 required two difference catalytic systems for the generation of hydrogen peroxide and methane activation, respectively. For instance, Park and co-workers combined heterogeneous Pd/C and homogeneous copper or vanadium based catalyst for the selective oxidation of methane with *in-situ* produced hydrogen peroxide.[11-13] The reaction under study is further benefited by the choice of water as reaction medium, as those in the open literature are typically performed in organic or acidic solvents, such a acetonitrile and triflouroacetic acid (TFA) as report in literature[14,15,10].

5.2.3. Effect of diluents and the acidity of the solvent

Most of the reactions carried out in this study utilised nitrogen as diluent for O_2 and H_2 instead of carbon dioxide. This was necessary in order to quantify the amount CO_2 evolved from the reaction, even though existing literature on hydrogen peroxide synthesis using similar catalyst generally used CO_2 as diluents.[6] This is based on the fact that the CO_2 diluent could act as "green" *in-situ* acid promoter by forming acid solution from dissolved CO_2 in water consequently increase the rate of formation and the stability of hydrogen peroxide. For that reason, further investigation has been undertaken to use CO_2 as diluent purposely to compare the effect of reaction diluent while other parameters were kept constant. The catalytic data in table 5.2 shows that the use of carbon dioxide did not improve catalytic activity, and that the increase in acidity (due to carbonic acid formation) was not beneficial. In fact, reaction carried out with CO_2 as diluent was inferior than the activity observed when nitrogen was used as diluent.

Table 5.2: Effect of diluents on catalytic performance of 5wt%Au-Pd/TiO_{2IW} for the selective oxidation of methane with *in-situ* formation of H_2O_2

Entry	Diluents	Product amount (μmol)				Methanol Selectivity (%)[c]	TOF [d]	H_2O_2 Remain (μmol) [e]
		CH_3OH [a]	HCOOH [a]	MeOOH [a]	CO_2 in gas[b]			
1[f]	N_2	0.81	0	<0.1	0.11	79.4	0.164	29
2[g]	CO_2	0.28	0	<0.1	nd	-	-	26

Reaction Time; 30 min, Reaction Temp; 70 °C, Stirring rate: 1500 rpm, Catalyst: 1.0 x 10^{-5} mol of metals (27.6 mg), Solvent: H_2O, 10 mL, [a] Analysis using ^{1}H-NMR, [b] Analysis using GC-FID, [c] Methanol selectivity = (mol of CH_3OH/ total mol of products) * 100, [d] Turn over frequency (TOF) = mol of oxygenates / mol of metal / reaction time (h), [e] Assayed by Ce^{+4} (aq) titration, nd: not determine.

[f]Gases: 1.38% H_2/2.77%O_2/61.11%CH_4/34.72%N_2, (Total pressure: 40 bar)

[g]Gases: 2.0% H_2/3.9%O_2/44.1%CH_4/49.9%CO_2, (Total pressure: 58 bar)

Catalyst: Catalysts was synthesised using impregnation method and calcined in air at 400 °C for 3 hours

It seems that at these particular reaction conditions, the acidity of the solution does not play an important role in affecting catalytic activity. In order to corroborate and verify the results obtained, the reactions were carried out in the presence of acids. It was reported by Van Weynbergh *et al.* that in the presence of phosphoric acid (H_3PO_4), H_2O_2 formation would increase.[16] In their case, Pd supported on TiO_2 was used as the catalyst, and N_2 was chosen as diluent gas. Therefore, solutions containing 0.1 M phosphoric acid with a pH equal to 1.6 were used. From the data presented in table 5.3, it is clearly demonstrated that the catalytic activity did not improve upon the addition of the acid, although its addition was successful produced higher formation of hydrogen peroxide (table 5.3). The increased production of H_2O_2 in the presence of phosphoric acid is to be expected, given that hydrogen peroxide is more stable in acidic conditions, where its decomposition is inhibited. Moreover, the availability of protons (H^+ ions from acid) in the aqueous reaction medium would increase the selectivity of the H_2 to H_2O_2 reaction.[17,18]

Table 5.3: Effect of acidic solution on catalytic performance of 5wt%Au-Pd/TiO_{2IW} for the selective oxidation of methane with *in-situ* formation of H_2O_2

Entry	Solvent	pH	Product amount (μmol)				Methanol Selectivity (%)[c]	TOF [d]	H_2O_2 Remain (μmol) [e]
			CH_3OH [a]	HCOOH [a]	MeOOH [a]	CO_2 in gas[b]			
1[f]	H_2O	6.4	1.31	0	0.29	0.32	68.2	0.320	56
2[g]	0.1 M H_3PO_4	1.6	0.10	0	nd	nd	-	-	225
3[f]	0.03M HNO_3	1.5	2.17	8.36	4.49	1.94	12.8	3.004	105

Reaction Time; 30 min, Reaction Temp; 50 °C, Stirring rate: 1500 rpm, Catalyst: 1.0 x 10^{-5} mol of metals (27.6 mg), Solvent: H_2O, 10 mL. [a] Analysis using ^{1}H-NMR, [b] Analysis using GC- FID, [c] Methanol selectivity = (mol of CH_3OH/ total mol of products) * 100, [d] Turn over frequency (TOF) = mol of oxygenates / mol of metal / reaction time (h), [e] Assayed by Ce^{+4} (aq) titration
[f]Gases: 1.38% H_2/2.77%O_2/61.11%CH_4/34.72%N_2, (Total pressure: 40 bar)
[g]Gases: 2.0% H_2/3.9%O_2/44.1%CH_4/49.9%CO_2, (Total pressure: 58 bar)
Catalyst: Catalysts were synthesised using impregnation method and calcined in air at 400 °C for 3 h

The pH of reaction solution with only water as solvent and N_2 as diluents was determined to be around pH 6, and thus H_2O_2 was expected to be less stable in this solution as opposed to an aqueous acidic solution. It could be suggested here that the presence of phosphoric acid could affect the active species and/or the active site of catalyst responsible for the oxidation methane to oxygenated species. In particular, phosphorus anions might strongly bind on to the metal, subsequently blocking some of the catalyst active sites. For that reason, another step has been taken by replacing the phosphoric acid with nitric acid (HNO_3). Earlier works by Edwards and co-workers on hydrogen peroxide synthesis have shown that the presence of nitric acid is beneficial for enhancing H_2O_2 formation.[6] Their studies employed an impregnated Au-Pd/TiO_2 catalyst that was calcined at 400 °C. As revealed in table 5.3 (entry 3), catalytic activity based on TOF value obtained from methane oxidation in aqueous 0.03 M nitric acid solution with pH 1.5 shows 9 times higher than a reaction carried out in water as solvent. However, the methanol selectivity was low (12.8%) with formic acid was observed as main product. The superior catalytic activity of the reaction in nitric acid medium could be attributed to the two different possible factors. The first factor may be due to the increased formation of hydrogen peroxide, and additionally its higher stability against decomposition into H_2O and O_2. The second factor

could originate from a background reaction of homogeneous metal (Au/Pd) which potentially leaches from the catalyst into solution during reaction in acid media. The later factor was further indicated by the observed product distribution, which followed a similar trend to the homogenous metal reaction, especially that of $PdCl_2$ (see section 5.2.2). In this case, formic acid was detected as main product, and a high formation of CO_2 observed.
The data indicates that acidity could play an important role, especially on the availability of hydrogen peroxide during the reaction. However, the acidity factor alone cannot explain the lower catalytic activity observed with the reaction in the presence of CO_2 as diluent, which is known to produce an acidic solution of carbonic acid. Another possible reason for this could be due to the displacement of methane molecules in the liquid reaction solution by solubilising large amounts of CO_2, thereby affected the availability of methane in solution, and decreasing its ability to interact with the catalyst active sites. Based on the solubility of various gases in an aqueous medium,[19] the solubility of CO_2 in water was around 66 times higher compared to solubility of N_2 and CH_4 under similar conditions.

5.2.4. Varying reaction conditions

Even though detailed discussions on the reaction parameters such as temperature, pressure, oxidant concentration have been shown and discussed in section 4.3.2, similar parameters were investigated here given that the one-pot catalytic set-up may require different reaction conditions, given the need to simultaneously synthesise hydrogen peroxide together with methane oxidation.

5.2.4.1. Effect of reaction temperature

It is reported in the literature that temperature plays an important factor in determining the rate and the amount of hydrogen peroxide produced during direct synthesis from hydrogen and molecular oxygen in presence of CO_2.[5,20,6] The highest rate was achieved at sub-ambient 2 °C, and it was found to decrease with increasing reaction temperature, mainly due to the decomposition or hydrogenation of the synthesised hydrogen peroxide. Therefore, a series of reactions were performed with reaction temperatures between 2 °C and 90 °C, in order to determine the optimum conditions (table 5.4).

Table 5.4: Effect of reaction temperature on catalytic performance of 5wt%Au-Pd/TiO_{2IW} for the selective oxidation of methane with *in-situ* formation of H_2O_2

Entry	Temp.	Product amount (μmol)				Methanol	Oxygenate	TOF	H_2O_2
	(°C)	CH_3OH [a]	HCOOH [a]	MeOOH [a]	CO_2 in gas[b]	Selectivity (%)[c]	productivity (Mol/kg_{cat}/ Hour)[d]	[e]	Remain (μmol) [f]
1	2	0.26	0	0.47	0.15	29.5	0.053	0.146	124
2	30	0.81	0	0.53	0.24	51.3	0.097	0.268	33
3	50	1.31	0	0.29	0.32	68.2	0.116	0.320	56
4	70	0.81	0	<0.1	0.11	79.4	0.059	0.164	29
5	90	0.74	0	0	0.56	56.9	0.054	0.148	25

Reaction Time; 30 min, Stirring rate: 1500 rpm, Catalyst: 1.0×10^{-5} mol of metals (27.6 mg), Solvent: H_2O, 10 mL, [a] Analysis using ^{1}H-NMR, [b] Analysis using GC-FID, [c] Methanol selectivity = (mol of CH_3OH/ total mol of products) * 100, [d] Oxygenates productivity = mol of oxygenates / Kg_{cat} / reaction time (h), [e] Turn over frequency (TOF) = mol of oxygenates / mol of metal / reaction time (h), [f] Assayed by Ce^{+4} (aq) titration

Gases: 0.86% H_2/1.72%O_2/75.86%CH_4/21.55%N_2, (Total pressure: 32 bar)

Catalyst: Synthesised using impregnation method and calcined at 400 °C in static air for 3 hours.

As illustrated earlier, both hydrogen peroxide and partial oxygenated species are not formed in the absence of a catalyst. It is also important to note that the 5wt%Au-Pd/TiO_{2IW} catalyst was capable of both synthesising hydrogen peroxide and activating methane over the entire range of tested temperatures, even at 2 °C. In addition to this, there is no literature reported on the synthesis of hydrogen peroxide using this particular catalyst at 90 °C. The higher amount of hydrogen peroxide detected after the reaction at 2 °C might due to higher rates of formation coupled with lower decomposition and hydrogenation at the particular temperature. Reactions at 50 °C gave the best compromise in terms of activity and selectivity. At higher temperatures, there were little or no traces of methyl hydroperoxide, probably due to its transformation to methanol and CO_2. Higher temperatures are known to induce the methyl hydroperoxide transformation, and in the presence of a catalyst it selectively converts to methanol. Detailed studies on the formation and stability of methyl hydroperoxide are discussed in section 5.4.2 of this chapter. The highest methanol selectivity was obtained at 70 °C, with the selectivity to methanol around 80%.

5.2.4.2. Effect of reaction time

As described in section 4.3.2.3, the conversion of methane was increased throughout the reaction time. Methyl hydroperoxide was observed as an intermediate product, and it progressively transformed to methanol in the presence of a catalyst. In view of the fact that the oxidant is introduced to the system differently, it is essential to know whether a similar behavior will be observed compared to the oxidation of methane with the addition of hydrogen peroxide. It is clear from figure 5.1 that time-online study of methane oxidation with *in-situ* generated H_2O_2 shows a similar pattern in which methyl hydroperoxide is the primary product, and that methanol and CO_2 are increasingly formed at longer reaction times.

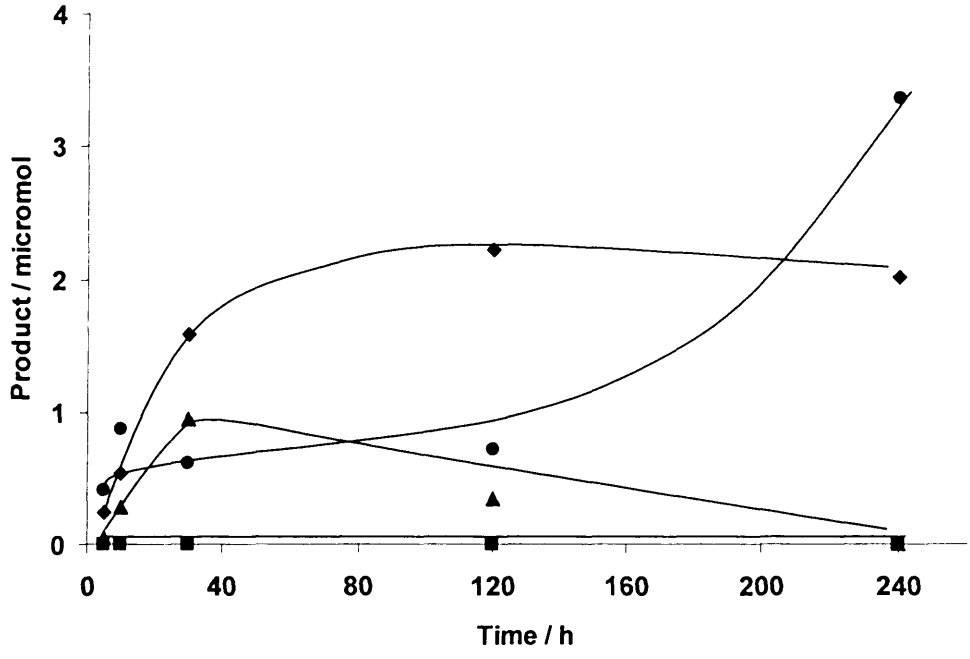

Figure 5.1: Time online plot of methane oxidation with *in-situ* generation H_2O_2 in the presence of 5wt%Au-Pd/TiO_{2IW} catalyst. Key: ▲ methyl hydroperoxide, ♦ methanol, ● carbon dioxide. Conditions, P=40 bar (Gases: 1.38% H_2/2.77%O_2/61.11%CH_4/34.72%N_2), T = 50 °C, 1500 rpm, catalyst mass = 28 mg.

For example, the selectivity to methanol increases up to 68% after 2 hours of reaction time, although further increases in time lead to a decrease in methanol selectivity and a significant increase in CO_2. Crucially however, no formic acid is observed even under these lengthened conditions. The results show that a similar mechanism and active species could be involved in both methane oxidation systems, either with H_2O_2 added as co-

reactant or with *in-situ* generated H_2O_2 from H_2 and O_2. In addition, by tuning the reaction time, there is the possibility of increasing the yield of methanol. However, prolonged reaction times will lead eventually to the over-oxidation of oxygenates and therefore CO_2 formation.

5.2.4.3. Effect of O_2/H_2 concentration

As it was shown in section 4.3.2.4, hydrogen peroxide concentration is first order toward the rate of methane oxidation when it was used as co-reactant. By increasing the hydrogen and oxygen pressures, an increase of oxygenate productivity and methanol formation was also observed (table 5.5). To verify the data, the test was carried out for two different reaction lengths, and both showed an increase of total oxygenates product. This is in agreement to the data observed for the oxidation with added hydrogen peroxide. It is important to emphasise that even with low amounts of oxidant present, high amounts of product were observed under the *in-situ* conditions.

Table 5.5: Effect of O_2/H_2 concentration in the liquid phase oxidation of methane using 5wt% Au-Pd/TiO_{2IW} with *in-situ* formation of H_2O_2

Entry	Time (min)	Product amount (μmol)				Methanol Selectivity (%)[c]	Oxygenate productivity (Mol/kg_{cat}/ Hour)[d]	TOF [e]	H_2O_2 Remain (μmol) [f]
		CH_3OH [a]	HCOOH [a]	MeOOH [a]	CO_2 in gas[b]				
1	30[g]	1.31	0	0.29	0.32	68.2	0.116	0.320	56
2	30[h]	1.59	0	0.95	0.61	50.5	0.184	0.508	35
3	120[g]	1.93	0	0	0.55	77.8	0.035	0.097	56
4	120[h]	2.23	0	0.35	0.71	63.4	0.204	0.562	62

Reaction Temp; 50°C, Stirring rate: 1500 rpm, Catalyst: 1.0 x 10^{-5} mol of metals (27.6 mg), Solvent: H_2O, 10 mL, [a] Analysis using ^{1}H-NMR, [b] Analysis using GC-FID, [c] Methanol selectivity = (mol of CH_3OH/ total mol of products) * 100, [d] Oxygenates productivity = mol of oxygenates / Kg_{cat} / reaction time (h), [e] Turn over frequency (TOF) = mol of oxygenates / mol of metal / reaction time (h), [f] Assayed by Ce^{+4} (aq) titration

[g]Gases: 0.86% H_2/1.72%O_2/75.86%CH_4/21.55%N_2, (Total pressure: 32 bar)

[h]Gases: 1.38% H_2/2.77%O_2/61.11%CH_4/34.72%N_2, (Total pressure: 40 bar)

Catalyst: Synthesised using impregnation method and calcined at 400 °C in static air for 3 hours.

This is based on the theoretical amount of hydrogen peroxide that can be synthesised at these particular conditions; in the case of entries 1 and 3 the maximum amount of hydrogen peroxide is less than 500 μmol, whereas the maximum amount of hydrogen peroxide that could be synthesised in entry 2 and 4 was calculated to be around 1000 μmol. At this level of oxidant (< 1000 μmol of H_2O_2) with oxidation carried out at 50 °C for 30 minutes reaction times, methane activation with added hydrogen peroxide gave 5 times less oxygenates (see section 4.3.2.4 of chapter 4).

It is essential to state here that the proposed active species is the hydroperoxy species (OOH) and this is known to participate in the *in-situ* generation of hydrogen peroxide. Theoretical modelling studies show the activation barrier for producing H_2O_2 from H_2 and O_2 is higher compared to the barrier for the formation of hydroperoxy species from H_2O_2,[21,22-24] hence it seems sensible to have higher catalytic activity toward methane oxidation even though the amount of H_2O_2 produced and/or detected after reaction is relatively low. This data effectively demonstrates that the generation of the oxidant in a one pot process at very low concentration is far more affective for the activation of methane than the addition of hydrogen peroxide at a large amount. From another point of view, the oxidant could be generated throughout the course of the reaction. This will overcome the financial problems associated with the high unselective decomposition of hydrogen peroxide, and also increases the product-oxidant stoichiometric ratio which is crucial in later scale-up stages.

5.2.5. Effect of Au/Pd metal ratio

As demonstrated in section 4.3.5, the Au-Pd metal ratio is important in controlling the catalytic activity and the product distribution. Theoretically, this parameter might be more important and prominent given that the reaction involves *in-situ* generation of hydrogen peroxide as well as methane oxidation. The ratio of Au/Pd should affect both the productivity of hydrogen peroxide as well as the oxidation of methane. In this study, the total 5wt%Au-Pd/TiO_{2IW} catalysts with three different Au to Pd weight ratio (4Au:1Pd, 2.5Au:2.5Pd, 1Au:4Pd) were synthesised and were tested for methane oxidation with *in-situ* generated H_2O_2. The 2.5wt%Au2.5wt%Pd/TiO_{2IW} was reported in literature as the optimised ratio for synthesising hydrogen peroxide.[5] The catalytic data for the bimetallic catalysts were then compared to monometallic 5wt%Au/TiO_{2IW} and 5wt%Pd/TiO_{2IW}

respectively. It is evident from table 5.6 that a clear activity and selectivity pattern has been observed by varying the Au-Pd ratio.

Table 5.6: Effect of Au:Pd ratio on catalytic performance of Au-Pd/TiO_{2IW} for the selective oxidation of methane with *in-situ* formation of H_2O_2

Entry	Au:Pd ratio (wt%:wt%)	Product amount (μmol)				Methanol Selectivity (%)[c]	Oxygenate Selectivity (%)[d]	TOF [e]	H_2O_2 Remain (μmol) [f]
		CH_3OH [a]	HCOOH [a]	MeOOH [a]	CO_2 in gas[b]				
1	5Au	0.23	0	0	1.24	15.6	15.6	0.012	21
2	4Au: 1Pd	0.96	0	0	0.65	59.6	59.6	0.048	17
3	2.5Au: 2.5Pd	2.23	0	0.35	0.71	67.8	78.4	0.129	62
4	1Au: 4Pd	2.34	0	0	1.01	69.9	69.9	0.117	20
5	5Pd	2.07	<0.1	0	2.43	45.4	46.7	0.107	20

Reaction Time; 2 hours, Reaction Temp; 50 °C, Stirring rate: 1500 rpm, Catalyst: 1.0 x 10^{-5} mol of metals, Solvent: H_2O, 10 mL, [a] Analysis using ^{1}H-NMR, [b] Analysis using GC- FID, [c] Methanol selectivity = (mol of CH_3OH/ total mol of products) * 100, [d] Oxygenates selectivity = (mol of oxygenates / total mol of products) * 100, [e] Turn over frequency (TOF) = mol of oxygenates / mol of metal / reaction time (h), [f] Assayed by Ce^{+4} (aq) titration
Gases: 1.38% H_2/2.77%O_2/61.11%CH_4/34.72%N_2, (Total pressure: 40 bar)
Catalyst: Catalysts were synthesised using impregnation method and calcined in air at 400 °C for 3 hours

The catalytic activity comparisons of the tested catalysts were based on TOF values. It can be seen that the highest TOF value for bimetallic catalysts (0.129 mole oxy./mole of metals/hrs) was obtained for the 2.5wt%Au2.5wt%Pd/TiO_{2IW} catalyst, whereas altering the weight ratio of Au into 4.0wt% with 1.0wt% of Pd clearly decreases the catalytic activity (TOF: 0.048 mole of oxy./mole of metals/hrs). On the other hand, by increasing the Pd content (4.0wt%Pd-1.0wt%Au), the observed catalytic activity was comparable to 2.5wt%Au2.5wt%Pd/TiO_{2IW} catalyst. The lower catalytic activity observed with 4.0wt%Au1.0wt% compared to 1.0wt%Au4.0wt%Pd was further explained by the catalytic data of the respective monometallic catalysts, 5wt%Au/TiO_{2IW} and 5wt%Pd/TiO_{2IW}. The monometallic Pd catalyst produced a TOF value around 9 times higher compared to the monometallic Au counterpart. The beneficial effect of Pd in obtaining higher catalytic activity is to be expected since Pd based metal catalysts are well known to have superior ability in generating hydrogen peroxide from H_2 and O_2 than monometallic Au catalyst.[9,17]

In addition to this, as discussed in chapter 4, palladium oxide (PdO) was believed to be responsible for activating the methane molecule, and the detail mechanisms are discussed in section 5.4 of this chapter. However, it is important to state that the excess of Pd species could enhance CO_2 formation and consequently affect the oxygenate selectivity, as shown in entry 4 and 5 of table 5.6. In this case, the highest oxygenate selectivity *i.e.* 78% was observed in the reaction with catalyst contained equal weight of Au/Pd ratio.

In addition to better catalytic activity, three times more H_2O_2 was detected after reaction by the 2.5wt%Au2.5wt%Pd/TiO_{2IW} catalyst compared to the other tested catalysts listed in table 5.6. This indicates a greater capability of synthesising H_2O_2 as reported in the literature. Further observation of the catalytic data also suggested that the presence of methyl hydroperoxide in the reaction with 2.5wt%Au2.5wt%Pd seems to be related to the amount of hydrogen peroxide (or hydroperoxy species) available during reaction. This statement is based on the fact that methyl hydroperoxide is believed to originate from the reaction involving hydroperoxy species. Moreover, it might due to the ability of catalyst in transforming methyl hydroperoxide either selectively to methanol or to carbon dioxide. It is apparent that it needs a combination of Au and Pd in a proper ratio in order to successfully transform the majority of the methyl hydroperoxide to methanol. Au itself is not selective and by a small addition of Pd to it improved almost 4 times methanol selectivity with similar amount of total products. Insignificant amount of formic acid observed with Pd monometallic could be due to the trace amount of Pd leached out into solution and this observation is in agreement with the homogeneous data which show the formation of formic acid even at lower temperature.

5.2.6. Effect of Au-Pd alloy

There is clear evidence from the catalytic studies of the Au-Pd ratio of the beneficial combination of both metals in order to obtain high activity and selectivity to oxygenate products, especially to methanol. To verify whether it is due to the presence of Au core-Pd shell structures, a series of reactions with physical mixtures of 2.5wt%Au/TiO_{2IW} and 2.5wt%Pd/TiO_{2IW} were carried out, either with the same weight or moles of metal. Both instances gave inferior activity and selectivity compared to the alloyed Au-Pd catalyst with core-shell structures (table 5.7).

Table 5.7: Effect of Au-Pd alloy on catalytic performance of 5wt%Au-Pd/TiO_{2IW} for the selective oxidation of methane with *in-situ* formation of H_2O_2

Entry	Au:Pd ratio	Product amount (μmol)				Methanol Selectivity (%)[c]	Oxygenate productivity (Mol/kg_{cat}/ Hour)[d]	TOF [e]	H_2O_2 Remain (μmol) [f]
		CH_3OH [a]	HCOOH [a]	MeOOH [a]	CO_2 in gas[b]				
1	2.5Au: 2.5Pd [g]	1.31	0	0.29	0.32	68.2	0.116	0.320	56
2	2.5Au: 2.5Pd [h]	0.12	0	0	0.54	18.2	0.009	0.024	33
3	2.5Au: 2.5Pd [i]	0.81	0	0	0.58	58.3	0.059	0.162	21

Reaction Time; 30 min, Reaction Temp; 50 °C, Stirring rate: 1500 rpm, Catalyst: 1.0 x 10^{-5} mol of metal (27.6 mg), Solvent: H_2O, 10 mL, [a] Analysis using ^{1}H-NMR, [b] Analysis using GC-FID, [c] Methanol selectivity = (mol of CH_3OH/ total mol of products) * 100, [d] Oxygenates productivity = mol of oxygenates / Kg_{cat} / reaction time (h), [e] Turn over frequency (TOF) = mol of oxygenates / mol of metal / reaction time (h), [f] Assayed by Ce^{+4} (aq) titration,

Gases: 0.86% H_2/1.72%O_2/75.86%CH_4/21.55%N_2, (Total pressure: 32 bar)

[g] Catalyst: 2.5wt%Au2.5wt%Pd/TiO_2 (impregnation method) and calcined at 400°C in static air for 3 h.

[h] Physical mixture of 2.5wt%Au/TiO_2 and 2.5wt%Pd/TiO_2 (impregnation method), 1:1 wt %

[i] Physical mixture of 2.5wt%Au/TiO_2 and 2.5wt%Pd/TiO_2 (impregnation method), 1:1 mol of metal

This observation is in line with synergistic effects observed with other substrates reported in the literature.[25,26] Therefore, it confirms the fact that it is necessary to have a specific catalyst structure to successfully generate the oxidant at some level, and then simultaneously use the oxidant to selectively oxidise methane. In this case, the core-shell structure of gold-palladium seems to play an important role. Detail explanation of the characterisation of 5wt%Au-Pd/TiO_{2IW} has been discussed in detail in chapter 4.

5.2.7. Catalyst pre-treatment and its influence on methane oxidation

As described in section 4.3.6, catalyst pretreatment affected both the catalytic activity and selectivity patterns. Therefore, a series of pretreatments were performed on a 5wt%Au-Pd/TiO_{2IW} catalyst, which were then studied under *in-situ* conditions. Initially, the study investigated the effect of heat treatment in static air where the calcined catalyst at 400 °C was compared to the as-prepared 5wt%Au-Pd/TiO_{2IW} catalyst dried at 110 °C. It was reported in literature that uncalcined Au-Pd catalyst gave 3 times higher rate of hydrogen

peroxide synthesis than the calcined catalyst,[20,27] although it was not particularly robust and deactivated significantly with successive uses. This is due to the fact that most of the metals leached into solution during the reaction mixture. It was reported that calcinations at 400 °C would generate a stable and reusable catalyst without loss of the catalytic activity.

Table 5.8 illustrates that the uncalcined catalyst produced more than double the turnover frequency (TOF) compared to the calcined catalyst counterpart. There are two possible reasons that could explain the higher activity of uncalcined catalyst. The first is due to the capability of the catalyst, in terms of hydrogen peroxide generation.

Table 5.8: Effect of calcinations on catalytic performance of 5wt%Au-Pd/TiO_{2IW} for the selective oxidation of methane with *in-situ* formation of H_2O_2

Entry	Calc. Temp. (°C)	Product amount (μmol)				Methanol Selectivity (%)[c]	TOF [d]	H_2O_2 Remain (μmol) [e]
		CH_3OH [a]	HCOOH [a]	MeOOH [a]	CO_2 in gas[b]			
1	110	1.14	4.59	0	3.36	12.5	1.146	32
2	400	1.59	0	0.95	0.61	50.5	0.508	35

Reaction Time; 30 min, Reaction Temp; 50 °C, Stirring rate: 1500 rpm, Catalyst: 1.0 x 10^{-5} mol of metals (27.6 mg), Solvent: H_2O, 10 mL, [a] Analysis using ^{1}H-NMR, [b]Analysis using GC- FID, [c] Methanol selectivity = (mol of CH_3OH/ total mol of products) * 100, [d] Turn over frequency (TOF) = mol of oxygenates / mol of metal / reaction time (h), [e] Assayed by Ce^{+4} (aq) titration
Gases: 1.38% H_2/2.77%O_2/61.11%CH_4/34.72%N_2, (Total pressure: 40 bar)

Secondly, the higher formation of formic acid and carbon dioxide may be contributed from the reaction catalysed by homogeneous Pd that had leached to the reaction mixture. This statement is based upon the fact that an analogue reaction with a homogeneous Pd solution (see section 5.2.2) generated 41% formic acid and 44% carbon dioxide. Homogeneous Au did not give any activity under similar reaction conditions. Atomic absorption spectroscopy (AAS) analysis revealed that higher amounts of metal were lost during reaction catalysed by the uncalcined 5wt%Au-Pd/TiO_{2IW} catalyst (table 5.9) whereas 5wt%Au-Pd/TiO_{2IW} catalyst calcined at 400 °C did not show any significant leaching of either Pd or Au, as it was calculated that more than 99.99% of both metals remained after reaction within the limit of detection (table 5.11). The AAS analysis was further supported by ICP-MS analysis in very high sensitivity up to part per billion (ppb) levels.

Table 5.9: Analysis of filtrate from methane oxidation with *in-situ* formation of H_2O_2 in the presence of uncalcined 5wt%Au-Pd/TiO_{2IW} catalyst

Catalyst	Metal	Metal leach, (%)
Uncalcined 5wt%Au-Pd/TiO_{2IW}	Au	57
	Pd	52

In addition to this, there is another possibility where leached metals might rapidly deposit onto the autoclave, stirrer or solid catalyst. Therefore, the uncatalysed 'blank' reaction has been performed by two ways, one for verifying the reactor itself and the other by carrying out the reaction with the filtrate solution (after performing hot filtration) after reaction. It is important to state here that both blank tests did not give any formation of products and that no hydrogen peroxide was detected following the titration method with cerium sulphate. In addition, the AAS analysis of filtrate after performing hot filtration also did not show that any significant metal leached out during reaction (table 5.10).

Table 5.10: Analysis of filtrate from methane oxidation with *in-situ* formation of H_2O_2 in the presence of calcined 5wt%Au-Pd/TiO_{2IW} catalyst

Entry	Uses	Metal	Metal leach, (%)	
			AAS	ICP-MS
1	Fresh	Au	<0.001	<0.001
		Pd	<0.001	<0.001
2	Fresh (hot filtration)	Au	<0.001	<0.001
		Pd	<0.001	<0.001

Hence it is possible that the activities observed with the uncalcined catalyst may be due to homogeneous Pd cations that are known to be an efficient catalyst for both hydrogen peroxide synthesis and methane activation.[10,12] Formic acid was not detected in the calcined Au-Pd catalyst and CO_2 levels were very low.

In another set of experiments, the effect of heat treatment was investigated (oxidative treatment versus reductive treatment, table 5.11). A dried 5wt%Au-Pd/TiO_2 catalyst

synthesised by impregnation was subjected to heat treatment in flowing of 5% hydrogen in argon for 3 hours at 400 °C and later compared to the static air calcined analogue.

Table 5.11: Effect of catalyst pretreatment on catalytic performance of 5wt%Au-Pd/TiO_{2IW} for the selective oxidation of methane with *in-situ* formation of H_2O_2

Entry	Catalyst Pretreatment	Product amount (μmol)				Methanol Selectivity (%)[c]	Oxygenate productivity (Mol/kg_{cat}/ Hour)[d]	TOF [e]	H_2O_2 Remain (μmol) [f]
		CH_3OH [a]	HCOOH [a]	MeOOH [a]	CO_2 in gas[b]				
1	Static air	1.59	0	0.95	0.61	50.5	0.184	0.508	35
2	Flowing 5%H_2/Ar	0.23	0	0	0.72	24.2	0.016	0.046	27

Reaction Time; 30 min, Reaction Temp; 50 °C, Stirring rate: 1500 rpm, Catalyst: 1.0 x 10^{-5} mol of metals (27.6 mg), Solvent: H_2O, 10 mL, [a] Analysis using ^{1}H-NMR, [b]Analysis using GC- FID [c] Methanol selectivity = (mol of CH_3OH/ total mol of products) * 100, [d] Oxygenates productivity = mol of oxygenates / Kg_{cat} / reaction time (h), [e] Turn over frequency (TOF) = mol of oxygenates / mol of metal / reaction time (h), [f] Assayed by Ce^{+4} (aq) titration,
Gases: 1.38% H_2/2.77%O_2/61.11%CH_4/34.72%N_2, (Total pressure: 40 bar)

It is apparent that reduction in hydrogen leads to a significant decrease in catalytic activity, determined at similar reaction conditions as the Au-Pd calcined catalyst in static air. This in line with the data observed using the addition of hydrogen peroxide approach, were lower activity was also observed for the reduced Au-Pd catalyst.

The observed decrease in activity might be due to two factors, either a lower capability of synthesising the hydroperoxy species, and/or a higher rate of hydrogen peroxide decomposition. Based on the available literature, a reduced 5wt%Au-Pd/TiO_{2IW} catalyst with metallic state Au and Pd and smaller particle sizes produced hydrogen peroxide at half the productivity of a 5wt%Au-Pd/TiO_{2IW} calcined catalyst.[27,28] The availability of Pd in metallic state can also accelerate the decomposition of the synthesised hydrogen peroxide. It was reported in the literature that the oxidation state of Pd had a greater effect on the yields of H_2O_2 produced versus the particle size and surface area properties of the catalyst system. An excellent correlation was observed between the H_2O_2 selectivity and H_2O_2 decomposition activity of the oxidised Pd catalysts. The oxidised Pd catalysts showed almost an order of magnitude lower H_2O_2 decomposition activity than the reduced catalysts.[9]

Moreover, as stated in chapter 4, theoretical modeling studies suggested that Pd^{2+} (PdO) available in calcined 5wt%Au-Pd/TiO_{2IW} catalyst was better in facilitating the abstraction of the proton from the methane molecule than Pd in the metallic state which is observed in reduced 5wt%Au-Pd/TiO_{2IW} catalyst.[22] Therefore, it could be concluded here that heat treatment environment was crucial in determining the overall catalytic activity and product distributions. Furthermore, both heat treatment conditions, either calcination in air or in hydrogen are required to obtain stable catalysts. Au-Pd in core-shell structures with PdO dominating the outer surface of catalyst was preferred to the presence of metallic palladium and smaller Au-Pd particles on the reduced sample.

5.2.8. Effect of different preparation techniques on Au-Pd/TiO_2 catalysts

Table 5.12 represent the effect of catalyst preparation technique on the catalytic activity of 1wt%Au-Pd/TiO_2 for methane oxidation using *in-situ* generated H_2O_2. Similar to section 4.3.4, an impregnated 1wt%Au-Pd/TiO_2 catalyst was compared directly to the 1wt%Au-Pd/TiO_2 catalyst synthesised via the sol-immobilisation technique.

Table 5.12: Effect of preparation technique on catalytic performance of 1%Au-Pd/TiO_2 for the selective oxidation of methane with *in-situ* formation of H_2O_2

Entry	Preparation techniques	Product amount (μmol)				Methanol Selectivity (%)[c]	TOF [d]	H_2O_2 Remain (μmol) [e]
		CH_3OH [a]	HCOOH [a]	MeOOH [a]	CO_2 in gas[b]			
1	Impregnation	1.58	0	0	0.33	82.7	4.37	32
2	Sol-Immobilisation.	0.66	0	0	0.20	76.7	1.83	37

Reaction Time; 30 min, Reaction Temp; 50 °C, Stirring rate: 1500 rpm, Catalyst: 10 mg, Solvent: H_2O, 10 mL, [a] Analysis using ^{1}H-NMR, [b] Analysis using GC-FID, [c] Methanol selectivity = (mol of CH_3OH/ total mol of products) * 100, [d] Turn over frequency (TOF) = mol of oxygenates / mol of metal / reaction time (h), [e] Assayed by Ce^{+4} (aq) titration
Gases: 0.86% H_2/1.72%O_2/75.86%CH_4/21.55%N_2, (Total pressure: 32 bar)

As observed for the oxidation with added H_2O_2, an impregnated catalyst gave TOF values over two times higher compared to the sol-immobilised catalyst. It has previously demonstrated that hydrogen peroxide formation is favoured on bigger metal particle sizes due to several factors, as previously discussed.[29]

Taking into account that the sol-immobilised catalyst was not subjected to calcination at high temperature, it was expected that a lack of a core-shell Au-Pd structure would be observed compared to the impregnated Au-Pd catalyst. Based on XPS characterisation studies of sol-immobilised Au-Pd catalysts, detailed in section 4.6.4 of chapter 4, there is no evidence of Pd enrichment at the surface and this indicates the absence of a core shell structure and the formation of a homogenous Au-Pd alloy in the immobilised catalyst. This was in agreement with the XPS study of similar materials reported in the literature.[30] Besides this, a more important aspect to consider for the inferior activity is the lack of oxide species on the catalyst surface. An impregnated catalyst generally composes of Pd^{2+} species whereas those prepared by sol-immobilisation contain mainly Pd^{0} with minor Pd^{2+} species. In the case of methane oxidation, it was proposed that cationic species (Pd^{2+}, (PdO)) have a prominent role in the oxidation process whereas metallic Pd mostly affected the decomposition of H_2O_2 and subsequently suppressed the overall catalytic activity.[9,22] Another important observation here is the ability of Au-Pd impregnated catalyst with 5 times lower Au-Pd metal loading to produce similar amount of oxygenated products compared to the 5wt% metal loading catalyst. The TOF value is calculated to be ~9 times higher with 82% methanol selectivity.

Furthermore, the methanol selectivity obtained in the reaction with *in-situ* H_2O_2 is higher than in the case of the addition of hydrogen peroxide. In the *in-situ* reaction conditions, the catalyst is steadily generating the active species, and at the same time selectively converting the intermediate species, CH_3OOH, into methanol. In this manner, the selective transformation of methyl hydroperoxide to methanol was more efficient and consequently enhanced the methanol selectivity. On the contrary, in the case of pre-loaded H_2O_2, the availability of proposed active species (hydroperoxyl species) is relatively high due to the higher concentration of added hydrogen peroxide (5000 μmol) which is 10 times higher than theoretical value of H_2O_2 could be synthesised through *in-situ* reaction condition. For that reason, at short reaction time (30 minutes), methane oxidation using added H_2O_2 with relatively higher availability of hydroperoxyl species during reaction probably undergoes competitive reaction between the formation of methyl hydroperoxide and its transformation to methanol. Hence methanol selectivity was lower due to the presence of unconverted methyl hydroperoxide. This observation again signifies the advantages of the *in-situ* capture of H_2O_2 concept over added oxidant for the selective oxidation of methane to methanol.

5.2.9. Effect of support on catalytic activity of Au-Pd bimetallic supported catalysts

In an attempt to elucidate the nature of the support, a series of reactions were conducted over 5wt%Au-Pd with different supports. The results from these experiments are summarised in table 5.13. The data showed a clear insight into the effect of support where TiO_2 still produced the highest catalytic activity and selectivity, as demonstrated in reactions performed with the addition of H_2O_2. The trend of activity was the following: $TiO_2 > Al_2O_3 > CeO_2 >$ Carbon whereas the selectivity pattern pursues the following trends, $TiO_2 > Al_2O_3 >$ Carbon$> CeO_2$. It is important to state that the selectivity trend reported here was calculated based on total products produced. The ideal selectivity comparison should be made at iso-conversion level.

Table 5.13: Effect of different support on catalytic performance of 5wt%Au-Pd supported catalyst for the selective oxidation of methane with *in-situ* formation of H_2O_2.

Entry	Catalyst	Product amount (μmol)				Methanol Selectivity (%)[c]	TOF [d]	H_2O_2 Remain (μmol) [e]
		CH_3OH [a]	HCOOH [a]	MeOOH [a]	CO_2 in gas[b]			
1	TiO_2	1.31	0	0.29	0.32	68.2	0.32	56
2	Carbon	0.31	0	0	0.43	41.9	0.03	24
3	CeO_2	0.26	0	0	0.39	40.0	0.05	24
4	γ-Al_2O_3	0.24	0	0.24	0.27	50.0	0.10	36

Reaction Time; 30 min, Reaction Temp; 50 °C, pressure: 30 bar, Stirring rate: 1500 rpm, Catalyst: 1.0 x 10^{-5} mol of metals (27.6 mg), Solvent: H_2O, 10 mL, [a] Analysis using ^{1}H-NMR, [b]Analysis using GC-FID, [c] Methanol selectivity = (mol of CH_3OH/ total mol of products) * 100, [d] Turn over frequency (TOF) = mol of oxygenates / mol of metal / reaction time (h), [e] Assayed by Ce^{+4} (aq) titration,
Gases: 0.86% H_2/1.72%O_2/75.86%CH_4/21.55%N_2, (Total pressure: 32 bar)
Catalyst: Catalysts were synthesised using impregnation method and calcined in air at 400 °C for 3 hours

Previous studies on hydrogen peroxide synthesis using Au-Pd supported catalysts demonstrated that carbon and SiO_2 were preferred supports for obtaining higher H_2O_2 productivity than TiO_2.[6] However, as demonstrated above, the carbon supported catalyst produced inferior catalytic activity than the TiO_2 support catalyst. It appears from the catalytic data that the nature of the catalyst plays a crucial role in determining the overall catalytic activity. To successfully oxidise methane at these particular conditions, the

catalyst must be able to accomplish a bi-functional role *i.e.* synthesising hydrogen peroxide and activating methane toward oxygenates.

5.3. Catalyst stability studies for methane oxidation: *In-situ* generated H_2O_2 and with addition of H_2O_2 as oxidant.

In order to study the catalyst reusability, a series of reactions were carried out for both *in-situ* H_2O_2 and H_2O_2 addition approaches respectively. In figure 5.2, it is shown that the activity of the 5wt%Au-Pd/TiO_{2IW} catalyst in the reaction with H_2O_2 added as co-reactant was reduced after first use, but then stabilised after successive uses. An opposite pattern observed for the selectivity of methanol, whereas oxygenate selectivity activity remained the same.

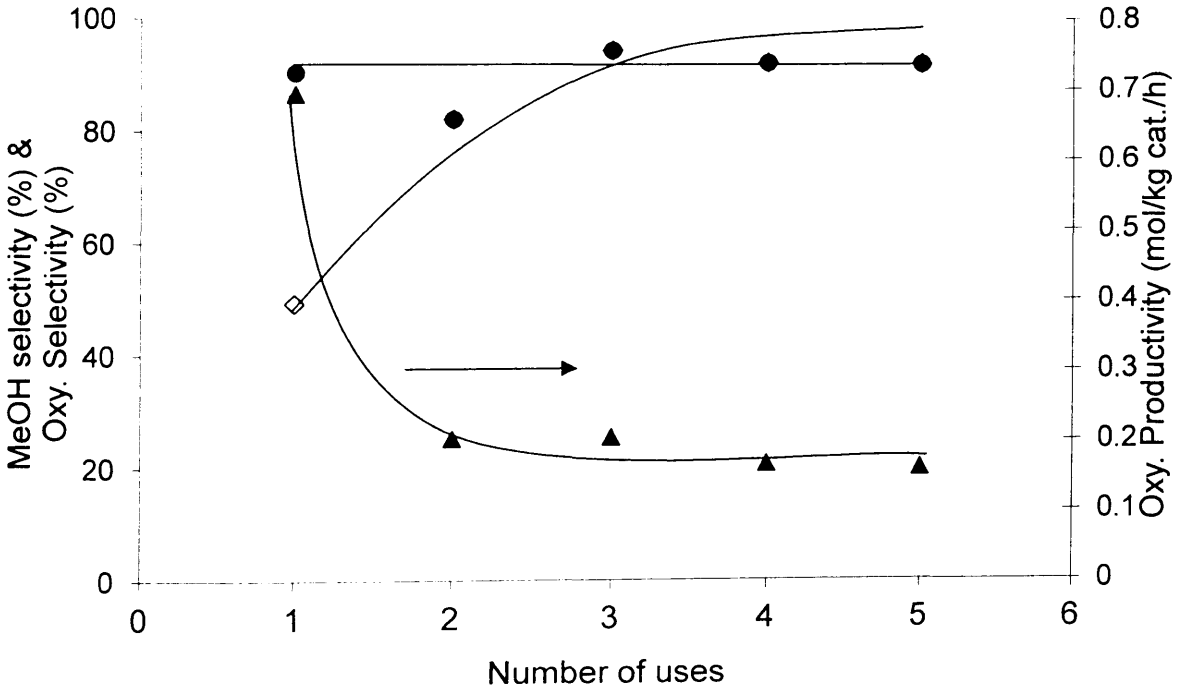

Figure 5.2: Plot of oxygenates productivity and selectivity to methanol and oxygenates, respectively as function of number of catalyst used in the reaction with addition of H_2O_2. Key: ▲ oxygenates productivity, ◊ methanol selectivity, ● oxygenates selectivity. Conditions: Time=0.5 hours, P(CH_4)=30 bar, [H_2O_2]=0.5M, T=50 °C, 1500 rpm, catalyst mass = 27.6 mg.

Providing that the differences in catalytic activity and selectivity patterns between fresh and used Au-Pd catalysts do not originate from the metal leaching issue (previously

confirmed by atomic absorption analysis (AAS)), another aspects that must be investigated is the catalyst structure, *i.e.* whether it is similar for the fresh and used Au-Pd catalyst. The used Au-Pd catalyst has been subjected to characterisation by XRD and XPS. XRD diffractogram (see figure 5.11) revealed that metallic Pd was detected on the used Au-Pd catalyst (peak at $2\theta = \sim 40.4^{o}$ corresponds to Pd^{0}). The same peak was observed in both reduced with H_2/Ar and H_2O_2 treated Au-Pd catalysts but not on the fresh calcined Au-Pd catalyst. The average metal particle size for the used catalyst was very similar compared to the fresh catalyst, which shows metal agglomeration did not occur.

The XRD data was further supported by XPS analysis of both fresh and used catalyst. It is clear from XPS spectrum of the fresh calcined catalyst (see figure 5.12(a)) that the dominant feature is the Pd ($3d_{5/2}$) peak, and that the contribution from the Au (4d) signal is reduced due to the nature of core-shell structure of the catalyst. The Pd ($3d_{5/2}$) signal at 336.8 eV was identified as oxidized Pd^{2+} (PdO) species. On the other hand, the Pd ($3d_{5/2}$) feature of the used catalyst (figure 5.12 (b)) shows two unresolved signals at 336.8 and 334.7 eV corresponding to Pd^{2+} and Pd^{0} respectively. In this case, the relative composition of Pd^{0} determined by deconvulation of Pd ($3d_{5/2}$) signal was around 43.5% and 56.5% for Pd^{2+} phase. The XPS spectrum of the used 5wt%Au-Pd/TiO_{2IW} catalyst also shows a similar pattern to those observed for the XPS spectra of both reduced (with 5%H_2/Ar) and H_2O_2 treated Au-Pd catalysts (see section 4.5.4 of chapter 4) where its consists both Pd^{2+} and Pd^{0} species. The Pd oxidation state composition between Pd^{2+} and Pd^{0} calculated on both samples (pretreated with H_2/Ar and H_2O_2 respectively) was also in a relatively similar range to the used Au-Pd catalyst. It is worth noting here that the activity level of 5wt%Au-Pd/TiO_{2IW} catalyst pretreated either in hydrogen stream or with hydrogen peroxide was of comparable activity to the used 5wt%Au-Pd/TiO_{2IW} catalyst, but in all cases these activities were inferior compared to the catalytic activity obtained with fresh 5wt%Au-Pd/TiO_{2IW} calcined catalyst. Consequently, this indicates that the catalytic performance of the catalyst toward methane oxidation with H_2O_2 as oxidant was strongly influenced by the characteristic properties of catalysts.

As previously mentioned, XRD analysis indicated that the metal particle size of used 5wt%Au-Pd/TiO_{2IW} catalyst was very similar to the fresh catalyst before reaction. The only clear difference between fresh and used samples is the occurrence of metallic Pd on used samples, as confirmed by XRD and XPS analyses. It seems that the presence of metallic Pd on used catalyst could be responsible for the lower catalytic activity. Therefore, since the presence of Pd^{0} lowered the catalytic activity, it was believed that the main active site is

PdO which then reduced to Pd^0 in the presence of hydrogen peroxide. The ability of hydrogen peroxide to act as reducing agent (together with oxidizing ability) was previously showed by Suss-Fink *et al.* in their vanadium based catalytic system, where H_2O_2 acted as a reducing agent for the reduction of V^V to V^{IV} species.[31] This was further support by the works of Liu and co-workers where they monitored the electrochemistry process using cyclic volumetric analysis in the presence of PdO and H_2O_2. Upon addition of H_2O_2, the peak current for the reduction of PdO (to metallic Pd) was enhanced, and the current was found to increase linearly with increasing concentrations of H_2O_2.[32] These studies indicate that PdO could well be reduced following the interaction with the hydrogen peroxide solution.

It is vital to know whether the catalytic activity could be restored by any means, therefore one step has been taken by recalcining the used catalyst in static air for 3 hours at 400 °C. Further analysis of the recalcined sample with XRD (see figure 5.11) showed that the peak corresponding to metallic Pd almost disappeared and that the crystallite size of Au-Pd calculated by Scherer equation was slightly increased from 23.4 to 24.8 nm. The additional step managed to slightly improve the catalytic activity, and at the same time suppressed the hydrogen peroxide decomposition (table 5.14). Higher amounts of oxidant remained following the reaction, and this is in line with the bigger crystallite size formed and the decrease in the amount of Pd in metallic state, as previously mentioned. It is essential to state here that at up to this stage, the catalyst regeneration procedure has not optimised and it has been shown that the original morphology of catalyst could be restored by varying the heat treatment procedure.

Table 5.14: Effect of heat treatment on used 5wt%Au-Pd/TiO_{2IW} catalyst

Entry	Catalyst	Product amount (μmol)				Methanol Selectivity (%)[c]	Oxygenate productivity (Mol/kg_{cat}/ Hour)[d]	H_2O_2 Remain (μmol) [e]
		CH_3OH [a]	HCOOH [a]	MeOOH [a]	CO_2 [b]			
1	Fresh	1.89	0	1.57	0.37	49.3	0.250	383
2	3rd used[f]	0.83	0	0	0.07	92.2	0.060	29
3	3rd used[g]	0.79	0	0	0.02	97.5	0.057	19
4	3rd used[h]	0.80	0	0.40	0.11	72.1	0.087	647

Reaction Time; 30 min, Reaction Temp; 50 °C, CH_4 pressure: 30 bar, Stirring rate: 1500 rpm, Catalyst: 27.6 mg., $[H_2O_2]$:0.5M, Solvent: H_2O, 10 mL, [a] Analysis using ^{1}H-NMR, [b] Analysis using GC-FID, [c] Methanol selectivity = (mol of CH_3OH/ total mol of products) * 100, [d] Oxygenates productivity = mol of oxygenates / Kg_{cat} / reaction time (h), [e] Assayed by Ce^{+4} (aq) titration,
Catalyst: Catalysts were synthesised using impregnation method and calcined in air at 400 °C for 3 hours
[f]Catalyst was dried at room temperature,
[g]Catalyst was dried at 110 °C in static air for 3 hours,
[h]Catalyst was dried at room temperature and calcined at 400 °C in static air for 3 hours

Reusability studies were also carried out for methane reaction with *in-situ* generated H_2O_2, and the data is shown in figure 5.3. Similar to the addition of hydrogen peroxide, the activity decreased after the first use. However, the selectivity patterns to either methanol or oxygenates follows an opposite trend and it was found to decrease with uses.

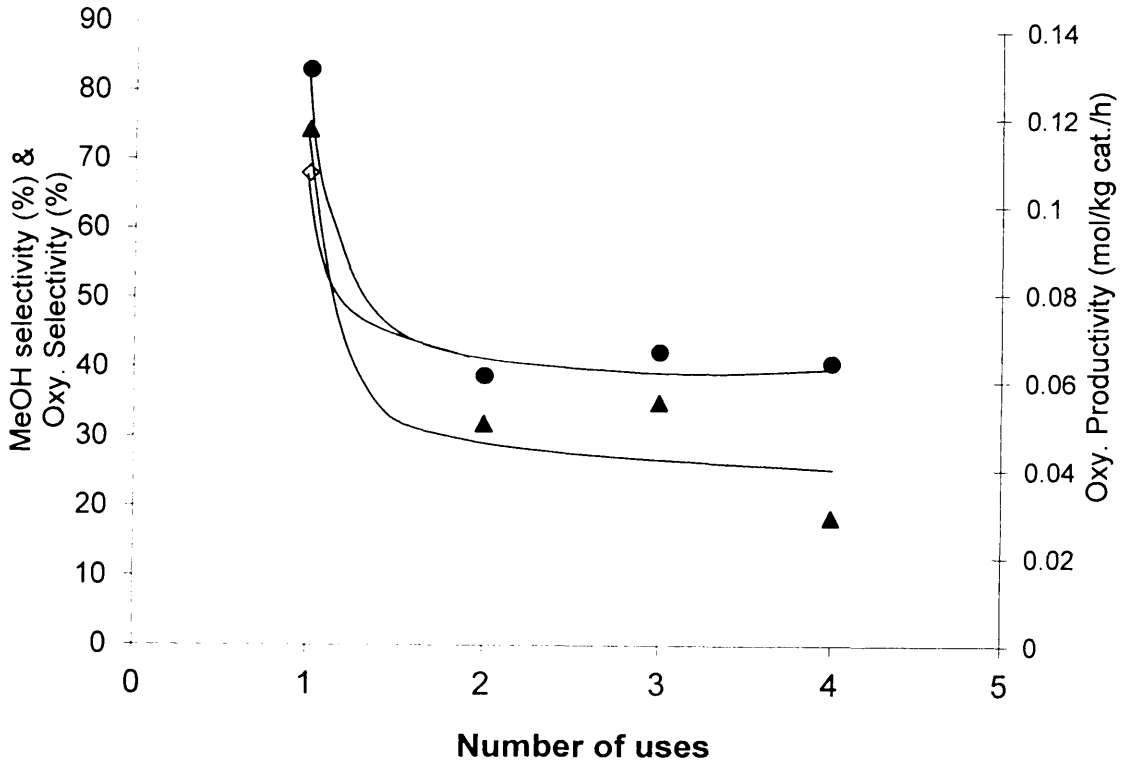

Figure 5.3: Plot of oxygenates productivity and selectivity to methanol and oxygenates, respectively as function of number of catalyst used in the reaction with *in-situ* H_2O_2. Key: ▲ oxygenates productivity, ◊ methanol selectivity, • oxygenates selectivity. Conditions: Time=0.5 hours, T=50°C, 1500 rpm, catalyst mass=28 mg. Gases: 0.86% H_2/1.72%O_2/75.86%CH_4/21.55%N_2

These differences could be attributed to the way that the hydroperoxy species is generated in the reaction. In case of methane oxidation with the addition of H_2O_2 as oxidant, the presence of metallic Pd on used catalysts favors the splitting of the H_2O_2, probably into surface bound hydroxyl species which later reacted with methyl species to produce methanol.[22] On the other hand, under *in-situ* H_2O_2 conditions, hydroperoxy species are generated from H_2 and O_2 gases which later interact with methyl species to form methyl hydroperoxide. As described in section 5.4.2, the methyl hydroperoxide intermediate is an unstable product and would transform either selectively to methanol or directly to carbon dioxide. Therefore, it was believed here that the alterations of the actives site are probably responsible for the unselective transformation of methyl hydroperoxide to CO_2, consequently decreasing the methanol and oxygenates selectivity observed in the presence of the used catalyst for the *in-situ* H_2O_2 approach. It is important to note here that the

catalytic activity of used catalyst is almost identical compared to H_2O_2-pretreated catalyst under similar reaction conditions. In both cases, palladium in the metallic state was observed.

It was evident from the experiment that reusability of the catalyst is strongly affected by the changes in the morphology of the catalyst. In parallel to role of the oxidant, the hydrogen peroxide concurrently reduced the palladium oxide into metallic palladium.

In order to verify the reusability pattern of 5wt%Au-Pd/TiO_{2IW} for another substrate *i.e.* ethane, the analogue experiments were carried out on the same batch of catalyst. The data obtained (figure 5.4) confirmed that a similar trend was observed to that of methane oxidation, where the oxygenate productivity reduced with used catalyst.

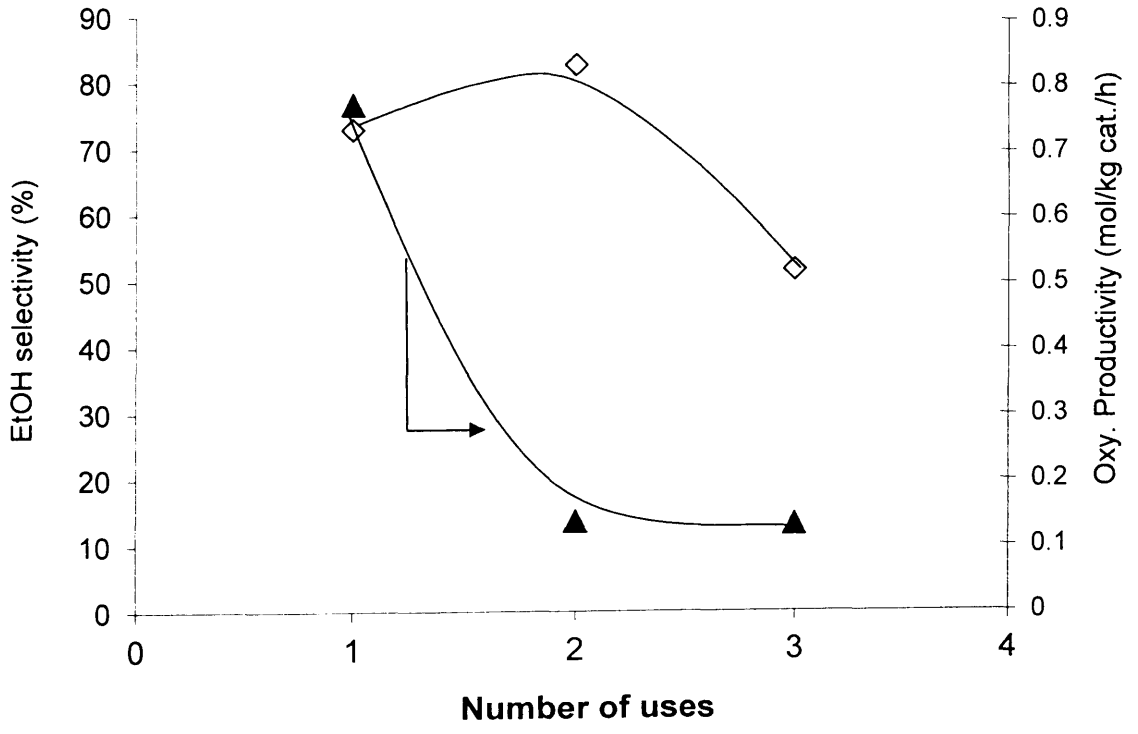

Figure 5.4: Plot of oxygenates productivity and selectivity to ethanol as function of number of catalyst used in ethane oxidation reaction with addition of H_2O_2. Key: ▲ oxygenates productivity, ◊ ethanol selectivity. Conditions: Time=0.5 hours, $P(C_2H_6)$=30 bar, $[H_2O_2]$=0.5M, T=50 °C, 1500 rpm, catalyst mass = 28 mg.

5.4. Mechanistic studies

5.4.1. Introduction

This section describes the possible reaction pathways and mechanistic aspects involved during the oxidation of methane using H_2O_2 as oxidant in the presence of 5wt%Au-Pd/TiO_{2IW} catalyst. Figure 5.5 shows the reaction pathways involved in methane/H_2O_2 mixtures reported by Olivera and co-workers, and is followed by a detailed mechanism based either on the reaction through methyl hydroperoxide as intermediate species (Scheme 1) or through other routes (Scheme 2).[33]

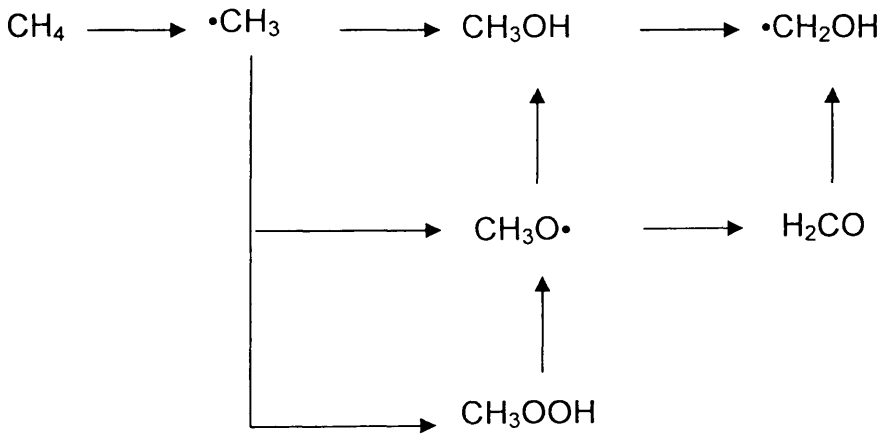

Figure 5.5: Reaction pathways involved in methane/hydrogen peroxide mixtures[33]

Scheme 1:

If the mechanism is via methyl hydroperoxide, the possible reaction pathways are presented below:

(1) $H_2O_2 \rightarrow \bullet OH + \bullet OH$

$H_2O_2 \rightarrow \bullet OOH + H$

$H_2O_2 \rightarrow 1/2O_2 + H_2O$

(2) $CH_4 + \bullet OOH \rightarrow \bullet CH_3 + H_2O_2$

$\bullet CH_3 + \bullet OOH \rightarrow CH_3OOH$

$CH_3OO\bullet + CH_4 \rightarrow CH_3OOH + \bullet CH_3$

$CH_3O\bullet + \bullet OH \rightarrow CH_3OOH$

(3) $CH_3OOH \rightarrow CH_3O\bullet + \bullet OH$

$CH_3OOH \rightarrow \bullet CH_3 + \bullet OOH$

$CH_3OOH \rightarrow CH_3OO\bullet + H$

$CH_3OOH + \bullet OH \rightarrow CH_3OO\bullet + H_2O$

$CH_3OOH + \bullet OH \rightarrow CH_3O\bullet + H_2O_2$

(4) $CH_3O\bullet + CH_4 \rightarrow CH_3OH + \bullet CH_3$

$CH_3O\bullet + \bullet OOH \rightarrow CH_3OH + O_2$

$CH_3O\bullet + H_2O_2 \rightarrow CH_3OH + \bullet OOH$

$\bullet CH_3 + \bullet OH \rightarrow CH_3OH$

Scheme 2:

If the mechanism is not via methyl hydroperoxide, the possible reaction pathways are presented below:

$H_2O_2 \rightarrow \bullet OH + \bullet OH$, or $H_2O_2 \rightarrow \bullet OOH + H$, or $H_2O_2 \rightarrow 1/2O_2 + H_2O$

$CH_4 + \bullet OH \rightarrow \bullet CH_3 + H_2O$

$\bullet OH + \bullet CH_3 \rightarrow CH_3OH$ [this pathway favour on Au]

If OH radical still available/excess:

$CH_3OH + \bullet OH \rightarrow CH_3O\bullet + H_2O$ or

$CH_3OH + \bullet OH \rightarrow \bullet CH_2OH + H_2O$ [favour pathway]

$\bullet CH_2OH + CH_4 \rightarrow CH_3OH + CH_3$

If OH radical still available/excess:

$\bullet CH_2OH + \bullet OH \rightarrow HCHO + H_2O$, from HCHO it can proceed to give carbon oxide

It seems the formation of oxygenated products from the oxidation of methane with H_2O_2 can proceed via different pathways, as indicated above. Therefore in order to confirm the species available in the reaction solution, Electron Paramagnetic Resonance (EPR) analysis was carried out and is described in section 5.4.4. In all cases, Au based supported catalysts produced only methanol, methyl hydroperoxide and carbon dioxide as products. No formation of formaldehyde, formic acid or methyl formate was observed even at longer reaction times. In order to confirm that all the products originated from methane, a reaction was carried with labelled methane ($^{13}CH_4$), and analysis of the reaction solution after reaction with ^{1}H-NMR showed the presence of $^{13}CH_3OOH$ and $^{13}CH_3OH$.

Time online studies indicate that methyl hydroperoxide, CH_3OOH, is the primary product, and that it gradually transforms to methanol in the presence of the catalyst. This profile was observed in both cases, either with the addition of H_2O_2 or by an *in-situ* generation of

H_2O_2 (see figure 4.2 and 5.1). This is in agreement with the scheme proposed (scheme 1) above, where the reactions proceed via methyl hydroperoxide which is later selectively transformed to methanol. In order to corroborate the mechanism that proceeds through methyl hydroperoxide route, further study on the transformation of the methyl hydroperoxide intermediate species in the presence of 5wt%Au-Pd/TiO_{2IW} has been carried out, and is briefly discussed in the following section.

5.4.2. Stability of methyl hydroperoxide in the presence of 5wt%Au-Pd/TiO_{2IW} catalyst

Since methyl hydroperoxide is not commercially available, and also due to the fact that the standard methyl hydroperoxide synthesis procedure reported in the literature is rather complex (involving Me_2SO_4 and H_2O_2)[34] an alternative route was undertaken in this study by synthesizing methyl hydroperoxide (CH_3OOH) under the standard reaction conditions for methane oxidation with the addition of H_2O_2, but in the presence of copper oxide catalyst. CH_3OOH was the major product of this reaction, though minor amounts of CH_3OH and CO_2 were also detected. The presence of methyl hydroperoxide was confirmed by ^{1}H-NMR, which showed a similar chemical shift (3.9 ppm) as reported in the literature.[35] To further confirm the presence of methyl hydroperoxide, reduction with sodium borohydride ($NaBH_4$) was carried out and the only product produced was methanol (table 5.15) in agreement with the studies reported by Shulpin *et al.*[35] The slightly lower amount of reduced product (CH_3OH) observed after reduction with sodium borohydride was within the instrumental and analysis error limits. It was noted here that the analysis was carried out using 250 MHz NMR machine where the signal to noise ratio was poorer compared to standard analysis using a 500 MHz NMR machine. Moreover, a similar test on ethyl hydroperoxide showed 100% product mass balance before and after reduction with sodium hydroperoxide. However, any possible formation of other compounds such as CO_2 could not be excluded at this stage.

Table 5.15: Reduction of methyl hydroperoxide (CH_3OOH) with sodium borohydride, ($NaBH_4$)

Entry	Solution	Initial (μmol)	After (μmol)		
		CH_3OOH	CH_3OH[a]	HCOOH [a]	MeOOH[a]
1	Before	17	0	0	0
2*	After	0	15	0	0

*Analysis 15 min after addition of $NaBH_4$ (2:1mol ratio of NaBH4 to oxygenates) [a] Analysis using ^{1}H-NMR (250MHz)

Since the procedure to synthesise and verify the presence of methyl hydroperoxide has been established, all studies requiring methyl hydroperoxide followed this procedure.

Methyl hydroperoxide is relatively stable at temperatures below 5 °C for up to 3 days. At room temperature (and in the presence of light), it slowly transformed to CO_2. In the presence of 30 bar CH_4, a CH_3OOH/H_2O_2 solution at room temperature did not give any increment in the total amount of product, and only slight changes of product distribution were observed. Less than 10% of CH_3OOH converted to CH_3OH and CO_2 (mostly CH_3OH). The total number of moles of products observed before and after reaction is shown in table 5.16.

Table 5.16: Reaction of methyl hydroperoxide (CH_3OOH) in the presence of H_2O_2 and CH_4 at room temperature without presence of catalyst

Entry	Time (min)	Solution	Products (μmol)			Total product
			CH_3OH	CH_3OOH[a]	CO_2[b]	(μmol)
1	5	Initial	1.28	20.24	-	21.52
		After	2.73	18.4	0.3	21.43
2	20	Initial	1.34	19.73	-	21.07
		After	1.73	18.88	0.57	21.18

CH_4 pressure: 30 bar, $[H_2O_2]$= 0.5M, Stirring rate: 1500rpm, Reaction temperature: room temperature, [a] Analysis using ^{1}H-NMR, [b] Analysis using GC-FID

However, a reaction at 50 °C showed an increment in the amount of products (mainly CH_3OOH) of 42% within 5 minutes reaction time. The reaction was repeated three times, and the results were similar within experimental error as illustrated in table 5.17.

Table 5.17: Reproducibility tests on reaction of methyl hydroperoxide (CH_3OOH) in the presence of H_2O_2 and CH_4 at 50 °C without presence of catalyst

Entry	Time (min)		Products (μmol)			Total product (μmol)	Increment (%)
			CH_3OH	CH_3OOH[a]	CO_2 in gas[b]		
1	5	Initial	1.11	18.4	-	19.51	42
		After	0.83	29.3	3.60	33.73	
2[c]	5	Initial	1.26	21.93	-	23.19	36
		After	0.77	32.41	3.07	36.25	
3[d]	5	Initial	1.05	21.41	-	22.46	43
		After	0.73	33.81	5.28	39.82	

CH_4 pressure: 30 bar. $[H_2O_2]$= 0.5M, Stirring rate: 1500rpm, Reaction temperature: 50 °C, Reaction time: 5 min, [a] Analysis using ^{1}H-NMR (500MHz), [b] Analysis using GC-FID. [c]Reaction in similar reactor, [d] Reaction in different reactor

The analogue reaction also has been performed in the presence of labelled methane ($^{13}CH_4$) and $^{12}CH_4$. $^{13}CH_3OOH$ was detected after 20 minutes reaction time and the ratio of CH_3OOH produced from $^{13}CH_3OOH$ and $^{12}CH_3OOH$ is similar to the ratio of $^{13}CH_4/^{12}CH_4$ used initially. No formic acid was observed in all cases (table 5.18).

In contrast, analogue reaction in the presence of Helium instead of CH_4 showed the transformation of CH_3OOH to CO_2 with no CH_3OOH detected after reaction. It is important to notice here that a standard uncatalysed 'blank' reaction of $H_2O_2/H_2O/CH_4$ at a similar reaction temperature and time did not produce any oxygenates products.

Table 5.18: Reaction of methyl hydroperoxide (CH_3OOH) in the presence of H_2O_2 and mixture of $^{12}CH_4$ and labelled methane ($^{13}CH_4$) at 50 °C without presence of catalyst

Entry	Gas		Products (μmol)				Total (μmol)	Increment (%)
			CH_3OH [a]	CH_3OOH [a]	HCOOH [a]	CO_2 in gas[b]		
1	$^{12}CH_4$ (30 bar)	Initial	0.78	13.19	0	-	13.97	
	$^{12}CH_4$ (30 bar)	After	1.03	28.26	0	8.06	37.35	62
2	$^{12}CH_4$ (30 bar)	Initial	0.62	14.77	0	-	15.39	
	$^{12}CH_4$ (24 bar) + $^{13}CH_4$ (6 bar)	After	0.77	33.47 ($^{12}CH_3OOH$) & 4.67 ($^{13}CH_3OOH$)	0	5.85	44.76	65

CH_4 pressure: 30 bar, $[H_2O_2]$= 0.5M, stirring rate: 1500rpm, Reaction temperature: 50°C, Reaction time: 20 min, [a] Analysis using ^{1}H-NMR, [b] Analysis using GC-FID.

In order to verify the origin of the activity observed during the reaction of the solution containing methyl hydroperoxide in the presence of methane and hydrogen peroxide at 50 °C did not occur from possible copper species available in the reaction media, an analysis of fresh solution before reaction was subjected to elemental analysis using atomic absorption spectroscopy (AAS). The results showed that less than 4 part per million (ppm) of copper leached during the pre-synthesis of methyl hydroperoxide. Therefore, the following experiments were performed in order to find out whether Cu homogeneous available in the solution could give the high level of CH_3OOH produced within 5 minutes reaction time (42% increment of product). The experiments were carried out with two different concentrations of Cu (~4 and ~11 ppm of copper chloride, a similar precursor to those used in the preparation of copper oxide). In this range of concentration, the amount of oxygenate products was much lower (~2 μmol) (see appendix B (3)) compared to the amount of products produced in the analogue reaction of $CH_3OOH/CH_4/H_2O_2$. To support this observation, an additional reaction of $CH_3OOH/CH_4/H_2O_2$ was carried out using a solution containing methyl hydroperoxide synthesised through reaction of CH_4 and H_2O_2 at higher temperature (>90 °C). The possible presences of any metals such as Fe, Cu, Au and Pd in the solution were verified by subjecting the solution into AAS analysis. The AAS analyses confirm that no metal was detected within the detection limit of the instrument (<

1 ppm). This therefore supports the argument that at the level of copper present in solution, Cu was not responsible for the propagation of methyl hydroperoxide.

From the observations discussed above, in order to have propagation of CH_3OOH, the presence of CH_4 and H_2O_2 at elevated temperatures is necessary. It seems that the experimental data are in an agreement with the mechanism mentioned in scheme 1. In this stability study, hydrogen peroxide was induced by heat to produce hydroxyl (•OH) and hydroperoxyl (•OOH) radicals into the reaction system. It was claimed in the studies by Olivera *et al.* that both hydroxyl and hydroperoxyl radicals were capable of abstracting a hydrogen atom from solubilised CH_4 and CH_3OOH to generate methyl ($•CH_3$) and methyl peroxide radical ($CH_3OO•$) respectively.[33] In addition to this, other radicals species such as $CH_3O•$ and •OOH could possibly originate from the cleavage of CH_3OOH and H_2O_2. The availability of the aforementioned radical species during the reaction exposed the possibility to produce the methyl hydroperoxide through different reactions as listed in scheme 1. In most cases, the turnover formation of CH_3OOH was believed to involve hydroxyl radicals. To support this statement, the reaction of $CH_3OOH/H_2O_2/CH_4$ with the presence of hydroxyl (•OH) radical scavenger (sodium sulfite (Na_2SO_3)) was carried out and the results clearly showed that the turnover effect of methyl hydroperoxide has been observed. (See appendix B (4)).

In addition, it is crucial to find out whether other alkyl hydroperoxides have similar behaviour to that observed with methyl hydroperoxide. Therefore, ethyl hydroperoxide (CH_3CH_2OOH) was synthesised in a similar manner to that mentioned above, and the obtained ethyl hydroperoxide was later subjected to a reduction procedure with sodium borohydride ($NaBH_4$). The reduction of ethyl hydroperoxide produced only ethanol. The reaction of CH_3CH_2OOH in the presence of C_2H_6 and H_2O_2 at 50 °C was carried out and the result showed a similar outcome as that observed with the CH_3OOH counterpart (see table 5.19).

Table 5.19: Reaction of CH_3CH_2OOH in the presence of H_2O_2 and C_2H_6 at 50 °C without presence of catalyst

Entry		Product amount (μmol)							Total (μmol)	Increment (%)
		EtOH [a]	CH_3COOH [a]	EtOOH [a]	MeOH [a]	CH_3CHO hydrated	CH_3CHO, hydrated	CO/ CO_2 in gas [b]		
1	Initial	<0.44	0	21.77	0.33	0.90	13.91	-	37.35	
2	After	<0.44	0.44	44.70	0.37	0.94	18.60	2.14	67.63	44%

C_2H_4 pressure=30 bar. [H_2O_2]= 0.5M, stirring rate: 1500rpm, Reaction temperature: 50 °C, Reaction time: 5 min, [a] Analysis using ^{1}H-NMR, [b] Analysis using GC-FID.

As previously discussed, reaction of $CH_3OOH + CH_4 + H_2O_2$ at 50 °C produced ~ 53% increment of the CH_3OOH within 20 minutes, whereas the amount of CH_3OH remained the same. Only in the presence of catalyst *i.e.* 5wt%Au-Pd/TiO_{2IW} catalyst was the selective transformation of CH_3OOH to CH_3OH observed, and it was proven by the labelled $^{13}CH_3OOH$ experiment as shown in following paragraph. Therefore, the presence of 5wt%Au-Pd/TiO_{2IW} is necessary for the transformation of the intermediate (methyl hydroperoxide) to methanol.

To verify the formation of methanol from methyl hydroperoxide the following experiments were carried out. In the first step, $^{13}CH_4$ was used for synthesising labelled $^{13}CH_3OOH$. Satellite peaks at 4.05 and 3.75 ppm correspond to $^{13}CH_3OOH$, whilst no peak observed at chemical shift that match up with $^{13}CH_3OH$, *i.e.* 3.53 and 3.23 ppm (figure 5.6). In the second step, the solution containing $^{13}CH_3OOH$ was subjected to a standard methane oxidation reaction in the presence of 5wt%Au-Pd/TiO_{2IW}. In this reaction, $^{12}CH_4$ was used instead of $^{13}CH_4$. It is clear from figure 5.7 that ^{1}H-NMR analysis of the products after reaction showed the presence of $^{13}CH_3OH$ and $^{12}CH_3OH$. In view of the fact that only $^{12}CH_4$ was used in the second step, it was confirmed that $^{13}CH_3OH$ was formed from $^{13}CH_3OOH$.

In order to justify the effect of the catalyst in selective transformation of methyl hydroperoxide, an analogue experiment was carried out in the absence of catalyst, and it was evident that labelled methanol ($^{13}CH_3OH$) was not detected after reaction. Therefore the data indicate that the presence of 5wt%Au-Pd/TiO_{2IW} is necessary for the transformation of the intermediate (methyl hydroperoxide) to methanol. It was reported by Suss-Fink *et al.* that at a reaction temperature around 40 °C and in the absence of catalyst, the methyl hydroperoxide gradually transforms to produce formaldehyde and then formic acid, but no methanol.[36] At the same range of temperature, methanol was only observed if the catalyst was present in the reactor vessel.

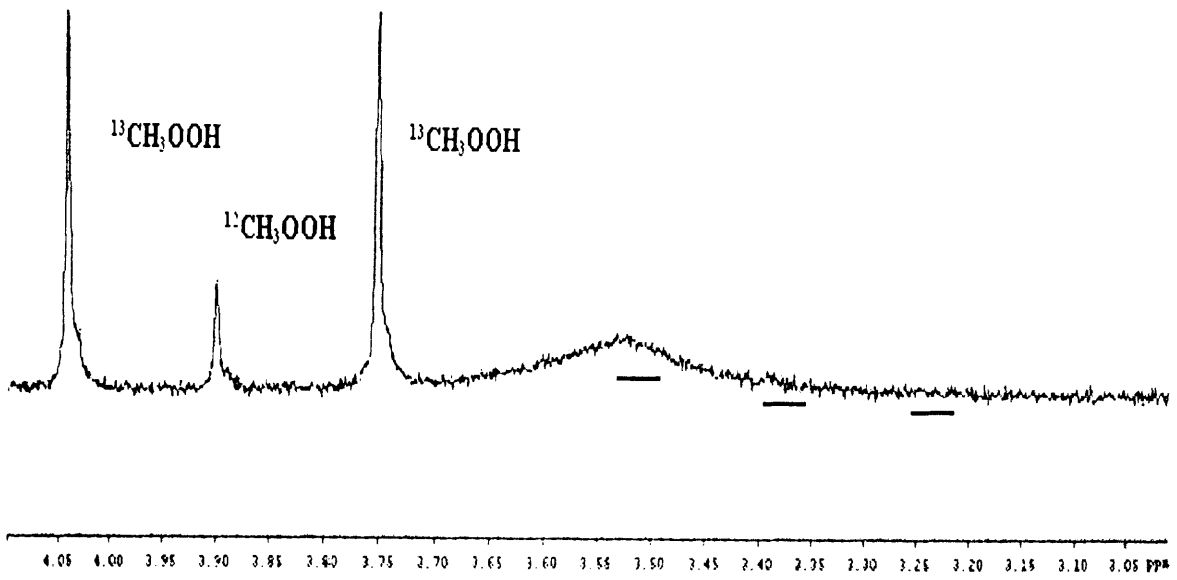

Figure 5.6: ^{1}H-NMR spectrum of solution containing $^{13}CH_3OOH$

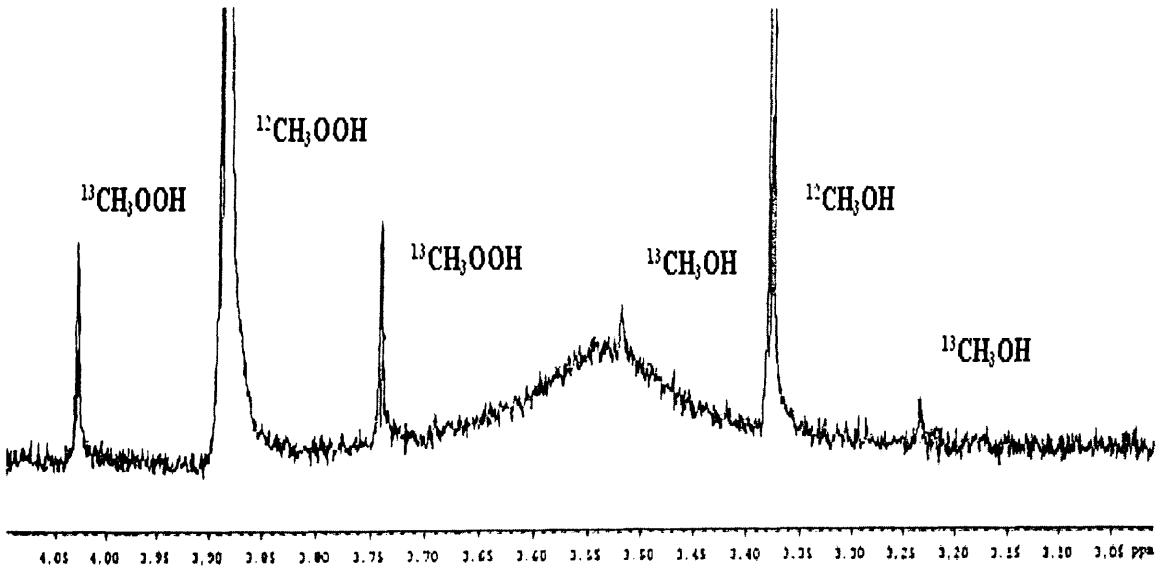

Figure 5.7: ^{1}H-NMR spectrum of solution after reaction in the presence of 5wt%Au-Pd/TiO_{2IW}. Conditions $P(CH_4)$=30 bar, $[H_2O_2]$=0.5M, T=50°C, Reaction time=30 min, Stirring rate: 1500 rpm, catalyst mass = 28 mg

5.4.3. Stability of the products

As part of elucidating the reaction pathways, stability studies on each product were carried out by using similar reaction conditions in the presence of selected catalysts. Instead of the alkane, inert gas was used, typically either He or N_2. All other parameters were kept constant. As described in section 2.6, the concentration of the products was compared before and after reaction and normally the products loss were presented as percentage losses. The products analyses were carried out both in ^{1}H-NMR for liquid and GC-FID for gases product. Therefore, the transformation pathway of the product could be traced. In some cases, labelled compounds were used. Methanol stability was performed first. If the reaction follows a standard consecutive oxidation pathway, methanol should oxidise through formaldehyde and later formic acid and finally fully combusted products (CO_x). In this study, within 30 min reaction time, consecutive oxidation of methanol could be observed due to the formation of formic acid and carbon dioxide. However, the formation of formaldehyde was not detected in any ^{1}H-NMR spectrum. The total amount of methanol converted was calculated to be around 29%, with CO_x species as the major product (80%). Formic acid was only observed as the minor product (20%) (table 5.20).

Table 5.20: Liquid phase reaction of methanol, formaldehyde and formic acid in water at 50 °C with 5wt%Au-Pd/TiO_{2IW} catalyst in the presence of H_2O_2 and helium

Entry	Substrate	Product distribution (%)				Substrate
		MeOH [a]	HCOOH [a]	HCHO, HCHO hydrated [a]	CO_x in gas[b]	Converted (%)
1	Methanol	-	12	0	80	29
2	Formaldehyde	0	9.0	-	91	81
3	Formic acid	5	-	0	67	72

Reaction Temp; 50 °C, He pressure: 30 bar, Catalyst: 27.6 mg (1.0 x 10^{-5} mol of metal), [H_2O_2]:0.5M, Solvent: H_2O, 10 mL. [a] Analysis using ^{1}H-NMR, [b] Analysis using GC-FID

Thus, further stability study with formic acid solution was carried out at similar reaction conditions and the results demonstrated that only 28% of formic acid remained after 30 minutes of reaction. In this case, only CO_2 was observed as a product, which confirmed the tendency of formic acid to over oxidise in the presence of 5wt%Au-Pd/TiO_{2IW} catalyst

and hydrogen peroxide at elevated temperature. The absence of formaldehyde as a consecutive product of methanol was proved by the higher oxidation rate of formaldehyde as more than 81% formaldehyde was converted after 30 minutes reaction. Formic acid product was only observed as a minor compound whereas the formaldehyde has higher tendency to form hydrated species. The stability studies are in line with the catalytic data observed for methane oxidation with hydrogen peroxide as oxidant, especially with time online reaction profile.

5.4.4. Identification of radical species available using Electron Paramagnetic Resonance (EPR)

EPR analysis has been used to identify the radical species available in the reaction solution. In this experiment, 5,5-dimethyl-pyrroline N-oxide (DMPO) was used as a radical trap and it was added as co-reactant in the standard methane reaction in the presence of 5wt%Au-Pd/TiO_{2IW} catalyst and hydrogen peroxide. The experiment was carried out for 5 minutes reaction time before the liquid solution was collected and kept in a glass tube, which was later transferred into liquid nitrogen. As illustrated in figure 5.8, two different adducts of DMPO were observed corresponding to methyl ($\bullet CH_3$ (DMPO-CH_3)) and hydroxyl radicals ($\bullet$OH (DMPO-OH)) species.

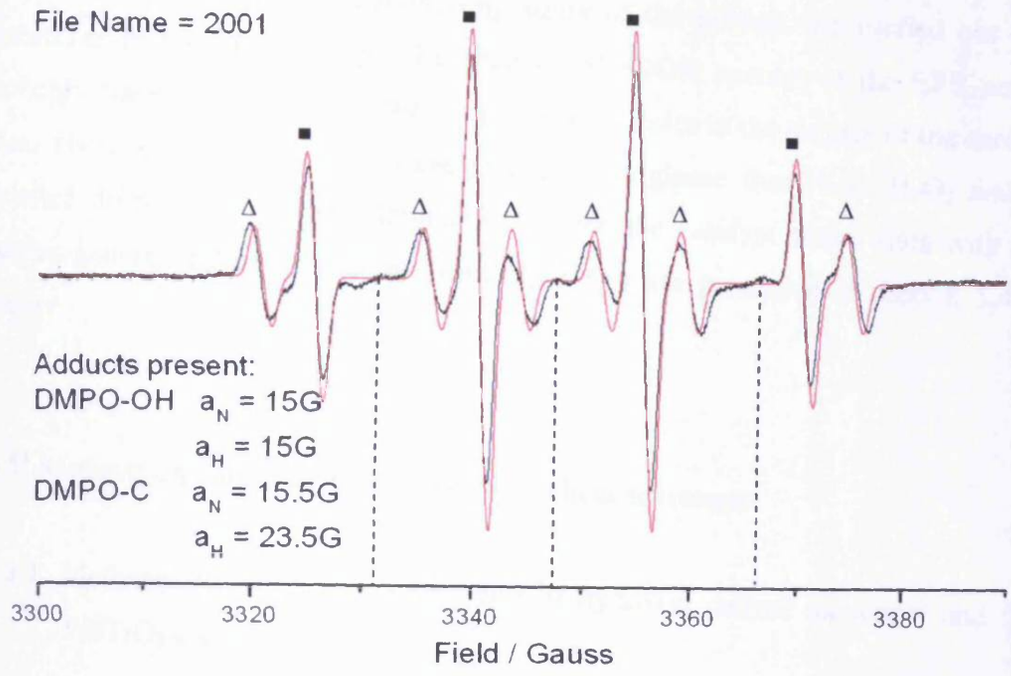

Figure 5.8: Electron paramagnetic resonance (EPR) spectrum of standard methane oxidation using 5wt%Au-Pd/TiO_{2IW} catalyst in the presence of DMPO as radical trap. Key: Black line: Experimental signal, Red line: Combined simulated signal for both •OH and •CH_3 adducts, (■) DMPO-OH adduct, (Δ) DMPO-CH_3 adduct, (---) Line referred decomposition of DMPO

Even though EPR is very sensitive analytical method with detectability levels approaching nanomolar concentration, the presence of other possible species such as •OOH and O_2^- cannot be excluded due to several factors relating to the experimental and analytical procedure, such as the time taken to sample the solution from the reactor. In this experiment, it takes around 1 minute between finishing the reaction and sampling the reaction solution by freezing with liquid nitrogen. It is known that the life time of radical reactions are very low, and for examples in case of •OH radical, the life time is 10^{-9} second.[37] Additionally, the possible decomposition of the radical adduct(s) could also happen before completing the EPR analysis, as shown by the minor peaks denoted by dashed line in figure 5.8. The information from EPR analysis was later corroborated with experimental evidence obtained using radical scavengers as well as from theoretical

modelling study. Theoretical modelling study of the system was carried out by another researcher in the same group. The absence of •OOH species in the EPR analysis was probably due to the bonding of the hydroperoxy species to the surface of the catalyst active sites. Hydroxyl (•OH) radical were shown to originate from both H_2O_2 and H_2O.[21,22] Detailed discussions on the interaction between the catalyst active sites with the active species generated from H_2O_2 (or from H_2 + O_2) are presented in section 5.4.6 of this chapter.

5.4.5. Methane oxidation in the presence of radical scavenger

5.4.5.1. Methane oxidation in the presence of hydroxyl radical scavenger and 5wt%Au-Pd/TiO_{2IW} catalyst

Since the EPR analysis showed the presence of radical species (•OH, •CH_3) in the reaction solution, attempts have been made to perform the standard methane reaction in the presence of radical scavengers. For an initial test, sodium sulfite (Na_2SO_3) was selected as •OH radical scavenger[38] and the results are illustrated in figure 5.9. In all cases, the total amount of products produced was almost at the same level; however it was clear that by increasing the amount of sodium sulphite in the reaction, the selectivity to methanol decreased whereas the selectivity to methyl hydroperoxide increased. The difference in methanol selectivity in the presence of •OH radical scavenger could be attributed to the blockage of the catalyst active sites responsible for selectively transforming methyl hydroperoxide to methanol. The presence of sodium sulfite also affected the active sites responsible for the decomposition of H_2O_2 where the amount of H_2O_2 left after reaction was increased upon increasing the concentration of Na_2SO_3.

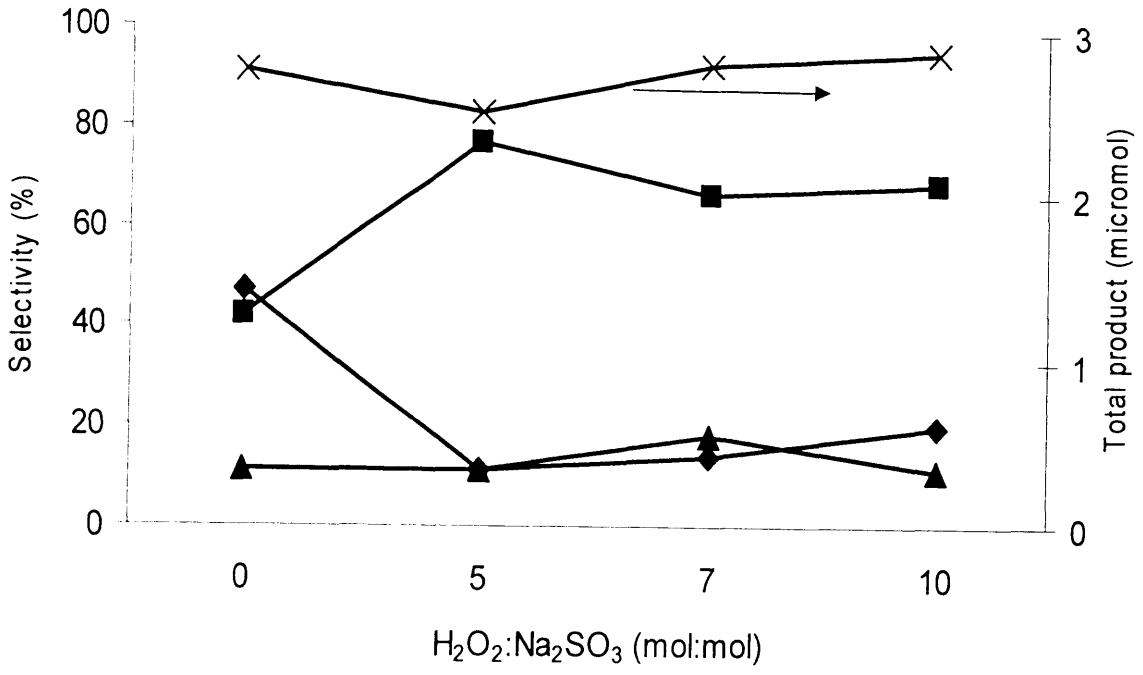

Figure 5.9: Effect of different H_2O_2 to scavenger ratio. Reaction condition: Time: 30 min, P(CH_4): 30 bar, [H_2O_2]: 0.5M, Temp: 50 °C, Catalyst mass: 27.6 mg, Scavenger: Sodium sulfite (Na_2SO_3). Key: ■ methyl hydroperoxide selectivity, ♦ methanol selectivity, ▲ carbon dioxide selectivity, and **X** total product.

5.4.5.2 Methane oxidation in the presence of carbon center/hydroperoxyl radical scavenger and 5wt%Au-Pd/TiO_{2IW} catalyst

In another set of experiments the effect of a carbon center/hydroperoxyl radical scavenger was studied. Sodium nitrite ($NaNO_2$) was used as radical scavenger. Based on the literature,[39] sodium nitrite is responsible to scavenge the carbon centre radicals while in another report is claimed that nitrite could work as $\cdot OOH/O_2^-$ scavenger.[38] In the first attempt, a series of reactions have been carried out by varying the oxidant to scavenger molar ratio as shown in table 5.21. The catalytic activity was completely shut off with the presence of high concentration of $NaNO_2$ whereas with low concentrations of $NaNO_2$ (where the H_2O_2 to $NaNO_2$ ratio equalled 200:1), 3 times less oxygenated product was observed compared to standard reaction conditions. Theoretically in this particular ratio (200:1), the amount of $NaNO_2$ present in the solution is 25 μmol which is almost 7 times higher than the total mol of oxygenates produced at standard reaction. It seems the oxidation could still proceed with lower amounts of scavenger.

Table 5.21: Standard methane oxidation with 5wt%Au-Pd/TiO_{2IW} in the presence sodium nitrite ($NaNO_2$) radical scavenger and H_2O_2 as oxidant

Entry	H_2O_2:$NaNO_2$ ratio	Product amount (μmol)				Total product (μmol)	H_2O_2 Remain (μmol)[c]
		CH_3OH [a]	HCOOH [a]	CH_3OOH [a]	CO_2 in gas[b]		
1	-	1.89	0	1.57	0.37	3.83	383
2	10:1	0	0	0	*<0.3	<0.3	518
3	20:1	0	0	0	*<0.3	<0.3	271
4	200:1	0.44	0	0.59	<0.1	1.13	1383

Reaction time: 30 min, Reaction temperature: 50 °C, CH_4 pressure: =30 bar, [H_2O_2]= 0.5M, stirring rate: 1500rpm, Catalyst: 1.0 x 10^{-5} mol of metals (27.6 mg) [a] Analysis using ^{1}H-NMR, [b] Analysis using GC-FID, [c] Assayed by Ce^{+4} (aq) titration, *Analysis using GC-TCD

Given the fact that the experiment could not give any clear indication regarding which of the species (methyl or hydroperoxyl) has been scavenged by $NaNO_2$, another step has been taken to perform the analogue reaction in *in-situ* generated H_2O_2. The reaction used two different concentration of $NaNO_2$; the calculation is based on the maximum H_2O_2 that could be produced with the presence of specific partial pressure of H_2 and O_2 gases. As shown in table 5.22, a similar observation to the reaction with addition of hydrogen peroxide was observed. High amounts of $NaNO_2$ completely switched-off the oxidation reaction, with no traces of oxygenates being observed in 30 minutes reaction time. Lowering the amount of scavenger to theoretically 25 μmol in 10 mL reaction solution produced a trace of methanol. The ability of the catalyst to synthesise hydrogen peroxide was not affected by the presence of radical scavenger where there was still an amount of hydrogen peroxide detected after reaction. Indeed, it was increased by increasing the amount of $NaNO_2$. It was reported in the literature that formation of hydrogen peroxide through H_2/O_2 gases on Au-Pd based catalyst proceeds via surface hydroperoxyl species. Therefore these results indicate that only methyl radical were terminated by nitrite species and the hydroperoxyl species were not affected.

Table 5.22: Standard methane oxidation with 5wt%Au-Pd/TiO_{2IW} in the presence of sodium nitrite ($NaNO_2$) radical scavenger and *in-situ* formation H_2O_2 as oxidant

Entry	Oxidant:$NaNO_2$ ratio	Product amount (μmol)				Total product (μmol)	H_2O_2 Remain (μmol)[c]
		CH_3OH [a]	HCOOH [a]	CH_3OOH [a]	CO_2 in gas[b]		
1	-	1.31	0	0.29	0.32	1.92	56
2	2:1	0	0	0	<0.3	<0.3	236
3	20:1	<0.1	0	0	<0.3	<0.4	80

Reaction temperature: 50 °C, CH_4 pressure: 30 bar, stirring rate: 1500rpm, Reaction time: 30 min, [a] Analysis using ^{1}H-NMR, [b] Analysis using GC-FID, [c] Assayed by Ce^{+4} (aq) titration,
Gases: 0.86% H_2/1.72%O_2/75.86%CH_4/21.55%N_2, (Total pressure: 32 bar)

A parallel modelling study proposed that hydroperoxyl species are bonded to the surface, but that surface methyl species should be desorbed, thereby producing methyl radicals in order to generate methyl hydroperoxide. Moreover, the experimental and theoretical data were supported by the EPR analysis shown in section 5.5.4 which indicates the presence of •OH and •CH_3 radical. Hydroperoxyl radicals (•OOH) were not detected probably due to formation of surface bonded hydroperoxyl species.[22]

5.4.6 General proposal on mechanistic pathways on methane oxidation using Au-Pd based supported nanoparticles catalyst and H_2O_2 as oxidant.

From the catalytic data mentioned above and together with theoretical modelling study,[22] it can be proposed that the reaction mechanism involved depends on the specific morphology, oxidation state and particle size of Au-Pd supported nanoparticles catalysts. Based on these catalyst properties, the types of Au-Pd catalysts used in this study could be divided into two. The first type consist of catalysts having Au core-Pd shell structures with average particle sizes bigger than 20 nm and the outer layer of the metal particles consisting of Pd in an oxidised phase (Pd^{2+}). An example of this type of catalyst was 5wt%Au-Pd/TiO_{2IW} catalyst calcined in static air. On the other hand, the second type of Au-Pd catalysts consist smaller particle size (< 15 nm) with the presence of Pd in metallic

state. Au-Pd catalysts synthesised via sol-immobilisation method or catalysts whose undergo reduction process were included in this group.

The former types of catalysts were shown to have better activity toward oxygenates formation and it strongly related to the presence of PdO phase. As it was shown in parallel theoretical studies on methane oxidation using hydrogen peroxide as oxidant and Au-Pd catalyst, the methane activation and the formation of hydroperoxy species was favoured on PdO phase rather than Pd in metallic state.[22] Pd and Au in metallic state could simultaneously cleave the hydrogen peroxide into hydroxyl species.[21,24] Therefore, different reaction pathways could evolve and it could explain the different product distribution observed between both types of catalysts.

It was plausible to suggest from combined catalytic reaction data with radical scavenger studies that in the presence of 5wt%Au-Pd/TiO_{2IW} catalyst calcined in static air, methane and H_2O_2 were probably activated on the catalyst surface. Both methyl and hydroperoxyl species were coordinated on the surface active site. The formation of another surface bonded species such as hydroxyl and proton were also possible. The hydrogen itself could originate from H_2O, H_2O_2 and CH_4 molecules available during reaction. Formations of methyl hydroperoxide as primary intermediate product was suggested to occur between the reactions of methyl species with surface bonded hydroperoxyl. Methyl hydroperoxide was confirmed as primary product by several means. Selective formation of methanol is believed to proceed via surface reaction. This statement is based on catalytic data observed in the reaction of methyl hydroperoxide with the presence of 5wt%Au-Pd/TiO_{2IW} calcined catalyst (see section 5.4.2). Selective formation of methanol possibly involves hydrogen transfer of surface methoxy (CH_3O) species. Summary of the possible steps of methane oxidation with hydrogen peroxide as oxidant and 5wt%Au-Pd/TiO_{2IW} calcined catalyst is shown below:

1. Adsorption of CH_4 and H_2O_2 onto catalyst surface
2. Dissociation or hydrogen abstraction from H_2O_2

   $H_2O_2 + M \rightarrow M\text{-}OOH + M\text{-}H$, (surface reaction),

   where M is catalyst active site and the reaction was favoured on PdO phase.
3. Interaction of/with CH_4 (step 2 and 3 occurred in parallel)

   Reaction with preadsorp CH_4, $M\text{-}CH_3$

   $M\text{-}CH_3 + M\text{-}OOH \rightarrow M\text{-}CH_3OOH$

   Or $\bullet CH_3 + M\text{-}OOH \rightarrow M\text{-}CH_3OOH$ (favour pathway)

4. Formation of CH_3OOH,

   Desorption from M-CH_3OOH, M-CH_3OOH → M* + CH_3OOH

5. Formation of CH_3OH,

   M + CH_3OOH → M-CH_3OOH

   M-CH_3OOH → M-CH_3O + M-OH

   M-CH_3O + M-H → M-CH_3OH (hydrogen transfer, M-H could be originated from H_2O_2, CH_4, H_2O)

Figure 5.10 illustrates a potential reaction scheme for the oxidation of methane with addition of hydrogen peroxide or with in-situ generated H_2O_2 from H_2/O_2 in the presence of 5wt%Au-Pd/TiO_{2IW} catalyst. Methanol is formed via a methyl hydroperoxide intermediate as major route, and over oxidises to formic acid (very unlikely in current condition) and CO_2 at longer reaction times. CO_2 may also be formed directly from methyl hydroperoxide and methanol.

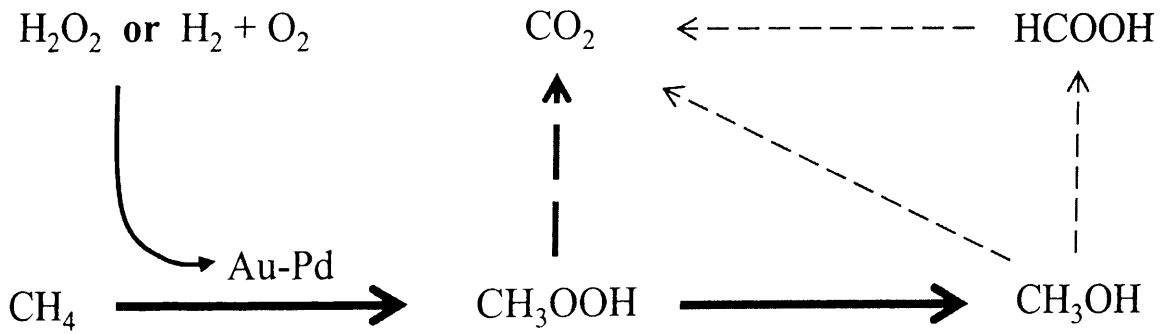

Figure 5.10: Possible reactions involved in methane oxidation using H_2O_2 as oxidant either added as co-reactant or by *in-situ* generation with Au-Pd based supported nanoparticles catalyst

In addition to the proposed mechanistic pathways discussed above, other possible pathways could be suggested for the methane oxidation reaction involving Au-Pd catalyst

having small particle sizes and metallic Pd. These types of catalysts have a higher tendency to cleavage the hydrogen peroxide into hydroxyl species over hydroperoxyl species and protons. Therefore, hydroxyl species might have a chance to interact with methyl species and directly produce methanol without undergoing the methyl hydroperoxide route. This proposed mechanism is based on catalytic activity data obtained in this study as well as suggestions from parallel theoretical modelling studies carried in the same research group.

5.5. Characterisation of used catalyst

5.5.1. X-ray diffraction (XRD) analysis

Figure 5.11 displays the XRD diffractogram of the 5wt%Au-Pd/TiO_{2IW} catalyst after subjecting the catalyst to methane oxidation in the presence of hydrogen peroxide. The diffractogram of the fresh 5wt%Au-Pd/TiO_{2IW} catalyst is plotted as a direct comparison with used samples. The used catalysts after filtration were either dried at room temperature overnight or were subjected to calcination (after drying in air) in static air at 400 °C for 3 hours. It can be observed that there was modification in the XRD patterns of both used samples (figure 5.11 (b and c)), indicating some structural change occurred to the catalyst during reaction. In particular, the diffraction peaks corresponding to metallic palladium were observed at $2\theta = 40.4^{\circ}$ and 46.9° and are assigned to (111) and (200) reflections, respectively (JCPDS file 01-087-0645). However, a close examination of the diffractogram of the re-calcined sample showed that the calcinations step could regenerate the catalyst to a state close to fresh catalyst, and the Pd^0 peaks were suppressed. This study has not yet optimised the regeneration procedure, and it was believed that the structure of used catalyst could still be restored comparable to fresh catalyst. In addition, the XRD data in table 5.23 illustrated that metal agglomeration on the used catalyst did not occur under reaction conditions, and the average crystallite size of Au-Pd in the used catalyst calculated using Scherrer equation was similar (23.4 nm) to that of the fresh catalyst (23 nm). As expected, the recalcination step at high temperature slightly increases the crystallite size to 24.8 nm due to a sintering effect.

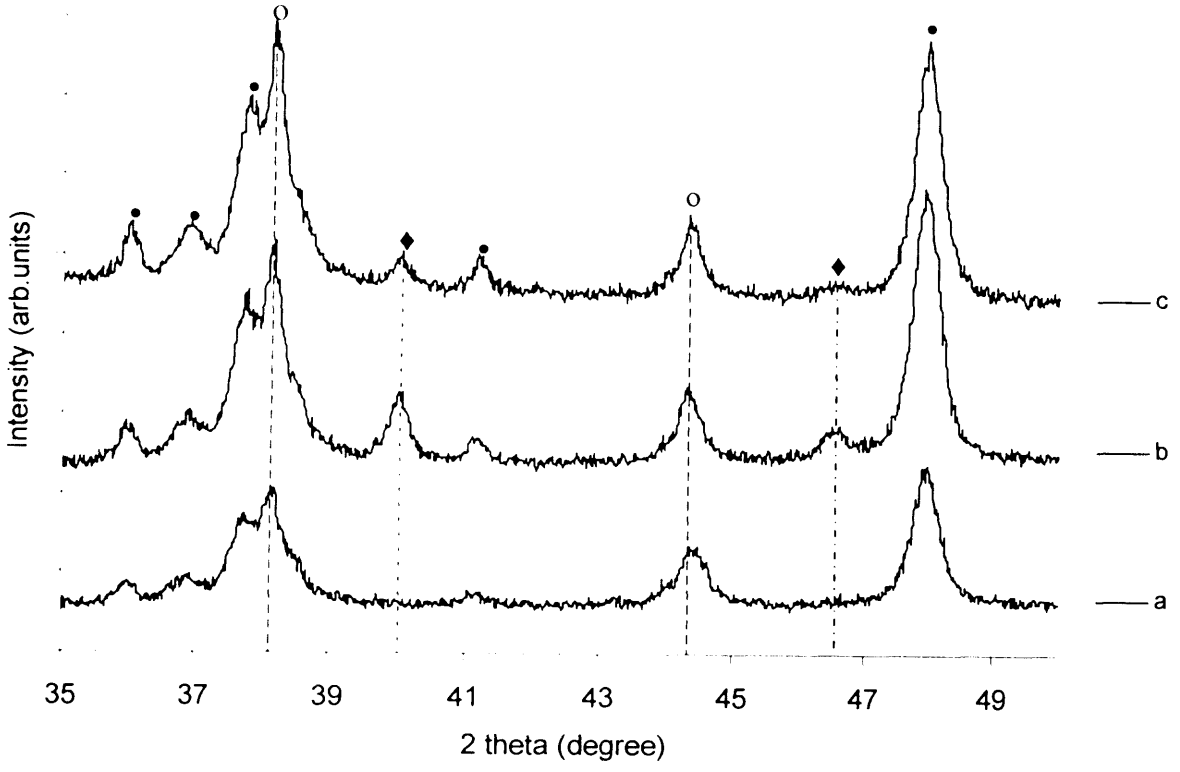

Figure 5.11: X-ray diffractogram of 5wt%Au-Pd/TiO_{2IW} catalyst. Key: (a) Calcined in static air at 400 °C for 3 h, (b) Calcined in static air at 400 °C for 3 h (after third used in standard methane oxidation with hydrogen peroxide then dried at room temperature), (c) Calcined in static air at 400 °C for 3 h (after third used in standard methane oxidation with hydrogen peroxide then recalcined in static air in similar condition), Symbol: (•) TiO_2, (o) Au/Au-Pd alloy, (♦) Palladium in metallic state (Pd^0)

Table 5.23: Crystallite size of used 5wt%Au-Pd/TiO_{2IW} catalysts with different pretreatment. For comparison, the data of fresh 5wt%Au-Pd/TiO_{2IW} catalyst is included.

Entry	Pretreatment[a]	Au-Pd, FWHM (200) (2θ; 44.3°)	Pd, FWHM (111) (2θ; 40.4°)	Au-Pd, FWHM (200) Crystallite size[b] (nm)	Pd, FWHM (111) Crystallite size[b] (nm)
1	Room temperature, 16 h	0.366	0.384	23.4	22.0
2	Static air, 400 °C for 3 h	0.345	0.326	24.8	25.9
3	Fresh catalyst	0.373	nd	23.0	nd

[a] Both catalysts have been used in three consecutive reaction of methane oxidation with presence of hydrogen peroxide before subjecting to respective pretreatment

[b] Crystallite size by means of Scherer's formula: $\frac{0.9 * \lambda}{\beta_{hkl} * \cos\theta}$

nd: not detectable

5.5.2. X-ray photoelectron spectroscopy (XPS) analysis

The X-ray photoelectron (XPS) spectra of the 5wt%Au-Pd/TiO_{2IW} was taken after reaction in an attempt to clarify the conformational changes of the catalyst during the reaction. Both used samples, from methane oxidation with both added and *in-situ* generated H_2O_2 were plotted together with the fresh catalyst calcined in static air. The spectra shown in figure 5.12 for samples after reaction are consistent with the XRD data in section 5.5.1, where the formation of metallic Pd was observed by a peak at a binding energy between 334 and 335 eV. However, the presence of an unresolved or 'shoulder peak' at a binding energy of 336 eV indicates the occurrence of some oxidised Pd^{2+} species.

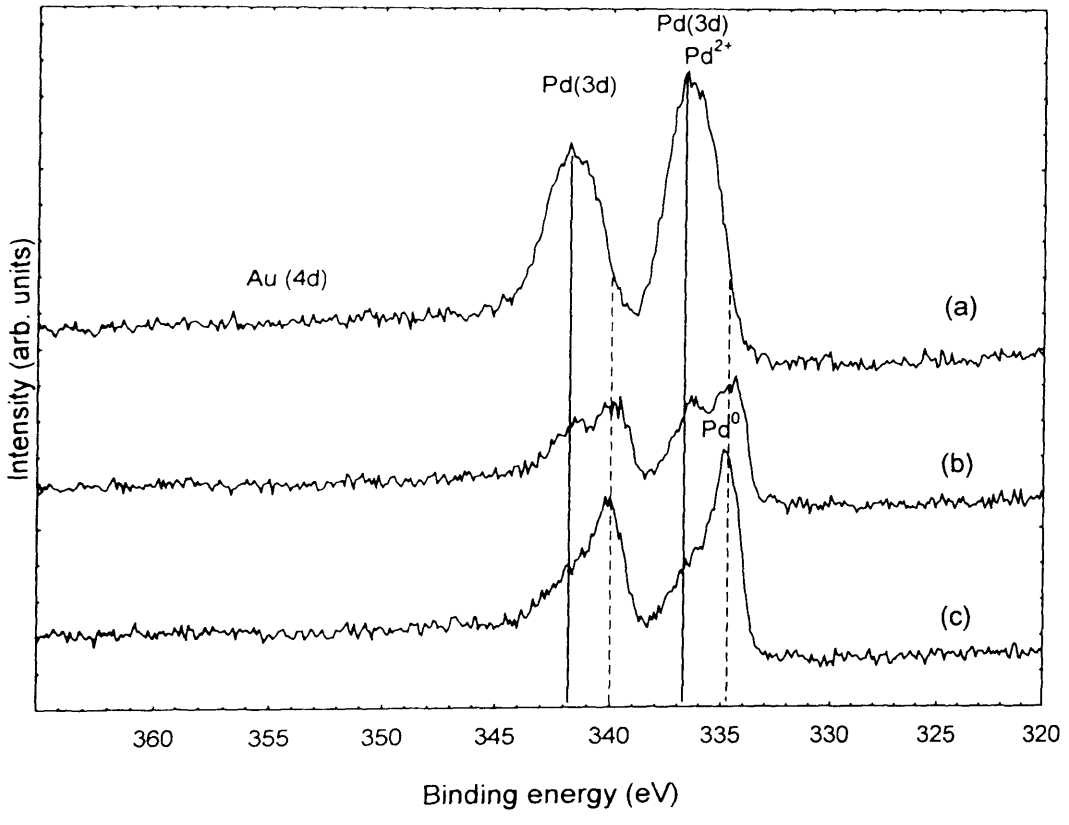

Figure 5.12: Pd (3d) spectra of 5wt%Au-Pd/TiO_{2IW} catalysts (a) Fresh after calcined at 400 °C in air, (b) After first used in methane oxidation with addition of H_2O_2, (c) After first used in methane oxidation with *in-situ* formation H_2O_2

The spectral intensities of both used catalysts were relatively lower compared to the fresh catalyst calcined in static air. Therefore, a question arises as to whether the decreased intensities may be due to the metal leaching during the reaction. However, it was confirmed by atomic absorption spectroscopy (AAS) that there were insignificant metals

(Au and Pd) detected in the reaction solution after reaction. In view of the fact that Pd^0 was detected in the used catalysts, it was useful to compare the XPS spectra to those of fresh catalysts having a similar phase composition. It has been shown in chapter 4 (section 4.5.4) that pre-treatment of a 5wt%Au-Pd/TiO_{2IW} catalyst in either a hydrogen environment at high temperature, or with a hydrogen peroxide solution produces a mixture of Pd^0 and Pd^{2+} species. It is worth noting here that the spectra intensities of fresh reduced catalysts are also lower compared to fresh calcined catalyst. A further surface atom composition derived from the integration of the XPS peaks in table 5.24 confirmed the similarity between both the used catalyst and the fresh, reduced sample. In all cases, the atomic percentages of each metal (Au and Pd) were relatively lower compared to fresh catalyst calcined in static air. Hence, the differences observed in the XPS were assigned to the reduction effect of the catalyst. From another point of view, the lower surface composition of each metal on the used catalyst could possible be due to the surface covering of the metal by a compound or species generated during the reaction, and consequently decreasing the XPS signals.

Table 5.24: Surface elemental compositions derived from XPS for fresh and used 5wt%Au-Pd/TiO_{2IW} catalysts

Entry	Type of reaction	No. uses	Composition (atom %)		Atom ratio
			Au/Ti	Pd/Ti	(Pd/Au)
1		Fresh[a]	0.0075	0.0518	6.91
	H_2O_2 addition	1	0.0028	0.0278	9.93
	In-situ H_2O_2	1	0.0030	0.0315	10.50
2		Fresh[b]	0.0049	0.0217	4.43
3		Fresh[c]	0.0049	0.0267	5.49

[a]Static air, 400 °C, 3 hours

[b]Flow of 5%H_2/Ar, 400 °C, 3 hours

[c]Static air, 400 °C, 3 hours followed by H_2O_2 treatment (H_2O_2, 0.5M)

Since the used samples have a mixture of Pd^0 and Pd^{2+}, the relative composition of each Pd species was determined by performing a deconvulation of each Pd (3d) spectra. The best fit spectra are displayed in figure 5.13. The percentage of Pd^{2+} calculated for each used catalyst after methane oxidation with the addition of H_2O_2 was slightly higher (56.5 %) compared to 52.7 % obtained for the used catalyst from the reaction with *in-situ*

generated H_2O_2. The presence of H_2 gas might assist the reduction process under the *in-situ* conditions.

(i)

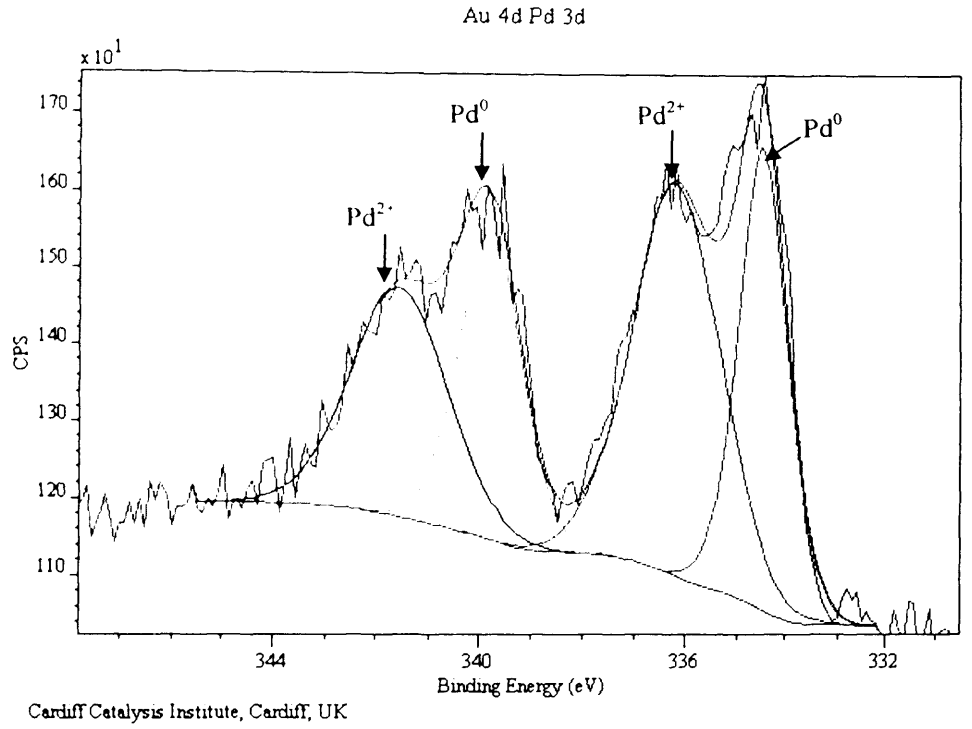

(ii)

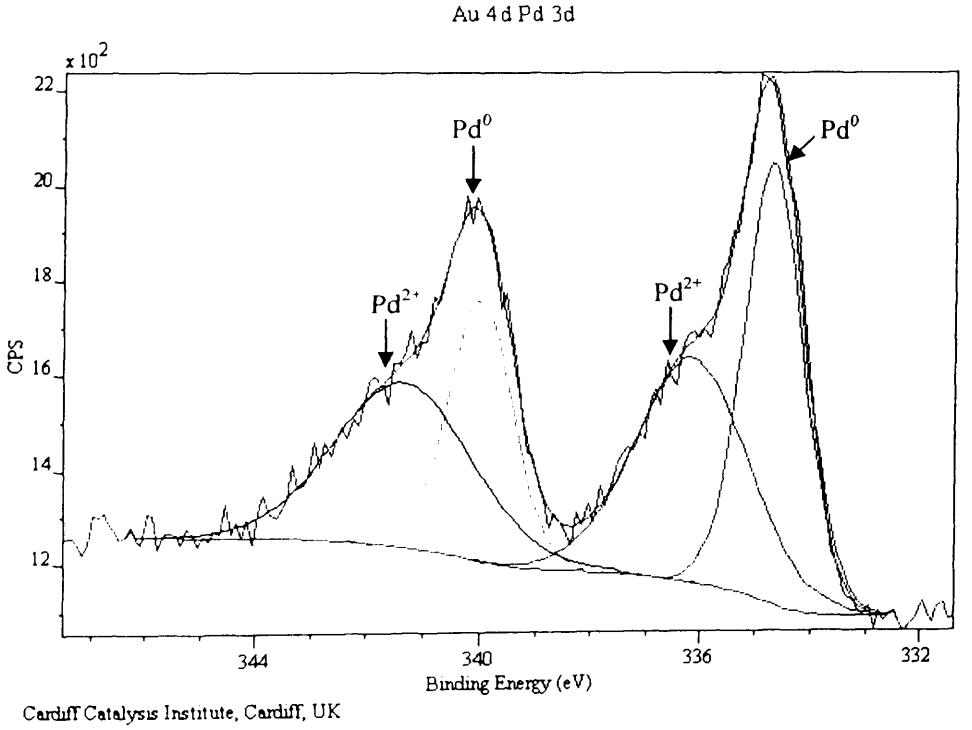

Figure 5.13: Deconvulation of Pd (3d) spectra of used 5wt%Au-Pd/TiO_{2IW} catalyst, (i) after reaction with added H_2O_2 (ii) after reaction with *in-situ* generated H_2O_2

5.6. Conclusions

Taking into consideration the fact that the Au-Pd alloy nanoparticles catalyst successfully oxidised methane to methanol using H_2O_2 as oxidant, and also considering the ability of 5wt%Au-Pd/TiO_{2IW} to synthesise hydrogen peroxide from a H_2/O_2 gas mixture, methane oxidation reactions using a gas composition of methane, hydrogen and oxygen diluted with nitrogen or carbon dioxide were carried out and discussed in this chapter. In typical experiments, the reactions were performed outside the explosive limit with a very low amount of hydrogen and oxygen introduced into the reactor (0.86% of H_2 and 1.72% of O_2) for the *in-situ* generation of hydrogen peroxide, and eventually the formation of methanol. In most cases, water was used as solvent and N_2 as diluents gas.

Through the catalytic data discussed in this chapter, it was proved that supported Au-Pd nanoparticles have the ability to concurrently generate the hydroperoxy species required for oxidation and activate methane at very mild conditions. It is important to state that the homogeneous gold system is not capable of oxidising methane to methanol using the *in-situ* approach, whereas a Pd-only or a combination of Au and Pd- homogeneous system shows activity for methane oxidation under the *in-situ* approach, albeit with low selectivity to methanol. Additionally, precipitation of the homogeneous catalysts was also observed. N_2 was found to be the preferred diluent compared to CO_2 and higher oxygenate formation was observed. The data could be explained by the methane displacement effect of CO_2 in solution, as this diluent consequently decreased the methane oxidation activity.

In the presence of a heterogeneous 5wt%Au-Pd/TiO_{2IW} catalyst, increase of the hydrogen and oxygen percentage leads to an increase of both methane conversion and methanol selectivity. Reactions at 50 °C gave the best compromise between catalytic activity and methanol selectivity. At higher temperatures (70 and 90 °C), a lower formation of oxygenate products was observed, and it was found to be associated with the poor ability of the catalyst to synthesise H_2O_2 *in-situ* at higher temperatures. Prolonging the reaction time up to two hours is accompanied with an enhancement of methanol formation, whereas at longer reaction time (> 2 hours) a decrease in methanol formation is observed, along with a significant increase in CO_2 formation. These results demonstrate that there is the possibility of increasing the yield of methanol, however a prolonged reaction time would lead eventually to the over-oxidation of oxygenates and increased CO_2 formation. From this, it can be concluded that the proper choice of reaction time is necessary. Moreover, the synergistic effect of Au and Pd is evidently observed. Physical mixtures of

Au/TiO_2 and Pd/TiO_2, either at the same mass or molar ratio gave inferior activity and selectivity compared to alloyed Au-Pd nanoparticle catalysts. This observation is in line with the synergistic effect observed in chapter 4.

The nature of the catalyst support is also crucial in order to successfully prepare a bi-functional catalyst. TiO_2 was found to be the best support for producing a bifunctional catalyst that can concurrently synthesise H_2O_2 as the oxidant, and perform the oxidation of methane. The ability of TiO_2 to interact and stabilise hydroperoxy species could be one of the reason behind this superior activity.

Furthermore, the activation of methane using *in-situ* generated H_2O_2 was preferred for larger particles of Au and Pd with a higher concentration of Pd metal cations on the surface of catalyst. Therefore, Au-Pd catalysts synthesised using an impregnation method that were calcined in static air and have Au core-Pd shell structures with PdO dominating the outer layer of the alloy were preferred as catalysts to those synthesised through the sol-immobilisation method. Calcined $Au-Pd/TiO_2$ catalysts were stable from a metal leaching point of view, and the used samples could be regenerated by a catalyst regeneration procedure.

By combining catalytic reaction studies, examining the stability of various reaction products, as well as experiments performed in the presence of radical scavengers, mechanistic pathways have been proposed for both the approach with added hydrogen peroxide, or *in-situ* generated hydrogen peroxide. By referring to the Au-Pd catalyst having a core shell structure with Pd^{2+} rich shell ($5wt\%Au-Pd/TiO_{2IW}$ catalyst), mechanistic pathways have been proposed to proceed through a methyl hydroperoxide intermediate product. Formation of methyl hydroperoxide as intermediate product occurs through interaction of a surface bound hydroperoxyl species and methyl species, and the methanol formed could be generated via several pathways, including the hydrolysis of methoxy species. The postulated mechanistic pathway was supported by theoretical molecular modelling studies carried out by another researcher in same research group.

References:

1. Gradassi, M. J.; Wayne Green, N. *Fuel Processing Technology* **1995,** *42*, 65-83.
2. Bharadwaj, S. S.; Schmidt, L. D. *Fuel Processing Technology* **1995,** *42*, 109-127.
3. www.icis.com. 2011.
4. Haruta, M. *Gold Bulletin* **2004,** *37*, 27.
5. Landon, P.; Collier, P. J.; Papworth, A. J.; Kiely, C. J.; Hutchings, G. J. *Chemical Communications* **2002**, 2058-2059.
6. Edwards, J. K.; Thomas, A.; Carley, A. F.; Herzing, A. A.; Kiely, C. J.; Hutchings, G. J. *Green Chemistry* **2008,** *10*, 388-394.
7. Liu, Q.; Lunsford, J. H. *Applied Catalysis A: General* **2006,** *314*, 94-100.
8. Lunsford, J. H. *Journal of Catalysis*, *216*, 455-460.
9. Choudhary, V. R.; Samanta, C.; Choudhary, T. V. *Applied Catalysis A: General* **2006,** *308*, 128-133.
10. Lin, M.; Hogan, T.; Sen, A. *Journal of the American Chemical Society* **1997,** *119*, 6048-6053.
11. Park, E. D.; Choi, S. H.; Lee, J. S. *Journal of Catalysis* **2000,** *194*, 33-44.
12. Park, E. D.; Hwang, Y. S.; Lee, J. S. *Catalysis Communications* **2001,** *2*, 187-190.
13. Park, E. D.; Hwang, Y.-S.; Lee, C. W.; Lee, J. S. *Applied Catalysis A: General* **2003,** *247*, 269-281.
14. Lin, M.; Sen, A. *Journal of the American Chemical Society* **1992,** *114*, 7307-7308.
15. Lin, M.; Hogan, T. E.; Sen, A. *Journal of the American Chemical Society* **1996,** *118*, 4574-4580.
16. J. Van Weynbergh, J. P. S., J. C. Colery. USPTO Ed.; Solvay Interox, 1993.
17. Samanta, C. *Applied Catalysis A: General* **2008,** *350*, 133-149.
18. Samanta, C.; Choudhary, V. R. *Catalysis Communications* **2007,** *8*, 73-79.
19. www.engineeringtoolbox.com. 2011.
20. Edwards, J. K.; Carley, A. F.; Herzing, A. A.; Kiely, C. J.; Hutchings, G. J. *Faraday Discussions* **2008,** *138*, 225-239.
21. Thetford, A.; Hutchings, G. J.; Taylor, S. H.; Willock, D. J. *Proceedings of the Royal Society A: Mathematical, Physical and Engineering Science* **2011.**
22. Thetford, A., Cardiff University, 2011.
23. Staykov, A.; Kamachi, T.; Ishihara, T.; Yoshizawa, K. *The Journal of Physical Chemistry C* **2008,** *112*, 19501-19505.
24. Li, J.; Staykov, A.; Ishihara, T.; Yoshizawa, K. *The Journal of Physical Chemistry C* **2011,** *115*, 7392-7398.
25. Kesavan, L.; Tiruvalam, R.; Rahim, M. H. A.; bin Saiman, M. I.; Enache, D. I.; Jenkins, R. L.; Dimitratos, N.; Lopez-Sanchez, J. A.; Taylor, S. H.; Knight, D. W.; Kiely, C. J.; Hutchings, G. J. *Science* **2011,** *331*, 195-199.
26. Lopez-Sanchez, J. A.; Dimitratos, N.; Glanville, N.; Kesavan, L.; Hammond, C.; Edwards, J. K.; Carley, A. F.; Kiely, C. J.; Hutchings, G. J. *Applied Catalysis A: General* **2011,** *391*, 400-406.
27. Edwards, J. K., Cardiff University, 2006.

28. Solsona, B. E.; Edwards, J. K.; Landon, P.; Carley, A. F.; Herzing, A.; Kiely, C. J.; Hutchings, G. J. *Chemistry of Materials* **2006,** *18*, 2689-2695.
29. Edwards, J. K.; Solsona, B. E.; Landon, P.; Carley, A. F.; Herzing, A.; Kiely, C. J.; Hutchings, G. J. *Journal of Catalysis* **2005,** *236*, 69-79.
30. Dimitratos, N.; Lopez-Sanchez, J. A.; Anthonykutty, J. M.; Brett, G.; Carley, A. F.; Tiruvalam, R. C.; Herzing, A. A.; Kiely, C. J.; Knight, D. W.; Hutchings, G. J. *Physical Chemistry Chemical Physics* **2009,** *11*, 4952-4961.
31. Süss-Fink, G.; Gonzalez, L.; Shul'pin, G. B. *Applied Catalysis A: General* **2001,** *217*, 111-117.
32. Liu, J.; Lagger, G.; Tacchini, P.; Girault, H. H. *Journal of Electroanalytical Chemistry* **2008,** *619-620*, 131-136.
33. Olivera, P. P.; Patrito, E. M.; Sellers, H. *Surface Science* **1995,** *327*, 330-357.
34. Hasegawa, S. *The Review of Physical Chemistry of Japan* **1946,** *20*, 21-30.
35. Süss-Fink, G.; Nizova, G. V.; Stanislas, S.; Shul'pin, G. B. *Journal of Molecular Catalysis A: Chemical* **1998,** *130*, 163-170.
36. Nizova, G. V.; Süss-Fink, G.; Shul'pin, G. B. *Tetrahedron* **1997,** *53*, 3603-3614.
37. www.wikipedia.org. 2011.
38. Bum Gun Kwon, J. H. L. *Bull. Korean Chem. Soc.* **2006,** *27*, 1785.
39. Elliot, A. J.; Simsons, A. S. *Canadian Journal of Chemistry* 1984, 62, 1831-1834.

CHAPTER 6

Catalytic Oxidation of Copper Based Catalysts

6.1. Introduction

This chapter is separated into two main sections. The first section focuses on the optimisation of the Au based catalysts for the liquid phase oxidation of methane through the addition of copper as a co-metal. In the second section, the focal point is a copper oxide system, where three different approaches have been used for the preparation of copper oxide materials. The synthesised copper oxide materials were then subjected to methane oxidation. Detailed characterisation of both systems are discussed and correlated with the observed catalytic activity.

6.2. Liquid phase methane with copper as co-metal on Au based support catalyst system

6.2.1. Introduction

As discussed in the preceding chapters, Au-Pd based catalysts demonstrate promising activity and selectivity for the activation of $C_1$and C_2 alkanes with H_2O_2 as oxidant, either by generating the H_2O_2 *in-situ* from a H_2/O_2 gas mixture, or by adding hydrogen peroxide as a co-reactant. Different approaches have been tried, including the variation of reaction parameters and the tuning of the catalyst itself. In this particular section, the influence of copper as third metal on to the Au-Pd system has been studied and compared with the reference Au-Pd bimetallic catalyst. Depositing copper on to supported Au nanoparticle catalysts has been reported by several studies.[1-3] Bimetallic Au-Cu nanoparticles supported on silica were active catalysts for the synthesis of acrolein from propene, and a synergistic effect was demonstrated.[1] In resemblance to the calcined Au-Pd/TiO_{2IW} catalysts, heat treatment of SiO_2-supported bimetallic Au-Cu nanoparticles under a reduction environment produced Au core-Cu shell structures. Switching the support to TiO_2

produced catalysts with the capability of epoxidising propene using N_2O as oxidant.[4] In addition to propene and CO oxidation reactions, Della Pina and co-workers demonstrated that supported Au-Cu bimetallic catalysts selectively oxidised benzyl alcohol to benzaldehyde at over 98% yield.[5] Previously, copper has been reported in theoretical studies to have the capability of oxidising methane to methanol as oxygenate product.[6] This was also shown by the integration of copper in to ZSM-5, where Cu played a crucial role in obtaining higher selectivity to methanol using O_2 (or air) as an oxidant at relatively low temperatures (150 °C).[7,8] In another set of experiments, the presence of copper is crucial in altering the selectivity pattern of methane oxidation. A study by Sen *et al.* using a Pd/C heterogeneous catalyst in a $CO/O_2/TFA/H_2O$ system initially showed the formation of formic acid as a main product, and through the addition of copper chloride, the selectivity could be switch to methanol and its derivative.[9]

Recently, CuO-Pd–Au/C materials synthesised by the impregnation method have been mixed with proton-conducting $Sn_{0.9}In_{0.1}P_2O_7$ particles and used for the direct oxidation of methane to methanol in an electrochemical cell and a fixed bed flow reactor.[10] The electrochemical cell was fed with mixtures of H_2O, O_2 and CH_4, whereby the active oxygen species was generated and later oxidized methane to methanol. Another observed product was carbon dioxide, but at much lower levels relative to methanol. Details reactions as follow:

Anode : $H_2O \rightarrow 1/2O_2 + 2H^+ + 2e^-$ Scheme 6.1

Cathode : $O_2 + CH_4 + 2H^+ + 2e^- \rightarrow CH_3OH + H_2O$

A similar electrocatalytic system in a gas phase fixed bed flow reactor gave three times higher methanol yield, though CO_2 was still observed as a consecutive oxidation product. It is important to note here that in both cases, the reactions were carried out at higher temperature *i.e.* > 200 °C, and with an optimised temperature of 400 °C. This is well above the reaction temperatures employed in this study. It is important to state here that methane oxidation using the Au-Pd-Cu supported catalysts reported in this work has been filed for patent in 2008.[11] Hence the initial concept was shown before any related published works. In order to have direct comparison, the catalytic testing was carried out at similar conditions to those employed for the Au-Pd bimetallic described in chapters 4 and 5.

6.2.2. Liquid phase methane oxidation with addition of H_2O_2 as oxidation

In view of the fact that TiO_2 was demonstrated to be the superior support for methane and ethane oxidation (as discussed in previous chapters), a series of mono, bi and trimetallic Au/Pd/Cu catalysts supported on TiO_2 have been prepared using the impregnation method. The catalytic performances of the calcined supported Au/Pd/Cu catalysts were probed with methane oxidation reaction in the presence of H_2O_2 as oxidant. Table 6.1 represents the catalytic data for methane oxidation with the addition of hydrogen peroxide at standard reaction conditions. It can be seen that monometallic copper generated similar types of oxygenate product as observed in the analogue reaction with supported Au-Pd catalysts, whereby methyl hydroperoxide is the primary intermediate species which then transforms either selectively to methanol or directly to carbon dioxide as combustible product. Other possible oxygenate products, such as formic acid and formaldehyde as well as carbon monoxide were not observed. However, the overall catalytic activity based on the calculated turnover frequency (TOF) was higher than the Au or Pd monometallic counterparts. Moreover, monometallic copper on TiO_2 also displayed higher oxygenate selectivity than both respective mono and bimetallic Au/Pd supported on the same TiO_2 material. Nevertheless, the opposite trend was observed in terms of methanol selectivity. In this case, methyl hydroperoxide selectivity accounted for 86% of the overall selectivity, suggesting that copper alone does not have the capability of selectively transforming methyl hydroperoxide to methanol. Incorporating Au into Cu showed an increase in the TOF value by a factor of two, although the synergistic effect observed did not affect the selectivity profile. Both Au-Cu and Pd-Cu supported catalysts showed inferior methanol selectivity compared to the supported Au-Pd reference catalyst.

Hence, it opens up the possibility of combining the concept of higher catalytic activity through using copper metal, and improving the selectivity to methanol by using Au-Pd nanoparticles. Initially, similar metal loadings (weight percent) of each metal were tested, and it was shown to improve both oxygenate productivity and selectivity. Comparisons based on TOF values showed that the trimetallic 5wt%AuPd2.5wt%Cu/TiO_{2IW} catalyst produced more than twice the amount of product compared to the bimetallic 5wt%Au-Pd/TiO_{2IW} catalyst. Oxygenate selectivity was calculated to be around 97% which was also 7% higher than the bimetallic 5wt%Au-Pd/TiO_{2IW} counterpart.

Table 6.1: Methane oxidation of Cu in mono, bi or trimetallic with Au/Pd metal supported on TiO_2

Entry	Catalyst	Product amount (μmol)				Oxygenate Selectivity (%)[c]	Methanol Selectivity (%)[d]	Oxygenate productivity (Mol/kg_{cat}/ Hour)[e]	TOF[f]	H_2O_2 Remain (μmol)[g]
		CH_3OH [a]	HCOOH [a]	MeOOH [a]	CO_2 in gas[b]					
1	2.5wt%Cu/TiO_{2IW}	0.76	0	4.40	0.19	96	14.2	0.406	1.032	338
2	2.5wt%Au2.5wt%Cu/ TiO_{2IW}	0.91	0	6.18	0.39	95	12.2	0.739	1.418	66
3	2.5wt%Pd2.5wt%Cu/ TiO_{2IW}	0.64	0	2.30	0.56	84	18.3	0.369	0.588	2434
4	2.5wt%Au2.5wt%Pd/ TiO_{2IW}	1.89	0	1.57	0.37	90	49.3	0.250	0.692	383
5	2.5wt%Au2.5wt%Pd/ 2.5wt%Cu/TiO_{2IW}	2.36	0	5.87	0.26	97	27.8	1.243	1.646	2483
6	2.5wt%Au2.5wt%Pd/ 1.0wt%Cu/TiO_{2IW}	6.08	0	0.94	0.33	96	82.7	0.729	1.404	842
7	Physical mixture of 5wt%AuPd/TiO_{2IW} and 2.5wt%Cu/TiO_{2IW}	0.49	0	1.23	0.34	83	23.8	0.128	0.344	845
8[h]	2.5wt%Cu/TiO_{2IW}	0.20	0	2.49	0.47	85	6.3	0.212	0.538	1139

Reaction Time; 30 min, Reaction Temp; 50 °C, CH_4 pressure: 30 bar, Catalyst: 1.0 x 10^{-5} mol of metal., [H_2O_2] 0.5M, Solvent: H_2O, 10 mL, [a] Analysis using ^{1}H-NMR, [b] Analysis using GC-FID, [c] Oxygenate selectivity = (mol of oxygenate/ total mol of products) * 100, [d] Methanol selectivity = (mol of CH_3OH/ total mol of products) * 100, [e] Oxygenates productivity = mol of oxygenates / Kg_{cat} / reaction time (h), [f] Turn over frequency (TOF) = mol of oxygenates / mol of metal / reaction time (h), [g] Assayed by Ce^{+4} (aq) titration. [h]Pretreat in flow of 5wt% H_2/Ar at 400 °C for 3 hours.
Catalysts: synthesised via impregnation method and calcined at 400 °C in static air for 3 hours.

However, the methanol selectivity observed for the 5wt%AuPd2.5wt%Cu/TiO_{2IW} was still inferior to the bimetallic counterparts, at only 27.8% compared to 49.3% obtained with 5wt%Au-Pd/TiO_{2IW} catalyst.

Interestingly, by depositing Cu on to the Au-Pd system, the decomposition of hydrogen peroxide was suppressed as almost 50% of the original oxidant was detected after reaction (table 6.1, entry 5). This is significantly higher than observed in the absence of Cu, where hydrogen peroxide utilization was much higher and only 8% of the H_2O_2 remained after reaction. This observation, together with higher methyl hydroperoxide selectivity indicates that some of the active sites responsible for both hydrogen peroxide decomposition and methanol formation were blocked by the presence of copper. Therefore, a step has been taken to vary the percentage of Cu metal loaded on to the catalyst. Two factors must be considered, in that the new catalyst should be able to minimise the unselective decomposition of hydrogen peroxide while at the same time amplifying the active sites responsible for the selective transformation of methyl hydroperoxide to methanol. Catalyst screening demonstrated that 1.0wt%Cu was the optimised loading in order to achieve both goals. Comparable activity to 5wt%AuPd2.5wt%Cu/TiO_{2IW} with 83% selectivity to methanol was obtained with this catalyst (5wt%AuPd1.0wt%Cu/TiO_{2IW}). A synergistic effect was later proved through an analogous reaction in the presence of physical mixtures of 2.5wt%Cu/TiO_{2IW} and 5wt%Au-Pd/TiO_{2IW} catalyst. In this case, both catalytic activity and selectivity to methanol were inferior, even compared to 5wt%Au-Pd/TiO_{2IW}.

In addition, the capability of the trimetallic 5wt%AuPd1.0wt%Cu/TiO_2 used in this study is clearly superior as higher TOF values and a higher selectivity to oxygenated products is observed compared to the Au-Pd-Cu on Carbon reported in the literature by Lee *et al.*[10] In their work, methane oxidation was carried out in the gas phase instead of liquid phase and with temperature above 350 °C. Carbon dioxide was detected as the main product.

Therefore, this study successful demonstrates the ability of trimetallic TiO_2-supported Au-Pd-Cu nanoparticle catalysts to enhance the catalytic activity and methanol selectivity whilst also suppressing the unselective decomposition of hydrogen peroxide. The ability of copper to generate methyl hydroperoxide is probably due to the ability of copper to form Cu-OOH species.[12,13] Surface hydroperoxy species were shown to involve in the formation of the CH_3OOH intermediate species in the Au-Pd catalyst system (see chapter 5). The interaction of copper with hydrogen peroxide is illustrated in scheme 6.2.

$Cu^{2+} + H_2O_2 \rightarrow Cu^{1+}\text{-}OOH + H^+$ Scheme 6.2

$Cu^{1+}\text{-}OOH + H_2O \rightarrow Cu^{2+} + O_2^- + H_3O^+$

As illustrated in scheme 6.2, the involvement of copper is mainly via a redox process during the reaction, where the oxidation state interchanges in the presence of hydrogen peroxide in aqueous medium. Therefore, in order to determine the effect of the copper oxidation state on the catalytic activity of methane, an analogous reaction has been performed in the presence of 2.5wt%Cu/TiO_{2IW} pre-treated in 5%H_2/Ar stream. Heat treatment in hydrogen environment is expected to reduce the Cu^{2+} species into metallic copper (Cu^0). It was claimed in the literature that the possibility of obtaining Cu^{1+} species only occurred at substantially low hydrogen flow rate (~1 mL/min).[14] In this study, the hydrogen flow was set to 5 mL/min. Catalytic data revealed in table 6.1 (entry 8) demonstrated that the presence of oxidised copper is preferred in order to obtain higher catalytic activity. On the other hand, unlike the bimetallic Au-Pd system, the reduced TiO_2-supported monometallic copper catalyst suppressed the decomposition of hydrogen peroxide as 23% still remained after reaction, compared to only 7% for the analogue oxidised catalyst. In order to verify this observation, a hydrogen peroxide decomposition experiment has been carried out in the presence of calcined and reduced 2.5wt%Cu/TiO_{2IW} catalysts. Experiments using glass vials at room temperature for 30 minutes duration demonstrated that in this particular experimental set-up, the outcome is slightly different as an opposite trend to the amount of hydrogen peroxide remaining after reaction was observed. The reduced catalyst decomposed around 11.6% of H_2O_2 whereas 5.5% decomposition was calculated with the calcined catalyst, indicating that there is more than one factor that could influence the hydrogen peroxide decomposition. Both oxidation and decomposition tests were repeated twice and gave similar observations. As a result, another set of H_2O_2 decomposition experiments were carried out under pressurised conditions, whereby N_2 was used instead of methane. Other experimental parameters were kept the same to the standard reaction conditions with methane. As shown in table 6.2, the reduced 2.5wt%Cu/TiO_{2IW} catalyst decomposed less hydrogen peroxide with 667 μmole H_2O_2 remaining after 30 minutes reaction time compared to 121 μmole calculated for the oxidised sample.

Table 6.2: Hydrogen peroxide decomposition test on calcined and reduced 2.5wt%Cu/TiO_{2IW} catalyst, respectively.

Entry	pretreatment	H_2O_2 remain (μmole)
1	Calcined in static air, 400 °C	121
2	Reduced in flowing 5%H_2/Ar, 400 °C	667

Reaction Time; 30 min, Reaction Temp; 50 °C, N_2 pressure: 30 bar, Catalyst: 1.0 x 10^{-5} mol of metal., [H_2O_2] 0.5M, Solvent: H_2O, 10 mL.

This observation is in line with the H_2O_2 utilisation trend examined in analogous methane reactions which suggested that the experimental pressure could affect H_2O_2 decomposition. In addition to this, the higher H_2O_2 decomposition observed under N_2 environment instead of methane was in agreement with similar tests with the Au-Pd/TiO_{2IW} catalyst, indicating that the type of gas also affects the decomposition process.

In order to identify the active site responsible for the observed catalytic activity and selectivity, it is important to corroborate the obtained catalytic activity with the catalysts properties. Thus, a selected number of catalysts have been subjected to characterisation analysis with X-ray diffraction (XRD), Temperature programmed reduction (H_2-TPR) and X-ray photoelectron spectroscopy (XPS). XRD analyses (see section 6.3.1) of all the samples tested in table 6.1 could not detect any copper phases (outside detection limit of instrument) and thus prevents differentiations of the type of copper species available in each catalyst. However, H_2-TPR was carried out for both calcined Au-Cu and Cu catalysts supported on TiO_2, and showed that the main peak corresponds to a CuO (Cu^{2+}) cluster (see section 6.3.3). As it was stated in scheme 6.2, copper involvement in methane oxidation with H_2O_2 as oxidant likely occurs by a redox process. In this case, the higher composition of Cu^{2+} with possible minor Cu^{1+}/Cu^0 phases was believed to be responsible for generating the hydroperoxy species that subsequently enhances the probability of obtaining higher catalytic activity toward oxygenate formation (mainly methyl hydroperoxide). In this study, the presence of Cu^{2+} species (with minor Cu^{+1}/Cu^0) in both monometallic Cu/TiO_2 and bimetallic Au-Cu/TiO_2 displayed higher selectivity toward methyl hydroperoxide.

Conversely, a combined analysis of fresh 5wt%AuPd1.0wt%Cu/TiO_{2IW} using XRD, XPS and H_2-TPR suggested that the Au-Pd was evolved as an alloy form whereas Cu was present at small crystallite size (< 5 nm) and was highly dispersed on the TiO_2 surface. Copper was identified as a mixture of Cu^{2+} and reduced Cu species, probably dominated by

Cu^0 phase. The availability of both the Au-Pd alloy and copper in a mixture of oxidation states in trimetallic 5wt%AuPd1.0wt%Cu/TiO_{2IW} catalyst improved the catalytic activity and a higher TOF value was obtained. Additionally, increase of methanol selectivity was also observed.

Therefore, it was suggested in this preliminary study that copper is responsible for enhancing the formation of the intermediate species. In some extent, copper is also believed to block the non-selective sites for hydrogen peroxide decomposition and hydrogenation by disrupting the surface structure of the Au-Pd alloy whilst at the same time maintaining the active sites responsible for the selective formation of methanol. As shown in chapter 5, the active sites for the selective transformation of methyl hydroperoxide to methanol were proposed to occur on Au-Pd active sites.

6.2.3. Liquid phase methane oxidation with *in-situ* generated H_2O_2 as oxidant

Taking into account the ability of copper to enhance the catalytic activity and selectivity of supported Au-Pd catalysts for methane oxidation using hydrogen peroxide as oxidant; the same series of catalysts have been subjected to methane oxidation using *in-situ* generated H_2O_2. Four different catalysts were prepared with copper metal loadings between 0.25, 0.5, 1.0, 2.5wt % Cu, though the percentage of Au and Pd were kept constant with 2.5wt% for each metal. The catalytic screening was carried out at standard reaction conditions, at 50 °C and for 30 minutes reaction time. As shown in table 6.3, an opposite effect with respect to the reaction with added hydrogen peroxide was observed in that the deposition of copper metal onto Au-Pd system suppressed the overall catalytic activity, regardless the percentages of copper loading. Moreover, by decreasing the percentage of copper, methanol formation reduced slightly and at the same time, increased CO_2 values were observed. A physical mixture of 5wt%Au-Pd/TiO_{2IW} and 2.5wt%Cu/TiO_{2IW} produced similar activity and selectivity compared to the trimetallic catalyst counterpart. Analogue methane reactions with 2.5wt%Cu on TiO_2 did not show any traces of product, and this observation was anticipated given the fact that the catalyst lacked the ability of generating the active species via the synthesis of hydrogen peroxide from H_2/O_2, as revealed from separated hydrogen peroxide synthesis experiments. In general, depositing Cu onto Au-Pd might alter or block the active sites responsible for the formation of the surface

hydroperoxy species from dissolved H_2 and O_2 and consequently limit the possible oxidation reaction from occurring.

Table 6.3: Liquid phase oxidation of methane using heterogeneous Au/Pd/Cu/TiO_{2IW} catalysts with *in-situ* formation of H_2O_2

Entry	Catalyst	Product amount (μmol)				Oxygenate Selectivity (%)[c]	TOF [d]	H_2O_2 Remain (μmol) [e]
		CH_3OH [a]	HCOOH [a]	MeOOH [a]	CO_2 in gas[b]			
1	5wt%AuPd 2.5%Cu/TiO_{2IW}	0.45	0	0	<0.1	98	0.090	18
2	5wt%AuPd 1.0%Cu/TiO_{2IW}	0.39	0	0	0.13	75	0.078	9
3	5wt%AuPd 0.5%Cu/TiO_{2IW}	0.31	0	0	0.20	61	0.062	17
4	5wt%AuPd 0.25wt%Cu/TiO_{2IW}	0.25	0	0	0.91	22	0.050	14
5	5wt%AuPd/TiO_{2IW}	1.31	0	0.29	0.32	83	0.320	56
6	Physical mixture 5wt%AuPd/TiO_{2IW} + 2.5wt%Cu/TiO_{2IW}	0.49	0	0	<0.1	98	0.098	9
7	2.5wt%Cu/TiO_{2IW}	0	0	0	0	0	0	0

Reaction Time; 30 min, Reaction Temp; 50 °C, Stirring rate: 1500 rpm, Catalyst: 1.0 x 10^{-5} mol of metal, Solvent: H_2O, 10 mL, [a] Analysis using ^{1}H-NMR, [b] Analysis using GC-FID, [c] Oxygenate selectivity = (mol of oxygenate/ total mol of products) * 100, [d] Turn over frequency (TOF) = mol of oxygenates / mol of metal / reaction time (h), [e] Assayed by Ce^{+4} (aq) titration, Gases: 0.86% H_2/1.72%O_2/75.86%CH_4/21.55%N_2, (Total pressure: 32 bar)
Catalyst: Synthesised using impregnation method and calcined in air at 400 °C for 3 hours

6.3. Catalyst Characterisation

In order to correlate the structure activity relationships, it was necessary to characterise the catalyst with appropriate techniques. The characterisation is also required given the fact that the catalytic properties of supported metal catalysts strongly depends on the nature of the metal, such as particle size, oxidation state, shape as well as the interaction with support

materials. In particular, combining the catalytic experiments with the information obtained from characterisation studies is useful in elucidating the real active site responsible in the catalytic activation system. In this study, the selected catalysts were characterised by means of XRD, XPS and H_2-TPR techniques.

6.3.1. X-ray diffraction (XRD) analysis

The X-ray diffraction (XRD) patterns of calcined (static air, 400 °C) Cu/Au/Pd catalysts in mono/bi or trimetallic form were recorded with Cu Kα radiation in the range of 20-70° and are displayed in figure 6.1. The detailed XRD diffraction patterns for Au/Pd monometallic and bimetallic including their characteristic peaks and reference file were previously shown in section 4.5.1 of chapter 4. Similar to the Au/Pd systems, the identification of the Cu phase was based on specific diffraction peaks observed in XRD diffractogram. Based on the reference JCPDS file (01-085-1326), metallic copper (Cu^0) showed diffraction peaks at 2θ values of 43.4°, 50.6° and 74.2°, which are indexed as the (111), (200) and (220) planes, respectively. The presence of Cu^{2+} species (CuO) on the other hand was characterised by specific peaks at 2θ = 36.1°, 38.7°, 48.8° corresponding to the (002), (111) and (-202) reflections respectively (JCPDS: 01-089-5986). In addition to Cu^{2+} and Cu^0, the Cu^{1+} (Cu_2O) phase could be monitored in the XRD pattern by referring to major peaks at 2θ = 36.4°, 42.3°, and 61.4° which are assigned to the (111), (200) and (220) planes respectively (JCPDS 01-071-3645).

It can be seen in figure 6.1 that there were no peaks corresponding to copper were observed in all cases either on monometallic or with presence of Au/Pd metals. The crystallite size of Cu on the surface of the support is suspected to be lower than detection limit (< 5 nm) of instrument. Moreover, it is reported in literature that if the part of copper exists in the form of copper oxide clusters, these clusters will not be detected using XRD.[15] However, clear signal corresponding to Au/Au-Pd were observed at 2θ=38.2°, 44.3° and 64.5° and are assigned to the (111), (200), (311) planes respectively (JCPDS File:03-065-2870).

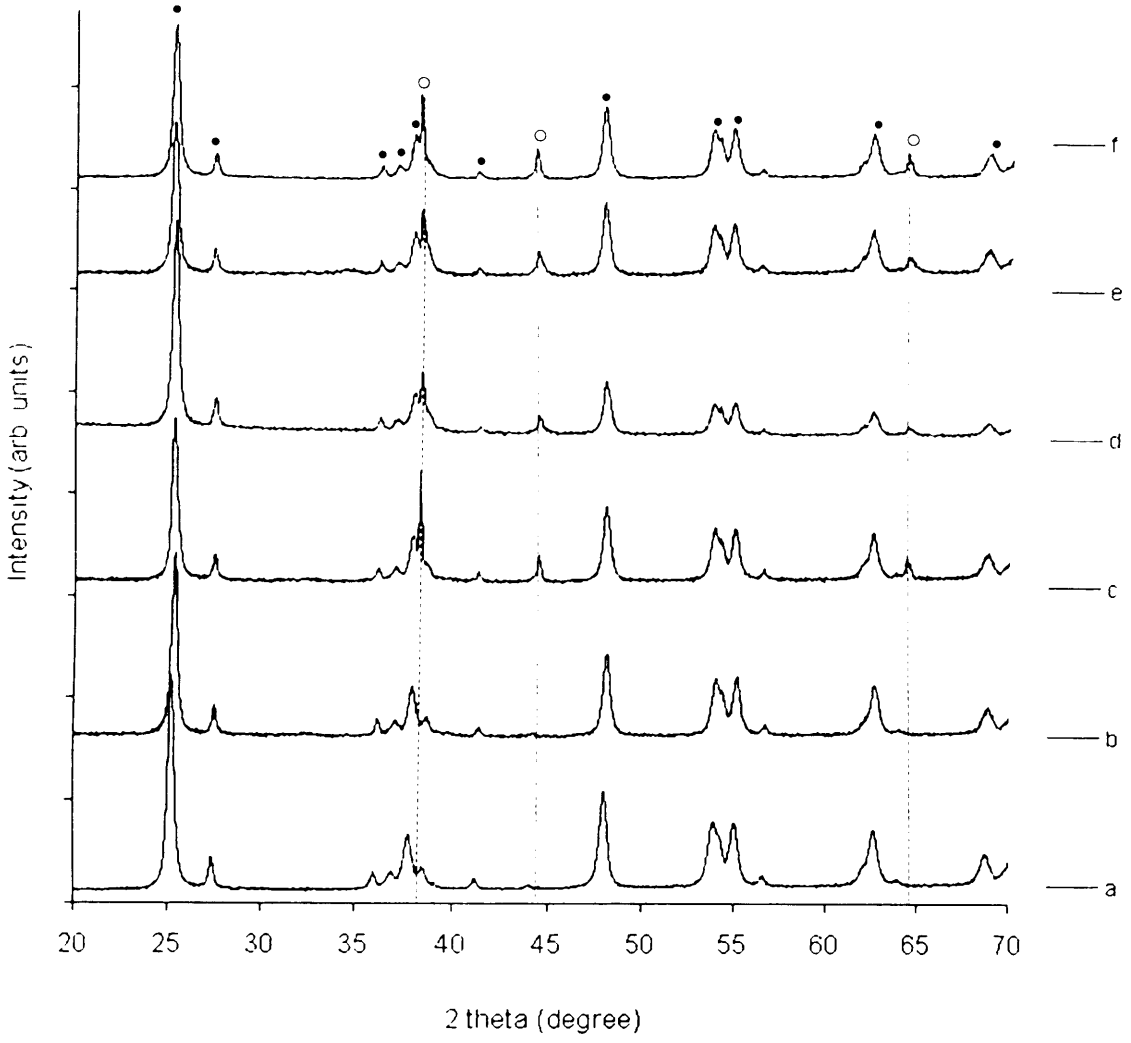

Figure 6.1: XRD diffractogram of (a) TiO_2, (b) 2.5wt%Cu, (c) 2.5wt%Au2.5wt%Cu, (d) 2.5wt%Au2.5wt%Pd1.0wt%Cu, (e) 2.5wt%Au2.5wt%Pd2.5wt%Cu, (f) 2.5wt%Au. Key: • is the TiO_2 phase, ○ is the Au/Au-Pd phase.

Even by subjecting the 2.5wt%Cu/TiO_{2IW} catalyst to a stream of 5% hydrogen in argon, no clear distinctions between the reduced sample and the calcined sample were observed (figure 6.2). It was reported in literature that typical XRD of the reduced Cu on TiO_2 showed 2θ values at 43.4°, 50.6° and 74.2°, which corresponds to metallic copper.[4] The non-detection of the Cu peaks prevents the use of X-ray powder diffraction analysis for the determination of size and phase composition of the copper metal particles. In all cases, characteristic peaks of the TiO_2 (P25) support were clearly observed, as detailed in section 4.5.1 of chapter 4.

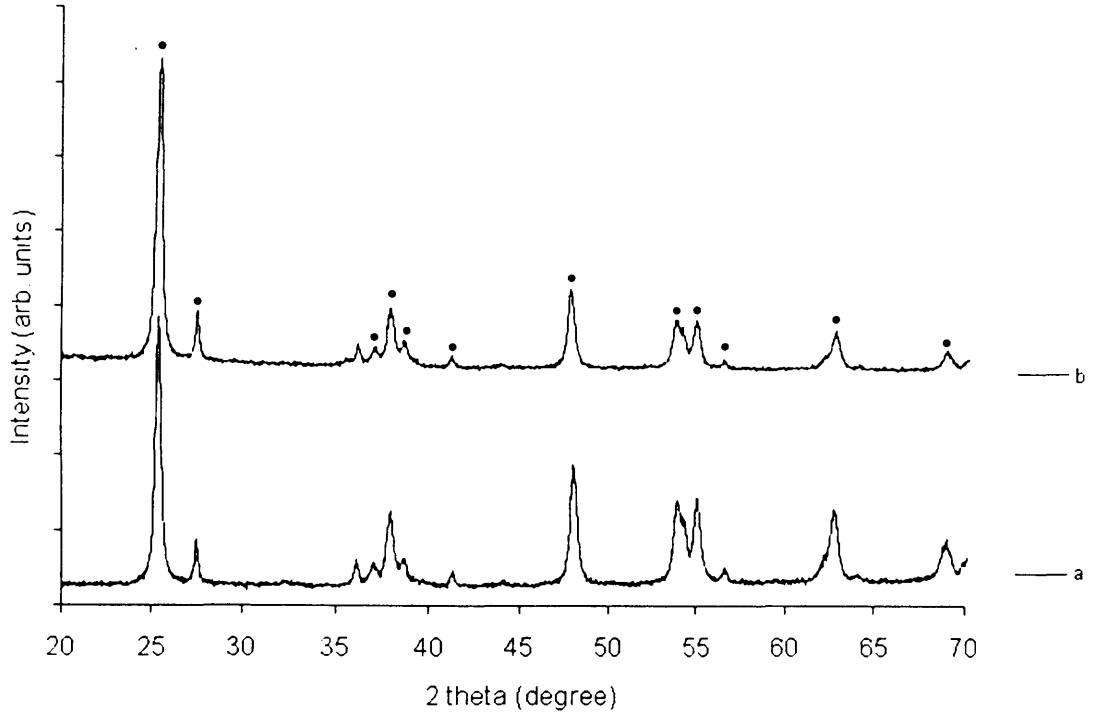

Figure 6.2: XRD diffractogram of 2.5wt%Cu/TiO_{2IW} with different heat treatment environment. (a) Static air, 400 °C, (b) 5%H_2/Ar, 400 °C. All peaks observed correspond to TiO_2 phase. Key: • is the TiO_2 phase

The mean crystallite size calculated for Au-Pd alloy in 2.5wt%Au2.5wt%2.5Cu/TiO_2 by the Scherrer equation from the 44.4° diffraction peak was 18.5 nm, whereas for 2.5wt%Au2.5wt%Pd1.0wt%Cu/TiO_2 the crystallite size was slightly bigger *cal.* 23.4 nm. This particular reflection was chosen instead of the (111) reflection due to the reasons mentioned in chapter 4, section 4.5.1. The possible formation of Au-Cu could be observed in the range of 43° and 44°; however no peak was detected in this particular range. It was reported in the literature that calcination of a supported Au-Cu catalyst in static air at 400 °C for 2 hours did not produce a Au-Cu alloy as a main phase.[3] Additionally, other possibilities such as the formation of Pd-Cu alloys were not detected in XRD diffractogram.

6.3.2. X-ray photoelectron (XPS) analysis

To evaluate the oxidation state and surface composition of Cu, Pd and Au species deposited on the TiO_2 support, as well as to determine the possible formation of alloy phases, the XPS spectra are presented for the Cu (2p), Au (4d) Pd (3d) and Au (4f) signals. Detailed XPS binding energies of each metal and its specific oxidation state are presented in table 6.4.

Table 6.4: Values of the Pd ($3d_{5/2}$), Au ($4d_{3/2}$), Au ($4f_{7/2}$) and Cu ($2p_{3/2}$) binding energies for different oxidation state of Pd, Au and Cu respectively.[16,17]

	Pd ($3d_{5/2}$): BE, eV[a]	Au ($4f_{7/2}$): BE, eV[a]	Cu ($2p_{3/2}$) BE, eV[a]
Au^0	-	83.5	-
Au^{1+}	-	84.0	-
Au^{3+}	-	86.0	-
Pd^0	335.5-335.8	-	-
Pd^{2+}	336.3–337.0	-	-
Cu^0	-	-	932.6
Cu^{1+}	-	-	932.4
Cu^{2+}	-	-	933.6.

[a]All binding energies referenced to C 1s=284.6 - 284.7 eV

Figure 6.3 displays the Cu (2p) spectrum acquired from fresh 5wt%AuPd1.0wt%Cu/TiO_{2IW} calcined catalyst. The main peak position was measured at a binding energy of 932.8 eV and corresponds to reduced copper species. This is further supported by the unclear satellite peak around 944 eV. However the observed weak shoulder peak at around 934 eV could indicate the presence of a minor amount of Cu^{2+}. According to literatures, the oxidation states of copper species can be differentiated by characteristic binding energies. In the Cu (2p) spectrum, only Cu^{2+} (934 eV) species show a satellite shake-up peak located around 10 eV (944 eV) higher than the Cu ($2p_{3/2}$) transition.[18] These satellites peaks are not seen for either Cu^{1+} or metallic Cu (Cu^0), and it was therefore used to differentiate between Cu^{2+} and other reduced species.[18,14,19]

In addition to that, by deconvoluting the Cu (2p) experimental peak, the percentages of reduced Cu and Cu^{2+} could be resolved. This was then shown to be around 32.2% (atomic percent) while the rest *cal.* 67.8% correspond to reduce phase, possibly Cu^0. It was claimed in the literature that a clear distinction between reduced phase (Cu^{1+} and/or Cu^0) is possible through examination of the Cu Auger spectra.[20]

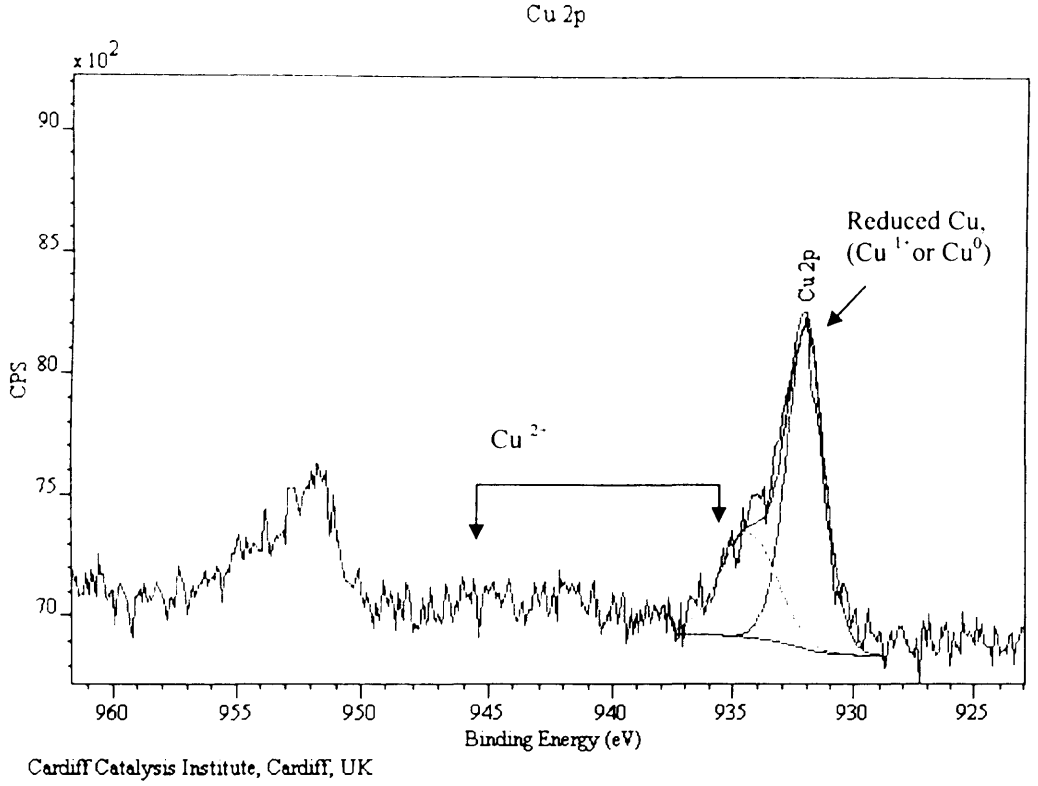

Figure 6.3: Cu (2p) spectra of fresh calcined 5wt%AuPd1.0wt%Cu/TiO_{2IW} catalyst

On the other hand, the combined Au (4d) and Pd (3d) XPS signals in figure 6.4 shows a resemblance to the calcined bimetallic Au-Pd catalyst, where the intensity of the Au ($4d_{3/2}$) feature was below the detection limit as it has been reported in the literature [21] and also to the XPS analysis of 5wt%Au-Pd/TiO_{2IW} used earlier in this study (section 4.5.4 of chapter 4). The decrease of the Au signal together with higher Pd/Au ratio (see table 6.5) probably indicates the presence of Au-core Pd-shell alloy nanoparticles. Additionally, Pd (3d) signals around 337 eV confirmed the occurrence Pd^{2+} oxidation state (see table 6.5).

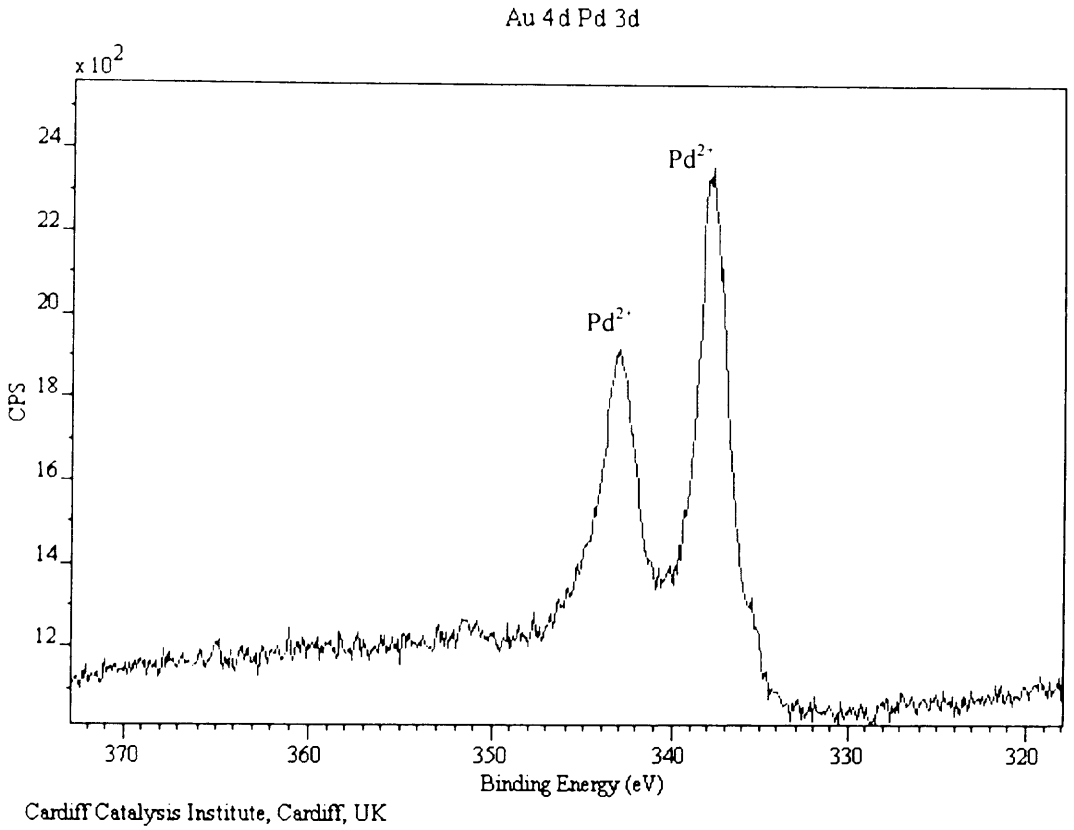

Figure 6.4: Combined Au (4d) and Pd (3d) spectra of fresh 5wt%AuPd1.0wt%Cu/TiO_{2IW} calcined catalyst

As mentioned in chapter 4, the formation of alloys occurred after calcinations at higher temperature, and alloys were not observed for the Au-Pd uncalcined catalyst. This was further proved by the XPS spectrum (figure 6.5 (i)) of an uncalcined 5wt%AuPd1.0wt%Cu/TiO_{2IW} catalyst where there were clear spectral contributions from both Au and Pd, leading to the several overlaps peaks. A detail comparison on Au (4f) transition between the uncalcined and calcined material (figure 6.5(ii)) again demonstrates the weak signal of Au on the calcined catalyst. The weak signal of Au could be explained by the inelastic scattering effect of the emitted electron from the Au core during transportation through the Pd shell.[22,21]

(i)

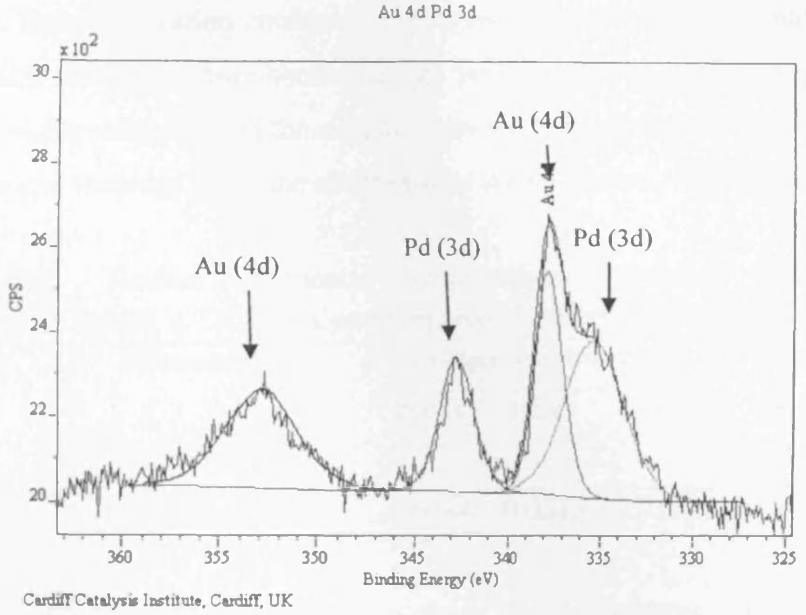

(ii)

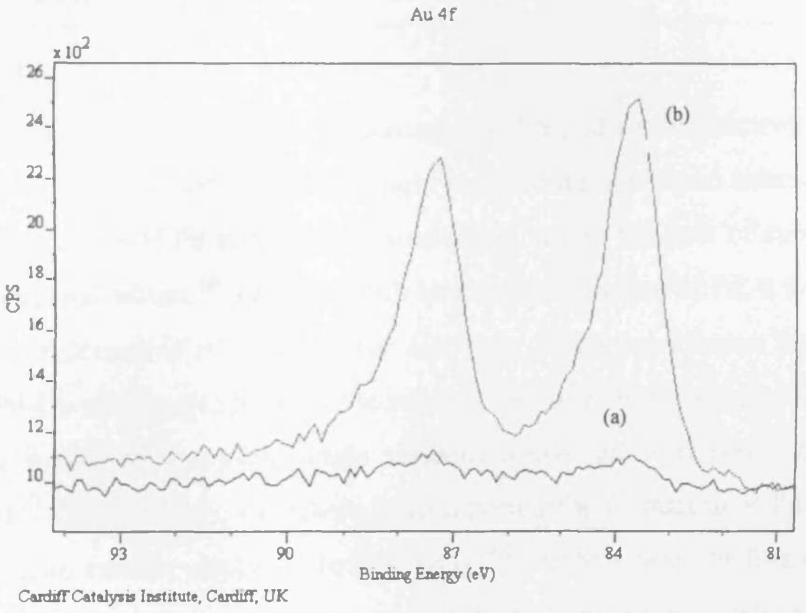

Figure 6.5: (i) Combined Au (4d) and Pd (3d) spectra of fresh 5wt%AuPd1.0wt%Cu/TiO_{2IW} uncalcined catalyst, (ii) Overlay Au (4f) spectra of uncalcined and calcined 5wt%AuPd1.0wt%Cu/TiO_{2IW} catalyst, (a) Calcined in static air at 400 °C for 3 hours, (b) Uncalcined (dried in air at 110 °C)

Table 6.5 represents the atomic percentages of each metal calculated from the integrated area of each peak in the XPS signal. The experimentally determined Pd/Au atomic ratio is again larger than the theoretical value (1.86), indicating the presence of Au core-Pd shell alloyed structures. Surface enrichment with Cu was also observed in the Au-Pd-Cu calcined

catalyst. This observation could arise from two reasons; either the particles are trimetallic and exhibit the typical core-shell structure with a gold core and Pd/Cu shell, or the copper is more highly dispersed on the support than the gold. Based on the XRD data and the low copper metal loadings used, the observations are consistent with the latter case.

Table 6.5: Surface elemental compositions derived from XPS for the 5wt%AuPd1.0wt%Cu/TiO_2 catalysts prepared by impregnation method

Entry	Treatment	Composition (atom %)			Atom ratio (Pd/Au)	Atom ratio (Cu/Au)	Atom ratio (Pd/Cu)
		Au/Ti	Pd/Ti	Cu/Ti			
1	Uncalcined	0.0384	0.0373	0.0134	0.97	0.39	2.78
2	Calcined in air, 400°C	0.0028	0.0380	0.0278	13.57	9.9	1.37

On the other hand, the atomic percentages of Pd and Cu are almost the same in both the uncalcined and calcined catalysts, roughly indicating a minimal interaction between Pd and Cu. If the nature of Pd and Cu are considered, where the heat of sublimation of copper is higher than palladium,[18] together with larger atomic radius of Pd, it would be expected that surface enrichment of Pd could occur. However, it has been shown that the type of alloying in the Pd-Cu system depends on the support. Surface segregation of Cu is favoured for the alumina-supported samples, while random alloys are observed with silica as support material.[23] Giorgio and co-workers have reported the formation of Pd core -Cu shell alloys supported on various oxides including TiO_2.[24,25] In their case, the formation of the alloy was obtained after heat treatment in a hydrogen environment, which is different to the calcination in air utilized in this study. Atomic percentages of Pd and Cu calculated based on the XPS spectrum does not clearly indicate the surface enrichment of either palladium or copper. In addition, the ratio of Pd to Cu in the XPS analysis of the bimetallic 2.5wt%Pd2.5wt%Cu/TiO_{2IW} (table 6.6) catalyst suggests that Pd-Cu alloys probably do not form, where the value obtained around 1.04 which is low compared to theoretical value 1.64. However, the formation of any trimetallic Au-Pd-Cu alloys cannot be excluded, though this particular alloy has not yet been reported in the literature. Further studies using STEM and EDX analysis are needed for clarifying the morphology of the Au/Pd/Cu supported catalysts.

Table 6.6: Surface elemental compositions derived from XPS for the 2.5wt%Pd2.5wt%Cu/TiO_{2IW} catalysts prepared by impregnation method and calcined in static air.

Catalyst	Composition (atom %)		Atom ratio
	Pd/Ti	Cu/Ti	(Pd/Cu)
2.5wt%Pd2.5wt%Cu/TiO_{2IW}	0.0558	0.0539	1.04

6.3.3. Temperature programmed reduction (H_2-TPR)

Temperature programmed reduction with hydrogen (H_2-TPR) could provide information concerning the reducibility of different chemical species present, in the catalyst as well as the degree of interaction between both metal-support and metal-metal. Figure 6.6 shows the H_2-TPR profiles of the mono, bi or trimetallic Au/Pd/Cu catalysts supported on TiO_2. In the examined temperature range, the TPR profile of trimetallic 2.5wt%Au2.5wt%Pd1.0wt%Cu/TiO_{2IW} catalyst was clearly different to the monometallic 2.5wt%Cu/TiO_{2IW} or bimetallic 2.5wt%Au2.5wt%Cu/TiO_{2IW} analogues, where only one broad peak was observed around 300 °C. No additional peaks were observed within the experimental limit. H_2-TPR profiles for both 2.5wt%Cu/TiO_{2IW} and 2.5wt%Au2.5wt%Cu/TiO_{2IW} catalysts showed two reduction peaks in the range of temperature, at 180 °C and between 300-325 °C. According to the literature, a peak at 180 °C is responsible for the reduction of highly dispersed CuO (Cu^{2+}) cluster species,[4] whereas a peak at higher temperature (300 °C) has been proposed to be associated with larger particles of bulk CuO on the TiO_2 surface.[26] There was no peak observed for the formation of a Au-Cu alloy, which is reported to be observable around 260-280 °C by Chimentão and co-workers.[4,27] The lack of a Au-Cu alloy peak was expected given the fact that the Au-Cu catalyst in this study was calcined in air instead of reduced in hydrogen. Bracey and co-workers claimed that the interaction between gold and copper in the calcined catalyst (static air, 400 °C, 2 hours) is minimal.[3] The lack of formation of a Au-Cu alloy was further proved by referring the second peak at 325 °C on TPR profile to a 2.5wt%Au2.5wt%Cu/TiO_{2IW} catalyst. This particular reduction peak was in accordance with a monometallic Au/TiO_2 catalyst reported in the literature.[2,4] In the case of the

trimetallic catalyst, the disappearance of the Cu^{2+} cluster peak at a reduction temperature of 180 °C is in agreement with the XPS data, where it illustrated that the reduced species was more prominent. However, there is still no clear information in order to assign the reduction peak for the trimetallic calcined catalyst. Therefore as comparison, a calcined 5wt%Au-Pd/TiO_{2IW} bimetallic was subjected to analogous TPR analysis. As illustrated in figure 6.-6 (d), almost similar TPR profiles were observed for the trimetallic 2.5wt%Au2.5wt%Pd1.0wt%Cu/TiO_{2IW} catalyst and the bimetallic Au-Pd catalyst. It was proven from XRD analysis (section 6.3.1) and also XPS analysis (section 6.3.2) that Au-Pd evolved as an alloy form. This further indicates a similar formation of Au-Pd alloy in the case of the trimetallic Au-Pd-Cu/TiO_{2IW} calcined catalyst. The negative peak below 100 °C, which was more intense in the bimetallic Au-Pd catalyst, could be speculated to be PdO-like species, as claimed in literature.[18]

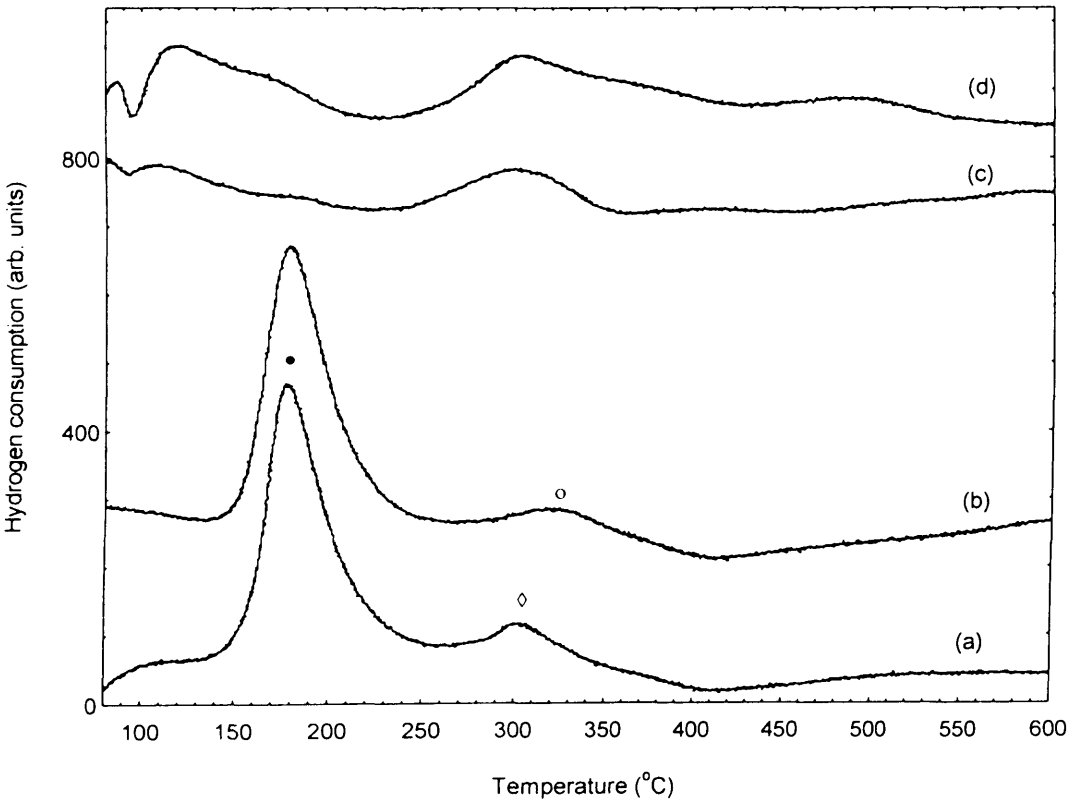

Figure 6.6: TPR profiles of (a) 2.5wt%Cu/TiO_{2IW}, (b) 2.5wt%Au2.5wt%Cu/TiO_{2IW}, (c) 2.5wt%Au2.5wt%Pd1.0wt%Cu/TiO_{2IW}, (d) 2.5wt%Au2.5wt% /TiO_{2IW}. Key: • associated with CuO cluster, ◊ associated with larger particles of bulk CuO on TiO_2, o associated with Au monometallic on TiO_2. All catalysts were calcined in static air at 400 °C for 3 hours.

The lack of a peak relating to the copper species might be due either to the detectability limit of instrument or the nature of the catalyst. XPS analysis was consistent with the former case. In addition, in all samples, no peak were observed that relate to the reduction of Ti species which occurs at around 415 °C for $Ti^{4+} \rightarrow Ti^{3+}$ and 551 °C for $Ti^{3+} \rightarrow Ti^{<3+}$.[28]

6.4. Copper oxide catalysts

6.4.1 Introduction

In order to discover and explore new catalytic systems for hydrocarbon activation, and given the fact that copper was shown to activate methane at these particular conditions using hydrogen peroxide as oxidant, the synthesis of copper oxide based materials was carried out for further understanding of the role played by the particle size and oxidation state of Cu. An initial study therefore focused on the synthesis of copper oxide catalysts using three different techniques namely, co-precipitation with urea, quick-precipitation with sodium hydroxide and a sol-gel technique. Detailed preparation procedures of each techniques were described in chapter 2, section 2.2.2.

6.4.2. Catalyst Characterisation

6.4.2.1. Thermogravimetric analysis (TGA)

Figure 6.7 illustrates the Thermogravimetric analysis (TGA) curves for copper oxide solid precursors, prepared through the precipitation method with urea, and later heated at a rate of 5 °C/min in a flowing air environment. The decomposition of the precursor started at a rather high temperature (250 °C) compared to the literature for a copper hydroxide compound (180 °C),[29] and complete decomposition into cupric oxide (CuO) occurred at a temperature above 520 °C. The higher decomposition temperature could indicate the presence of more than one phase. Further analysis using XRD (see section 6.4.2.2 of this chapter) showed that the precursor consisted of a copper chloride hydroxide phase.

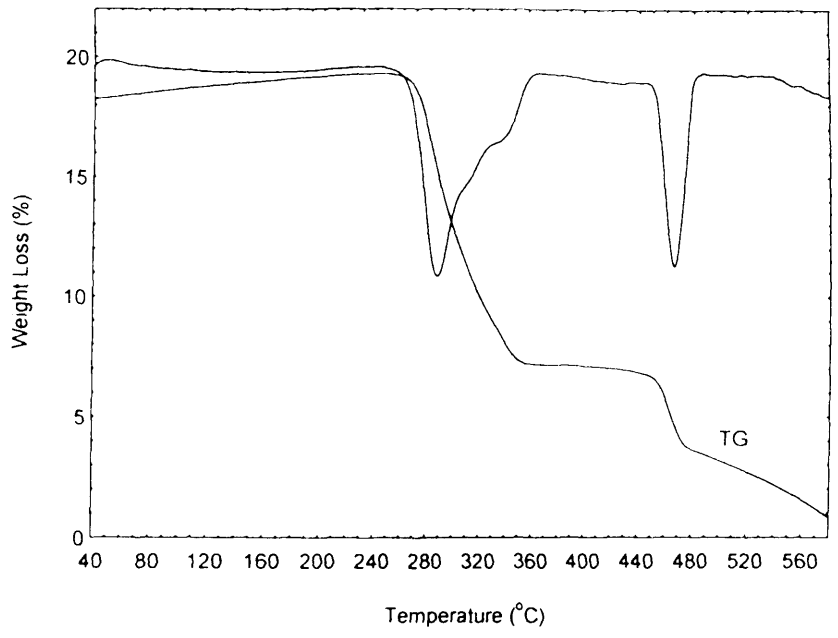

Figure 6.7: TGA of copper oxide precursor synthesised via precipitation method with urea

The TGA curve of the copper oxide precursor prepared through the sol-gel technique is presented in figure 6.8. With this material, three weight losses were observed, starting from around 120 °C and up to 360 °C. In the first stage (temperature above 120 °C), surface and crystalline water are volatilized, and in the second stage rapid decomposition was observed starting at a temperature of around 200 °C. This is due to the decomposition of citric acid and/or copper citrate. The slight weight decrease between 240 and 360 °C may be indicative of the formation of oxide.[30]

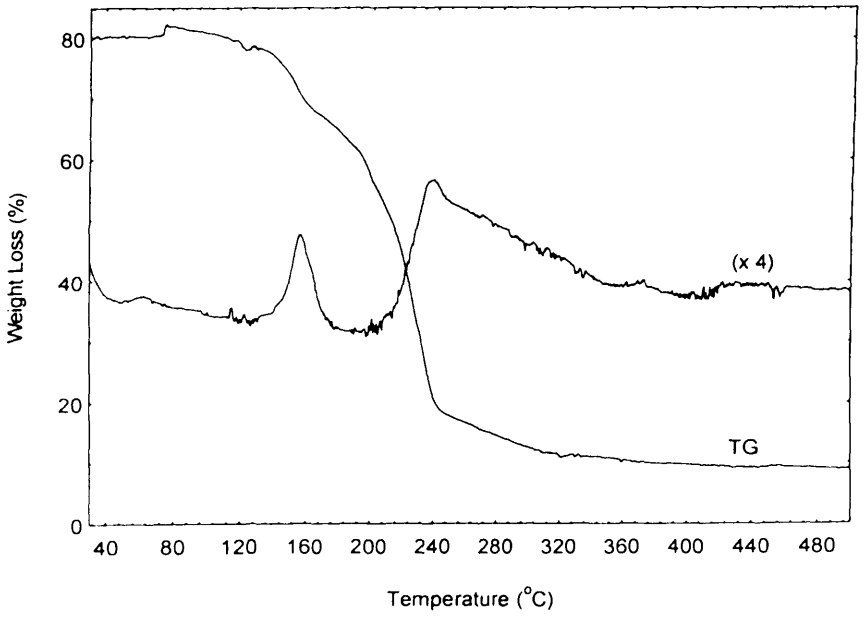

Figure 6.8: TGA of copper oxide precursor synthesised via sol gel method

6.4.2.2. X-ray diffraction (XRD) analysis

The powder X-ray diffraction patterns of copper oxide synthesised through different preparation techniques are presented in figure 6.9. Calcination of the solid precursors obtained through the precipitation of copper chloride with urea generated a single phase CuO, identified with three main characteristic peaks at $2\theta = 36.1^{\circ}$, 38.7°, 48.8°. These correspond to the (002), (111) and (-202) planes respectively. These specific diffraction peaks were referred to the reference JCPDS file (03-065-2309). The solid precursor itself was confirmed to be the copper chloride hydroxide ($CuCl_2 \cdot 3Cu(OH)_2$) phase by reference of the XRD diffractogram to JCPDS file number 01-078-0372. The XRD patternof copper chloride hydroxide (see appendix B (5)) was rather complex compared to the well crystalline CuO phase. The characteristic peaks were observed at $2\theta = 16.1^{\circ}$, 17.6°, 31.5°, 32.2°, 32.4°, 39.5° and 39.8° from which the three main peaks at $2\theta = 31.5^{\circ}$, 32.2° and 39.8° were indexed to the (121), (013) and (220) planes respectively. A similar CuO phase was also observed with the sample prepared via quick-precipitation with sodium hydroxide. Compared to the slow precipitation procedure with urea, the peaks were much broader, indicating smaller crystallite size. The formation of other copper phases, such as Cu_2O and metallic copper, were not observed in both samples. This could be confirmed by examining the characteristic peaks for Cu_2O and metallic copper respectively. According to reference JCPDS file, the Cu_2O phase could be identified by referring to main diffraction peaks at $2\theta = 36.4^{\circ}$, 42.3°, and 61.4° which are assigned to the (111), (200) and (220) reflections respectively (JCPDS 01-071-3645). The typical diffraction peaks for metallic copper could be observed at $2\theta = 43.4^{\circ}$, 50.6° and 74.2° (JCPDS file, 01-085-1326). In contrast to both precipitation techniques, the diffraction pattern from copper oxide synthesised via the sol-gel technique showed a mixture of CuO and Cu_2O phases, but the intensity of the Cu_2O signal was relatively low compared to CuO phase.

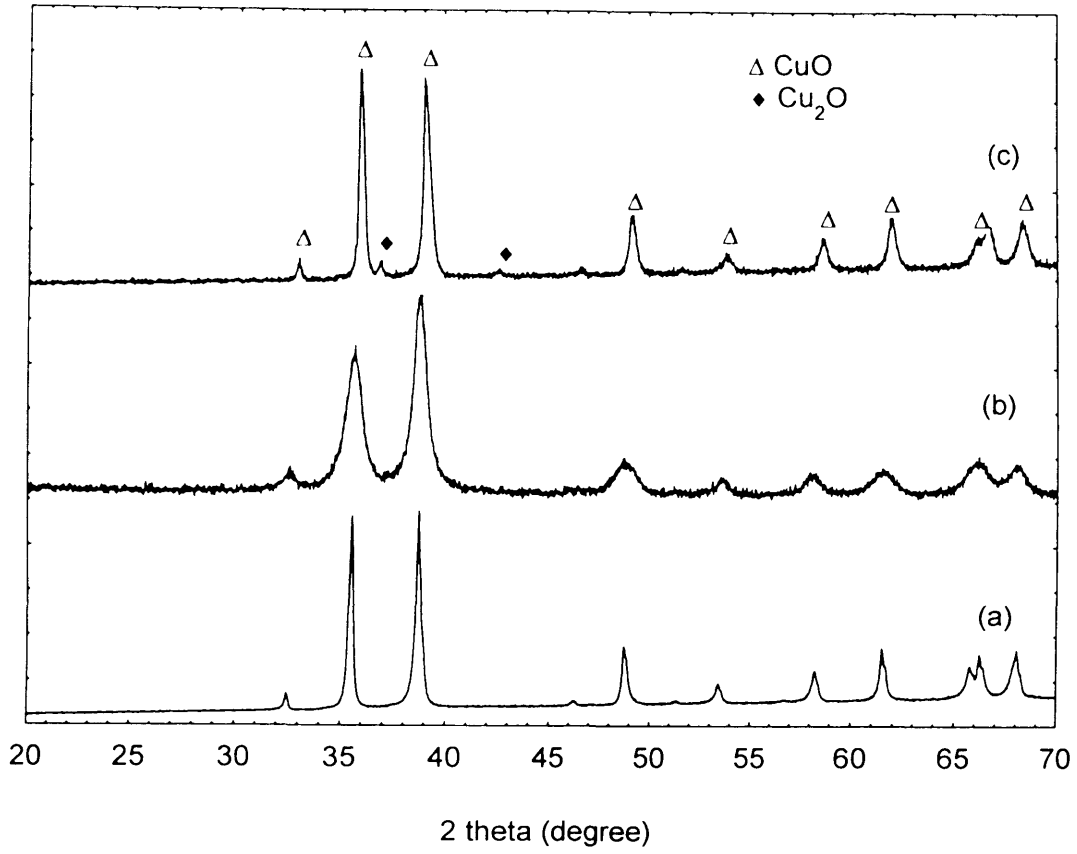

Figure 6.9: XRD diffractogram of copper oxide synthesised via different method. (a) Precipitation with urea, (b) Quick precipitation with sodium hydroxide, (c) Sol-gel with citric acid

Table 6.7 listed the average crystallite size of each material. This was calculated by using using the Scherrer formula on the main CuO peak at $2\theta = 35.7^{o}$. As expected from the XRD pattern, the broad CuO peak observed in samples synthesised through quick precipitation method produced the smallest crystallite size at *ca.* 9.3 nm, compared 35.8 and 31.4 nm for CuO_{Cp} and CuO_{Sg}, respectively.

Table 6.7: Crystallite size of copper oxide synthesised via three different methods

Catalyst	FWHM (2θ: 35.7°)	Crystallite size* (2θ: 35.7)/nm
CuO_{Cp}	0.233	35.8
CuO_{Qp}	0.894	9.3
CuO_{Sg}	0.266	31.4

*Crystallite size by means of Scherer's formula: T (Å) = (0.9 x λ) / (β_{hkl} x cos θ)

The smaller crystallite size of copper oxide observed in samples synthesised through quick-precipitation technique could be explained by the specific procedure used during the catalyst preparation, where solid NaOH was added into the boiling solution of copper acetate and acetic acid at relatively higher temperature. Precipitation at high temperature increases the rate of reaction and consequently forces large amounts of nuclei to form in a short time, while at the same time preventing the agglomeration of CuO nanoparticles.[31]

The following diffraction pattern in figure 6.10 illustrated the effect of calcination temperature on the structure of the copper oxide catalyst prepared through the sol-gel technique. The dried samples did not show any reflections from an amorphous phase (figure 6.10 (a)). Increasing the calcination temperature in static air decreased the contribution from the Cu_2O phase, and it was almost completely eradicated at 400 °C. The average crystallite size was calculated to increase from 24.9 nm (at 250 °C) to 31.2 nm (at 400 °C), possibly due to the sintering process (table 6.8).

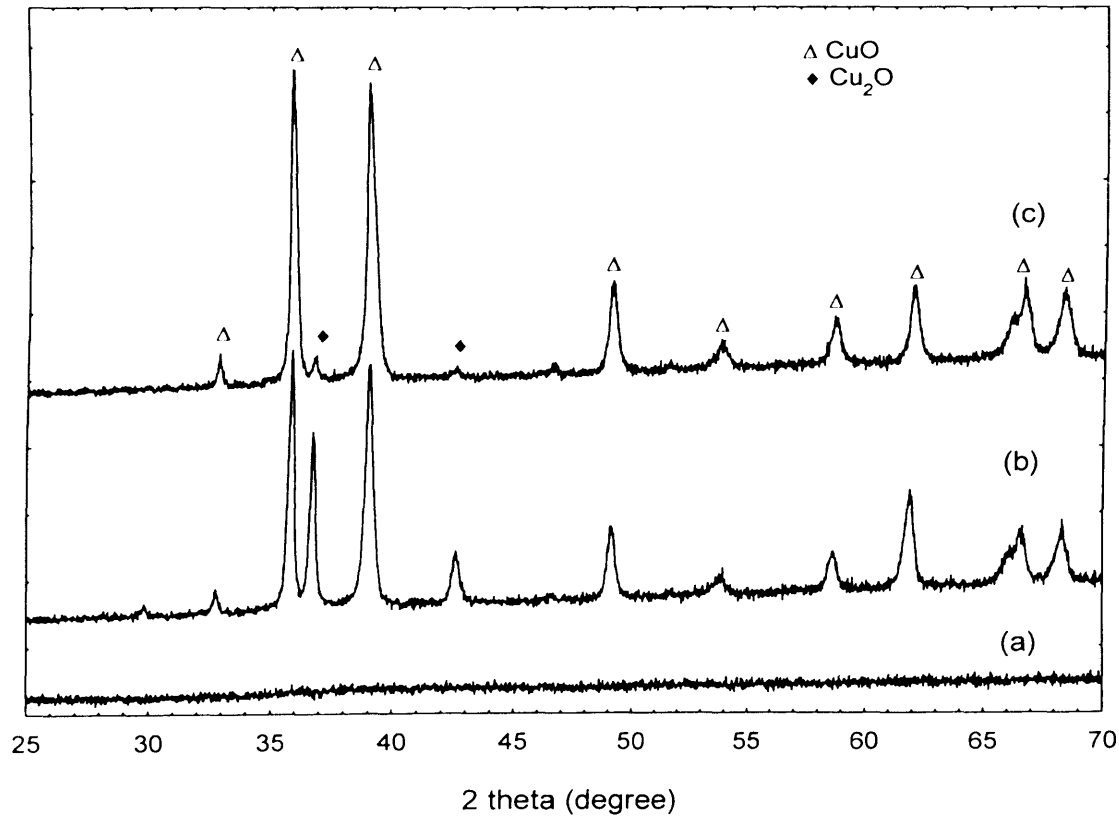

Figure 6.10: XRD diffractogram of copper oxide synthesised via sol-gel method. (a) Precursor, copper citrate, (b) Calcined at 250 °C in air, (c) Calcined at 400 °C in air

Table 6.8: Crystallite size of copper oxide synthesised via sol-gel method and calcined in different temperature

Calcinations temp. (°C)	FWHM (2θ: 35.7°)	Crystallite size* (2θ: 35.7°)/nm
250	0.335	24.9
400	0.266	31.4

*Crystallite size by means of Scherer's formula: T (Å) = (0.9 x λ) / (β_{hkl} x cos θ)

By subjecting similar sol-gel precursor to reduction with 5% hydrogen in argon stream at 400 °C for 3 hours, metallic copper species were produced (JCPDS 01-085-1326) where the main peak was observed at 2θ = 43.4 ° and 50.6°. These peaks correspond to the (111) and (200) planes, respectively (figure 6.11). Formation of CuO species was not detected whilst a broad peak at 36.7° was attributed to a Cu_2O phase. Although, it was reported by Rodriquez *et al.* that under standard reduction conditions with hydrogen (H_2 flow > 1 mL/min) Cu^{1+} is not a stable intermediate and the direct transformation from CuO to Cu occurred instead, following the sequential reduction of CuO → Cu_4O_3 → Cu_2O → Cu.[14] On the other hand, chemical reduction of the calcined copper oxide with sodium borohydride produced Cu_2O as main phase. This was confirmed by standard Cu_2O samples obtained from a commercial source and also the reference XRD pattern (JCPDS 01-071-3645). Metallic copper was detected as a minor contribution. In this case, an equal mole ratio (1:1) of sodium borohydride to CuO was used and the treatment was carried out at room temperature with moderate stirring for 30 min before the material was subjected to the drying process in air. The occurrence of Cu_2O as main phase instead of metallic copper could be due to the concentration of sodium borohydride which was probably insufficient to fully reduce the CuO phase.

As presented in table 6.9, by reducing the precursor in a flow of hydrogen, the crystallite size of copper reduced to 5.3 nm. The influence of a flowing gas rather than static conditions, as well as presence of a reducing gas assisted in the removal of chloride species. The presence of Cl species in catalyst during heat treatment process is well known to accelerate the agglomeration metal particles, subsequently producing larger particles.

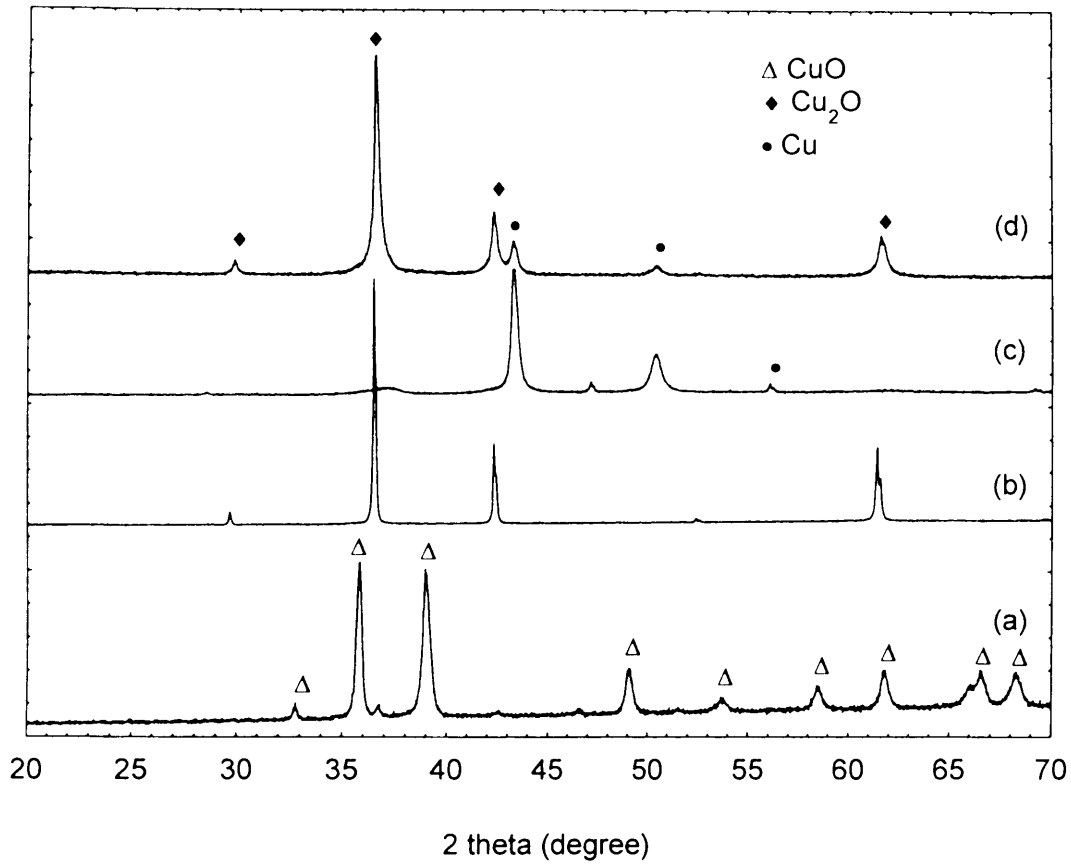

Figure 6.11: XRD diffractogram of copper oxide synthesised via sol-gel method followed by different pretreatment (a) Calcined at 400 °C in air, (b) Standard Cu_2O, (c) Reduced at 400 °C in H_2/Ar, (d) Calcined at 400 °C in air and reduced with sodium borohydride

Table 6.9: Crystallite size of copper oxide synthesised via sol-gel method followed by different pretreatment

Treatment / Phase of copper	FWHM	Crystallite size* (nm)
Static air, 400 °C (CuO)	0.268 (2θ: 35.7°)	31.2
Flow 5%H_2/Ar, 400 °C, (Cu)	1.625 (2θ: 43.4°)	5.3
Static air, 400°C and $NaBH_4$ treatment (Cu_2O)	0.349 (2θ: 36.6°)	24.1

*Crystallite size by means of Scherer's formula: T (Å) = (0.9 x λ) / (β_{hkl} x cos θ)

6.4.2.3. BET surface area measurement

Catalyst surface areas determined by BET method are summarised in table 6.10. In line with the smaller crystallite size, the highest surface was obtained for quick-precipitate catalyst *cal.* 103 m^2/g. On the other hand, samples synthesised through the co-precipitation method with urea, as well as with sol gel technique generated lower BET surface areas. To verify the analysis, two different instruments with optimized degassing procedures were used and this resulted in similar values.

Table 6.10: BET surface areas of prepared copper oxide catalyst

Catalyst	BET surface area (m^2/g)*
CuO_{Cp}	4.2
CuO_{Qp}	103.0
CuO_{Sg}	3.6

* Determined using BET surface area analyzer (Micrometics Gemini 2360 surface analyzer and Autosorb 1, Quantachrome instruments, respectively)

6.4.2.4. Scanning electron microscopy (SEM) analysis

The morphology of prepared samples was investigated by SEM using the methods described in the experimental section. The results are presentedin figure 6.12. Different preparation techniques produced different morphologies. A slow precipitation technique with urea produced cubic structures of almost similar size, which is clearly different with the inhomogeneous shape of the quick-precipitation technique with sodium hydroxide. Calcinations of gel-like structure (see appendix B (6)) from the sol-gel technique produced foam-like structure with an observable hole on the surface of the catalyst. Post-synthesis reduction with either flowing hydrogen or sodium borohydride did not change the physical morphology of the sol-gel catalyst.

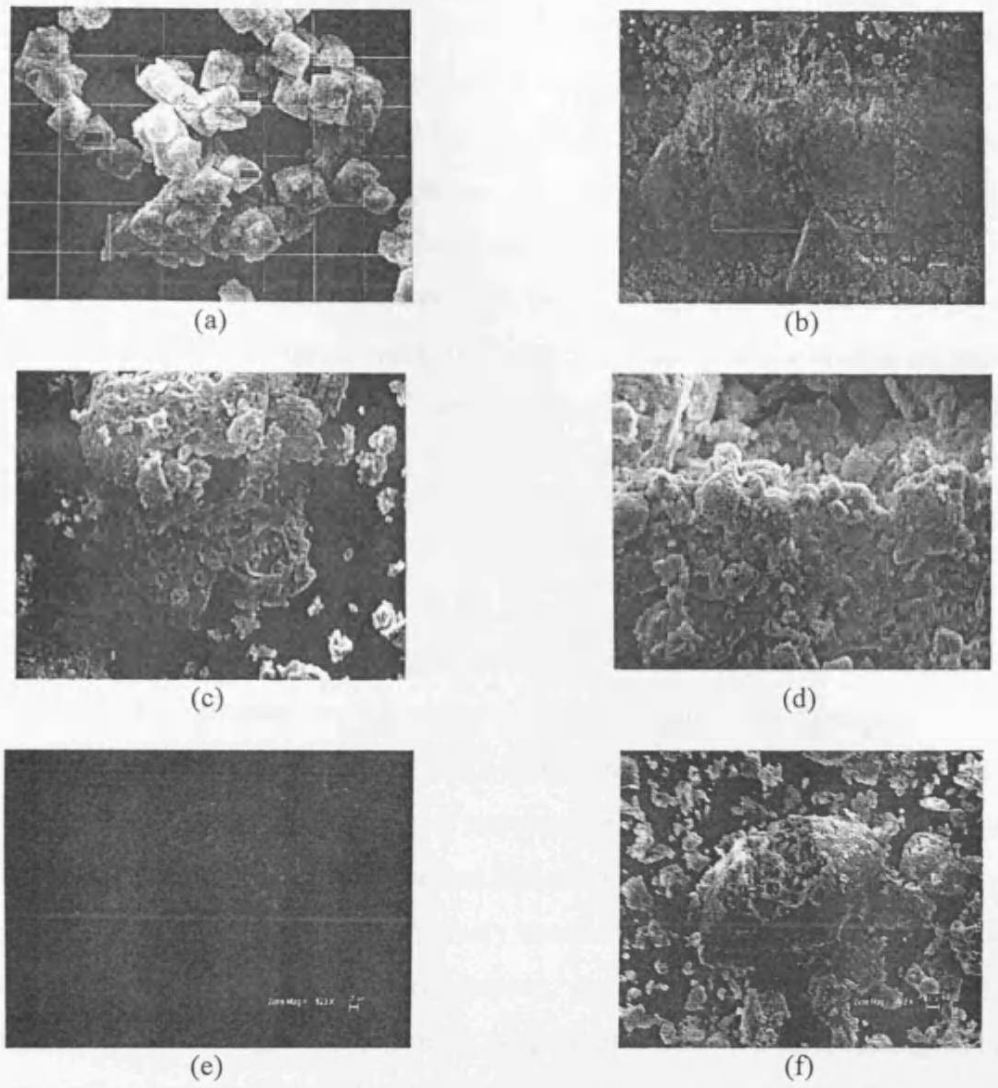

Figure 6.12: SEM micrograph of copper oxide (a) precipitation with urea (b) quick precipitation with sodium hydroxide, (c) sol gel and calcined in air at 250 °C, (d) sol gel and calcined in air at 400 °C, (e) Sol gel and calcined in H_2/Argon at 400 °C, (f) sol gel and calcined in air at 400 °C followed sodium borohydride treatment.

It is well reported in the literature that the morphologies (and other catalyst properties) of copper oxide can be tuned by changing the preparation technique as well as the copper precursor.[31,34-36] For example, in the case of copper oxide synthesised via the homogeneous precipitation of copper salt solutions in the presence of urea, it was shown that the nature of the salt precursor (*i.e.* chloride, nitrate, and sulfate) played an essential role in the properties of the generated solid phase.[36] While a nitrate precursor yielded spherical amorphous particles, switching nitrate to sulfate produced needle-shape materials. The particle morphology of solid precursor samples were claimed to be retained even after heat treatment at higher temperature where CuO was produced. Similar observation to the

literature[36] were observed in this study when copper chloride was used as a precursor in the presence of urea. In this case, the bipyramidal particles of solid copper chloride hydroxide were obtained. However, in contrast to the literature, this study observed a slight change of the particle morphology by a heat treatment procedure, especially after calcination in air at 400 °C where it showed a cubic-like structure.

In the case of copper oxide prepared via quick-precipitation with NaOH, it was reported by Zhu and co-workers that in the absence of glacial acetic acid, copper acetate solution might hydrolyze at temperatures above 80 °C, and that needle-like CuO nanocrystals may form.[31]

6.4.2.5. X-ray photoelectron (XPS) analysis

The surface composition and oxidation state of selected copper oxide catalysts were measured by X-ray photoelectron spectroscopy (XPS). Figure 6.13 displays Cu (2p) X-ray photoelectron (XPS) spectra acquired from a fresh copper oxide catalyst synthesised via the sol-gel technique and calcined at different temperature, along with a catalyst prepared using the quick-precipitation method with sodium hydroxide. The characteristic binding energies for this transition (Cu $Pd_{3/2}$) were previously detailed in table 6.3. In agreement with the XRD analysis (section 6.4.2.2 of this chapter), the presence of a distinctive shake-up satellite peak in the XPS spectra confirmed the presence of Cu^{2+} phase. The signal is rather intense in CuO_{Qp} compared to CuO_{Cp} samples and again indicates the surface composition of copper. A slightly weaker signal for CuO_{Sg} that was calcined at 250 °C supported the presence of a minor Cu^{1+} phase, as shown in the XRD pattern.

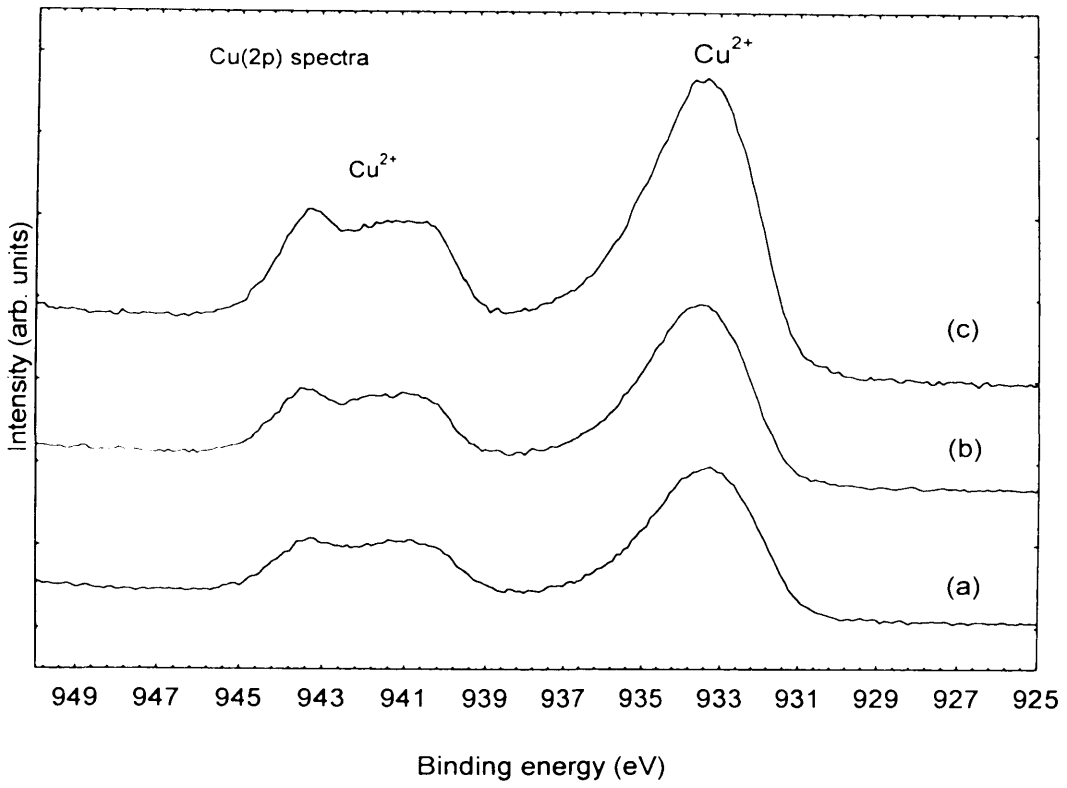

Figure 6.13: Cu 2p spectra of copper oxide catalyst. (a) Sol gel and calcined at 250 °C in air, (b) Sol gel and calcined at 400 °C in air, (c) Precipitation (NaOH) and dried at 25 °C in air.

As previously mentioned, Cu LMM Auger spectra are required in order to clearly differentiate between Cu^{1+} and Cu^0 phases.[20] The characteristic binding energy, along with the kinetic energy for Cu LMM Auger spectra with different oxidation states of Cu are presented in table 6.11.

Table 6.11: Values of the Cu LMM Auger binding and kinetic energy, respectively for Cu metal, Cu_2O and CuO[37]

	Cu LMM Binding energy, eV[a]	Cu LMM Kinetic energy, eV[a]
Metallic Cu	568.1	918.4
Cu_2O	570.3	916.5
CuO	569.5	917.8

[a]Peaks referenced to C 1s=284.6 - 284.7 eV

Cu Auger spectra (Cu LMM) for CuO_{Sg} as shown in figure 6.14 gave almost identical spectra for both samples (calcined at 250 and 400 °C, respectively) with a main peak at a binding energy of 569 eV corresponding to Cu^{2+} species, and a shoulder peak at 572 eV. This shoulder peak is higher than those reported in the literature for the Cu^{1+} species.[37] However, given the fact that metallic copper species were not detect through XRD analysis, and that the binding energy of Cu^0 is reported to be lower than Cu^{2+} species, it was assumed here that the shoulder peak was due to the presence of a Cu_2O (Cu^{1+}) phase. In general, the XPS analysis was in agreement with the XRD data where CuO was shown as the main phase.

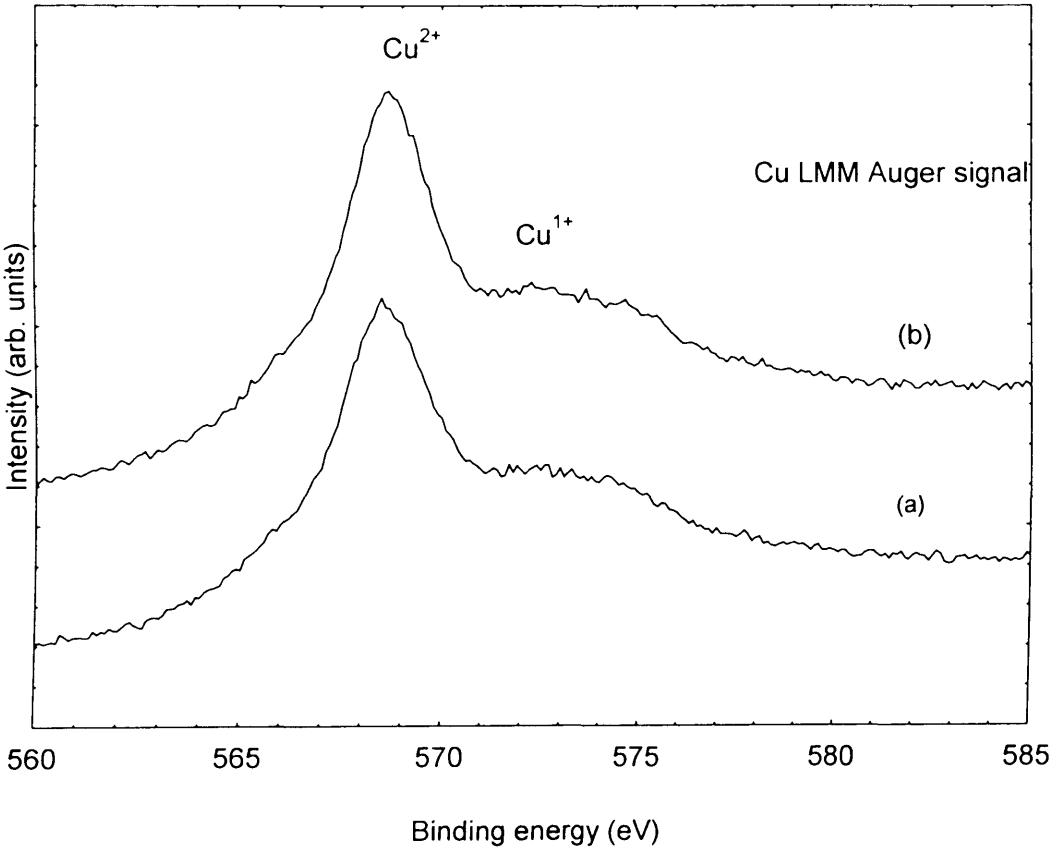

Figure 6.14: Cu LMM Auger spectra of copper oxide catalyst. (a) Sol gel and calcined at 250 °C in air, (b) Sol gel and calcined at 400 °C in air

6.5. Liquid phase methane oxidation with copper oxide catalyst systems

6.5.1. Copper catalysts: effect of preparation technique

As shown in table 6.12, the copper oxide materials prepared via the precipitation technique with urea (CuO_{Cp}) gave comparable oxygenates productivity to the Au-Pd supported nanoparticles catalysts, though in this case methyl hydroperoxide was the major product. A higher selectivity to the intermediate species rather than methanol seems to strongly relate to the Cu^{2+} species available on the CuO_{Cp} catalyst, which is in agreement with the data observed for a calcined monometallic Cu/TiO_2 catalyst.

Table 6.12: Liquid phase methane oxidation with copper oxide based catalyst synthesised via different technique and comparison with $5wt\%Au\text{-}Pd/TiO_{2IW}$ catalyst.

Entry	Preparation technique	Product amount (μmol)				Methanol selectivity (%)[c]	Oxygenate productivity (Mol/kg_{cat}/ Hour)[d]	H_2O_2 Remain (μmol) [e]
		CH_3OH [a]	HCOOH [a]	MeOOH [a]	CO_2 in gas [b]			
1	Co-precipitate (urea)	0.41	0	2.85	0.24	11.7	0.236	19
2	Sol-gel	1.60	0	3.03	0.90	28.9	0.336	275
3	Quick-precipitate (NaOH)	1.93	0	0.67	0.52	61.9	0.188	105
4	$5wt\%AuPd/TiO_{2IW}$	1.89	0	1.57	0.37	49.3	0.250	383

Reaction Time; 30 min, Reaction Temp; 50 °C, CH_4 pressure: 30 bar, Catalyst: 28 mg, H_2O_2: 0.5M, Solvent: H_2O, 10 mL. [a] Analysis using ^{1}H-NMR, [b]Analysis using GC-FID, [c] Methanol selectivity = (mol of CH_3OH/ total mol of products) * 100, [d] Oxygenates productivity = mol of oxygenates / Kg_{cat} / reaction time (h), [e] Assayed by Ce^{+4} (aq) titration.

Implementing a sol-gel technique for the preparation of copper oxide (CuO_{Sg}) increased both oxygenates activity and methanol selectivity, as well as there being more oxidant remaining after reaction. However, similar to the precipitation method, methyl hydroperoxide still evolved as a main product. Since the particle size and surface area of CuO_{Sg} is in a similar range compared to CuO_{Cp} catalyst, it was believed here that the difference in catalytic activity and selectivity might relate to the oxidation state of copper.

Detailed X-ray diffraction analysis revealed that minor peaks corresponding to Cu_2O (Cu^{1+}) were observed in the CuO_{Sg} catalyst, and these are believed to take part in the reaction. Modification of the precipitation method using NaOH instead of urea in addition to the quick precipitation process generated crystalline CuO phases with smaller average particle size and a higher surface area. An analogue methane reaction shows 62% methanol selectivity which is higher compared to the 12% and 29% obtained for CuO_{Cp} and CuO_{Sg} catalysts, respectively. In contrast, oxygenates productivity followed the opposite trend where only 0.188 mol/kg_{cat}/hrs was observed compared to 0.236 and 0.336 mol/ kg_{cat}/hrs for the CuO_{Cp} and CuO_{Sg} catalysts respectively. It seems that an increase in methanol selectivity with CuO_{Qp} catalyst may be attributed to the smaller crystallite size of the catalyst (see table 6.6), and the lower overall activity could originate from the type of copper species evolved during the reaction. In this case, the presence of Cu^{2+} with minor amounts of Cu^{1+} in the CuO_{Sg} catalyst was preferred for obtaining higher oxygenates productivity compared to the single Cu^{2+} oxidation state observed in both CuO_{Cp} and CuO_{Qp} respectively. Further discussion on the effect of Cu oxidation state on catalytic methane oxidation is covered in the following section.

6.5.2. Effect of copper oxidation state

In order to verify the effect of the oxidation state on the catalytic activity, product distribution and additionally hydrogen peroxide decomposition, an effort has been made to tune the distribution of the copper oxidation state by subjecting the copper oxide precursor prepared using sol-gel technique to different calcinations temperatures. The crystallite size calculated using the Scherrer equation shows that the average crystallite size is in the range of 25–31 nm. Phase composition analysis from the XRD data illustrated that both samples (calcined at 250 °C and 400 °C) consist of CuO with minor amounts of Cu_2O phase, as detailed in section 6.4.2.2. The presence of Cu^{1+} was more prominent in the catalyst calcined at 250 °C. In general, catalysts with a mixture of Cu^{1+} and Cu^{2+} showed a higher oxygenate productivity than the single CuO phase catalyst, particularly on the formation of the methyl hydroperoxide intermediate. The dual-phase catalyst also showed a lower rate of hydrogen peroxide decomposition (table 6.13). The formation of the intermediate species was enhanced by increasing the percentage of Cu^{1+} species, and this is in line with the data presented in previous section. The exact percentages of copper species calculated from the

XRD data for the CuO_{Sg} catalyst (calcined at 250 °C) show 78% of Cu^{2+} (CuO) with 22% of Cu^{1+} (Cu_2O). CuO_{Sg} catalyst calcined at 400 °C consists of 96% of Cu^{2+} with only 4% of Cu^{1+} oxidation state.

Table 6.13: Liquid phase methane oxidation with copper oxide based catalyst synthesised via sol-gel technique and calcined at different temperature.

Entry	Calcinations in air (°C)	Product amount (μmol)				Methanol Selectivity (%)[c]	Oxygenate productivity (Mol/kg_{cat}/ Hour)[d]	H_2O_2 Remain (μmo) [e]
		CH_3OH [a]	HCOOH [a]	MeOOH [a]	CO_2 in gas[b]			
1	250	1.83	0	6.00	0.18	22.8	0.567	2074
2	400	1.60	0	3.03	0.90	28.9	0.336	275

Reaction Time; 30 min, Reaction Temp; 50 °C, CH_4 pressure: 30 bar, Catalyst: 28 mg, H_2O_2 0.5M, Solvent: H_2O, 10 mL. [a] Analysis using ^{1}H-NMR, [b]Analysis using GC-FID, [c] Methanol selectivity = (mol of CH_3OH/ total mol of products) * 100, [d] Oxygenates productivity = mol of oxygenates / Kg_{cat} / reaction time (h), [e] Assayed by Ce^{+4} (aq) titration.

The amount of hydrogen peroxide detected after reaction for the catalyst calcined at 250 °C is 7 times higher compared to the higher calcination temperature counterpart. It was noted here that the crystallite size of the copper oxide catalyst calcined at 250 °C was smaller (25 nm) compared to the sample calcined at 400 °C (31 nm). This data again indicates a lower rate of hydrogen peroxide decomposition observed for samples with smaller particle sizes, as it was shown in the previous section. It is important to state here that both samples have similar characteristics, where a mixture of Cu^{2+} and Cu^{1+} are observed. An increase in the amount of Cu^{1+} significantly suppresses the hydrogen peroxide decomposition. Thus, it was believed that hydrogen peroxide decomposition was strongly affected by the type of copper evolved during the reaction, rather than a particle size effect alone.

In view of the fact that the copper oxidation state can play a significant role in controlling the activity and selectivity of methane oxidation, it is crucial to separately verify each catalyst with distinctive oxidation states. In the case of Cu^{1+}, the reaction was conducted using commercial Cu_2O with an average crystallite size of 81 nm. It is interesting that only traces of CO_2 were observed after reaction, and that a methanol selectivity of 42% was obtained. However, oxygenates productivity was less than half of the catalyst containing

both 1+ and 2+ oxidation states, or catalysts with the 2+ oxidation state alone (table 6.14). Given that the copper oxide catalysts discussed above only contain Cu^{1+}/Cu^{2+} species, another step has been taken in order to obtain metallic Cu, by subjecting the copper oxide precursor to a stream of 5% hydrogen in argon. The presence of metallic copper as major phase, though with minor amounts of Cu^{1+}, was confirmed by XRD analysis. It is noteworthy that the oxygenate productivity is almost identical to the calcined catalyst. However, the reduced catalyst also shows higher methanol selectivity as well as significantly suppressing the H_2O_2 decomposition. Higher amounts of H_2O_2 were detected after reaction for the reduced catalyst, and this is in agreement with the data observed with the reduced 2.5wt%Cu/TiO_{2IW} catalyst (see section 6.2.2 of this chapter). Moreover, the higher methanol selectivity with the reduced catalyst is in line with catalytic data observed for methane oxidation catalysed by 5wt%AuPd1.0wt%Cu/TiO_{2IW}, as discussed in section 6.2.2 of this chapter. In both catalysts, metallic copper was the major phase whereas the oxidised state of copper evolved as minor phase.

Table 6.14: Liquid phase methane oxidation with copper oxide based catalyst synthesised via sol-gel technique followed by different pretreatment

Entry	Catalyst/ pretreatment	Product amount (μmol)				Methanol Selectivity (%)[c]	Oxygenate productivity (Mol/kg_{cat}/ Hour)[d]	H_2O_2 Remain (μmol) [e]
		CH_3OH [a]	HCOOH [a]	MeOOH [a]	CO_2 in gas[b]			
1	Static air, 400 °C	1.60	0	3.03	0.90	28.9	0.336	275
2	Flow H_2/Ar 400 °C	2.15	0	2.54	0.73	39.7	0.335	520
3	Static air, 400 °C & $NaBH_4$ treatment	2.13	0	0.20	<0.1	87.7	0.166	179
4	Cu_2O (Commercial, Fisons)	0.93	0	1.21	0.1	41.5	0.153	61

Reaction Time; 30 min, Reaction Temp; 50 °C, CH_4 pressure: 30 bar, Catalyst: 28 mg, H_2O_2: 0.5M, Solvent: H_2O, 10 mL. [a] Analysis using ^{1}H-NMR, [b]Analysis using GC-FID, [c] Methanol selectivity = (mol of CH_3OH/ total mol of products) * 100, [d] Oxygenates productivity = mol of oxygenates / Kg_{cat} / reaction time (h), [e] Assayed by Ce^{+4} (aq) titration.

In addition to reduction in hydrogen flow environment, the phase composition of the copper oxide synthesised via the sol-gel technique was also tuned by chemical reduction with sodium borohydride ($NaBH_4$). In this case, the reduction step was carried out after post-synthesis calcinations of the CuO sample at 400 °C in static air. Since the reduction utilised a chemical compound rather than reducing gas, it is possible that both the structural composition and the oxidation state could easily be tuned by controlling the molar ratio of $NaBH_4$ and copper. Brief analysis using XRD on a CuO material pre-treated with an equimolar amount of $NaBH_4$ to copper indicated the presence of Cu_2O as a main phase, plus a minor peak corresponding to metallic copper. Catalytic activity data shows comparable oxygenate productivity to the pure Cu_2O catalyst as only trace amounts of CO_2 were detected in the gas phase. Conversely, oxygenates distribution was shifted from methyl hydroperoxide into methanol (88%) while the amount of hydrogen peroxide remaining was slightly higher than the pure Cu_2O catalyst. In addition to the effect of the oxidation state, the higher methanol selectivity observed with $NaBH_4$-treated copper oxide may originate from the induced effect of trace amounts of sodium borohydride remaining on the catalyst, which could potentially reduce methyl hydroperoxide to methanol.

To corroborate the observation of hydrogen peroxide utilisation, H_2O_2 decomposition studies were performed on catalysts containing different phases of copper. The results in table 6.15 indicate that pure Cu_2O with 1+ oxidation state gave higher peroxide decomposition (up to 48%) whereas only 4.2% decomposition was observed with the calcined catalyst (Cu^{2+} as a main phase). However, slightly higher H_2O_2 decomposition (12%) was calculated on the reduced copper oxide catalyst. This indicates that the hydrogen peroxide utilisation is not controlled by either the crystallite size or oxidation state alone, but that it is a combination of both factors.

Table 6.15: Hydrogen peroxide decomposition test using different copper oxide catalyst

Entry	Catalyst/pretreatment	H_2O_2 decomposition (%)
1	CuO_{Sg} (static air, 400°C)	4.2
2	CuO_{Sg} (Flow of H_2/Ar, 400°C)	12.0
3	Cu_2O (Fisons)	48.0

Based on catalytic data, it seems that the oxidation state of copper considerably affects the oxygenate productivity, the selectivity to methanol and additionally hydrogen peroxide utilisation. However, this is rather complex as a combination of more than one oxidation state is preferred to any single oxidation state. In particular, higher oxygenate productivity and selectivity to methanol is favoured on catalysts having a combination of metallic copper with minor oxidised copper species. It is possible that the copper species available at the beginning of reaction is crucial, and that in the presence of hydrogen peroxide as oxidant, a redox process might occur throughout the reaction progress.

6.6. Conclusions

In this chapter, copper metal was selected as a co-metal for supported Au based catalysts, or copper was used in the form of copper oxide for the selective oxidation of methane. Copper oxide was prepared with different preparation techniques, and post-synthetically modified by calcination treatments. Depositing copper together with Au/Pd on to the surface of TiO_2 significantly enhanced the catalytic activity for methane oxidation, as well as improving the hydrogen peroxide utilization. In particular, a trimetallic 5wt%AuPd1wt%Cu/TiO_{2IW} catalyst achieved selectivity to methanol of around 83% with oxygenates productivity three times higher compared to the bimetallic 5wt%Au-Pd/TiO_{2IW} analogue. It was found that the Cu/Au-Pd ratio was crucial in obtaining higher activity and selectivity to methanol. The most active ratio was obtained in the presence of 2.5wt%Cu, whereas the highest methanol selectivity was obtained with 1.0wt% of copper loading. Further catalyst characterisation using XPS, XRD and H_2-TPR indicate either that the Au-Pd nanoparticles evolved as an alloy where Cu was highly dispersed on the TiO_2 surface, or that the Au-Pd nanoparticles were covered by copper. The origin of the increased productivity and selectivity to methanol over the reference 5wt%Au-Pd/TiO_{2IW} catalyst was based on the specific role of Cu and Au-Pd metals. Copper seems to enhance the formation of the intermediate product (methyl hydroperoxide), though the selective transformation of methyl hydroperoxide to methanol still required the Au-Pd active sites.

To demonstrate the effect of copper, another set of experiments were carried out by utilizing copper oxide catalysts synthesised by different methods and post-synthetically modified by different treatment procedures. These studies successfully developed copper oxide materials with different oxidation states, particle sizes, surface areas and

morphologies. After a series of methane oxidation reactions using the prepared copper oxide materials, the oxidation state of copper was observed to be the most prominent factor for controlling oxygenates productivity and selectivity, compared to other factors such as the particle size and surface area. The oxidation state, either as a single or a mixture of copper species, could be tuned by several means of pretreatment technique. A combination of copper species, either Cu^{2+}/Cu^{1+} or Cu^{1+}/Cu^{0} is preferred over a single copper oxidation state. A redox reaction is proposed to occur throughout the reaction.

Overall, the presence of copper was shown to significantly beneficial for enhancing the catalytic activity and selectivity of the Au-based catalysts. The roles of copper were briefly shown with the copper oxide catalytic system.

References:

1. H. Sinfelt, R. J. B.; Patent, U. Ed., 1976.
2. Bracey, C. L.; Ellis, P. R.; Hutchings, G. J. *Chemical Society Reviews* **2009,** *38*, 2231-2243.
3. Bracey, C. L.; Carley, A. F.; Edwards, J. K.; Ellis, P. R.; Hutchings, G. J. *Catalysis Science & Technology* **2011,** *1*, 76-85.
4. Chimentão, R. J.; Medina, F.; Fierro, J. L. G.; Llorca, J.; Sueiras, J. E.; Cesteros, Y.; Salagre, P. *Journal of Molecular Catalysis A: Chemical* **2007,** *274*, 159-168.
5. Della Pina, C.; Falletta, E.; Rossi, M. *Journal of Catalysis* **2008,** *260*, 384-386.
6. Shiota, Y.; Yoshizawa, K. *Journal of the American Chemical Society* **2000,** *122*, 12317-12326.
7. Groothaert, M. H.; Smeets, P. J.; Sels, B. F.; Jacobs, P. A.; Schoonheydt, R. A. *Journal of the American Chemical Society* **2005,** *127*, 1394-1395.
8. Smeets, P. J.; Groothaert, M. H.; Schoonheydt, R. A. *Catalysis Today* **2005,** *110*, 303-309.
9. Lin, M.; Hogan, T.; Sen, A. *Journal of the American Chemical Society* **1997,** *119*, 6048-6053.
10. Lee, B.; Sakamoto, Y.; Hirabayashi, D.; Suzuki, K.; Hibino, T. *Journal of Catalysis* **2010,** *271*, 195-200.
11. Lopez-Sanchez, J. A. D., Nikolaos; Jenkins, Robert Leyshon; Carley, Albert Frederick; Willock, David James; Taylor, Stuart Hamilton; Hutchings, Graham John; Rahim, Mohd Hasbi. . Office, E. P. Ed.; Cardiff University: United Kingdom, 2011.
12. Okuno, T.; Ohba, S.; Nishida, Y. *Polyhedron* **1997,** *16*, 3765-3774.
13. Park, E. D.; Hwang, Y.-S.; Lee, C. W.; Lee, J. S. *Applied Catalysis A: General* **2003,** *247*, 269-281.
14. Rodriguez, J. A.; Kim, J. Y.; Hanson, J. C.; Pérez, M.; Frenkel, A. I. *Catalysis Letters* **2003,** *85*, 247-254.
15. Coq, B.; Tachon, D.; Figuéras, F.; Mabilon, G.; Prigent, M. *Applied Catalysis B: Environmental* **1995,** *6*, 271-289.
16. B. Pawelec, A. M. V., V. La Parola, E. Cano-Serrano,; J.M. Campos-Martin, J. L. G. F. *Applied Surface Science* **2005,** *242*, 380-391.
17. Venezia, A. M.; La Parola, V.; NicolI; V.; Deganello, G. *Journal of Catalysis* **2002,** *212*, 56-62.
18. Batista, J.; Pintar, A.; Mandrino, D.; Jenko, M.; Martin, V. *Applied Catalysis A: General* **2001,** *206*, 113-124.
19. S. Poulston, P. M. P., M. Bowker. *Surface and Interface Analysis* **1996,** *24*, 811-820.
20. Corma, A.; Palomares, A.; Márquez, F. *Journal of Catalysis* **1997,** *170*, 132-139.
21. Edwards, J. K.; Solsona, B. E.; Landon, P.; Carley, A. F.; Herzing, A.; Kiely, C. J.; Hutchings, G. J. *Journal of Catalysis* **2005,** *236*, 69-79.
22. Hilaire, L.; Légaré, P.; Holl, Y.; Maire, G. *Surface Science* **1981,** *103*, 125-140.

23. Molenbroek, A. M.; Haukka, S.; Clausen, B. S. *The Journal of Physical Chemistry B* **1998,** *102*, 10680-10689.
24. Giorgio, S.; Henry, C. R. *The European Physical Journal - Applied Physics* **2002,** *20*, 23-27.
25. Zhang, F.; Miao, S.; Yang, Y.; Zhang, X.; Chen, J.; Guan, N. *The Journal of Physical Chemistry C* **2008,** *112*, 7665-7671.
26. Chen, C.-S.; You, J.-H.; Lin, J.-H.; Chen, Y.-Y. *Catalysis Communications* **2008,** *9*, 2381-2385.
27. Llorca, J.; Domínguez, M.; Ledesma, C.; Chimentão, R. J.; Medina, F.; Sueiras, J.; Angurell, I.; Seco, M.; Rossell, O. *Journal of Catalysis* **2008,** *258*, 187-198.
28. Z. Gu, L. L., S. Chen. *Indian Journal of Chemical Technology* **2009,** *16*, 175-180.
29. L. Durand-Keklikian, E. M. *Colloid & Polymer Science* **1990,** *268*, 1151-1158.
30. Faungnawakij, K.; Shimoda, N.; Fukunaga, T.; Kikuchi, R.; Eguchi, K. *Applied Catalysis B: Environmental* **2009,** *92*, 341-350.
31. Zhu, J.; Li, D.; Chen, H.; Yang, X.; Lu, L.; Wang, X. *Materials Letters* **2004,** *58*, 3324-3327.
32. www.wikipedia.org. In *Wikipedia*, 2011.
33. Howard Sanders, A. J.; Porous Material Inc, 2000.
34. Vaseem, M.; Umar, A.; Hahn, Y. B.; Kim, D. H.; Lee, K. S.; Jang, J. S.; Lee, J. S. *Catalysis Communications* **2008,** *10*, 11-16.
35. Sun, L.; Zhang, Z.; Wang, Z.; Wu, Z.; Dang, H. *Materials Research Bulletin* **2005,** *40*, 1024-1027.
36. Matijević, S. K. a. E. *Journal of Material Research* **1991,** *6*, 766-777.
37. Poulston, S.; Parlett, P. M.; Stone, P.; Bowker, M. *Surface and Interface Analysis* **1996,** *24*, 811-820.

CHAPTER 7

Conclusions and Recommendation for Future Work

7.1. Conclusions

Activation of short chain alkanes and their catalytic oxidation into useful organic oxygenates is a major challenge for industry and academia. Due to the recent discoveries related to the ability of gold based nanoparticles to perform a variety of reactions, further work into the activation of carbon-hydrogen bonds by gold and gold alloyed nanoparticles was the central topic of this study and has been addressed in this PhD thesis. The research intends to develop a catalytic system that can activate methane under very mild conditions. Additionally, environmentally benign catalysis was focused on these studies. An area of heterogeneous catalysis including catalyst characterisation, reaction design, product analysis and validations, proposed reaction mechanisms and key reaction parameters for controlling selectivity and activity were covered briefly in this thesis.

It is clear from the work outlined in the proceeding chapters that the activation of primary C-H bond in saturated alkanes was successfully carried out using heterogeneous Au, Pd, Cu based catalyst. In **chapter 3**, bimetallic Au-Pd supported nanoparticles catalysts have been shown to oxidise primary C-H bond in toluene and toluene derivative at relatively mild solvent-free reaction conditions in the presence of molecular oxygen as oxidant. Catalytic activity and product distribution was shown to strongly relate to the nature of catalyst where smaller and narrower metal particle sizes were observed to give enhanced catalytic performance. Sol-immobilised technique was preferred method in synthesising Au-Pd supported nanoparticles catalyst in this particular reaction due to the possibility of forming small metal particle size and narrow particle size distribution with this particular technique. Given the fact that Au-Pd catalyst has been demonstrated to activate primary C-H bond, further studies were performed by switching the aromatic hydrocarbons with lower chain alkanes *i.e.* methane and ethane.

In **chapter 4**, liquid phase methane oxidation was carried out using addition of hydrogen peroxide as oxidant. Comparison between heterogeneous with analogue homogeneous metal catalyst has been performed where only methanol and methyl hydroperoxide was

observed in former case. In later case, the product distribution was different which preferred formation of formic acid and carbon dioxide as overoxidation product. In addition, precipitation of metal was occurred in homogeneous system. Therefore, particular attention was made in the investigation of reaction parameters on heterogeneous Au-Pd supported catalyst. In general, oxygenates productivity was observed to increase by increasing the pressure of gas substrate, hydrogen peroxide concentration, reaction temperature up to 70 °C as well as by prolong the reaction time. The hydrogen peroxide utilisation was identified as one of the important factors where the developed catalyst should not unselectively decompose pre-loaded H_2O_2. Hence, an impregnated synthesise Au-Pd supported catalyst with oxidised state of metal (*i.e.* PdO, Pd^{2+}) and bigger particle size was preferred than smaller and reduced state (Pd^0 and Au^0) of metal obtained in sol-immobilisation technique. The presence of metal in metallic state especially Pd was identified to accelerate the decomposition of hydrogen peroxide subsequently decreased the catalytic activity. Moreover, the Au core Pd shell structure with surface dominance with PdO in impregnated catalyst was found to have better ability to abstract hydrogen from methane molecule as well as to stabilise the hydroperoxy species compared to Pd and Au in metallic state observed in sol-immobilised catalyst. The better catalytic activity of Au-Pd catalyst consist Pd in oxidised state (Pd^{2+}) was further strengthened by lower catalytic activity and higher hydrogen peroxide decomposition observed with the methane reaction carried out in the presence of Au-Pd/TiO_2 catalyst reduced in H_2/Ar environment. The presence of Pd in metallic state in reduced catalyst was confirmed by XRD and XPS analysis, respectively. In term on the types of supported materials, TiO_2 was discovered as the superior support compared to other tested support such as SiO_2, CeO_2, Al_2O_3 and activated carbon. This particular support was suggested to stabilise the surface hydroperoxy species consequently enhanced the probability to oxidise methane to oxygenated products. By varying the Au to Pd ratio, oxygenates productivity and selectivity could be tuned where the surface composition of Au/Pd indicated to play an important role. A balance between Au and metal ratio was favoured in transforming methyl hydroperoxide to methanol. At the end of the chapter, the applicability of the developed Au-Pd catalytic system was examined on ethane. Ethane with better solubility in water and weaker C-H bond strength compared to methane was found to enhance catalytic activity with three times higher oxygenates productivity. In standard reaction condition, the product distribution favoured on alcohol and intermediate alkyl hydroperoxide as main products. In addition, acetaldehydehyde in hydrated form was

obtained. Increasing the reaction temperature enhances the C-C splitting products where methanol was detected at standard reaction condition.

In view of the fact that primary C-H bond in methane and ethane have been successfully activated using H_2O_2 as oxidant, in **chapter 5**, particular attention was made to generate the oxidant in *in-situ* condition with the presence of H_2 and O_2 gases. The Au-Pd supported nanoparticles catalyst was known to synthesise H_2O_2 using *in-situ* approach and it was reported to work *via* formation of hydroperoxy species. This parallel one-pot process might slowly provide the active species into the system and in general, higher methanol selectivity compared to similar reaction conditions with pre-loaded H_2O_2 was observed. Manipulating reaction parameters such as temperature and concentration of feed H_2/O_2 gases affected the formation of oxygenates and its distribution. Synergistic effect of Au-Pd bimetallic catalyst has been shown where it is active and selective compared to monometallic catalyst counterpart. Nature of support is crucial in order to successfully utilised as bi-functional catalyst. Therefore, TiO_2 was discovered as the suitable support for methane oxidation with *in-situ* generated H_2O_2 approach. Activation of methane using *in-situ* generated H_2O_2 was preferred on larger metal particle size with Au-Pd in Au core Pd shell structure and the Pd was preferred in oxidised state (PdO). On the basis of the results obtained, mechanistic pathways have been proposed via methyl hydroperoxide as the key intermediate product. Formation of methyl hydroperoxide as intermediate product was occurred through interaction of surface bound hydroperoxyl species with methyl species and the methanol formation could be generated via several pathways including hydrolysis of methoxy species. Minor reaction pathways cannot be neglected.

Since most of the catalytic studies used Au-Pd supported nanoparticles, an improvement of the system has been shown in **chapter 6** by integrating copper metal and the reactions were carried out using addition of H_2O_2 as oxidant. Depositing copper successfully enhanced catalytic activity and selectivity as well as improved hydrogen peroxide utilisation. It was suggested that copper might assist in generating methyl hydroperoxide intermediate whereas Au-Pd alloy responsible in selective formation of methanol. The presence of Au-Pd alloyed phase was confirmed by XPS and XRD studies whereas majority of Cu was proposed to evolve as single species (with mixture of copper in oxidised and reduced state) and small in particle size. In addition, with the aims to explore new catalyst and to corroborate the role of copper, a series of copper oxide catalysts have been developed and tested in methane oxidation reaction using H_2O_2 as oxidant. Based on the catalytic data, it seems the oxidation state of copper was shown to be an important

factor in controlling the catalytic activity and selectivity. A mixture of copper oxidation state was preferred than a single state and the redox process was deemed to occur throughout the reaction progress.

7.2. Recommendation for future work

Further investigations are possible for all fields explored in this thesis. Brief recommendations are shown below:

1. It was demonstrated in this study that supported Au-Pd nanoparticles catalysts were successfully oxidised methane and ethane using hydrogen peroxide as oxidant. However, it is important in the future study to utilise molecular oxygen or air as oxidant and it is possible to achieve by tuning the reaction conditions and morphology as well as characteristics of metal supported catalysts. For instance, activation of oxygen can possibly occur in the presence of very small metal particles of catalyst.
2. It has been proven in this study that Au-Pd supported catalysts are capable in oxidising methane using *in-situ* generated H_2O_2 approach. Therefore, another step could be taken by combining the H_2O_2 generating capability of Au-Pd system with another active catalyst such as ZSM-5.
3. Solubility of the H_2/O_2 is crucial in generating higher amount of oxidant consequently improved the catalytic activity. An alternative way to do it other than chemical means is by changing the reactor configuration. Since the study used the autoclave batch reactor, one of the steps can be taken is by replacing the impeller purposely to improve the gas dispersion into the liquid medium. Better dispersion might improve the *in-situ* generation of H_2O_2 and also enhance the concentration of solubilised methane in water.
4. One of the limitation in batch system is the product produced is overoxidised. The flow reactor set-up will facilitate the problem by limiting the exposure of the product to the catalyst consequently increase the selectivity of target product by varying contact time. Besides, the system allowing a dilute H_2O_2 as oxidant, this is important in order to avoid the change of the catalyst structure *i.e.* oxidation state and particle size since this factor will affect the reusability of the catalyst.

5. Other than one-pot single stage reaction system utilised in this study, the alternative two stage process where H_2O_2 synthesis and alkane oxidation operated at different reactors possibly can be used. In this case, the H_2O_2 generated in the first reactor could be continuously supplied to the second reactor.
6. The possible used of another characterisation technique such as STEM could further help in identifying the nature of developed catalyst especially on complex trimetallic Au-Pd-Cu supported systems. Combination between STEM, XPS and XRD data might give a clear picture on any possible formation of alloy and also the average particle size of metal. In case of copper oxide system, an *in-situ* XRD analysis especially in the present of gas substrate could be beneficial in monitoring the phase changing during reactions.

Appendix A: Products identification and validation

Appendix A (1a): Calibration Factor and R^2 data from the calibration curve for oxidation of toluene.

Standard	CF / Mole %	R^2 / Mole %	CF / Concentration	R^2 / Concentration
Benzyl alcohol	657520.673	0.992	7134835.611	0.994
Benzaldehyde	564804.557	0.995	3257665.026	0.998
Benzoic acid	520965.696	0.999	5594474.037	0.999
Benzyl benzoate	1170606.036	1.000	12571797.575	1.000
Toluene	715628.567	0.999	7667894.856	1.000

Appendix A (1b): Calibration factor, conversion (mol %), selectivity (%) and mass balance (%) based on external standard (2-propanol).

Standard	2.5%				5%			
	Calibration factor	Selectivity (%)	Conversion (mol %)	Mass balance (%)	Calibration factor	Selectivity (%)	Conversion (mol %)	Mass balance (%)
Benzyl alcohol	0.2656113884	28.70			0.284530504	29.51		
Benzaldehyde	0.31965637	30.61			0.333400725	29.88		
Benzoic acid	0.361317902	25.42	7.95	99.99	0.357393409	24.68	16.18	99.99
Benzyl benzoate	0.168394082	15.27			0.157188503	15.93		
Toluene	0.270081966	-			0.261466543	-		

Appendix A (1c): Calibration Factor and R^2 data from the calibration curve for oxidation of 4-methoxytoluene.

Standard	CF / Mole %	R^2 / Mole %	CF / Concentration	R^2 / Concentration
4- Methoxybenzyl alcohol	323152.608	0.996	4099393.782	0.996
4- Methoxybenzaldehyde	324988.284	0.993	4122549.942	0.993
4- Methoxybenzoic acid	212355.617	0.996	2693909.308	0.996
4- Methoxytoluene	416634.741	0.947	5288746.513	0.947

Appendix A (1d): Calibration factor, conversion (mol %), selectivity (%) and mass balance (%) based on external standard (2-propanol).

Standard	1%				2%			
	Calibration factor	Selectivity (%)	Conversion (mol %)	Mass balance (%)	Calibration factor	Selectivity (%)	Conversion (mol %)	Mass balance (%)
4-Methoxybenzyl alcohol	0.14182182	36.31			0.162761534	35.66		
4-Methoxybenzaldehyde	0.150309843	34.00	2.83	100	0.164067094	36.03	5.77	99.99
4-Methoxybenzoic acid	0.244294052	29.70			0.240707769	28.30		
4-Methoxytoluene	0.140260577	-			0.136402856	-		

Appendix A (2): Gas chromatography-mass spectroscopy analysis of liquid phase solution from methane oxidation using H_2O_2 as oxidant

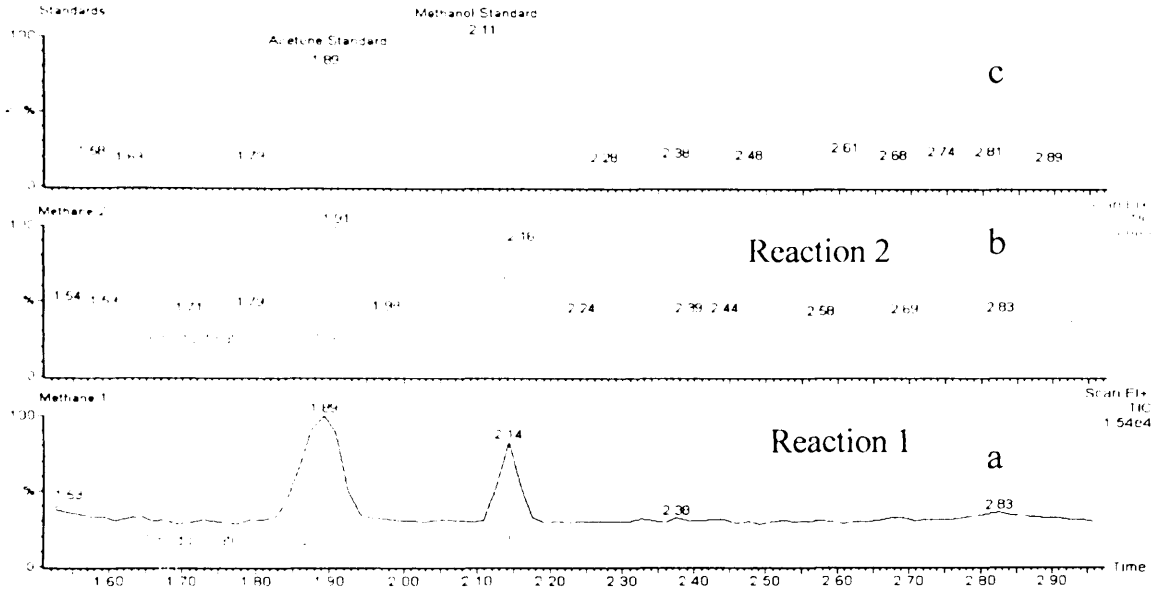

Figure A.2: GC-MS chromatograph (a), (b) for CH_4 oxidation and (c) of an aqueous solution of methanol and acetone.

Appendix A (3): Calibration of carbon dioxide using gas chromatography-flame ionisation detector (GC-FID)

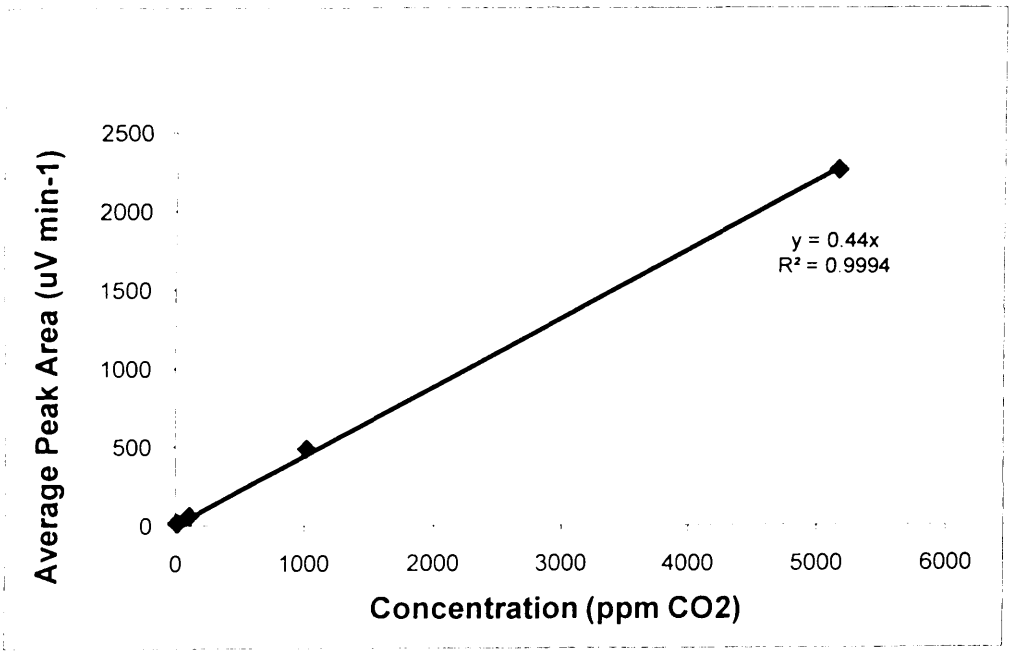

Figure A (3): Carbon dioxide (CO_2) calibration curve

Appendix B: Catalytic data and catalyst characterisation

Appendix B (1): Liquid phase oxidation of methane at various temperatures without catalyst in *in-situ* formation of H_2O_2 condition

Entry	Temp. (°C)	Product amount (μmol)				Methanol Selectivity (%)[c]	Oxygenate productivity (Mol/kg_{cat}/ Hour)[d]	TOF [e]	H_2O_2 Remain (μmol) [f]
		CH_3OH [a]	HCOOH [a]	MeOOH [a]	CO_2 in gas[b]				
1	2	0	0	0	0	-	-	-	0
2	30	0	0	0	0	-	-	-	0
3	50	0	0	0	0	-	-	-	0
4	70	0	0	0	0.13	-	-	-	0
5	90	0	0	0	0.13	-	-	-	0

Reaction Time; 30 min, Stirring rate: 1500 rpm, solvent: H_2O, 10 mL. [a] Analysis using ^{1}H-NMR, [b] Analysis using GC-FID, [c] Methanol selectivity = (mol of CH_3OH/ total mol of products) * 100, [d] Oxygenate productivity = mol of oxygenates / Kg_{cat} / reaction time (h), [e] Turn over frequency (TOF) = mol of oxygenates / mol of metal / reaction time (h), [f] Assayed by Ce^{+4} (aq) titration, Gases: 0.86% H_2/1.72%O_2/75.86%CH_4/21.55%N_2 (Total pressure: 32 bar)

Appendix B (2): UV-Vis analysis of filtrate reaction solution from methane oxidation with homogeneous Au using *in-situ* H_2O_2 approach

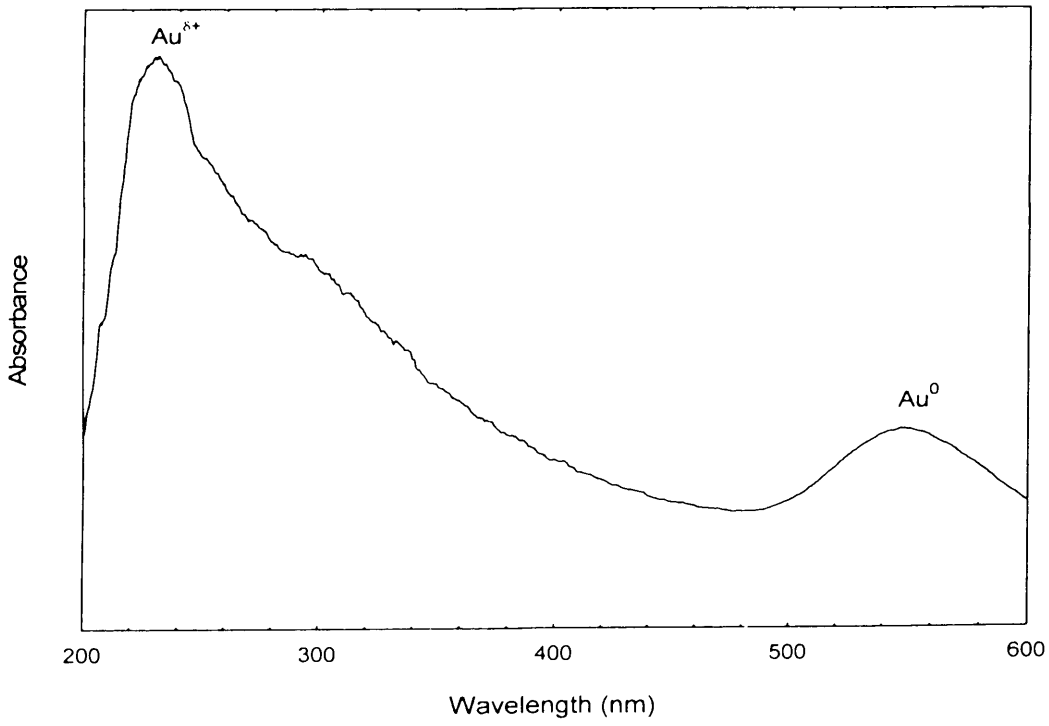

Figure B (2): UV-Vis spectra of filtrate reaction solution from methane oxidation with homogeneous Au using *in-situ* H_2O_2 approach

Appendix B (3): Oxidation of methane with the presence of copper chloride ($CuCl_2 \cdot 2H_2O$) solution

Entry	Metal (ppm)	Products (μmol)			
		CH_3OH[a]	HCOOH [a]	CH_3OOH[a]	CO_2 in gas[b]
1	4	0.98	0	1.02	<0.05
2	11	0.86	0	2.25	0.21

P_{CH4}=30 bar. $[H_2O_2]$= 0.5M, stirring rate: 1500rpm, Reaction temperature: 50 °C, Reaction time: 20 min, [a] Analysis using ^{1}H-NMR, [b] Analysis using GC-FID.

Appendix B (4): Blank reaction of (CH_3OOH + H_2O_2 + CH_4) with presence of OH radical scavenger

Entry		Products				Increment (%)
		CH_3OH[a]	CH_3OOH[a]	CO_2 in gas[b]	Total	
1	Initial	0.78	13.19	-	13.97	62
	After	1.03	28.26	8.06	37.35	
2*	Initial	0.45	13.39	-	13.84	22
	After	1.78	15.56	0.60	17.94	

P_{CH4}=30 bar. $[H_2O_2]$= 0.5M, stirring rate: 1500rpm, Reaction temperature: 50 °C, Reaction time: 20 min, [a] Analysis using ^{1}H-NMR (500MHz), [b] Analysis using GC-FID.
* H_2O_2/scavenger: 5/1 (mol/mol).

Appendix B (5): X-ray diffraction (XRD) analysis of CuO_{Cp} precursor

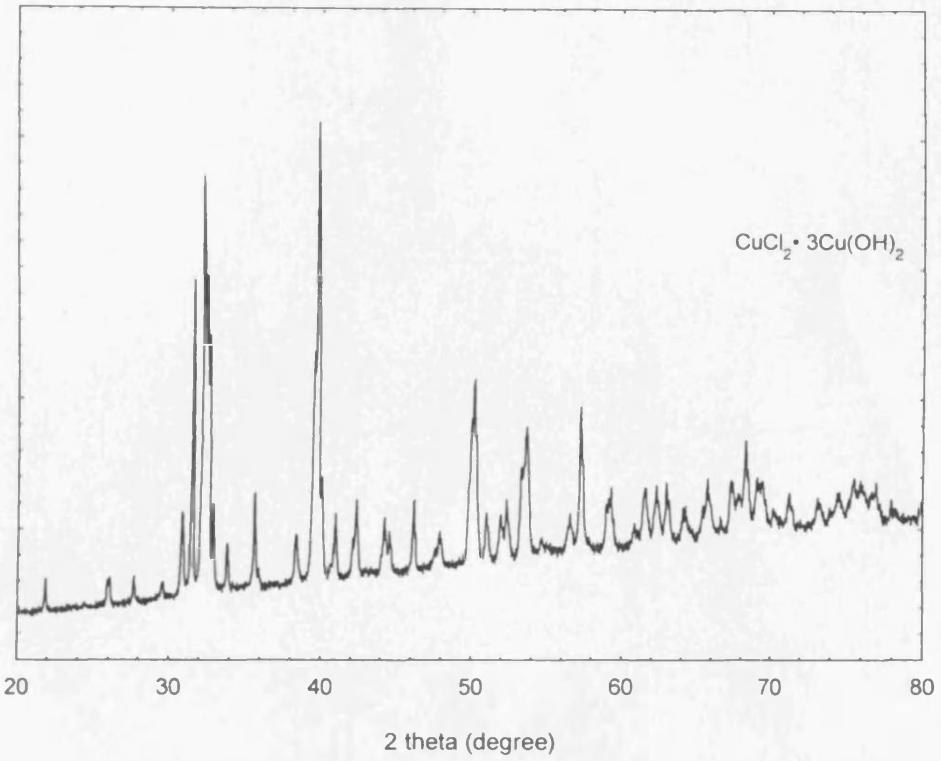

Figure B (5): XRD diffractogram of copper chloride hydroxide

Appendix B (6): Scanning electron microscopy analysis of CuO_{Sg} precursor

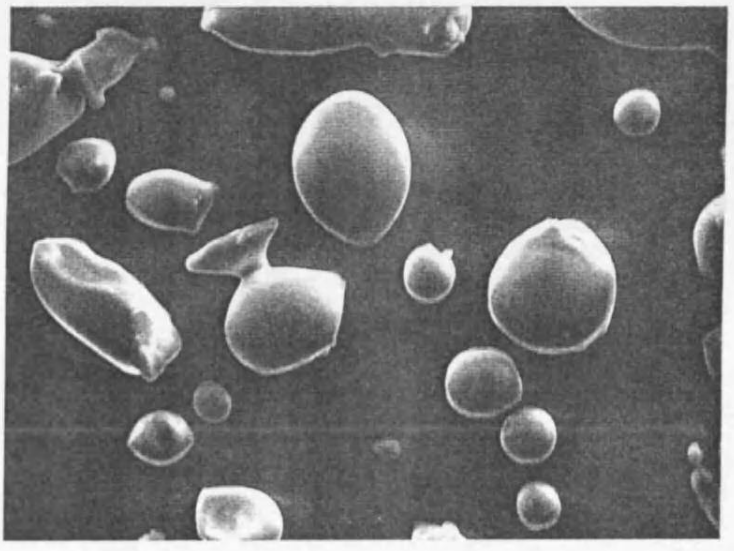

Figure B (6): SEM micrograph of copper oxide precursor synthesized using sol-gel technique